SCIENTIFIC COMMITTEE
THIRTEENTH REGULAR SESSION
Rarotonga, Cook Islands
9–17 August 2017

Background analyses for the 2017 stock assessments of bigeye and yellowfin tuna in the western and central Pacific Ocean

WCPFC-SC13-2017/SA-IP-06

S. McKechnie[1], L. Tremblay-Boyer[1], G. Pilling[1]

[1]Oceanic Fisheries Programme, The Pacific Community

Contents

1 Introduction **3**

2 Regional structure and fisheries definitions **5**

2.1 Background and modifications 5

2.2 Consequences for fisheries definitions and data 5

3 Alternative catch history **6**

4 Growth of BET **7**

4.1 Background 7

4.2 Model fitting 8

4.3 Results 11

4.4 Construction of conditional length-at-age input file 12

5 Natural mortality **12**

5.1 Background and methods 12

5.2 Results 14

6 Maturity and spawning potential **14**

6.1 Background and methods 14

6.2 Results 15

7 CPUE analyses **16**

7.1 Background and methods 16

7.2 Results and discussion 18

8 Construction of tagging datasets **20**

8.1 Results 22

9 General Discussion **23**

10 Acknowledgements **24**

1 Introduction

Stock assessment models for tuna in the Western and Central Pacific Ocean (WCPO) conducted by the Pacific Community (SPC) generally utilise the statistical software MULTIFAN-CL[2] (MFCL; Fournier et al., 1998; Hampton and Fournier, 2001; Kleiber et al., 2014). Most models are spatially explicit, consisting of several discrete geographical regions containing region-specific sub-populations linked by biological parameters such as movement and spatially-explicit recruitment. The basic unit of the fishing component of these models is a "fishery" - defined as a set of fishing activity extending over a region (or subregion) with similar characteristics, such as catch per unit effort (CPUE) and size compositions of the catch.

It is common when conducting a stock assessment in the WCPO for there to be changes to fisheries definitions, and possibly the regional boundaries themselves, between assessments. These changes are typically presented in papers ancillary to the stock assessment (e.g. McKechnie et al., 2014; Tremblay-Boyer et al., 2015; McKechnie, 2016), and the first part of this paper (Section 2) will cover these details for the 2017 bigeye (BET) and yellowfin (YFT) tuna stock assessments in the WCPO (McKechnie et al., 2017; Tremblay-Boyer et al., 2017). Most of these changes to fisheries definitions made in 2017 result from the recommendation of the pre-assessment workshop (PAW; Pilling and Brouwer, 2017) to shift the boundary between the northern temperate regions and the equatorial regions from 20° N to 10° N. Consequently there are modifications to the fisheries definitions and changes in both the distribution of data among regions for those fisheries that were maintained, and the regional weights applied to the standardised CPUE indices (see McKechnie et al., 2017; Tremblay-Boyer et al., 2017 for details of the modelling of the CPUE indices in the stock assessments).

In addition, this paper presents other analyses of input data in more detail than can be addressed in the stock assessment papers (McKechnie et al., 2017; Tremblay-Boyer et al., 2017). This includes all analyses where stand-alone papers were not considered warranted in each case. The exceptions to this were the alternative analyses of CPUE for the operational longline dataset that were a substantial body of work, and this is presented in detail by Tremblay-Boyer and Pilling (2017a,b), and the biological data analyses of BET in the WCPO undertaken by CSIRO (growth and sexual maturity), which are detailed in Farley et al. (2017).

After defining the changes to stock assessment region boundaries, fisheries definitions and data summaries (Section 2), each discrete set of analyses will be presented in-turn, with the background, methods, results and their discussion presented together in each section. These analyses can be briefly summarised as;

- **Alternative catch history** (Section 3); Based upon the request of WCPFC13 (see also Pilling and Brouwer, 2017), this section outlines initial analyses that construct an alternative

[2] http://www.multifan-cl.org

catch history for longline (LL) fisheries based on the indications of under reporting of BET in logbooks suggested by MRAG Asia Pacific (2016).

- **Growth analyses** (Section 4); Additional data in the form of aged otoliths were available for the 2017 stock assessment of BET, and are presented in detail by Farley et al. (2017). This section presents externally (to MFCL) fitted integrated growth models and the construction of conditional age-at-length input files for use in MFCL for the BET assessment.
- **Natural mortality analyses** (Section 5); The age-specific natural mortality function (M-at-age) in previous assessments of BET/YFT have been input as fixed values to MFCL. Changes in estimated or fixed growth functions, and maturity, affect the form of calculated M-at-age. This section updates M-at-age for new growth functions, maturity data and the sex ratio data used to estimate natural mortality for BET.
- **Maturity and spawning potential analyses** (Section 6); Spawning potential is used to modify model estimates of total biomass into an index of spawning biomass for spawner-recruit analyses and reference points, and is also input to MFCL as a fixed vector of values-at-age. This section updates estimates to be used in the 2017 assessment of BET for a new maturity function (Farley et al., 2017) and new growth functions.
- **CPUE analyses** (Section 7); This section presents the CPUE standardisations undertaken on the operational longline dataset using techniques very similar to those presented by McKechnie et al. (2015b). These are the CPUE indices used in the diagnostic case models, and most sensitivity and uncertainty analyses model runs of McKechnie et al. (2017) and Tremblay-Boyer et al. (2017). Alternative standardisations using the "proxy" method of classifying missing vessels in the early time series, and geostatistical techniques are presented in Tremblay-Boyer and Pilling (2017a) and Tremblay-Boyer and Pilling (2017b), respectively, and are utilised in sensitivity model runs of the assessments.
- **Construction of tagging datasets** (Section 8); Small modifications to the construction of tagging files for input into MFCL have occurred since the previous BET/YFT stock assessments in 2014, although the methods remain largely similar to those previously presented in detail by Berger et al. (2014) and McKechnie et al. (2016b). This section briefly details the process of constructing these files and presents summaries of the updated datasets, including new data provided for the Japanese Tagging Programme (JPTP).

Finally, a summary section is presented that addresses outstanding issues and avenues of further analyses that would be beneficial for future stock assessments of BET and YFT in the WCPO (Section 9). The reader should also refer to the individual stock assessment reports for stock assessment conclusions and recommendations based on the analyses herein.

2 Regional structure and fisheries definitions

2.1 Background and modifications

The major change between the 2011 and 2014 stock assessments of BET and YFT was the modification of the regional structure of the stock assessments, with three additional regions being established, largely to improve the modelling of the tagging data. Subsequent to the 2014 stock assessments, the study of Schaefer et al. (2015) highlighted a lack of movement of tagged fish between the equatorial zone (10° N–10° S) and more temperate waters, and the PAW consequently recommended that re-configuring the boundaries of the northern and equatorial regions from 20° N to 10° N be investigated as part of the 2017 stock assessments of both species (Pilling and Brouwer, 2017).

The two options for regional structures are displayed in Figures 1–2 and will be referred to throughout as the 2014 and 2017 regional structures, respectively. Note that it is difficult to modify the northern latitudinal boundary of region 7 due to the distribution of the Philippines fisheries, the scale of the data provision of those fisheries and the fact that one of those fisheries (F18) can receive a standardised CPUE index for YFT (Bigelow and Garvilles, 2017). Consequently, the boundary of regions 1 and 7 was maintained at 20° N for the 2017 regional structure.

Further changes to fisheries data included in the 2017 stock assessments result from ongoing improvements to the annual catch estimates for Indonesia (ID) and the Philippines (PH), and are outlined in Williams and Terawasi (2017). Additionally, the estimates of catch and effort of Japanese (JP) purse seine (PS) vessels in the WCPO have been improved for 2017 by utilising port sampling data (Peatman et al., 2017) and these changes are included in the data summaries presented in Figures 17–80.

2.2 Consequences for fisheries definitions and data

The consequences of the boundary shifts with respect to the fisheries definitions were relatively minor, with the data summaries of the new fisheries definitions shown in Figures 17–80. Note that throughout this section we refer to the fisheries by their 2017 fisheries numbers, which do not always correspond directly to those from 2014 due to the reduction in the number of fisheries by one (e.g. F32 will refer to MISC-VN7 - the Vietnam miscellaneous fishery in region 7, which was previously referred to as F33 in 2014).

There were already pole and line fisheries (PL) in both region 1 and region 3 and so a small amount of data shifts from region 3 (F21) to region 1 (F20). PL fisheries were not present in region 2 or region 4 in the 2014 stock assessment and so the boundary change for these regions is inconsequential for this gear type.

There was a significant amount of LL fishing in the 10–20° N zone over the assessment period and so the boundary shifts have some consequences for the LL fisheries definitions. In the 2014 assessments

there were US LL fisheries established in both region 2 and region 4, however there is a negligible amount of US LL fishing south of 10° N, so the fisheries definitions were modified by combining that small US LL fishery in region 4 with the "all flags fishery" (F9; the small amount of catch for US LL in region 4 can now be observed in Figures 25 and 57, for BET and YFT respectively) thus reducing the overall number of fisheries from 33 to 32. The US LL fishery in region 2 (F3) thus receives most of the data that was formerly in R4 (Figures 19 and 51) and the all flags fishery in region 2 (F2) also receives a substantial amount of data that was formerly included in the northern 10° band of R4 (Figures 18 and 50).

The movement of the 1-3 and 2-4 boundaries south raised the potential for some PS data to now be present in the northernmost regions (region 1 and 2; in addition to that already included in F20). However, extraction of all available data revealed that this occurrence was negligible ($<$ 100 mt over the assessment period), and it was not therefore necessary to establish a PS fishery in region 2 or add flags to F20 in region 1. However, a very small amount of JP PS data shifts from region 3 (F13 and F14, the associated and unassociated PS fisheries, respectively) to region 1 (F19).

3 Alternative catch history

The PAW requested that an additional one-off sensitivity model be undertaken as a preliminary assessment of the consequences of potential under reporting of BET catch in longline fisheries, as recently reported by MRAG Asia Pacific (2016). That study compared the catch of the main longline-caught species between the numbers of fish recorded by observers and those reported on vessel logsheets. It also compared the catch estimates from logsheets with port sampling of catch in Fiji. The estimated total under reporting of BET (including both retained and discarded catch) was 21% (MRAG Asia Pacific, 2016; Table 29) for the period 2010–2012.

The recommendation of the PAW was to construct a preliminary alternative catch history for LL fisheries in the BET stock assessment based on these results, by scaling the catches of all LL fisheries upwards based on the ratios reported in MRAG Asia Pacific (2016). The suggested approach makes a number of assumptions about the rate of under reporting and how to apply these to the stock assessment LL fisheries, including how to implement changes over time.

The approach proposed during the PAW can be defined as

$$\hat{C}_{f,t} = \begin{cases} C_{f,t}/(1 - r_{min}) & \text{for} \quad t <= 2005 \\ C_{f,t}/(1 - (r_{max} - r_{min})/(t_{max} - t_{min})) & \text{for} \quad 2005 < t <= 2011 \\ C_{f,t}/(1 - r_{max}) & \text{for} \quad t > 2011 \end{cases} \tag{1}$$

where $\hat{C}_{f,t}$ are the "corrected" catch estimates in numbers of fish for fishery f in time-step t, $C_{f,t}$ are the equivalent catches that are used in the other assessment model runs, $r_{min} = 0.04$ and $r_{max} = 0.21$ are the minimum and maximum under reporting ratios, respectively, and t_{min} and t_{max} are 2005

and 2012, respectively. Thus the correction assumes that under reporting up to 2005 (r_{min}) was at a low base rate and then increases linearly over the period from 2005 to 2012; the period between when the tropical tuna CMMs were implemented and when the estimates of under reporting by MRAG Asia Pacific (2016) were made. The ratio estimated for 2012 was assumed constant for the remaining years in the model (2013–2015). The minimum ratio was assumed to be equivalent to the ratio estimated for albacore tuna from the same study (MRAG Asia Pacific, 2016; Table 29), which again included estimates for retained and discarded catch (a total under reporting of 4%).

The basis of this alternative catch history is that before the onset of management measures the incentive to under report BET catch was low (assumed to be similar to the recent estimates for albacore tuna) but has increased steadily to the recent levels estimated by MRAG Asia Pacific (2016). For simplicity, it is assumed that these ratios apply equally to all LL fisheries in the assessment model, despite widely varying contributions of different fleets.

4 Growth of BET

4.1 Background

Stock assessments fitted using MFCL assume a common, time-invariant growth over all regions in the model. Typically, growth is estimated internally (inside the stock assessment model; e.g. a Von Bertalanffy growth function) for tuna stock assessments in the WCPO, rather than being estimated externally to the model and input as fixed parameter values. This has been the case in previous assessments of BET in the WCPO (Davies et al., 2011; Harley et al., 2014), although it should be noted that sensitivity analyses fixing certain growth parameters at alternative values to determine the impacts on model output often occur.

The reliance on internally estimated growth functions can be attributed to at least three factors; the inability to model conditional age-at-length data in older versions of MFCL, the difficulties in estimating the age of individual tuna from hard parts (Schaefer and Fuller, 2006), which limits the availability of externally estimated growth functions for these species, and the presence of strong modes in the size frequency data of some fisheries which allows robust growth modelling for some species. It should be noted however that development of MFCL has recently allowed the integration of conditional age-at-length data directly into the model if these data are available from, for example, studies of otoliths or other hard parts. This feature has previously been utilised in the 2015 stock assessment of albacore tuna in the south Pacific (Harley et al., 2015).

Recent developments in the reading of BET otoliths using annual rings are outlined in Farley et al. (2017). This research follows on from the recommendations of the 2014 stock assessment of BET. Otoliths collected for YFT are yet to be analysed, which precludes otolith-based growth estimation for this species for the moment. Farley et al. (2017) outline the results for a study of growth of BET

over a wide region of the Pacific and present analyses of area- and sex-specific growth curve estimates. The growth scenarios investigated in the 2017 BET stock assessment are detailed in McKechnie et al. (2017) and so only the detailed methodology of the growth curves that were estimated externally to MFCL are presented herein.

Two approaches to estimating growth functions using the new otolith data were undertaken; simple growth estimates using only the otolith data, and models that integrate both otolith and tagging increment data. Development of the latter models can be considered as an attempt to help validate the representativeness of the otolith data for use in WCPO assessment models and/or to provide alternative growth functions to be utilised in sensitivity analyses within the stock assessment.

Integrated models simultaneously model data of several types (in this case otoliths and tagging increments) and have a long history for estimating tuna growth (Laslett et al., 2002; Everson et al., 2004). Several recent studies (Aires-da-Silva et al., 2015; Francis et al., 2015) have attempted to reparameterise these models into forms that could be integrated within age-based stock assessment software based on assumptions of the software and computational limitations. Our aim is to investigate externally estimated growth functions that can be provided to MFCL as fixed values and so the advantages of the Laslett et al. (2002) approach outweigh the computational burden that prompted the developments in the latter studies. We therefore restrict out models to the former.

4.2 Model fitting

Two types of otolith information are available for analysis - annual and daily, which are logically read by counting the annual and daily bands, respectively (see Farley et al., 2017 for more details). The CSIRO daily otolith dataset includes a subset of the annual otolith fish for which daily readings were also made for comparative purposes. Further daily otolith ages are available for fish previously read by SPC scientists in the early 1990's and which have been previously used for fitting integrated growth models by McKechnie et al. (2015a). There is a choice about whether annual and/or daily otoliths are utilised for a given model. In this analysis, if both types are combined, the annual readings for those fish in the CSIRO daily otolith dataset must be excluded to prevent fish contributing more than one data point to the analysis. The available otolith data is displayed in Figure 3.

Initially we fit a simple von Bertalanffy (VB) model to the annual otoliths provided by Farley et al. (2017) (model *Annual-Ot-VB-NoDay*). The decision to include all fish, even those slightly to the east of the stock assessment model boundaries (see the green points in Figure 3) was made based on the extreme paucity of fish available at old ages, with those present displaying a tendency to have negative residuals compared to fish less than 10 years of age. This also relates to the very high connectivity of fish over the 150° W boundary that have been detected during the central Pacific tagging research. There is a strong likelihood that many of the otolith fish just to the east originated from the WCPO and thus share similarities in growth with fish within the eastern part of the WCPO where a significant proportion of the stock is located (McKechnie et al., 2017). Furthermore, we

detect some differences between the otolith and tag increment datasets (which will be presented in Section 4.3), which suggest an asymptotic size more consistent with models fitted to the full dataset, rather than just those otoliths located in the WCPO. We also fit equivalent models to the same dataset but with these fish outside the stock assessment boundaries excluded, to assess the effect this has on the estimated growth curve.

We fit this model using the usual parameterisation of the VB

$$l_t = L_\infty(1 - \exp(-K(t - t_0)))$$

where l_t is length at time t (in years), L_∞ is the asymptotic length, K is the (annual) growth rate parameter and t_0 is the theoretical age at which length would be zero. For use in MFCL the VB growth function is parameterised as

$$l_t = L_1 + (L_n - L_1)\left(\frac{1 - \exp(-K^q(t-1))}{1 - \exp(-K^q(n-1))}\right)$$

where t is now a quarterly time-step, L_1 and L_n are the lengths at the first and maximum (n; 40 quarters of age for BET) age-class, respectively, and K^q is the quarterly growth rate parameter, and we also report these values herein to be consistent with the BET stock assessment report of McKechnie et al. (2017).

To estimate the VB parameters, we fit a simple Bayesian regression model to the annual otoliths which is given by

$$l_i \sim \text{Normal}(\mu_i, \sigma^2) \quad \text{and} \quad \mu_i = L_\infty(1 - \exp(-K(t_i - t_0))) \ ,$$

thus the growth curve is assumed to have a normal error distribution with a constant variance (σ^2; which is checked by examining the residuals). Additional models are fitted for comparison that also included the daily otoliths provided by CSIRO (with the associated annual otolith for that fish then excluded), model *Annual-Ot-VB*, and a model with both the CSIRO and SPC read daily otoliths (the latter were previously used in McKechnie et al., 2015a), or model *Annual-Ot-VB-withSPC*.

In addition to the otolith data we constructed a "high quality" dataset of tag increments. These consist of the the lengths of fish measured at release and then also measured on recapture (along with the time-at-liberty), which if measured accurately in both cases, can provide information about growth rates of fish (noting that the age at release or recapture remains unknown). Unfortunately, it is difficult to construct such a dataset for release-recapture data in the WCPO owing to inaccuracies in recapture measurements (usually by the recapture fisherman) and in the dates of recapture. We attempt to overcome these by filtering data to only leave those considered to be the most accurate; those with higher rewards (rewarded for measurement by trained observers/port samplers), and those measured by Japanese scientists. These are further filtered to exclude fish with a time-at-liberty of less than 180 days, leaving 612 fish for inclusion in the integrated models.

The models that integrated the otolith and tagging increment data followed the methods of Laslett et al. (2002). Three likelihoods are established for: the otolith data; the length-at-release data; and the length-at-recapture data. Each assumes an underlying VB growth with normally distributed error structure, however individual-level variation is permitted by modelling the asymptotic length as a random effect where the individual asymptotic lengths of otolith fish i (L_i), and tagged fish j (L_j) are normally distributed with mean (μ_∞), and variance (σ^2_∞), hyperparameters. Another difference from the simple VB model is that the unknown ages at tag release of fish j (a_j) are modelled as a log-normally distributed random effect (with mean μ_a, and variance σ^2_a) and from this the age at tag recapture can be derived as the estimated age-at-release plus the known time-at-liberty (T_{dif}). It should also be noted that the variance parameter of the length of tagged fish at recapture (σ^2_c) is different to the parameter assumed for the otoliths and tagged fish at release (σ^2), as these measurements are often made by fishers and so are susceptible to additional measurement error. The model is outlined below

$$
\begin{array}{lll}
l_i & \sim \text{Normal}(\mu_i, \sigma^2) & \text{and} \quad \mu_i = L_i(1 - \exp(-K(t_i - t_0))) \\
l_{1j} & \sim \text{Normal}(\mu_j, \sigma^2) & \text{and} \quad \mu_i = L_j(1 - \exp(-K(a_j - t_0))) \\
l_{2j} & \sim \text{Normal}(\mu_j, \sigma^2_c) & \text{and} \quad \mu_i = L_j(1 - \exp(-K(a_j + T_{dif} - t_0))) \\
L_i, L_j & \sim \text{Normal}(\mu_\infty, \sigma^2_\infty) & \\
a_j & \sim \text{LN}(\mu_a, \sigma^2_a) &
\end{array}
$$

where the tagging increment datasets (l_{1j}, l_{2j}, T_{dif}) can be constructed in different models using two datasets. The first is the same annual otolith dataset that *Annual-Ot-VB-NoDay* is fitted to, and this model is identified as *Annual-Integrated-VB*. The second combines only the daily otoliths of the CSIRO study (Farley et al., 2017; with only otoliths for fish less than a year of age included, as suggested in that paper) and the daily otoliths previously analysed by SPC and used in the external growth estimates of the Pacific-wide BET stock assessment (McKechnie et al., 2015a). This model is notated *Daily-Integrated-VB*. For comparative purposes in the results we also show the growth function estimated in the 2014 reference case stock assessment model and refer to it as *MFCL 2014*.

Given the models fitted and presented by Farley et al. (2017) and the general lack of significant differences (and limited sample sizes in most regions) in growth between sexes and over space, we restrict our modelling to data aggregated over sex and the full region of the dataset.

All models were fitted using the Bayesian statistical software STAN (Stan Development Team, 2016). Uninformative priors were placed on all parameters in each model, as a mix of diffuse normal distributions (t_0, μ_∞, μ_a) and uniform distributions ($1/K$, σ, σ_c, σ_∞, σ_a). MCMC chains were run for different numbers of evaluations dependent on the speed of convergence identified during preliminary model runs which determined the length of the burn-in period and the number of samples needed post-convergence. Convergence was assessed using widely implemented statistics such as $\hat{R}$ (Brooks and Gelman, 1997) and visual inspection of trace plots.

4.3 Results

As shown in Farley et al. (2017), the annual otolith data suggest a growth curve with a considerably lower asymptotic length than previously assumed in the WCPO (Figure 3). The estimate of L_n for *Annual-Ot-VB-NoDay* is 152cm, 32cm shorter than the value estimated by the 2014 reference case model (Figure 3, Table 1). The other growth parameters also differed to those in 2014, including a slightly faster growth rate K^q (Table 1). The daily otoliths were similar between the SPC and CSIRO datasets and were also generally consistent with the annual otoliths at least up to about one year of age, although the SPC daily otoliths also provide additional data for very small fish that were absent from the CSIRO data (Figure 3). Adding in each of these datasets in turn produced almost identical parameter estimates to *Annual-Ot-VB-NoDay* (Table 1), presumably due to the low sample sizes of these daily otoliths and the large mass of annual otoliths at intermediate ages, which prevents the model from allowing a lower L_1 estimate (which one might expect due to the small sizes of the SPC daily otoliths in particular). When the *Annual-Ot-VB-NoDay* model was re-fitted with otoliths outside the WCPO being excluded, the estimate of L_1 was 1cm lower (39.2cm) the L_n parameter was 5cm lower (147cm) and the quarterly growth rate (K^q) was slightly higher at 0.081.

The integrated LEP model fitted to the annual otoliths (*Annual-Integrated-VB*) and the tag increments estimated an overall growth curve relatively similar to the simple annual otolith models, with estimates of L_1, L_n and K^q of 37.8cm, 156cm and 0.073 (Figure 4, Table 2). However, there appears to be some conflict between the datasets with the residuals for the tag releases and recaptures tending to be generally negative and positive, respectively. Partly this suggests that the growth rates of the tagged fish may be very slightly faster than the otolith fish. Figure 5 attempts to display this by placing the tag release lengths on the growth curve estimated on only the otoliths (*Annual-Ot-VB*), which shows an apparent pattern of small fish with shorter times-at-liberty having slower growth (the recaptures fall below the line), but most large fish and small fish with higher times-at-liberty appearing to grow faster than the otolith fish (recaptures above the line).

Model *Daily-Integrated-VB* attempts to avoid some conflict by allowing the tag increment data to be more influential at older ages. This model suggests less conflict between the datasets but does not produce a substantially different overall growth function, although size of the youngest and oldest age classes were smaller and larger than *Annual-Integrated-VB*, respectively (Figure 6). The estimates of L_1, L_n and K^q were 33.2cm, 155cm and 0.090 (Table 2), respectively, and the estimates of growth curves for individual fish were more variable (individual parameters were less "shrunken" towards the hyper parameters) as there was no longer otolith data for older fish to impose additional constraints on the model. This is evident in the high standard deviation of the individual L_{inf} parameters (σ_{inf}) which was 17.9cm for *Daily-Integrated-VB*, although it was also relatively high for *Annual-Integrated-VB* as well (12.2cm).

Some lack of fit to the tag increment dataset for small fish with relatively short times-at-liberty was detected which may be related to a tagging effect on growth. This was explored using models that

included tagging effects (Wang and Jackson, 2000) but they failed to substantially improve the fit or change growth parameters and are not displayed for concision.

4.4 Construction of conditional length-at-age input file

Recent development of MFCL has enabled conditional age-at-length data to now be integrated into the stock assessment model with the addition of an auxiliary input file (Davies et al., 2015) and the stock assessment of south Pacific Albacore (Harley et al., 2015) utilised this feature of the software. Consequently, a sensitivity analysis model run fitted by McKechnie et al. (2017) used these new growth data internally in MFCL.

The data used to construct these files were the same as used for external growth modelling above. Therefore the file was constructed by combining a combination of annual and daily (combining CSIRO and SPC fish) otoliths. These data were then aggregated by year, quarter and recapture fishery (the stock assessment fishery that captured the fish that was sampled), and within each unique combination of these factors, a matrix was developed with rows consisting of the model length bins (95 2cm bins) and columns consisting of the model age-classes (40 quarterly bins). The body of the table is the count of the otoliths relating to each combination of ages and lengths.

5 Natural mortality

5.1 Background and methods

Natural mortality (M) is an important parameter (or parameters if age-dependent M is modelled) in integrated stock assessment models, however it is a very difficult parameter to estimate reliably (Hewitt et al., 2007). In previous stock assessments of BET/YFT (Davies et al., 2011; Langley et al., 2011; Davies et al., 2014; Harley et al., 2014) age-specific natural mortality has been assumed and the function has either been estimated within the model, or externally to the model and input to MFCL as a vector of fixed values. In some cases the alternative natural mortality functions have been included as one-off sensitivity runs or in the structural uncertainty grid (e.g. Harley et al., 2014). The fixed values used in all reference case models since 2009 were derived from the methods presented by Hoyle (2008) and Hoyle and Nicol (2008), and result in an estimate of natural mortality-at-length. This function is back transformed to a function at-age by using a growth function. This is essential as MFCL is parameterised by M-at-age rather than M-at-length. Consequently, if there are significant changes to the growth function (either estimated internally or externally to MFCL), then the natural mortality function will be biased unless the fixed vector of mortality-at-age is also updated with the new information. In the case of the 2017 YFT assessment, growth was estimated to be almost identical to the 2014 assessment, and given that no new maturity data were available, the M-at-age

vector was maintained at the same values used in 2014 (see the M-at-age function presented in Tremblay-Boyer et al., 2017).

The methods for estimating natural mortality external to MFCL (note that a sensitivity model, *Lorenzen*, in McKechnie et al., 2017 estimates natural mortality within MFCL) for the 2017 stock assessment of BET in the WCPO were the same as those used in the previous assessment (Harley et al., 2014) and are outlined in detail in Hoyle and Nicol (2008). The basis for the estimation method is the observation of a substantial positive relationship between the length of fish caught and the proportion of males in the catch of longline vessels for BET in the WCPO (Hoyle and Nicol, 2008). This phenomenon is widespread among other tuna species (Farley et al., 2007; Hoyle, 2008) and may be attributed to sex-specific differences in susceptibility to fishing, growth or natural mortality. The hypothesis behind the latter is that reproduction is more physically demanding for females than males, and so the natural mortality-at-age increases for the former. Consequently, models have been developed to estimate sex-specific natural mortality by fitting to available data on the sex ratio of catch at-length in the fisheries (Harley and Maunder, 2003; Hoyle, 2008; Hoyle and Nicol, 2008).

The models fitted were identical to those previously used (e.g. Hoyle and Nicol, 2008, with the methods first presented by Harley and Maunder, 2003). It is therefore assumed that natural mortality is highest ($M0$) in the first age-class and then declines linearly to a common mortality rate for both males and females at the so-called breakpoint age-class (a_{brk}), which is three quarters of age, consistent with all previous assessments of BET in the WCPO. The male mortality rate then remains constant over all subsequent age-classes, however after the breakpoint age-class the mortality rate of females is determined by the proportion of females that are mature (ψ) in that age-class, with immature and mature individuals having mortality rates of $M1$ and $M2$, respectively. Note that a lag can be imposed that delays the increase in mortality by l quarters after maturity. The model for natural mortality can therefore be defined for males as:

$$M_a^m = \begin{cases} M0 & \text{for} \quad a = 1 \\ M_{a-1}^m - (M1 - M0)/(a_{brk} - 1) & \text{for} \quad a = 1, 2, ..., a_{brk} \\ M1 & \text{for} \quad a = a_{brk} + 1, a_{brk} + 2, ..., a_N \end{cases}$$

and for females as:

$$M_a^f = \begin{cases} M0 & \text{for} \quad a = 1 \\ M_{a-1}^f - (M1 - M0)/(a_{brk} - 1) & \text{for} \quad a = 1, 2, ..., a_{brk} \\ M1(1 - \psi_{a-l}) + M2(\psi_{a-l}) & \text{for} \quad a = a_{brk} + 1, a_{brk} + 2, ..., a_N \end{cases}$$

where $M0$ is fixed at $2 \times M1$, and quarterly age-classes are notated a, and range from 1 to 40 (a_N). The parameters in the mortality model were estimated by optimising an objective function use the χ^2 distribution and the observed and model-predicted sex-ratios-at-length.

The changes to the external estimate of age-dependent natural mortality made for the 2017 assessment were:

- Updating the sex ratio data (collected by observers on LL vessels) that the model is fitted to.
- Updating the maturity curve using the most recent data presented by Farley et al. (2017).
- Updating the growth curves used to backtransform M-at-length to M-at-age, to those that were used in the stock assessment (McKechnie et al., 2017).

5.2 Results

The natural mortality functions corresponding to the variations in growth functions utilised in the 2017 BET stock assessment (McKechnie et al., 2017), or investigated in part of this study, are presented in Figure 7 along with the function used in the 2014 assessment. Each function is parameterised identically except for the growth function used to back transform the M-at-length into M-at-age. The four new functions are identical to the 2014 function, and each other, up to around 10 quarters of age. Subsequently, an earlier increase in mortality is seen, due to the higher mortality of females as they mature earlier with the new maturity function compared to that assumed for the 2014 function. The 2014 function reaches a higher natural mortality mode (around age-class 20) than the new functions and the right hand limb declines more steeply. Each of the lower asymptotic growth scenarios produce very similar functions.

6 Maturity and spawning potential

6.1 Background and methods

The maturity function is routinely input to stock assessment models as a fixed vector of age-specific values as there is very little information to inform the model of its shape. In MFCL, maturity is currently assumed to be age-based, although it is expected that an option of implementing a length-based maturity will soon be developed. Until that time, a fixed maturity function suffers from the same problems as natural mortality (Section 5) if the assumed, or estimated, growth function differs significantly from that used to originally estimate maturity-at-age.

Since 2008, stock assessments of BET and YFT have modified the usual definition of maturity (the proportion of fish-at-age that are sexually mature) to that of "spawning potential", where it is recognised that the contribution of fish of different age-classes to the production of the next generation is non-uniform (Hoyle, 2008; Hoyle and Nicol, 2008). For instance, it is well recognised that larger fish produce more eggs and there is a higher proportion of males in the population at older ages in these species, and so these factors must be taken account of when estimating the spawning potential of the modelled population. This is why reference points for these species refer to spawning potential

rather than spawning biomass (although the latter is utilised for skipjack tuna, e.g. McKechnie et al., 2016a). Consequently, previous estimates of spawning potential for BET/YFT have been calculated as the product of model-estimated biomass and an index of age-specific contribution to the next generation, which is itself a product of "classic" maturity (proportion of fish sexually mature at-age), egg production, sex ratio and spawning fraction (Hoyle, 2008). Note that the situation for YFT in 2017 is the same as for M, that is; the growth curve is almost identical to the 2014 estimate, and no new maturity estimates have become available and so the spawning potential-at-age function used in 2014 was maintained (see the spawning potential-at-age function presented in Tremblay-Boyer et al., 2017).

The process to estimate spawning potential for the 2017 stock assessment of BET in the WCPO again follows very closely from that used in the previous assessment (Harley et al., 2014) which directly utilised the methods of Hoyle and Nicol (2008). For BET, we update the sex ratio estimate as described in section 5 and also estimate alternative spawning potential functions based on the growth functions investigated in the full stock assessment outlined by McKechnie et al. (2017). The function for the proportion of fish estimated to be sexually mature is updated based on a logistic function fitted to the data presented by Farley et al. (2017) and is presented in Figure 8. The data used in the modelling were restricted to fish caught in the equatorial regions 3 and 4, as recommended by Farley et al. (2017). The sex ratio-at-length used was that estimated in Section 5, and the remaining functions (egg production and spawning frequency) are identical to those used in previous assessments (Hoyle and Nicol, 2008). Each of these functions are shown in Figure 8, and have been taken from previous biological studies (Schaefer, 1998; Sun et al., 2006).

Once the spawning potential-at-length relationship has been calculated, it is transformed into a relationship at-age based on the growth function used in the focal assessment model. In the 2017 assessment of BET the growth function is an important component of model uncertainty, with several alternative functions applied. Consequently, for each growth function an alternative spawning potential function is also adopted.

6.2 Results

Figure 9 displays the spawning potential functions utilised in the stock assessment and investigated in this study, along with the function used in 2014. The estimate using the 2014 growth function and the updated maturity and sex ratio data (2014 update in the figure) shows behaviour more similar to the low growth scenarios rather than the function used in 2014 itself (red line). The more rapid increase in spawning potential over the quarterly age classes 6–12 compared to the 2014 function (Figure 9) results from the earlier maturity estimated based on the data from Farley et al. (2017), compared to the function used in 2014 which was based on data from the EPO. However, the spawning potential for the 2014 model also declines more rapidly than the 2014 update at older age-classes due to the higher mortality at these ages that was used in 2014 (red line; Figure 7).

In general, all scenarios with a low growth rate produce very similar spawning potential-at-age functions, with the rate of increase and decrease, at young and old ages, determined by the small differences in estimated natural mortality (Figure 7) that result from the impacts of the growth curves on the transformation of the sex ratio-at-length relationship (Figure 9) onto the age-scale. These low growth scenarios do however produce slightly different results due to differences in growth rate (K), which affects the slope of the increasing left hand limb, and asymptotic size (L_{inf}), which affects the slope of the declining right hand limb of Figure 9.

7 CPUE analyses

7.1 Background and methods

This section describes the analyses that produced the standardised CPUE indices used in the diagnostic case models and structural uncertainty grids for the BET and YFT stock assessments (McKechnie et al., 2017; Tremblay-Boyer et al., 2017). The methods follow very closely those presented by McKechnie et al. (2015b), although they relate to an updated version of the operational longline CPUE dataset, with indices being estimated up to the end of 2015 (the terminal year of the stock assessments). The dataset analysed is the same as that utilised in the associated papers on the geostatistical approach to standardising CPUE (Tremblay-Boyer and Pilling, 2017a) and the analyses that attempt to account for the missing vessel identifiers for Japanese vessels in the early years of the dataset (Tremblay-Boyer and Pilling, 2017b). We therefore refer readers to these papers for the details of the construction of the dataset, the filtering of the data, and discussion of further work necessary to improve the data.

While the detailed methods associated with the collation and filtering of the data are not repeated herein (see Tremblay-Boyer and Pilling, 2017b for further details) we briefly summarise these steps. The dataset used to standardise the raw CPUE data is exactly the same as that presented by Tremblay-Boyer and Pilling (2017b) and these data were constructed by:

- Following the methods of data cleaning outlined in McKechnie et al. (2015b) and Tremblay-Boyer and Pilling (2017a) - removing data with missing critical fields, highly unusual values for hooks set, fishing outside the assessment boundaries, no catch of the key tuna species etc.
- The remaining data were assigned to the assessment regions 1–8 (2014 or 2017 regions, depending on which assessment model the indices were being produced for). Note that no standardisations were undertaken in region 9 as the data were too sparse to produce valid estimates. The nominal CPUE indices were utilsed in the stock assessments with lower effort deviation penalties applied.
- For data where vessel identification was available, only vessels fishing for a minimum number of quarters (see Table 3 for the region-specific values used, column "Min qtrs/ves") were retained

in an attempt to remove fishing activity for vessels that are not representative of the general fishing practices in the region.

- Data were then thinned further to reduce the total number of sets retained for model fitting, given the substantial sample sizes involved which preclude practical fitting of GLMs, given computer memory limitations. The thinning was applied by randomly excluding vessels from the dataset, and then applying the resulting ratio of retained to excluded effort to the data where vessel identifiers were missing (Japanese vessels in the early years). The rates of thinning were determined by trial and error based on the sample sizes in each region (see Table 3 for the final thinning rates), such that the maximum number of samples that could be practically modelled were retained.

- These datasets were then analysed using kmeans clustering methods (see McKechnie et al., 2015b and Tremblay-Boyer and Pilling, 2017a for details) such that designated groups of fishing sets were assigned to clusters that attempt to define the targeting practices of the fishing activity. Decisions on the numbers of clusters to use for each region were decided at the PAW and are displayed in Table 3 (column "clusters"). All clusters were retained in the dataset, again on the recommendation of the PAW, and the defined cluster values were used as a factor in the standardisation (see below).

The same modelling approach as McKechnie et al. (2017) was utilised to standardise the CPUE indices. Delta log-normal models were used to model the presence/absence of BET/YFT catch in individual sets (binomial component), and conditional on presence, the positive catch data were modelled with a log-normal GLM (positive component). The binomial component comprises modelling a binary response variable (y_i; 1 = at least 1 fish caught, or 0 = zero fish caught, in set i)

$$y_i \sim \text{Bernoulli}(p_i) \quad \text{and,} \tag{2}$$

$$\log(\frac{p_i}{1-p_i}) = \beta_0 + \beta_{T[i]} + \beta_{S[i]} + \beta_{C[i]} + \beta_H h_i \tag{3}$$

where p_i is the probability of at least one BET (or YFT when modelling that species) being caught in set i, the logit link function is used to express this probability in terms of the linear predictor and the coefficients are the intercept (β_0), the year-quarter factor ($\beta_{T[i]}$), the 5×5 spatial cell factor ($\beta_{S[i]}$), the targeting cluster factor ($\beta_{C[i]}$), and a coefficient for the continuous variable of hooks fished (divided by 100), $\beta_H h_i$. Note that it is also possible to include a vessel factor but this assumes that all vessels in the early time period are a single "missing" vessel (as was assumed by Hoyle and Okamoto, 2011). For this reason, the vessel factor was not included in the model that produced the standardised CPUE indices (which is consistent with the models used in the Pacific-wide analyses in 2015; McKechnie et al., 2015b), but it is included in the step plots to demonstrate its potential impact on the resulting indices.

The positive component of the delta log-normal model was then modelled using a Gaussian GLM

given by

$$\log c_i \sim \text{Normal}(\log \mu_i, \sigma^2) \quad \text{and,} \tag{4}$$

$$\log \mu_i = \beta_0 + \beta_{T[i]} + \beta_{S[i]} + \beta_{C[i]} \tag{5}$$

where $\log c_i$ is the log CPUE of the focal species (number caught divided by hundred hooks). The parameters in the linear predictor have the same interpretation as for the binomial component.

7.2 Results and discussion

We display the standardised indices used in the 2017 diagnostic case models (2017 regions) for BET (McKechnie et al., 2017) and YFT (Tremblay-Boyer et al., 2017), along with the models used in the 2014 reference case models of the same species (BET, Figure 10; YFT, Figure 11). Step plots are presented for the 2017 standardisation models in Figures 12–13, and diagnostic plots are presented in Figures 81–112. There are number of notable differences between the sets of indices which can be summarised for BET as:

- In a number of regions (especially regions 3, 5 and 7) the standardised indices cover a much longer time period, owing to the provision of the longline operational dataset subsequent to the 2014 assessment. Previously, many of the indices were only able to be estimated over the period where SPC holds operational data, which is often from about 1980.
- Several indices are relatively similar between the sets, at least over the time periods where both sets are available (e.g. regions 3, 5 and 8).
- Other regions show moderate differences in both the estimated trends, and the inter annual variation: Region 1 declines less than in 2014; region 2 declines by a similar amount in 2017, but shows less variability; region 6 in 2017 shows slightly higher abundance over the last two decades, but shows lower abundance during the late-1970s and 1980s; region 4 in 2017 shows a more moderate decline but over a longer time period (note that in 2014 this index caused problems in the assessment and was subsequently replaced with the standardised index from Hoyle and Okamoto, 2011, so the 2017 index can be considered more robust than previously); and region 7 shows a significant decline in the first decade, before a standardised index was available for the 2014 assessment.
- Significant increases in CPUE have been detected in several regions in the last two years, particularly regions 3, 4 and 5.

For YFT (Figure 11), the differences between the sets of indices can be summarised as:

- There are again substantial differences in the time periods covered by the two sets of indices in some regions.
- Regions 1, 3, 5, 6 and 7 show relatively similar indices in 2017 to those estimated in 2014, not

withstanding the different coverage of the assessment period that the 2017 indices provide.

- The index for region 4 in 2017 shows a similar decline to that estimated in 2014 but over a slightly longer time period. The 2017 index for this region is also slightly less variable.
- The index for region 2 estimated in 2014 displayed a substantial increase in CPUE over the first several decades followed by a significant decline from the mid-1990s until the present time. The 2017 index for this region shows more stable dynamics (though still has significant inter annual variation) in the early years, and while the recent substantial decline is also estimated, it is more moderate for this series.
- The index for region 8 in 2017 is significantly different to that estimated in 2014. For the latter the index was shorter, but also estimated a variable, slightly increasing trend in CPUE, while in 2017 the index displays a strong, relatively consistent decline over most the the time-series.
- Similar significant increases in CPUE in the last two years were estimated in several regions, as was observed for BET.

The step plots for the full year-quarter-scale CPUE indices estimated in 2017 are displayed in Figures 12–13. In general it can be observed that the factors introduced to the model had only a limited impact on modifying the indices from the nominal indices. Adding the cell factor and the cluster factor both removed some temporal variation from the time series, especially in the more uncertain early years, although the former factor had little effect on the trends in CPUE over time. In contrast, the cluster factor did estimate indices with different trends from the preceding model (the year-quarter/cell model). These impacts were species- and region-specific, with the cluster factor leading to higher declines for BET in regions 3 and 4, especially in recent years (Figure 12). For YFT, the most notable changes when the cluster factor was added were a less severe decline in CPUE in regions 3 and 7 (Figure 13).

Diagnostics were examined for departure from the error distribution assumed for the GLM model (i.e. binomial for the occurrence data and lognormal for the positive catch rates) and temporal trends in the estimated effects, for all levels of covariates are included in plot summaries (Figures 81–112). As has been the case for all recent CPUE standardisations of operational data for these species in the WCPO, the fits of the models are generally adequate. However, there are still cases where the model has difficulty predicting the observed catch rates for some parts of the distribution, particularly in the tails (Figures 81–112). For the lower tail in the LN component models this is often due to the lower bound of zero on the natural scale, while the model tends to underestimate the very high CPUE observed in some regions. This is presumably due to the high diversity of fishing activity included in the models which a relatively simple model has difficulty in always taking into account.

The final comparison between the indices used in 2014 and 2017 concerns the purse-seine standardised CPUE in region 8 (see Pilling et al., 2014 and Tremblay-Boyer et al., 2016 for the previous standardisations of these analyses - methods used in 2017 were as per Tremblay-Boyer et al., 2016,

with the addition of three further years data subsequent to the 2014 assessment), which are displayed in Figure 14. The new CPUE index is generally similar to the 2014 index, although there is certainly some time-series variation between them. The overall trends (flat overall but highly variable) are similar, and the index shows perhaps a slight upwards (though highly variable) trajectory over the subsequent three years added since the 2014 assessment.

A comparison of the 2017 CPUE indices used in the models assuming the 2014 regions (e.g. the sensitivity model *2014Reg* in McKechnie et al., 2017 and Tremblay-Boyer et al., 2017) and the diagnostic case models that assume the 2017 regions (and have previously been presented above), are displayed in Figures 15–16. These show predictable results in that the indices for regions 5–8 are identical, given that the boundaries of these regions are maintained in both regional structures. For regions 3 and 4 for both species, there are only marginal differences in estimated indices, which is presumably because the data shifted from these regions to the northern temperate regions is a relatively small component of the total effort in those regions. For BET the indices in region 1 and 2 were also very similar between the regional structures, with slight differences in some years, and a slightly less variable time-series estimated in region 2 for the 2017 regions. For YFT, there was a slight deviation between the indices for the different regional structures in region 1 in the late 1970s, although for region 2 a more stable time series was estimated for the 2017 regions. The differences in that region are very similar to the differences between the 2017 region indices and the indices used in the 2014 reference case model (Figure 11).

8 Construction of tagging datasets

The construction of the tagging files (hereafter .tag files) for use in MFCL for the 2017 assessments of BET and YFT closely follow the methods previously outlined by Berger et al. (2014) which were updated by McKechnie et al. (2016b). The raw .tag data files constructed from SPC databases underestimate recapture rates of tagged fish due to: not all recaptured tags being usable in MFCL (e.g. tags without recapture dates, location or vessel identification often cannot be attributed to a model fishery and are therefore excluded from the stock assessment); some fish shed tags immediately, or some time after tagging; and some tagging-induced mortality occurs such that tagged fish assumed to be present in the population will have already died. This results in fishing mortality being underestimated by this data component, which will potentially lead to underestimates of biomass.

These issues were addressed prior to the 2014 assessments by accounting for estimates of tag usability, tag-induced mortality and tag shedding in the reporting rate penalties input to MFCL (Davies et al., 2011; Langley et al., 2011). Development of MFCL in 2014 allowed for non-integer numbers of released fish, thus enabling the corrections for these factors to be applied directly to the releases (by scaling them downwards) rather than through the reporting rate penalties, which the model has the ability to adjust to fit other sources of data.

The methodology of correcting releases and filtering of the data for input into MFCL is covered in detail by McKechnie et al. (2016b), and so we provide only the following brief overview of the process and refer readers to that study for relevant details, especially the formulae used to correct release numbers which are presented in Section 3.4 of that report. Three tagging programmes for which SPC holds data were used for the 2017 assessments; the Regional Tuna Tagging Programme (RTTP; 1989–1992), Coral Sea Tagging Programme (CSTP; sporadically over 1991–2001) and the Pacific Tuna Tagging Programme (PTTP; 2006–2015; this programme is ongoing). The methodology used to construct the .tag file consists of:

- The "raw" .tag file for MFCL is produced using software written in FoxPro (Long, 1994) and only includes usable tags (those that can be assigned to a fishery and time period).
- A parallel programme written in the R statistical language (R Core Team, 2013) uses identical SQL queries with the exception that it extracts all recaptures (usable and unusable) and produces a "full" .tag file.
- The usability ratio is calculated as the ratio of usable to total recaptures at the scale of the length bin within a tagging release event.
- The number of releases is then scaled down by the correction ratio and then further scaled down by a tag shedding rate (0.059; for both species), base tag-induced mortality (0.07; for both species) and additional mortality from sub optimal tagging (inexperienced taggers etc.; species specific estimates were derived from Berger et al., 2014).
- All release events with less than 10 released fish are excluded.
- All release events after the second quarter of 2015 were excluded to prevent biases from the occurrence of re-caught fish not being reported or entered into the database by SPC at the time of the assessment (there is often a substantial lag between recapture and reporting).

The reporting rate penalties were calculated using identical methods to those outlined by Peatman et al. (2016). The datasets were updated to include tag seeding data that have become available since the 2014 assessments, and separate sets of penalties were estimated for the 2014 and 2017 regional structures.

The methods used for constructing the 2017 tagging files adopt the improved methodology of McKechnie et al. (2016b), with only some minor technical differences implemented compared to that study. These can be described briefly as;

- The exclusion of all archival tags from the .tag file as these tags were unlikely to share the same tagging-induced mortality and tag shedding rates, and their reporting rates are likely to be higher than conventional tags.
- If there was a positive count for total recaptures, but zero usable recaptures in a certain length bin, then the usability ratio is undefined. The previous approach (Berger et al., 2014) was to

apply the median usability ratio calculated over the focal release event to the length bin in question, but this has relatively little relationship with the true recapture rate for tags in that length-bin/release event. Therefore, in the current analyses (and previously implemented by McKechnie et al., 2016b) these releases are considered to provide no information about fishing mortality and are removed via the correction factor.

- All tagging programmes received the full process of correcting the release numbers whereas, in 2014 the CSTP data for instance, were not corrected for usability ratio (Berger et al., 2014).

An additional dataset from the Japan Tagging Programme (JPTP) was available in 2017 that was not used in either of the 2014 stock assessments. This programme has included several subprojects including large scale BET and YFT tagging and opportunistic tagging of these species during the ongoing SKJ tagging project (Pilling and Brouwer, 2017). These have been conducted by the Japanese government, NRIFSF and Ajinomoto Co. Inc. and have been focused on the Nansei Islands area (southwest of the main Japan islands) and offshore from central Japan. Tag release events for this programme that are usable in the stock assessment span the period 2000–2014. The methods used to construct tagging data suitable for MFCL for this programme were identical to those presented above. For the purposes of the corrections for tagger effects we assume correction factors similar to the PTTP are suitable. It should be noted that there are a moderate number of recaptures for this tagging programme from small-scale fisheries not included in the model (JP troll fishing, JP gill netting) and so these are corrected for when calculating the usability correction ratios.

8.1 Results

An additional 10 tagging release events were added to the BET tagging file since the 2014 stock assessments contributing an extra 5,953 effective releases and 2,878 usable recaptures. The corrections of tag releases for usability, tag shedding and tag-induced mortality reduced the effective number of releases to 2,938, 11,377 and 3,571 from the raw releases for the RTTP, PTTP and CSTP tagging programmes, respectively, giving a total of 17,886 effective releases and 6,348 usable recaptures in the updated tagging file (Table 4). The correction ratio for the PTTP releases is particularly severe owing to the number of fish tagged near the eastern boundary of the assessment region which are recaptured in the EPO (Schaefer et al., 2015) which significantly affects the usability ratio, and hence the correction factor applied to the effective number of releases.

Ten tagging release events were also added to the tagging file for YFT in 2017. This comprised an additional 3,572 effective releases and 786 usable recaptures. The corrections of tag releases for usability, tag shedding and tag-induced mortality reduced the effective number of releases to 2,343, 55,888 and 20,574 from the raw releases for the RTTP, PTTP and CSTP tagging programmes, respectively. This gave a total of 78,805 effective releases and 20,104 usable recaptures in the updated tagging file (Table 4).

The JPTP provided an additional 41 and 57 release events for BET and YFT respectively, with 2,180 and 5,657 effective releases and 357 and 652 usable recaptures. A feature of this tagging programme is the frequency with which tags are recaptured relatively soon after tagging and so the effective number of recaptures after the model-imposed mixing period is not large. However, these data are located in regions where little data is available from the other programmes and so provides potentially important information on mortality and biomass in these areas and so they are included in sensitivity model runs for the 2017 assessments for both species.

9 General Discussion

The changes made to the region definitions of the 2017 stock assessments led to a reduction in the number of fisheries from 33 to 32, however changes to the remaining fisheries were relatively minor. Despite this, some of the largest changes between assessments can potentially occur when modifying regional structures. For this reason it is important to quantify these changes clearly and this is outlined in McKechnie et al. (2017) and Tremblay-Boyer et al. (2017) where the modification of regions was a very early change in the stepwise development of the 2017 assessments.

The other substantial change to the development of the BET stock assessment addressed herein, was the provision of the BET annual otolith dataset (Farley et al., 2017). This dataset is extremely important for the 2017 stock assessment of this species and changes in the growth function either estimated or fixed in the model have substantial consequences for model output (McKechnie et al., 2017). We present alternative growth curves that are suitable for use in MFCL and also outline the construction of the conditional age-at-length input file to allow the otolith data to be integrated directly into MFCL. Any significant changes to the growth curve require recalculation of natural mortality and spawning potential and we have shown that moderate differences in these updated functions exist when compared to the 2014 stock assessment model parameters. We recommend that the development of length-based maturity (and hence spawning potential) and natural mortality in MFCL be given high priority as this would negate the need to continually adjust these functions under different growth scenarios. Given the significant changes to the BET stock assessment output following the inclusion of growth functions consistent with the new otolith data, it is recommended that a similar study is undertaken for YFT, if the techniques developed for BET can be extended to that species.

These analyses provide the basis for many of the sensitivity model runs and the uncertainty analyses in the BET and YFT stock assessments (McKechnie et al., 2017; Tremblay-Boyer et al., 2017), as do several of the other analyses presented here (catch uncertainty, inclusion of the JPTP data etc.). The stock assessments themselves quantify the impact of these developments on model output and management quantities and this paper aims only to provide the necessary background and detail to better interpret the model development and summaries presented in McKechnie et al. (2017) and Tremblay-Boyer et al. (2017).

10 Acknowledgements

We thank Keisuke Satoh and Takayuki Matsumoto for the provision of the JPTP tagging data and the Japanese government, NRIFSF and Ajinomoto Co. Inc. for supporting the JPTP tagging programme. We also thank participants at the pre-assessment workshop (Noumea, April 2017) for their contributions to these analyses, particularly Jess Farley for her advice on the analyses of the new biological datasets for bigeye tuna.

References

Aires-da-Silva, A. M., Maunder, M. N., Schaefer, K. M., and Fuller, D. W. (2015). Improved growth estimates from integrated analysis of direct aging and tag-recapture data: An illustration with bigeye tuna (*Thunnus obesus*) of the eastern pacific ocean with implications for management. *Fisheries Research*, 163:119–126.

Berger, A. M., McKechnie, S., Abascal, F., Kumasi, B., Usu, T., and Nichol, S. J. (2014). Analysis of tagging data for the 2014 tropical tuna assessments: data quality rules, tagger effects, and reporting rates. WCPFC-SC10-2014/SA-IP-06, Majuro, Republic of the Marshall Islands, 6–14 August 2014.

Bigelow, K. and Garvilles, E. (2017). Relative abundance of yellowfin tuna for the purse seine and handline fisheries operating in the Philippines Moro Gulf (Region 12) and High Seas Pocket 1. WCPFC-SC13-2014/SA-IP-07, Rarotonga, Cook Islands, 9–17 August 2017.

Brooks, S. P. and Gelman, A. (1997). General methods for monitoring convergence of iterative simulations. *Journal of Computational and Graphical Statistics*, 7:434–455.

Davies, N., Fournier, D. A., Hampton, J., and Bouye, F. (2015). Recent developments and future plans for MULTIFAN-CL. WCPFC-SC11-2015/SA-IP-01, Pohnpei, Federated States of Micronesia, 5–13 August 2015.

Davies, N., Harley, S., Hampton, J., and McKechnie, S. (2014). Stock assessment of yellowfin tuna in the Western and Central Pacific Ocean. WCPFC-SC10-2014/SA-WP-04, Majuro, Republic of the Marshall Islands, 6–14 August 2014.

Davies, N., Hoyle, S., Harley, S., Langley, A., Kleiber, P., and Hampton, J. (2011). Stock assessment of bigeye tuna in the western and central Pacific Ocean. WCPFC-SC7-2011/SA-WP-02, Pohnpei, Federated States of Micronesia, 9–17 August 2011.

Everson, J., Laslett, G., and Polacheck, T. (2004). An integrated model for growth incorporating tag-recapture, length-frequency, and direct aging data. *Canadian Journal of Fisheries and Aquatic Science*, 61:292–306.

Farley, J., Eveson, P., Krusic-Golub, K., Sanchez, C., Roupsard, F., McKechnie, S., Nichol, S., Leroy, B., Smith, N., and Chang, S.-K. (2017). Age, growth and maturity of bigeye tuna in the western and central Pacific Ocean. WCPFC-SC13-2017/SA-WP-01, Rarotonga, Cook Islands, 9–17 August 2017.

Farley, J. H., Davis, T. L. O., Gunn, J. S., Clear, N. P., and Preece, A. L. (2007). Demographic patterns of southern bluefin tuna, *Thunnus maccoyii*, as inferred from direct age data. *Fisheries Research*, (83):151–161.

Fournier, D., Hampton, J., and Sibert, J. (1998). MULTIFAN-CL: a length-based, age-structured model for fisheries stock assessment, with application to South Pacific albacore, *Thunnus alalunga*. *Canadian Journal of Fisheries and Aquatic Sciences*, 55:2105–2116.

Francis, R. I. C., Aires-da Silva, A. M., Maunder, M. N., Schaefer, K. M., and Fuller, D. W. (2015). Estimating fish growth for stock assessments using both age-length and tagging-increment data. *Fisheries Research*, 180:113–118.

Hampton, J. and Fournier, D. (2001). A spatially-disaggregated, length-based, age-structured population model of yellowfin tuna (*Thunnus albacares*) in the western and central Pacific Ocean. *Marine and Freshwater Research*, 52:937–963.

Harley, S. J., Davies, N., Hampton, J., and McKechnie, S. (2014). Stock assessment of bigeye tuna in the Western and Central Pacific Ocean. WCPFC-SC10-2014/SA-WP-01, Majuro, Republic of the Marshall Islands, 6–14 August 2014.

Harley, S. J., Davies, N., Tremblay-Boyer, L., Hampton, J., and McKechnie, S. (2015). Stock assessment of south Pacific albacore tuna. WCPFC-SC11-2015/SA-WP-06, Pohnpei, Federated States of Micronesia, 5–13 August 2015.

Harley, S. J. and Maunder, M. N. (2003). A simple model for age-structured natural mortality based on changes in sex ratios. Technical Report SAR-4-01, Inter-American Tropical Tuna Commission, La Jolla, California, USA, 19–21 May 2003.

Hewitt, D. A., Lambert, D. M., Hoenig, J. M., Lipcius, R., Bunnell, D. B., and Miller, T. J. (2007). Direct and indirect estimates of natural mortality for chesapeake bay blue crab. *Transactions of the American Fisheries Society*, 136:1030–1040.

Hoyle, S. and Nicol, S. (2008). Sensitivity of bigeye stock assessment to alternative biological and reporductive assumptions. WCPFC-SC4-2008/ME-WP-01, Port Moresby, Papua New Guinea, 11–22 August 2008.

Hoyle, S. D. (2008). Adjusted biological parameters and spawning biomass calculations for south Pacific albacore tuna, and their implications for stock assessments. WCPFC-SC4-2008/ME-WP-02, Port Moresby, Papua New Guinea, 11–22 August 2008.

Hoyle, S. D. and Okamoto, H. (2011). Analyses of Japanese longline operational catch and effort for Bigeye and Yellowfin Tuna in the WCPO. WCPFC-SC7-2011/SA-IP-01, Pohnpei, Federated States of Micronesia, 9–17 August 2011.

Kleiber, P., Hampton, J., Davies, N., Hoyle, S. D., and Fournier, D. (2014). *MULTIFAN-CL User's Guide*. http://www.multifan-cl.org/.

Langley, A., Hoyle, S. D., and Hampton, J. (2011). Stock assessment of yellowfin tuna in the Western and Central Pacific ocean. WCPFC-SC7-2011/SA-WP-03, Pohnpei, Federated States of Micronesia, 9–17 August 2011.

Laslett, G., Everson, J., and Polacheck, T. (2002). A flexible maximum likelihood approach for fitting growth curves to tag-recapture data. *Canadian Journal of Fisheries and Aquatic Science*, 59:976–986.

Long, J. (1994). *FoxPro 2.6 for Windows: developer's guide (2nd ed)*. Sams Pub, Carmel, Ind.

McKechnie, S. (2016). Summary of fisheries structures for the 2016 stock assessment of skipjack tuna in the western and central Pacific Ocean. WCPFC-SC12-2016/SA-IP-06, Bali, Indonesia, 3–11 August 2016.

McKechnie, S., Hampton, J., Abascal, F., Davies, N., and Harley, S. J. (2015a). Sensitivity of WCPO stock assessment results to the inclusion of EPO dynamics within a Pacific-wide analysis. WCPFC-SC11-2015/SA-WP-04, Pohnpei, Federated States of Micronesia, 5–13 August 2015.

McKechnie, S., Hampton, J., Pilling, G. M., and Davies, N. (2016a). Stock assessment of skipjack tuna in the western and central Pacific Ocean. WCPFC-SC12-2016/SA-WP-04, Bali, Indonesia, 3–11 August 2016.

McKechnie, S., Harley, S. J., Davies, N., Rice, J., Hampton, J., and Berger, A. (2014). Basis for regional structures used in the 2014 tropical tuna assessments, including regional weights. WCPFC-SC10-2014/SA-IP-02, Majuro, Republic of the Marshall Islands, 6–14 August 2014.

McKechnie, S., Ochi, D., Kiyofuji, H., Peatman, T., and Caillot, S. (2016b). Construction of tagging data input files for the 2016 skipjack tuna stock assessment in the western and central Pacific Ocean. WCPFC-SC12-2016/SA-IP-05, Bali, Indonesia, 3–11 August 2016.

McKechnie, S., Pilling, G., and Hampton, J. (2017). Stock assessment of bigeye tuna in the western and central Pacific Ocean. WCPFC-SC13-2017/SA-WP-05, Rarotonga, Cook Islands, 9–17 August 2017.

McKechnie, S., Tremblay-Boyer, L., and Harley, S. J. (2015b). Analysis of Pacific-wide operational longline CPUE data for bigeye tuna. WCPFC-SC11-2015/SA-WP-03, Pohnpei, Federated States of Micronesia, 5–13 August 2015.

MRAG Asia Pacific (2016). *Towards the quantification of illegal, unreported and unregulated (IUU) fishing in the Pacific Islands Region*. MRAG Asia Pacific, 101p.

Peatman, T., Caillot, S., Leroy, B., McKechnie, S., Roupsard, F., Sanchez, C., Nicol, S., and Smith, N. (2016). Analysis of tag seeding data and reporting rates. WCPFC-SC12-2016/SA-IP-13, Bali, Indonesia, 3–11 August 2016.

Peatman, T., Smith, N., Park, T., and Caillot, S. (2017). Better purse seine catch composition estimates: recent progress and future work plan for Project 60. WCPFC-SC13-2017/ST-WP-02, Rarotonga, Cook Islands, 9–17 August 2017.

Pilling, G. and Brouwer, S. (2017). Report from the spc pre-assessment workshop, noumea, april 2017. Technical Report WCPFC-SC13-2017/SA-IP-02, Rarotonga, Cook Islands, 9–17 August 2017.

Pilling, G. M., Usu, T., Kumasi, B., Harley, S., and Hampton, J. (2014). Purse seine cpue for skipjack and yellowfin in the png purse seine fishery. WCPFC-SC10-2014/SA-WP-03, Majuro, Republic of the Marshall Islands, 6–14 August 2014.

R Core Team (2013). *R: A language and environment for statistical computing*. R Foundation for Statistical Computing, Vienna, Austria.

Schaefer, K. and Fuller, D. (2006). Estimates of age and growth of bigeye tuna (*Thunnus obesus*) in the eastern Pacific Ocean, based on otolith increments and tagging data. Technical Report 23. 32–76, Inter-American Tropical Tuna Commission, La Jolla, California, USA.

Schaefer, K., Fuller, D., Hampton, J., Caillot, S., Leroy, B., and Itano, D. (2015). Movements, dispersion, and mixing of bigeye tuna (*Thunnus obesus*) tagged and released in the equatorial Central Pacific Ocean, with conventional and archival tags. *Fisheries Research*, 161:336–355.

Schaefer, K. M. (1998). Reproductive biology of yellowfin tuna (*Thunnus albacares*) in the eastern Pacific Ocean. Technical Report 21: 205–272., IATTC Bulletin.

Stan Development Team (2016). *Stan Modeling Language: User's Guide and Reference Manual*, version 2.12.0 edition.

Sun, C.-L., Chu, S.-L., and Yeh, S.-Z. (2006). Reproductive biology of bigeye tuna in the Western and Central Pacific Ocean. Technical Report WCPFC-SC2-2006/BI-WP-01, Manila, Philippines, 7–18 August 2006.

Tremblay-Boyer, L., McKechnie, S., and Harley, S. J. (2015). Spatial and fisheries structure and regional weights for the 2015 south Pacific albacore tuna (*Thunnus alalunga*) assessment. WCPFC-SC11-2015/SA-IP-07, Pohnpei, Federated States of Micronesia, 5–13 August 2015.

Tremblay-Boyer, L., McKechnie, S., Pilling, G., and Hampton, J. (2017). Stock assessment of yellowfin tuna in the Western and Central Pacific Ocean. WCPFC-SC13-2017/SA-WP-06, Rarotonga, Cook Islands, 9–17 August 2017.

Tremblay-Boyer, L. and Pilling, G. (2017a). Geo-statistical analyses of operational longline CPUE data. WCPFC-SC13-2017/SA-WP-03, Rarotonga, Cook Islands, 9–17 August 2017.

Tremblay-Boyer, L. and Pilling, G. (2017b). Use of operational vessel proxies to account for vessels with missing identifiers in the development of standardised CPUE time series. WCPFC-SC13-2017/SA-WP-04, Rarotonga, Cook Islands, 9–17 August 2017.

Tremblay-Boyer, L., Pilling, G., Kumasi, B., and Usu, T. (2016). Standardized CPUE for skipjack tuna (*Katsuwonus pelamis*) from the Papua New Guinea archipelagic purse seine fishery. WCPFC-SC12-2016/SA-IP-04, Bali, Indonesia, 3–11 August 2016.

Wang, Y.-G. and Jackson, C. J. (2000). Growth curves with time-dependent explanatory variables. *Environmetrics*, 11:597–605.

Williams, P. and Terawasi, P. (2017). Overview of tuna fisheries in the Western and Central Pacific Ocean, including economic conditions–2016. WCPFC-SC13-2017/GN-WP-01, Rarotonga, Cook Islands, 9–17 August 2017.

Table 1: Parameter estimates for Von Bertalanffy growth functions fitted using different statistical models and different datasets. Note that the L_N of 184cm shown for the 2014 reference case model was fixed, not fully estimated in the stock assessment model. The models are presented in Section 4.

Model	t_0	sd	K	sd	L_{inf}	sd	σ	sd	L_1	L_N	K^q	n otoliths
MFCL 2014	-0.22	NA	0.25	NA	200	NA	NA	NA	21.7	184	0.061	NA
Annual-Ot-VB-NoDay	-0.76	0.05	0.29	0.01	158	1.76	9.7	0.2	40.3	152	0.073	1,039
Annual-Ot-VB	-0.76	0.05	0.29	0.01	158	1.8	9.6	0.2	40.4	152	0.073	1,039
Annual-Ot-VB-withSPC	-0.71	0.04	0.30	0.01	157	1.75	9.5	0.2	39.2	151	0.074	1,116

Table 2: Parameter estimates for integrated Von Bertalanffy growth functions fitted to a combination of otolith and tag increment data. The models are presented in Section 4.

Model	$t0$	sd	K	sd	μ_{inf}	sd	σ_{inf}	sd	σ	sd	σ_c	sd	$\mu\log_a$	sd	$\sigma\log_a$	sd	L_1	L_N	K^q	n ots	n tags
Annual-Integrated-VB	-0.66	0.04	0.29	0.01	163	1.8	12.2	1.0	6.7	0.4	9.0	0.5	0.24	0.03	0.47	0.02	37.8	156	0.073	1,039	612
Daily-Integrated-VB	-0.4	0.03	0.36	0.02	159	2.8	17.9	2.8	1.6	0.7	6.9	0.5	0.21	0.02	0.4	0.02	33.2	155	0.090	77	612

Table 3: Summary of the region-specific settings used when cleaning, thinning and clustering the datasets used to estimate the standardised CPUE indices for the 2017 diagnostic case models for bigeye and yellowfin tuna. The column Min qtrs/ves shows the number of quarters that a vessel had to fish in the focal region to be retained in the dataset. The thinning rate shows the proportion of vessels retained after the random thinning of vessels to allow practical compution, given the substantial quantities of data available for some regions.

Region	Min qtrs/ves	Thinning rate	Min sets/vessel	Clusters
1	20	0.5	200	4
2	10	0.6	200	3
3	20	0.5	200	3
4	20	0.7	200	3
5	10	1	200	3
6	10	0.5	200	2
7	10	1	200	3
8	20	1	100	4

Table 4: Summary of the tagging file used in for the 2017 stock assessments of BET and YFT, showing the raw number of usable releases, the corrected effective number of releases, the correction ratio and the raw and effective recapture rates

Species	Programme	Raw	Effective	Recaptures	Correction	Raw rate	Effective rate
BET	CSTP	4,831	3,571	340	0.74	0.07	0.10
-	PTTP	37,701	11,377	5386	0.30	0.14	0.47
-	RTTP	3,757	2,938	622	0.78	0.17	0.21
YFT	CSTP	3,003	2,343	70	0.78	0.02	0.03
-	PTTP	105,461	55,888	14,883	0.53	0.14	0.27
-	RTTP	36,668	20,574	4,151	0.56	0.11	0.20

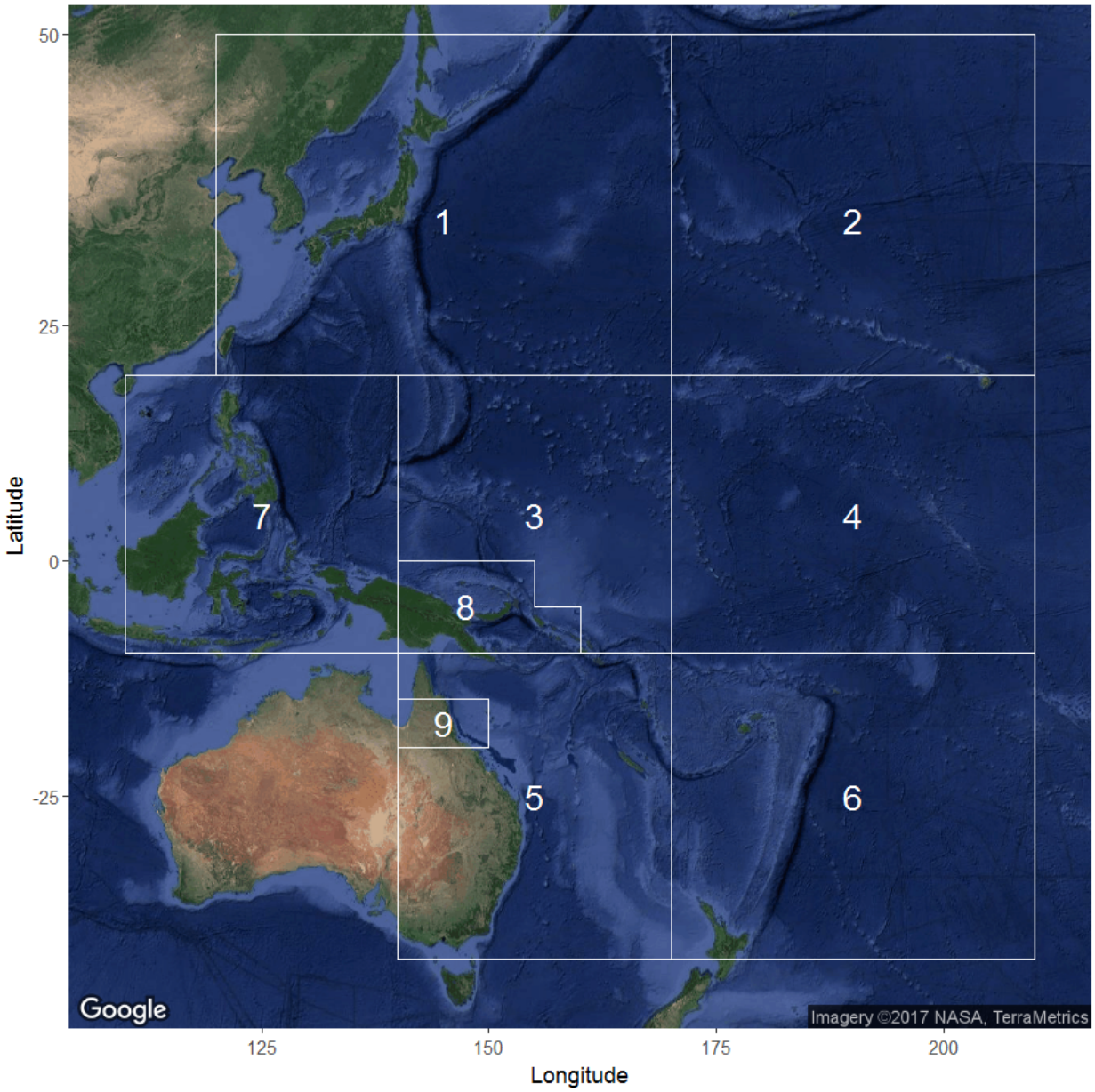

Figure 1: Regional structure of the reference case models for the 2014 BET and YFT stock assessment models in the WCPO.

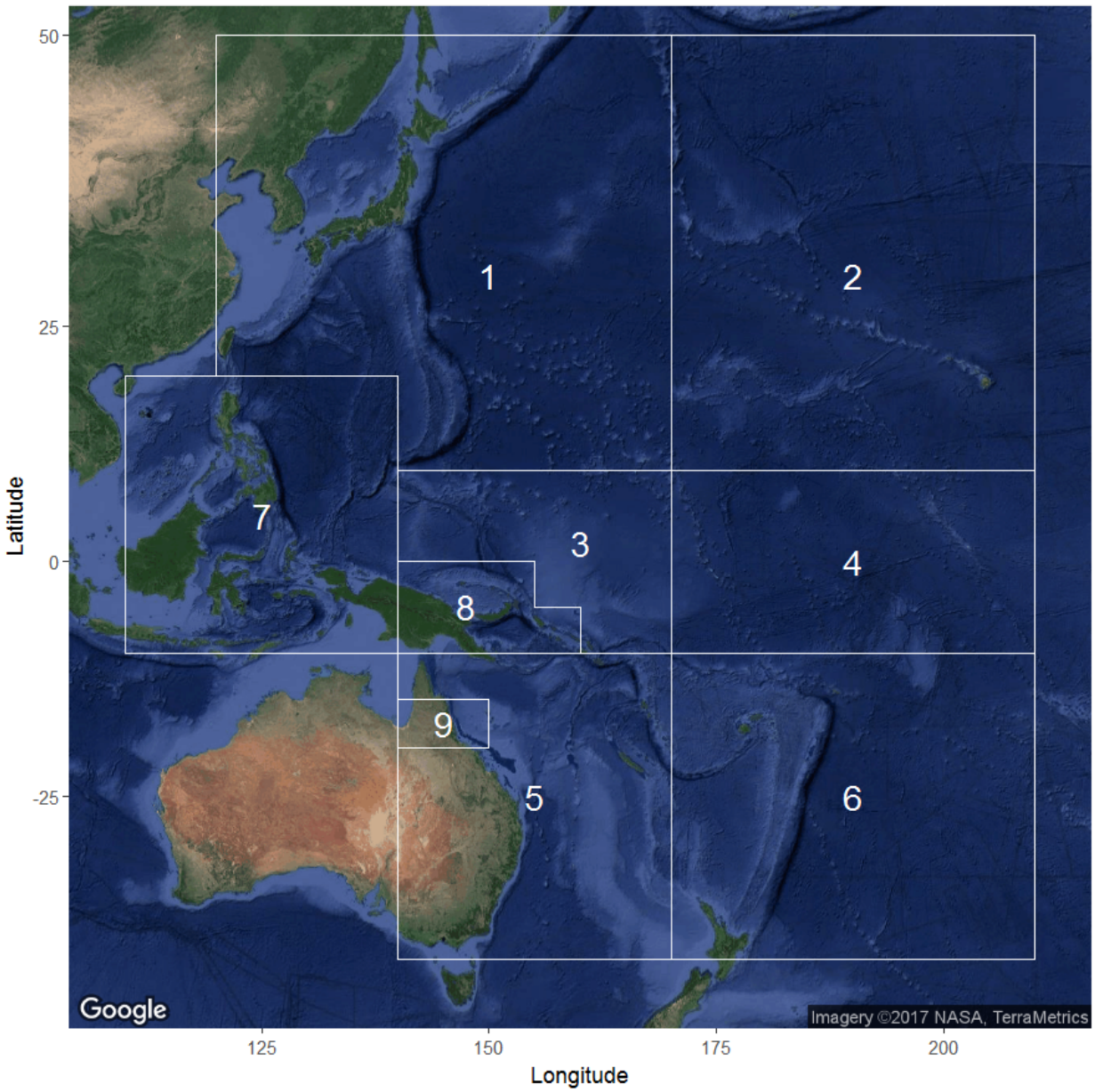

Figure 2: Regional structure of the reference case models for the 2017 BET and YFT stock assessment models in the WCPO.

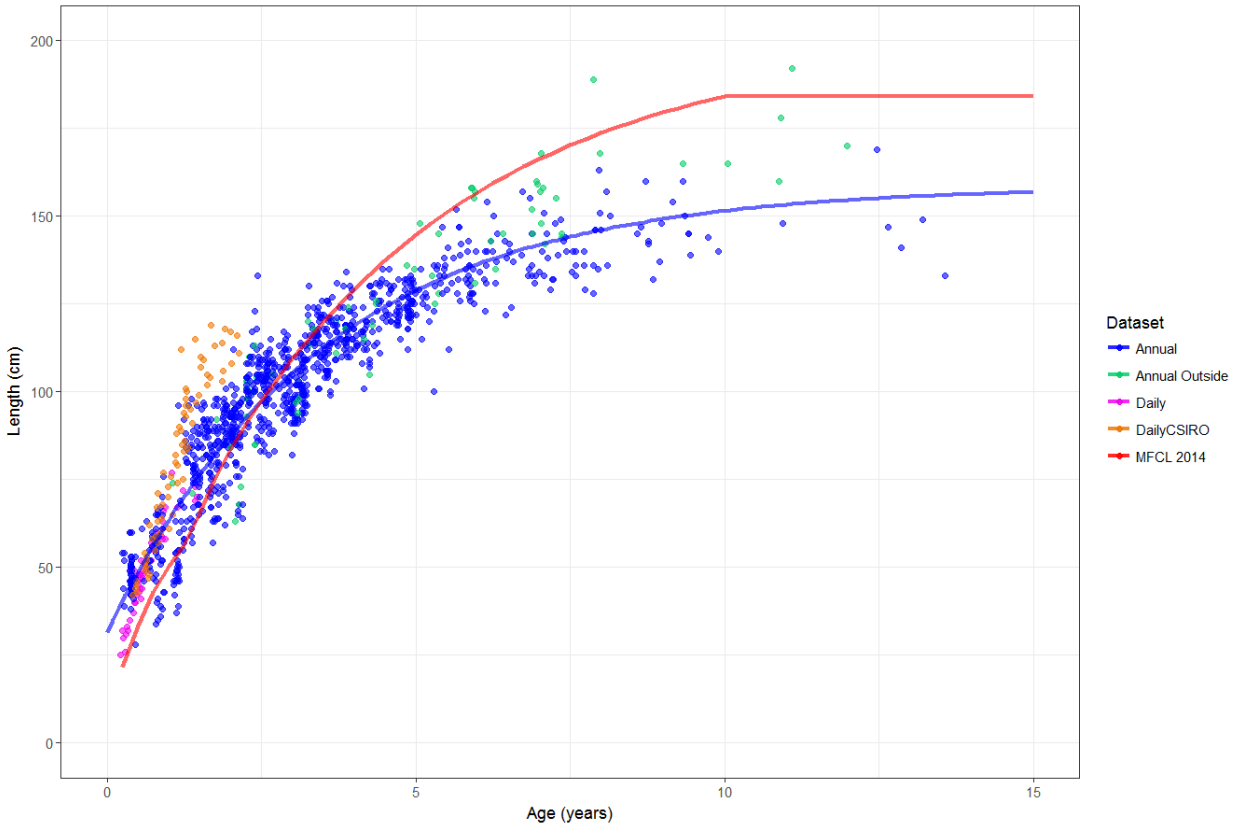

Figure 3: Comparison of otolith data and growth functions in the WCPO. The dots represent the CSIRO daily ring readings (pink), the SPC daily ring readings (orange) and the CSIRO annual ring readings (blue). The green points show the CSIRO annual ring readings for fish outside the stock assessment area. The blue line is the esimated von Bertalanffy growth function for the annual otoliths (*Annual-Ot-VB-NoDay*) and the red line is the growth function estimated in the 2014 BET stock assessment.

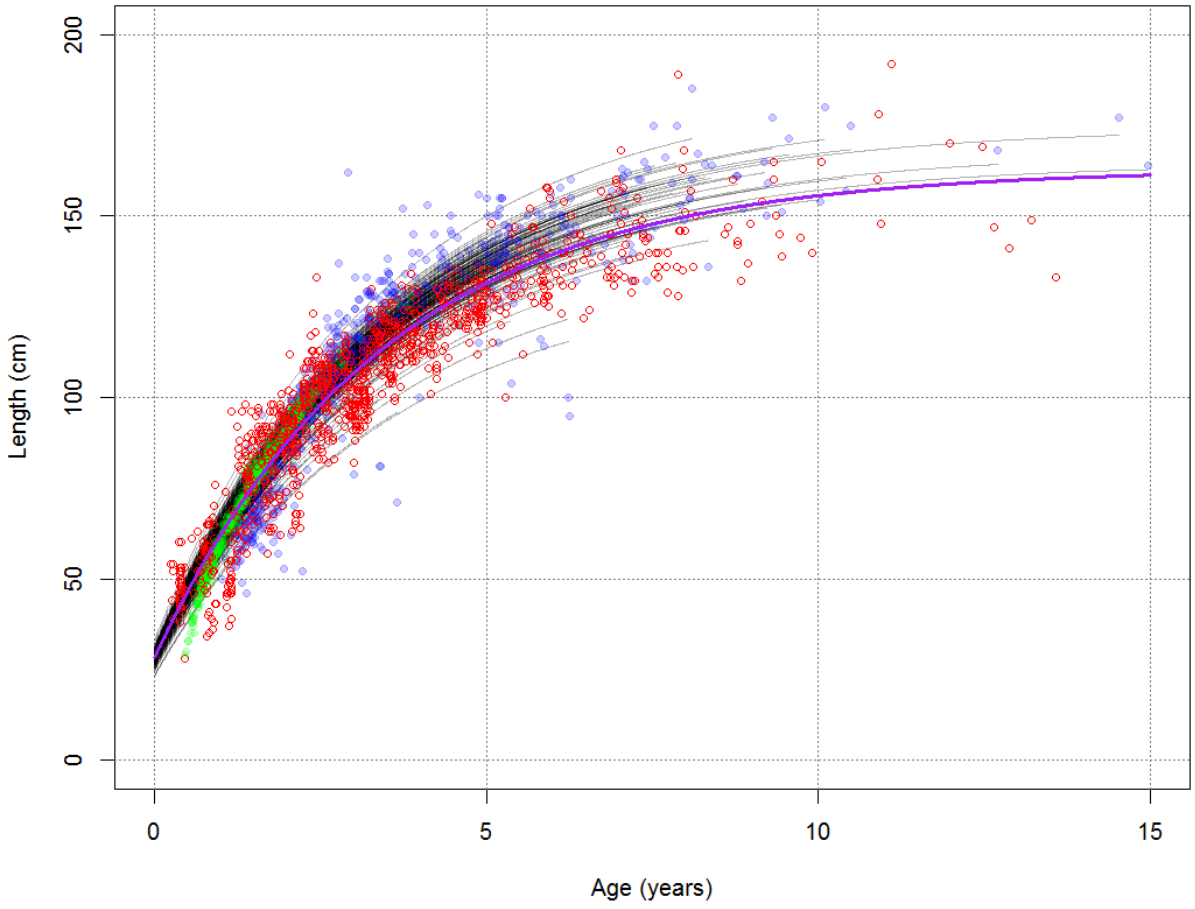

Figure 4: Fit of the LEP integrated model (*Annual-Integrated-VB*) to annual otolith data (red dots) and the high quality set of tag increment data - releases (green dots) and recaptures (blue dots). The black lines show the estimated von Bertalanffy curves for the individual tag increments and the purple line shows the estimated overall (hyperparameters) growth curve.

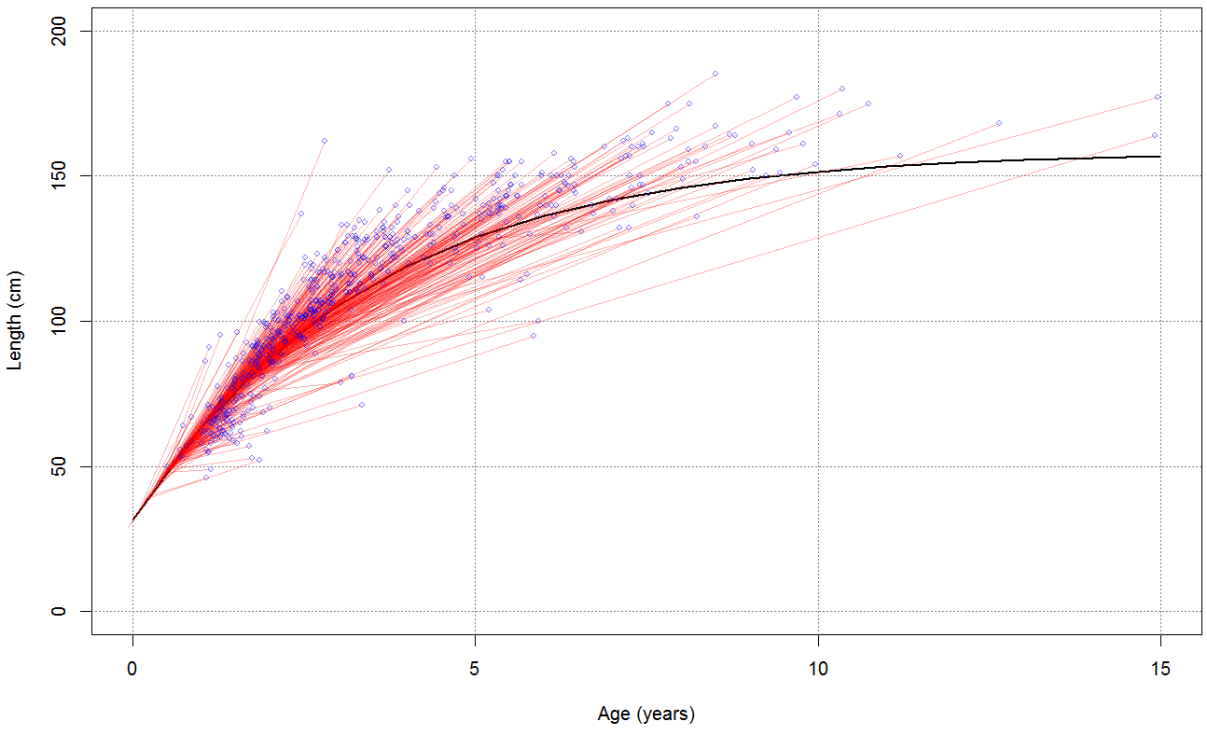

Figure 5: Figure displaying some conflict in growth rates between the annual otolith and high quality tag increment datasets. The black line is the estimate of the von Bertalanffy growth for a model fitted to just the annual otoliths in the WCPO. The tag increment data is overlayed by positioning the release lengths at the appropriate place on the line and the position of the recaptures is consequently determined by the recapture length and time-at-liberty.

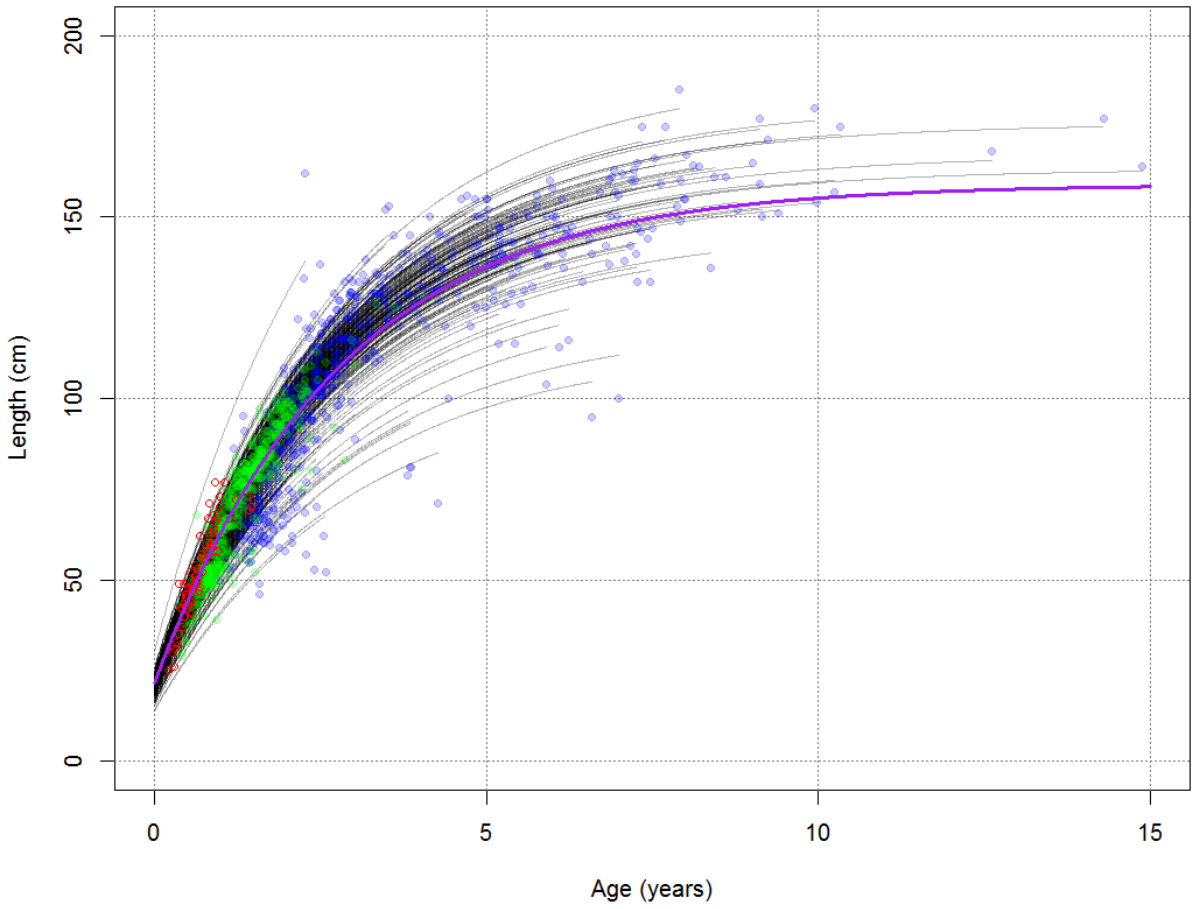

Figure 6: Fit of the LEP integrated model (*Daily-Integrated-VB*) to daily otolith data (red dots; both historical SPC and current CSIRO data) and the high quality set of tag increment data - releases (green dots) and recaptures (blue dots). The black lines show the estimated von Bertalanffy curves for the individual tag increments and the purple line shows the estimated overall (hyperparameters) growth curve.

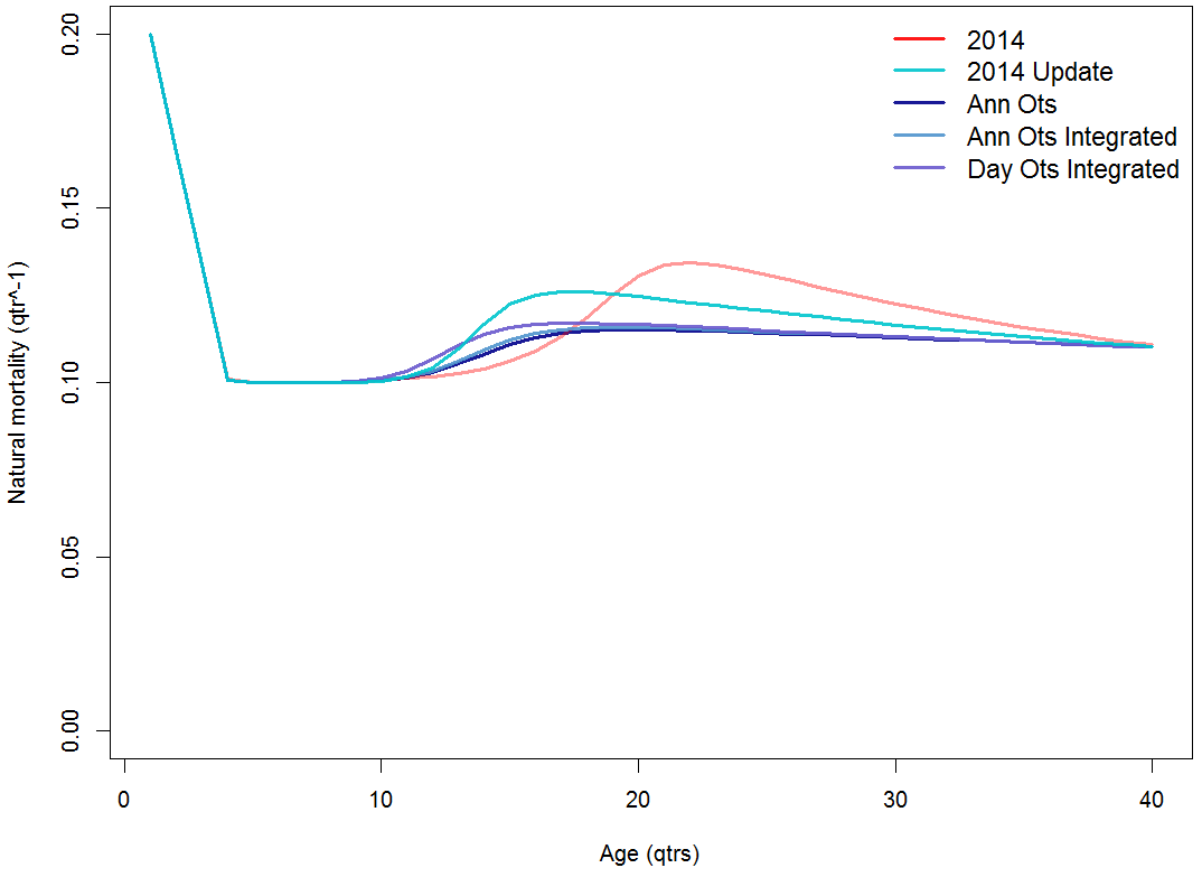

Figure 7: Comparison of the age-specific natual mortality functions utilised in the 2017 stock assesssment of BET in the WCPO.

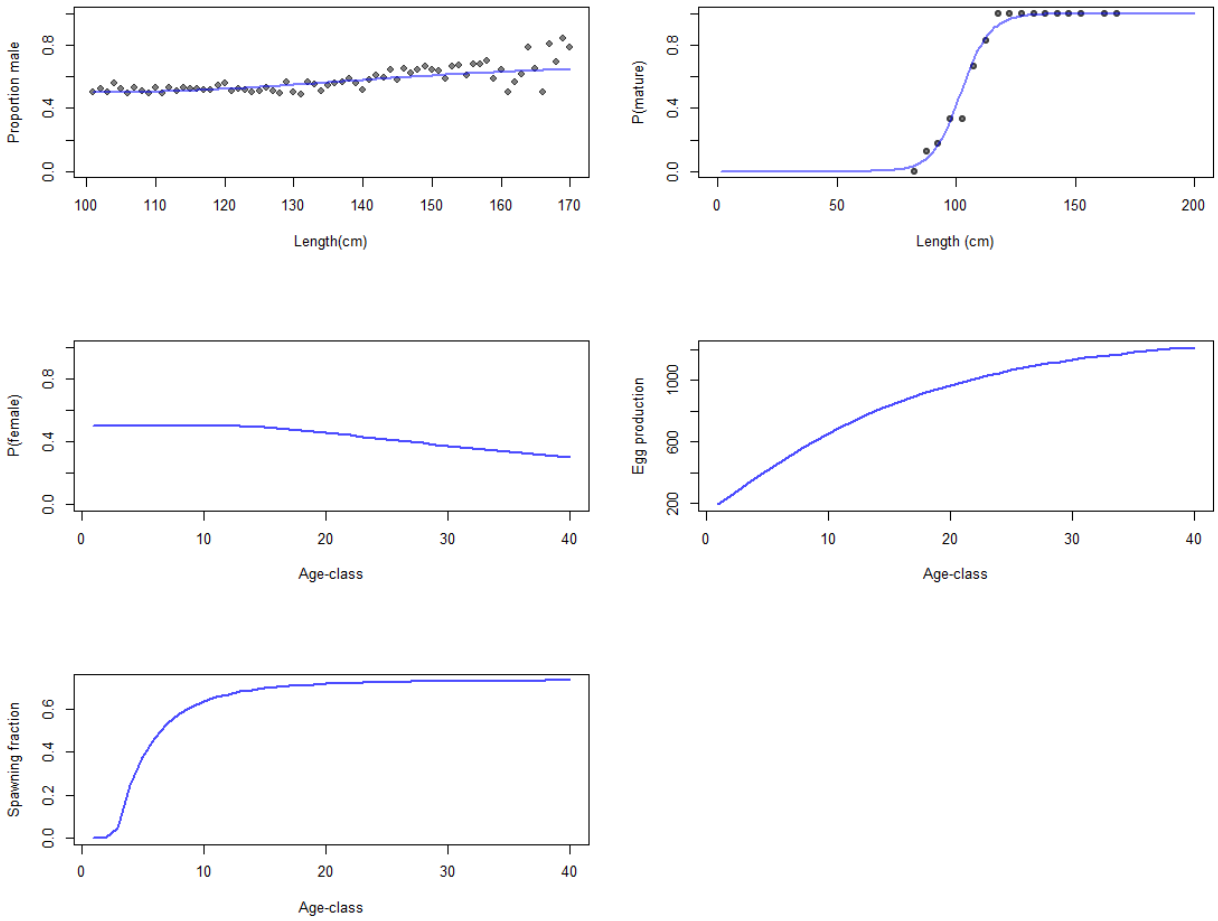

Figure 8: Biological functions used in the model fitting or calculation of natural mortality-at-age and spawning potential-at-age for BET. The panels show; top left - the proportion of males caught by length from the observer data with the model fit (blue line) used for fitting the natural mortality model; top right - the proportion of fish assessed to be sexually mature at-length for the data of Farley et al. (2017) for regions 3 and 4; middel left - the proportion female (1-P(male) from top left panel) using in the spawning potential calculations; middle right - the function used for egg production-at-age; bottom left - spawning fraction-at-age.

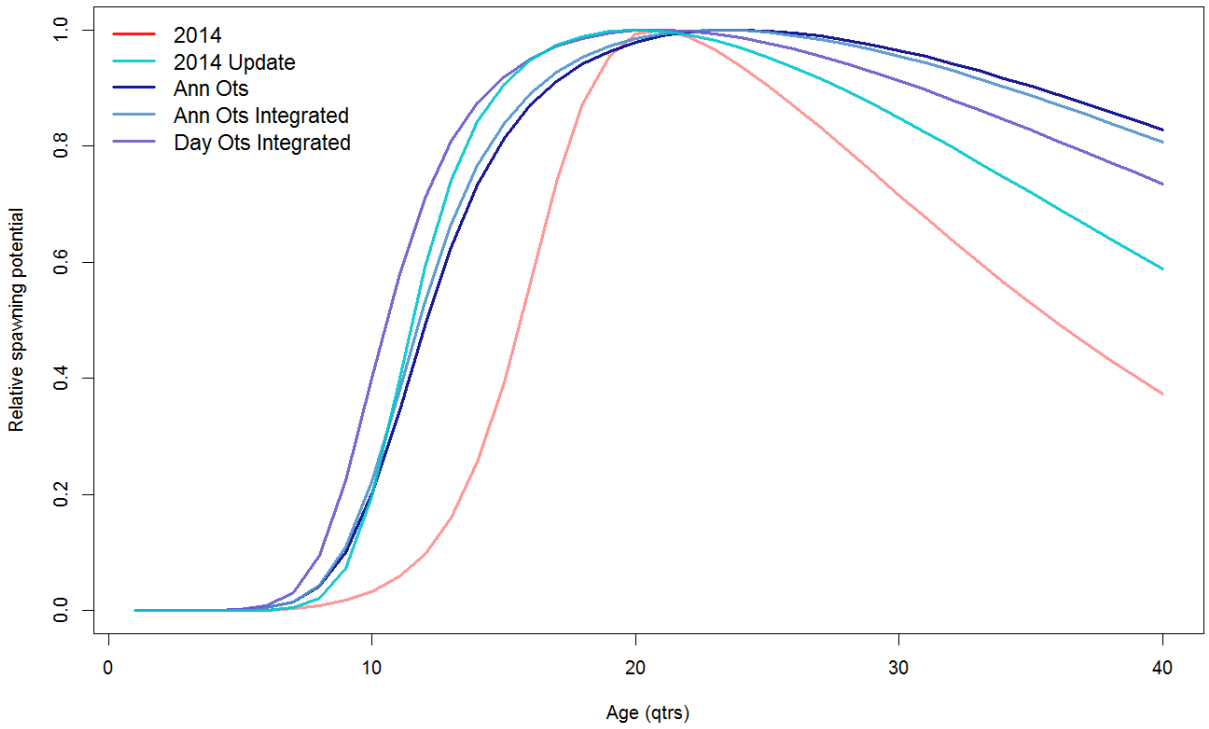

Figure 9: Comparison of the age-specific spawning potential functions utilised in the 2017 stock assesssment of BET in the WCPO.

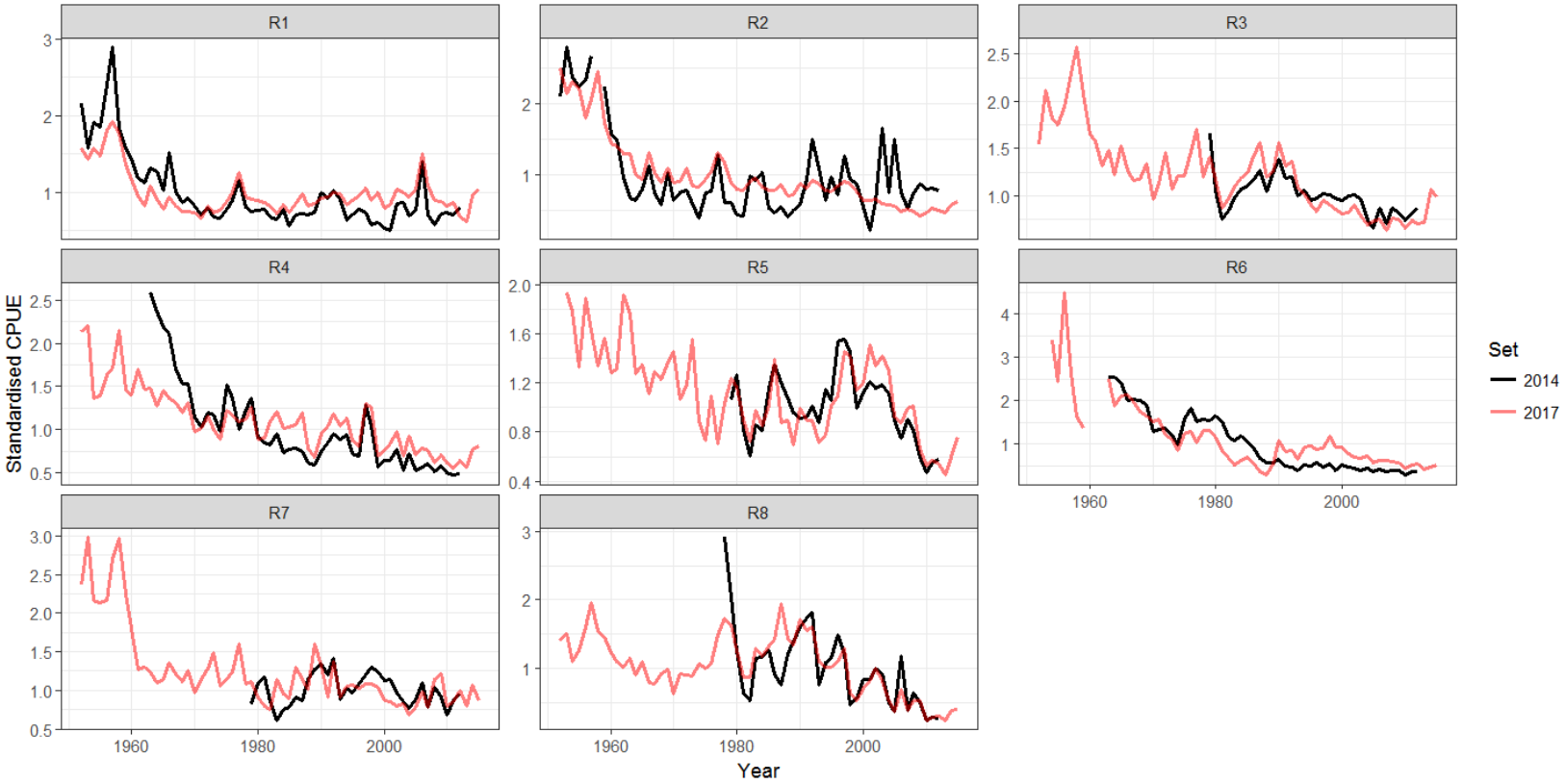

Figure 10: Comparison of the annualised standardised CPUE indices used in the 2014 reference case model (black) and the 2017 diagnostic case model (red), for BET. Note that both sets of indices are normalised to a mean of one over the period they share in common, not over the entire period, which makes them more comparable in cases where one index covers a different time period than the other.

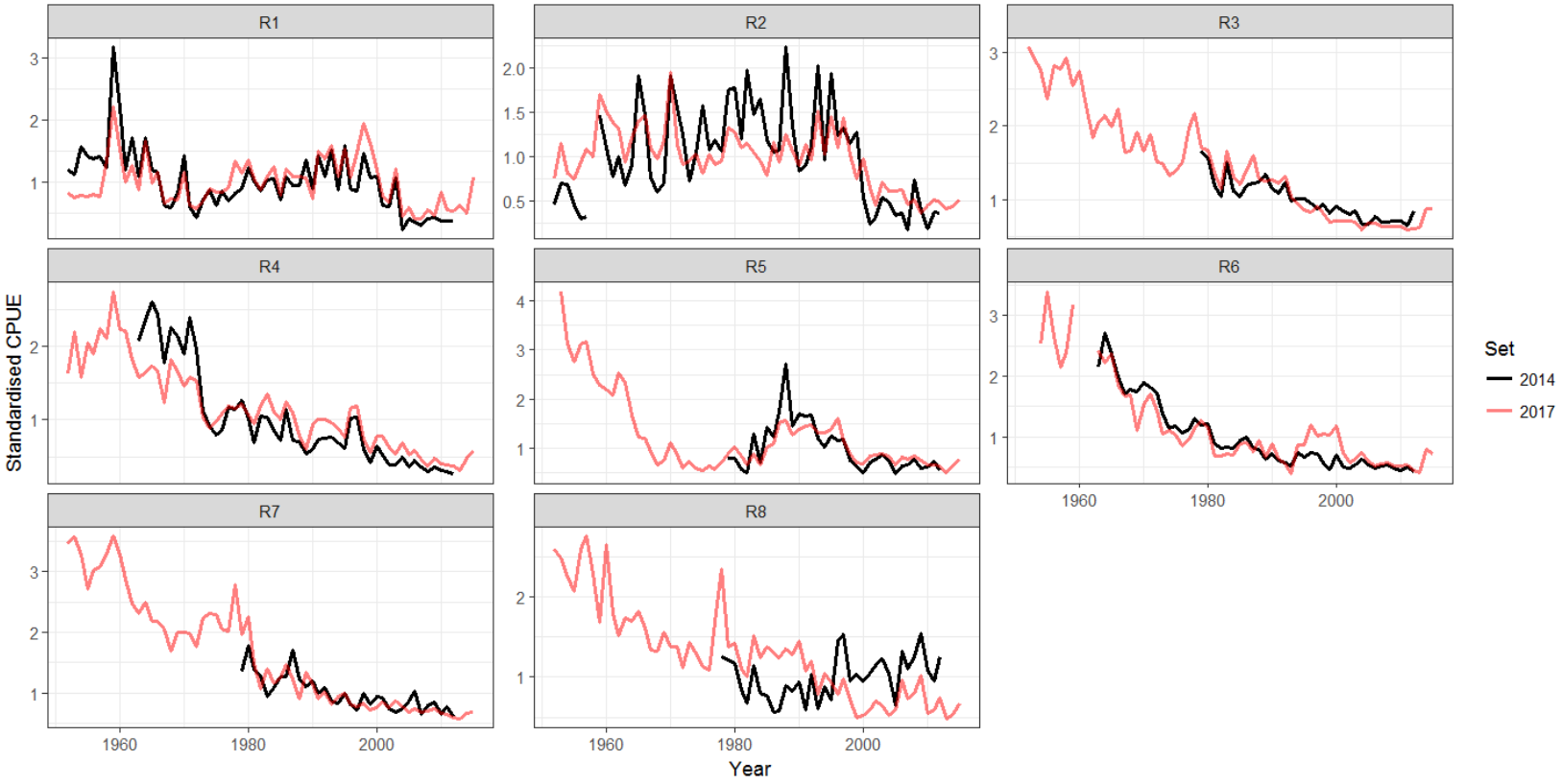

Figure 11: Comparison of the annualised standardised CPUE indices used in the 2014 reference case model (black) and the 2017 diagnostic case model (red), for YFT. Note that both sets of indices are normalised to a mean of one over the period they share in common, not over the entire period, which makes them more comparable in cases where one index covers a different time period than the other.

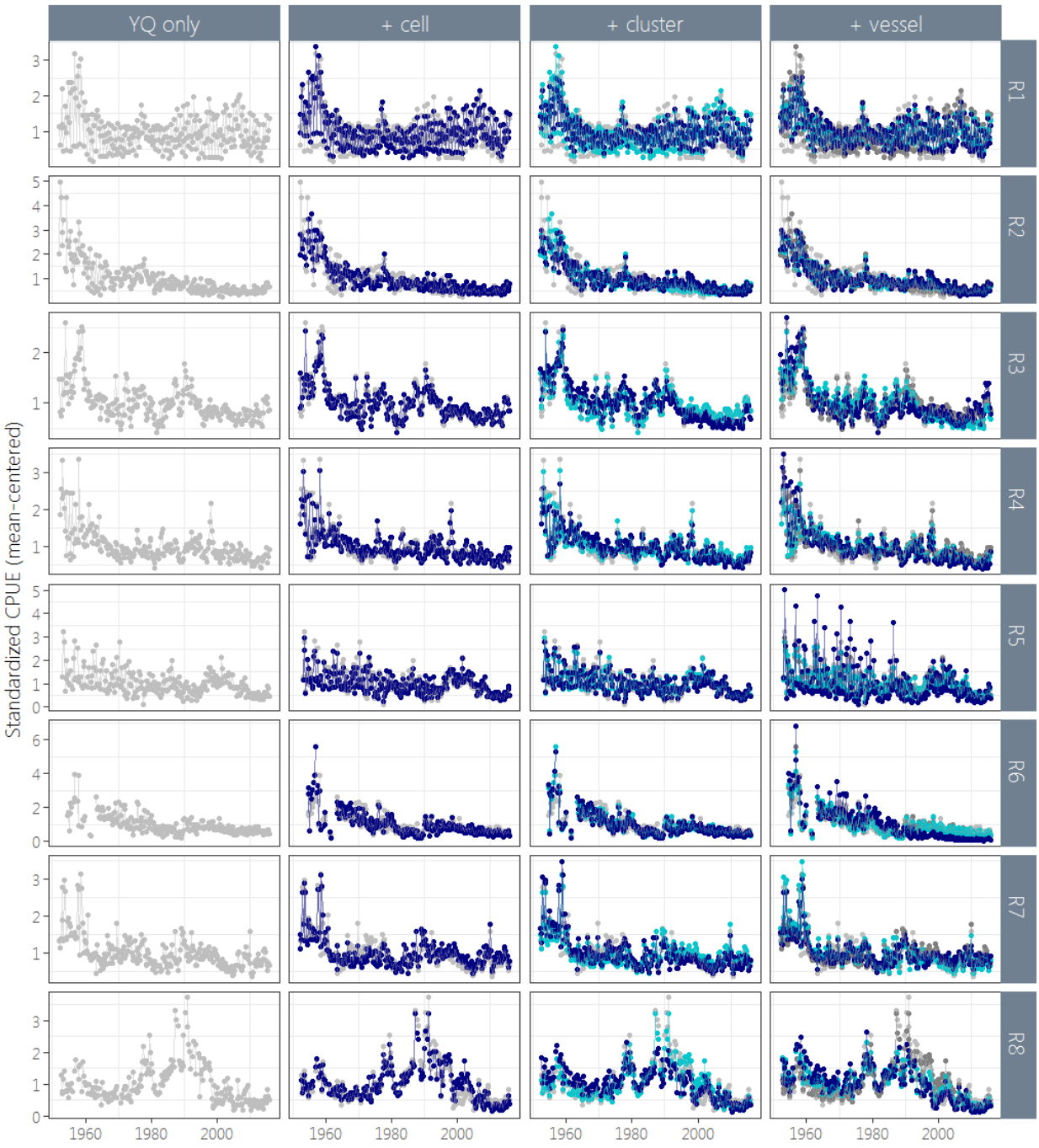

Figure 12: Step plots showing the effects of removing individual factors from the GLM model with respect to the estimated CPUE indices produced by standardisations for the diagnostic case model of BET. The left hand panel shows the model fitted with just a year-quarter factor, the panel second from the left shows the model with the cell factor added (dark blue line; grey line is the year-quarter-only model), the next panel shows the model with the cluster factor added (dark blue line; light blue line is the cell + year-quarter model, etc.) and finally the right panel shows a model with the vessel factor added (dark blue line; the light blue line is the previous model - cluster + cell + year-quarter, etc.).

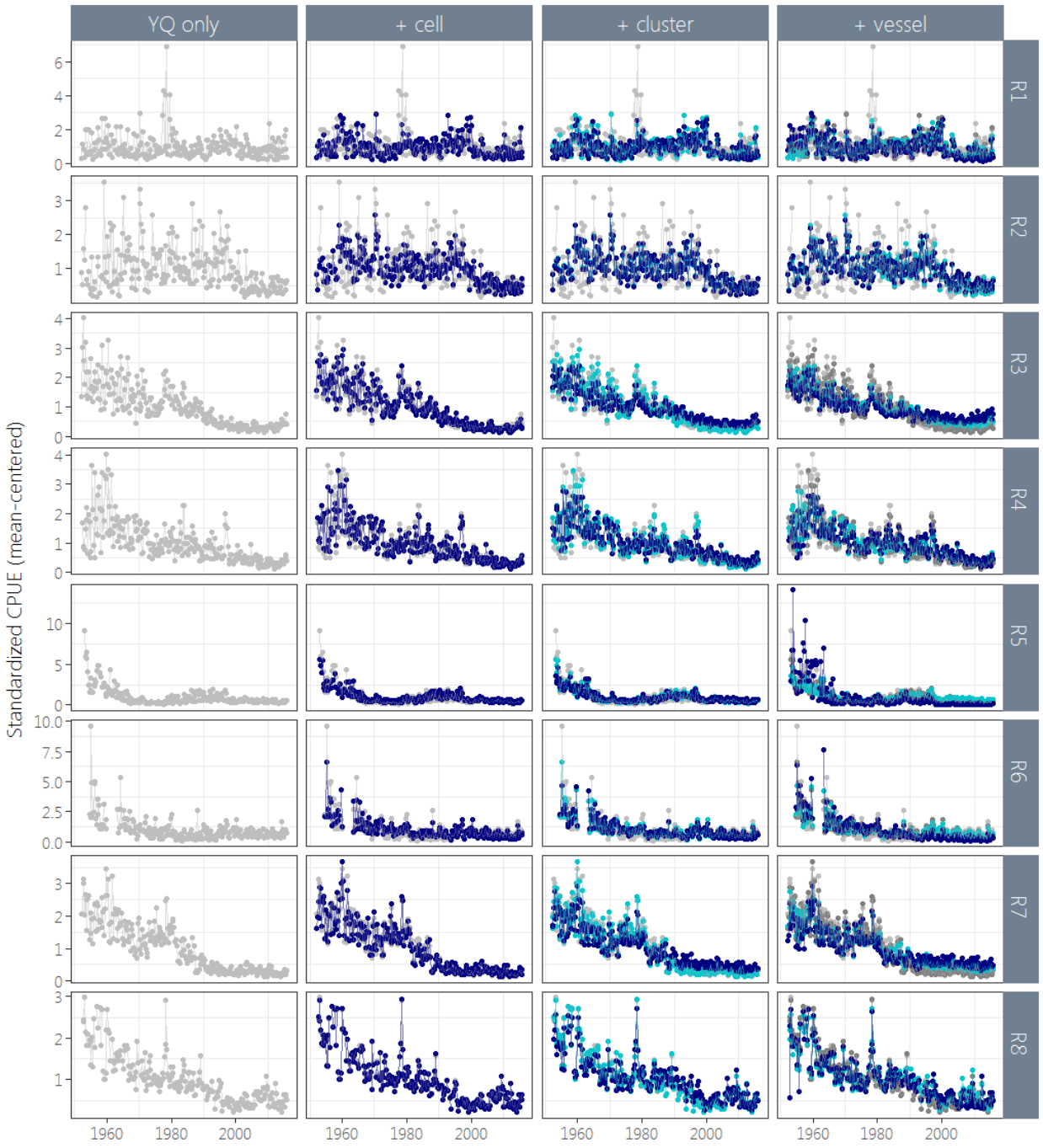

Figure 13: Step plots showing the effects of removing individual factors from the GLM model with respect to the estimated CPUE indices produced by standardisations for the diagnostic case model of YFT. The left hand panel shows the model fitted with just a year-quarter factor, the panel second from the left shows the model with the cell factor added (dark blue line; grey line is the year-quarter-only model), the next panel shows the model with the cluster factor added (dark blue line; light blue line is the cell + year-quarter model, etc.) and finally the right panel shows a model with the vessel factor added (dark blue line; the light blue line is the previous model - cluster + cell + year-quarter, etc.).

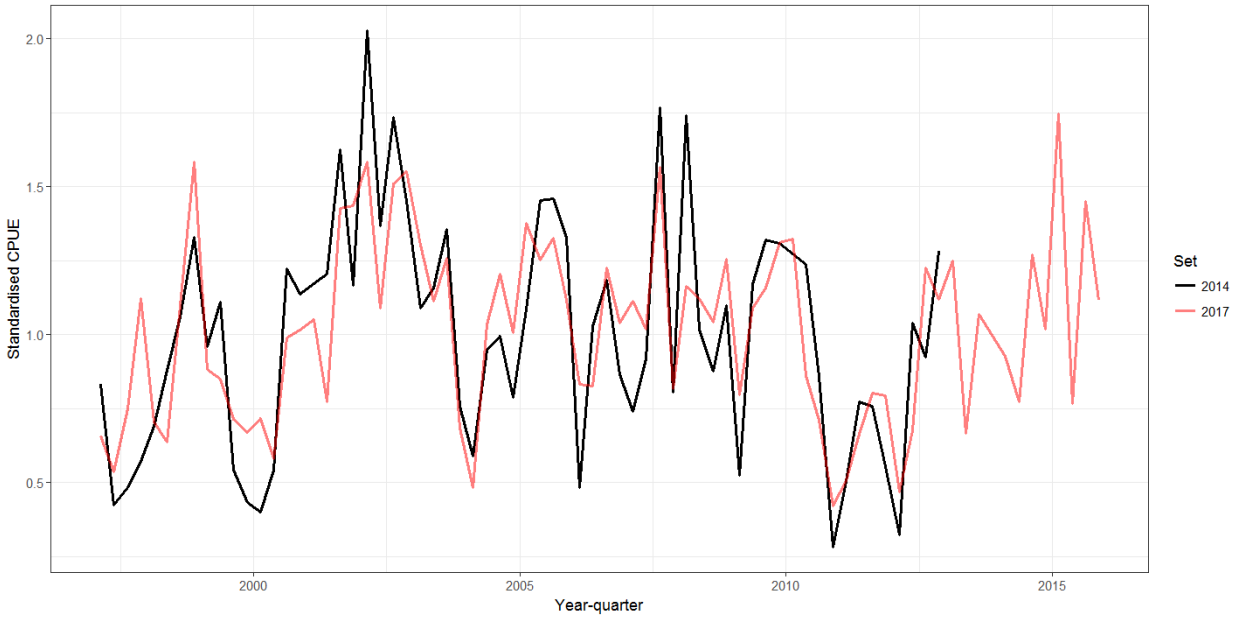

Figure 14: Comparison of the standardised CPUE indices used in the 2014 reference case model (black) and the 2017 diagnostic case model (red), for YFT for the purse seine fishery in region 8. Note that both sets of indices are normalised to a mean of one over the period they share in common, not over the entire period, which makes them more comparable as they cover a different time periods.

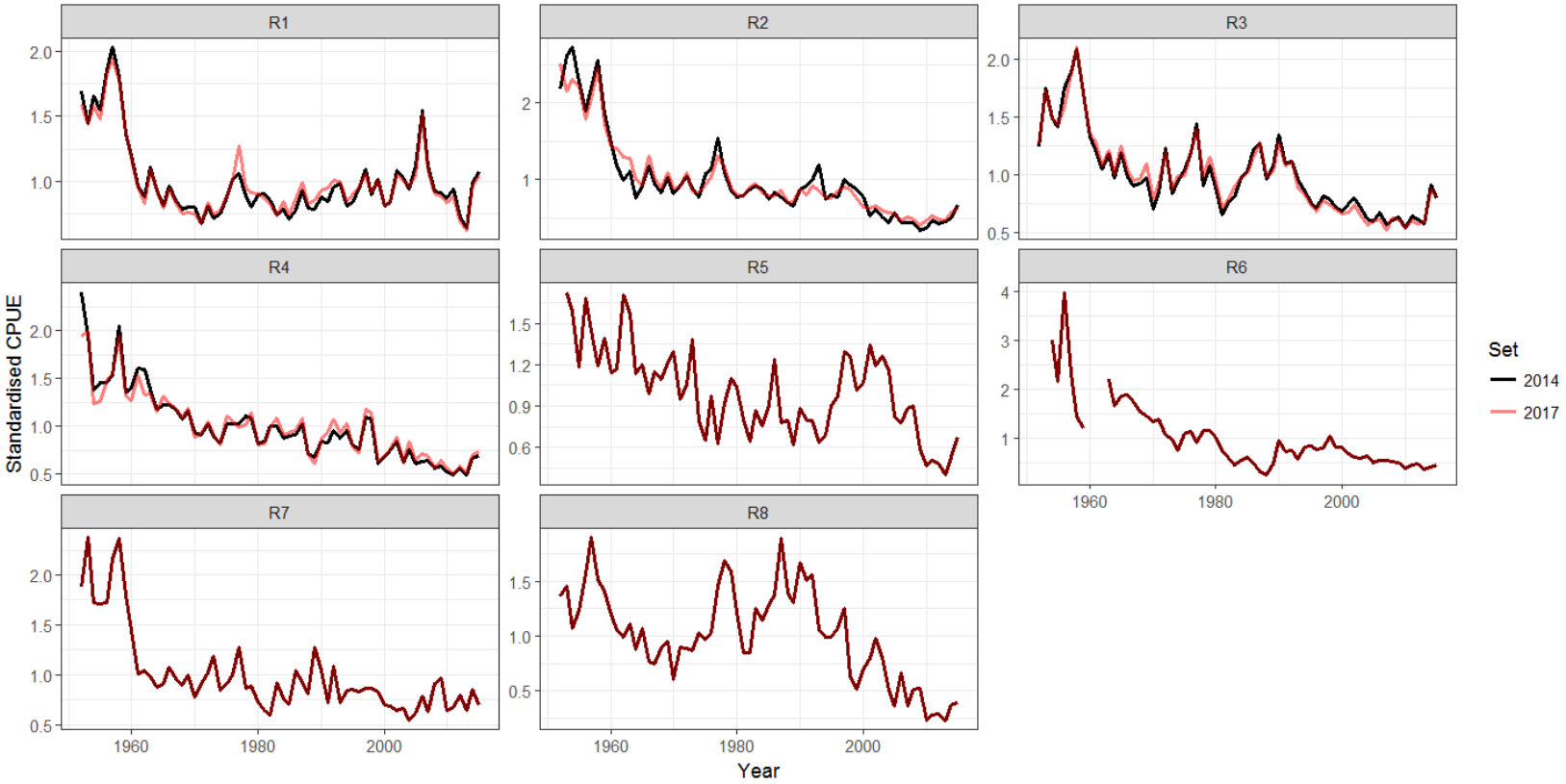

Figure 15: Comparison of the annualised standardised CPUE indices used in the 2017 sensitivity model with 2014 regions (model *2014Reg* in McKechnie et al., 2017; black) and the 2017 diagnostic case model which uses the 2017 regions (red), for BET.

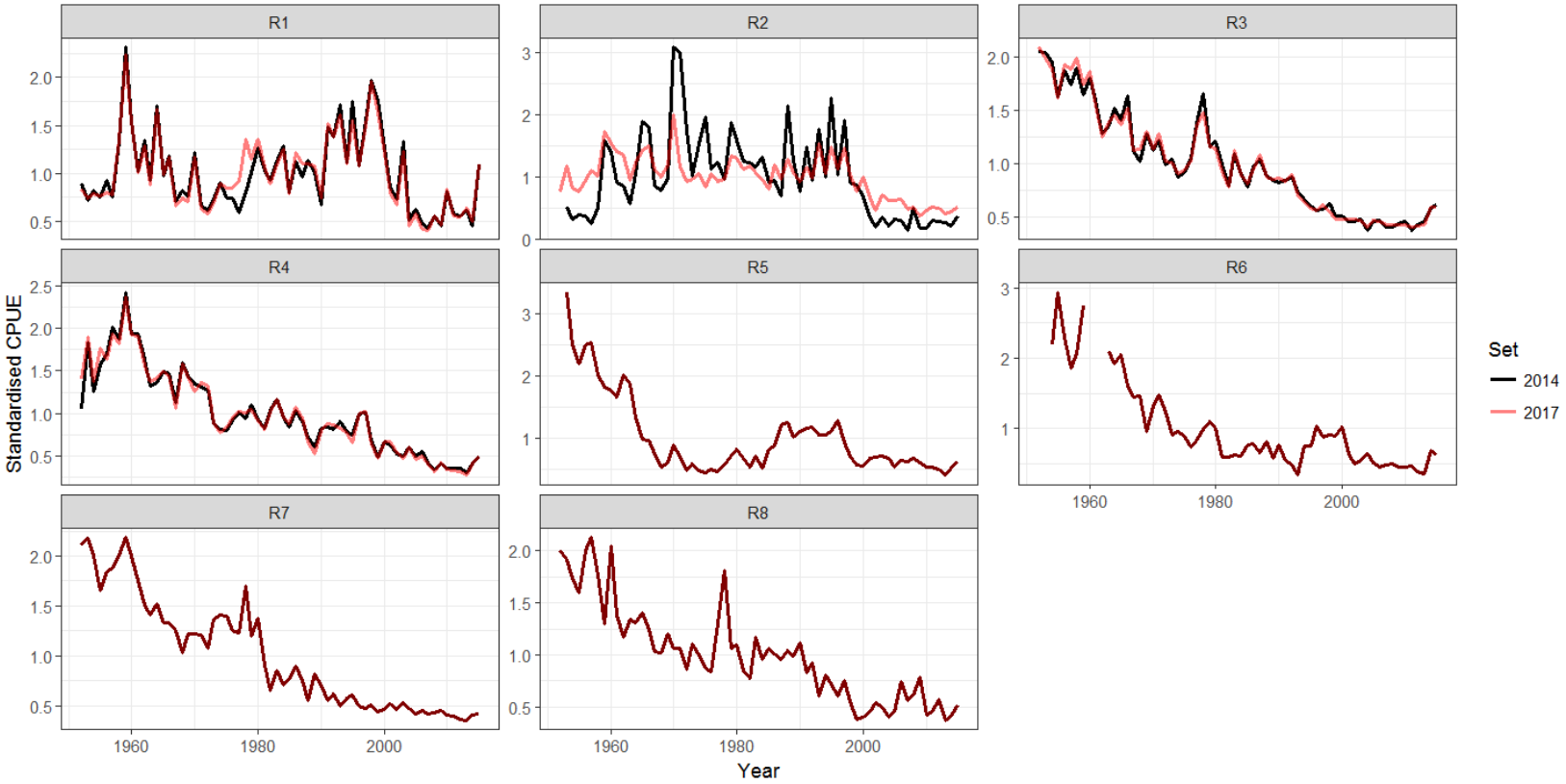

Figure 16: Comparison of the annualised standardised CPUE indices used in the 2017 sensitivity model with 2014 regions (model *2014Reg* in McKechnie et al., 2017; black) and the 2017 diagnostic case model which uses the 2017 regions (red), for YFT.

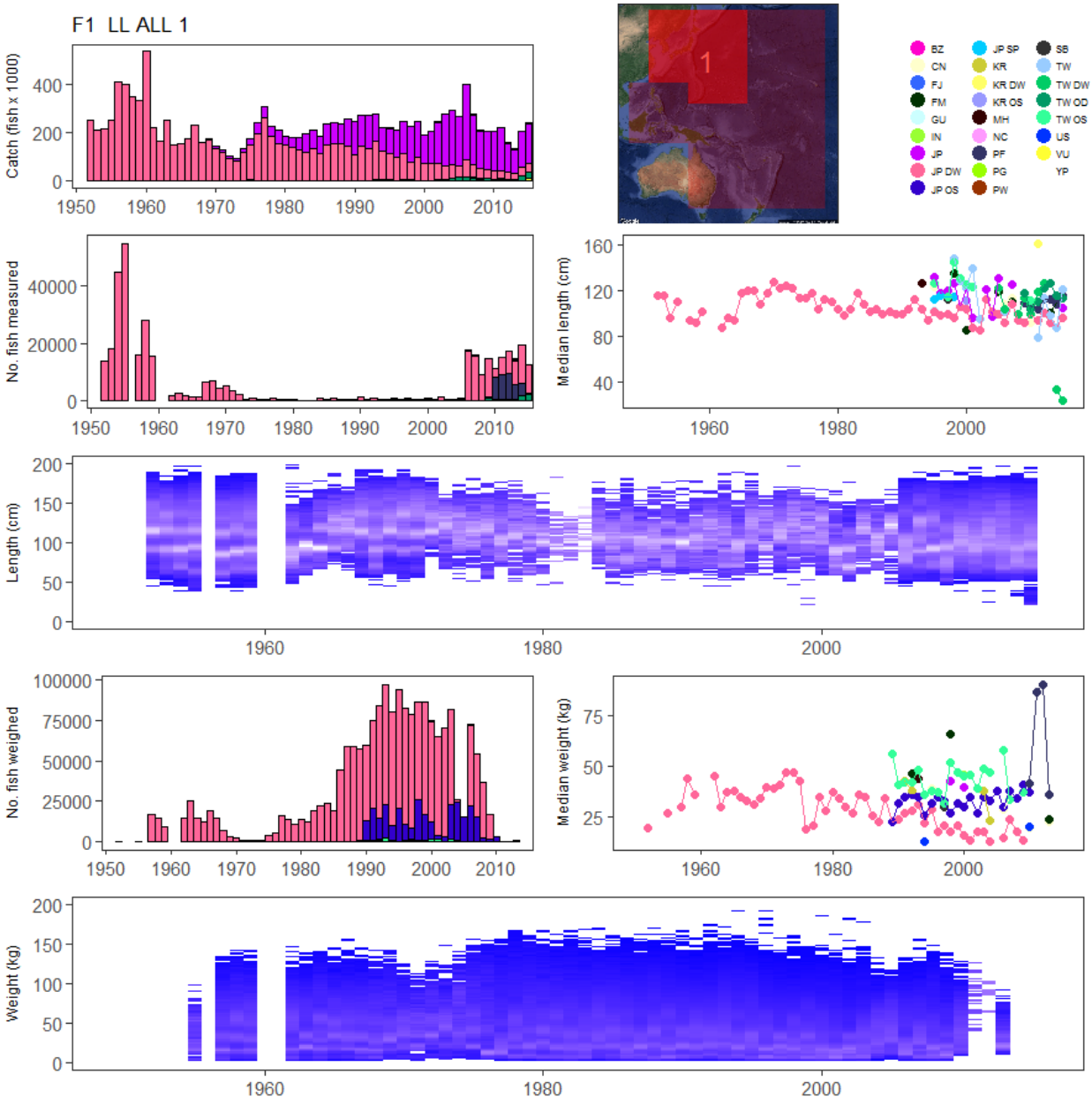

Figure 17: Summary of raw data available for fishery 1 of the 2017 BET stock assessment in the WCPO. The panels display; annual catch (top left), region of occurrence (top right), the annual number of fish with measured length (top middle left), median length of available length composition data (top middle right), a tile plot of the annual length distribution of fish (middle), the annual number of fish with measured weight (bottom middle left), median weight of available weight composition data (bottom middle right), and a tile plot of the annual weight distribution of fish (bottom).

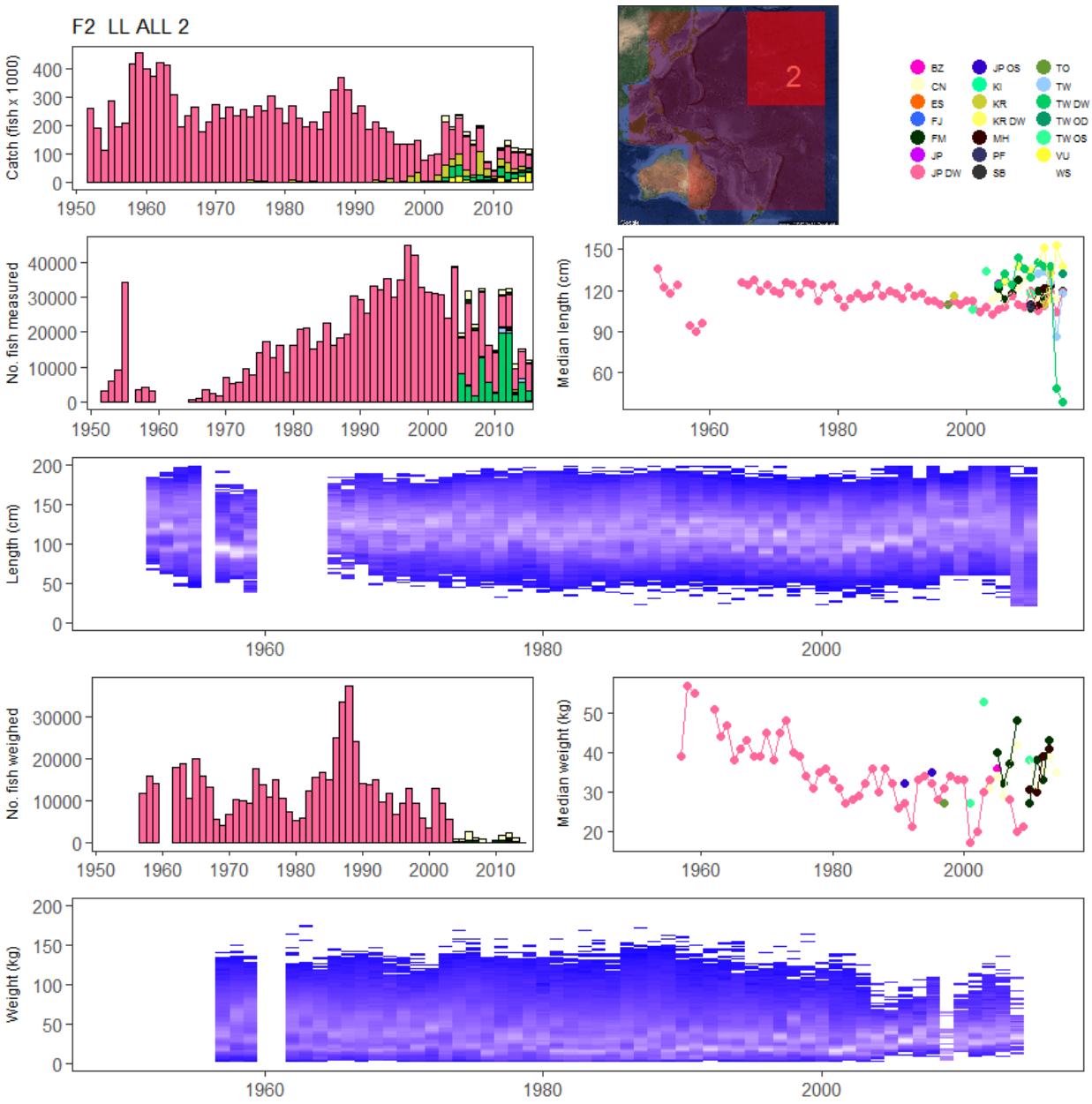

Figure 18: Summary of raw data available for BET fishery 2.

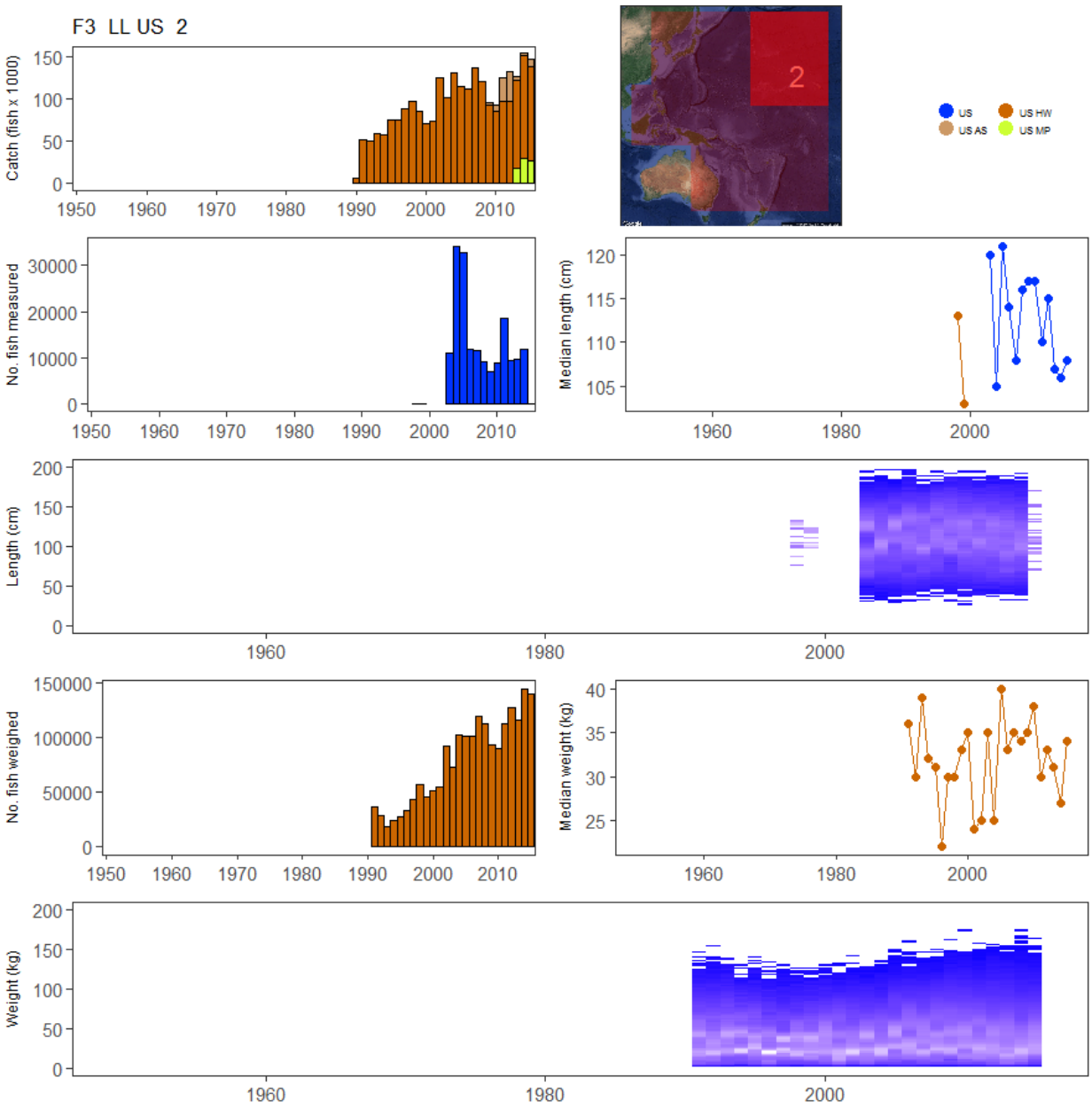

Figure 19: Summary of raw data available for BET fishery 3.

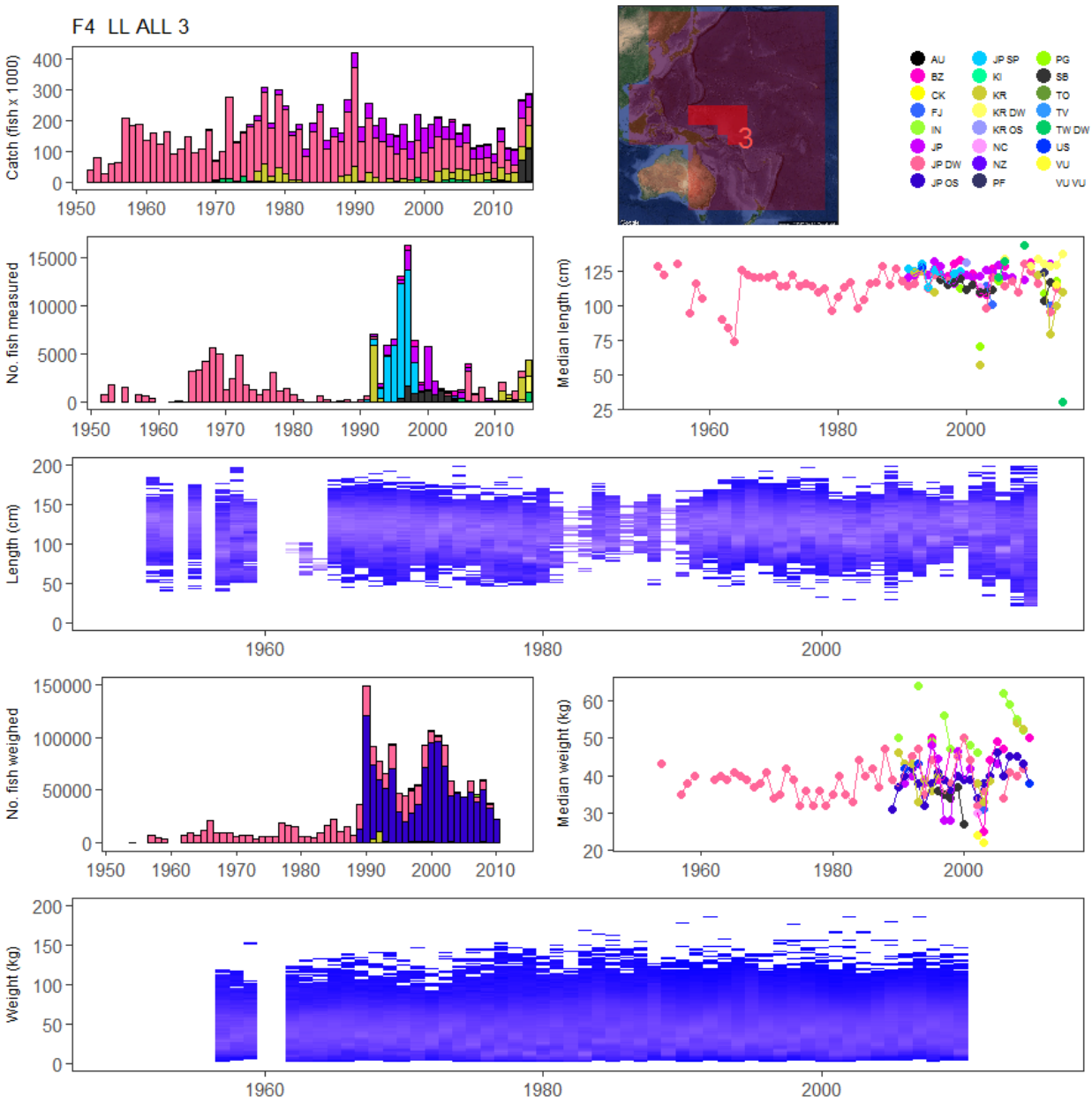

Figure 20: Summary of raw data available for BET fishery 4.

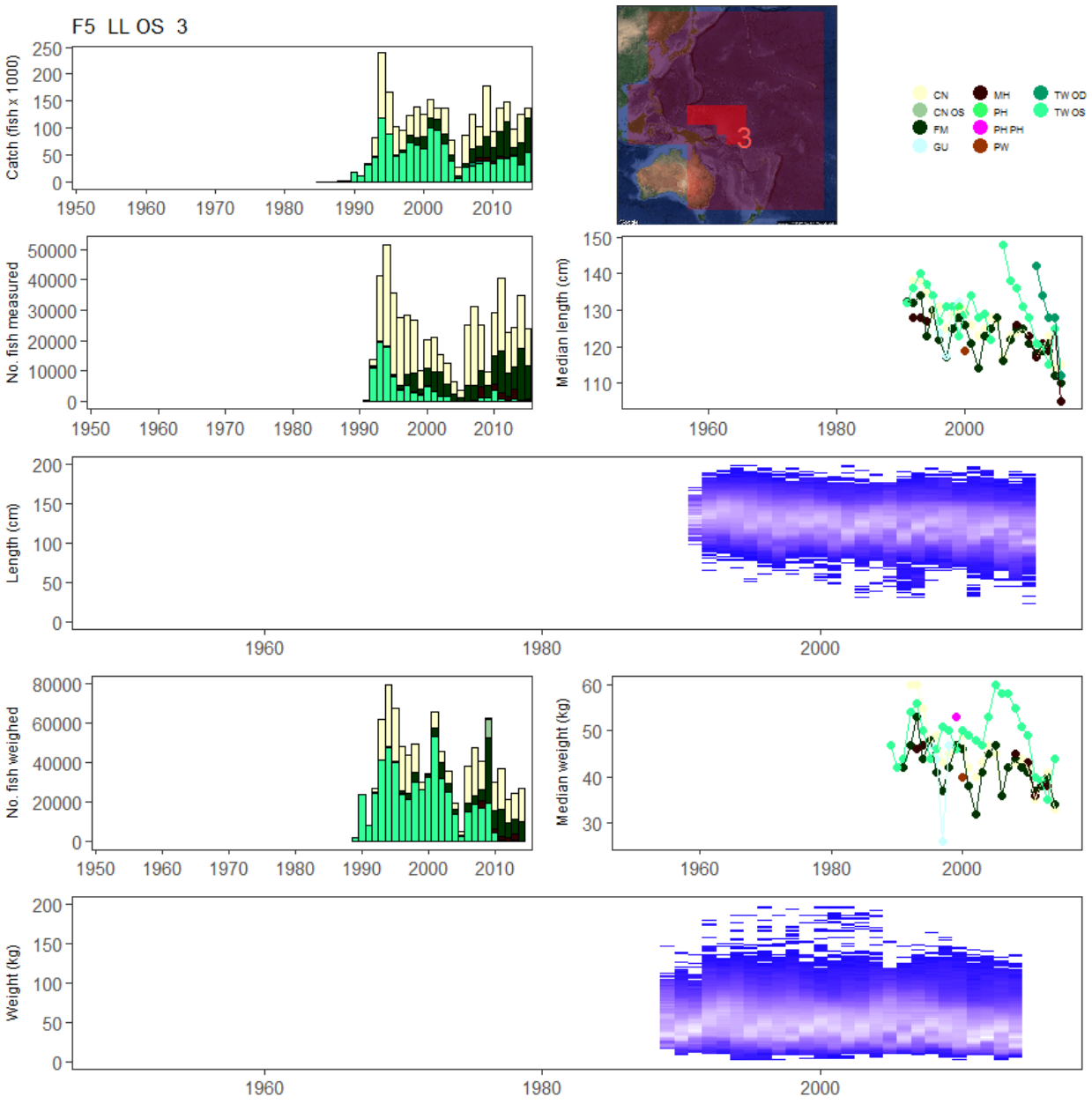

Figure 21: Summary of raw data available for BET fishery 5.

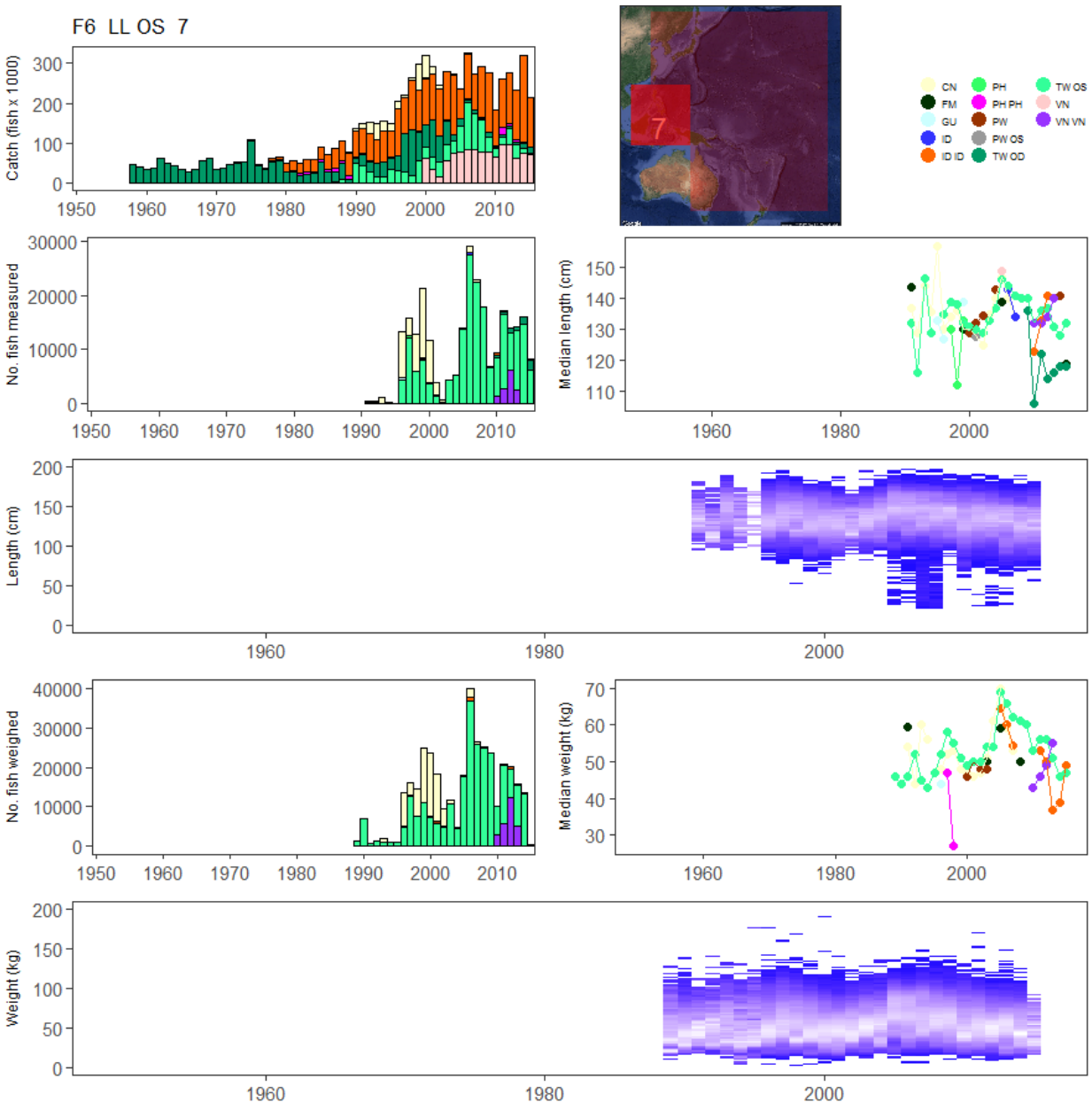

Figure 22: Summary of raw data available for BET fishery 6.

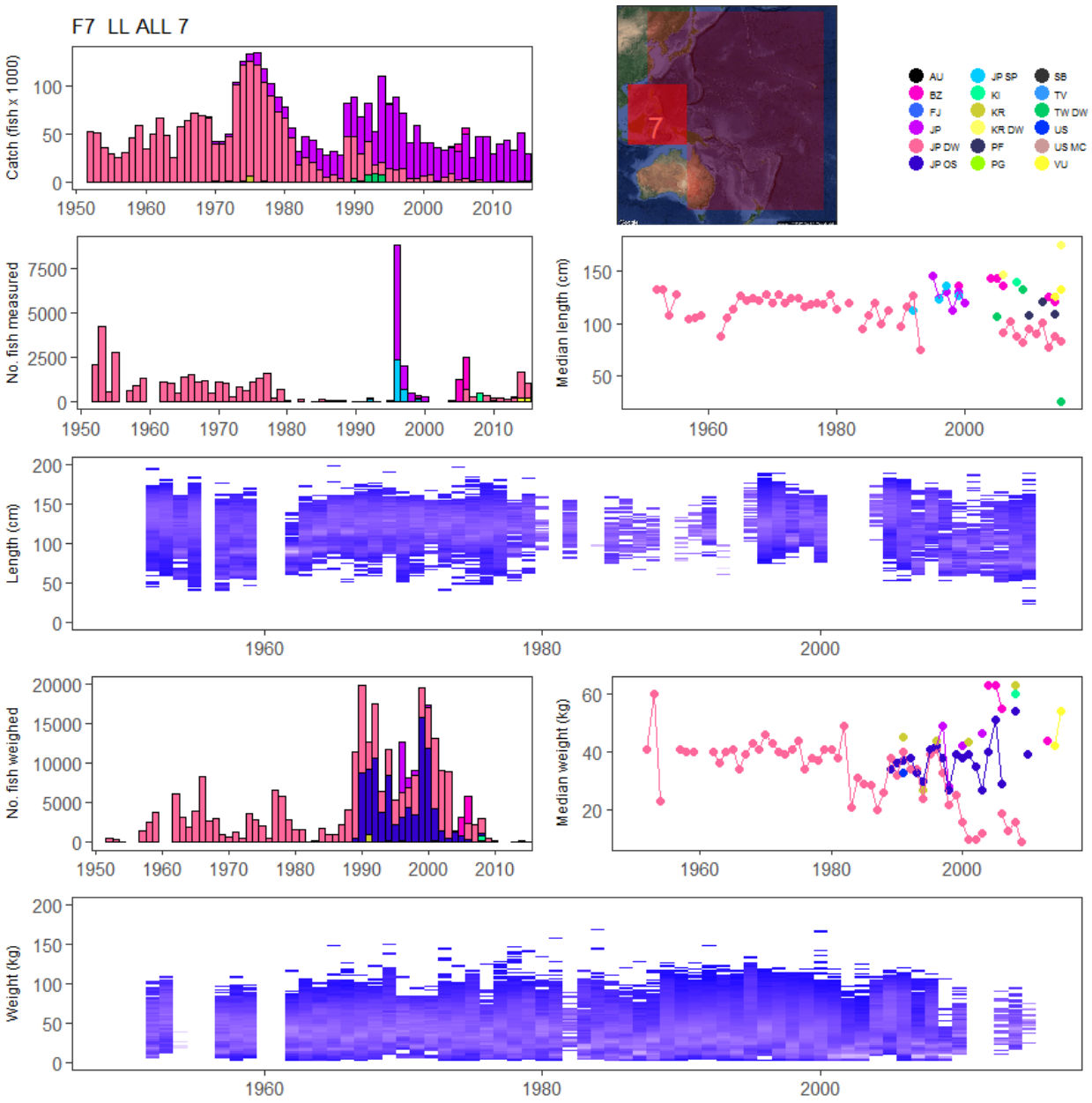

Figure 23: Summary of raw data available for BET fishery 7.

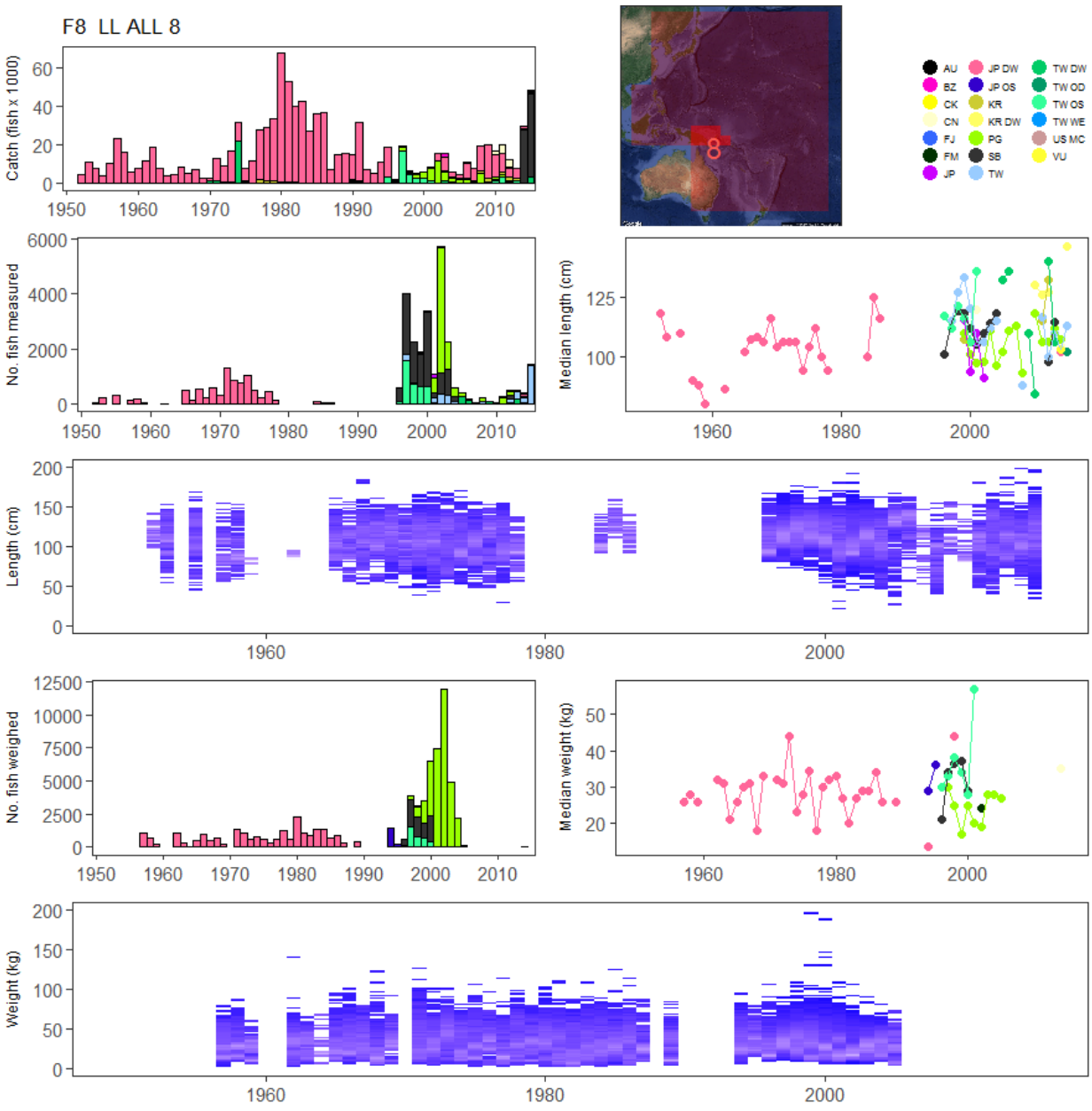

Figure 24: Summary of raw data available for BET fishery 8.

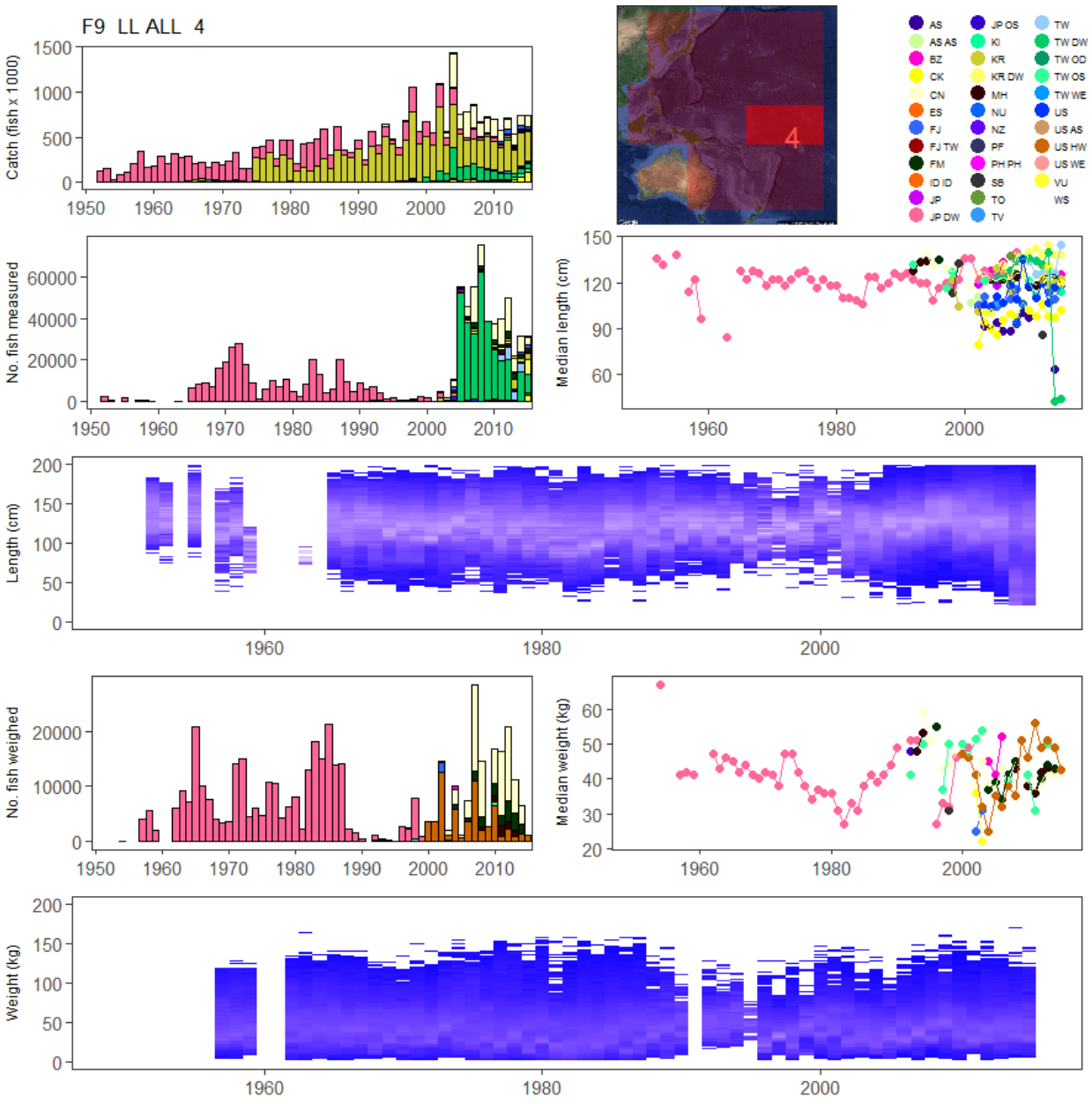

Figure 25: Summary of raw data available for BET fishery 9.

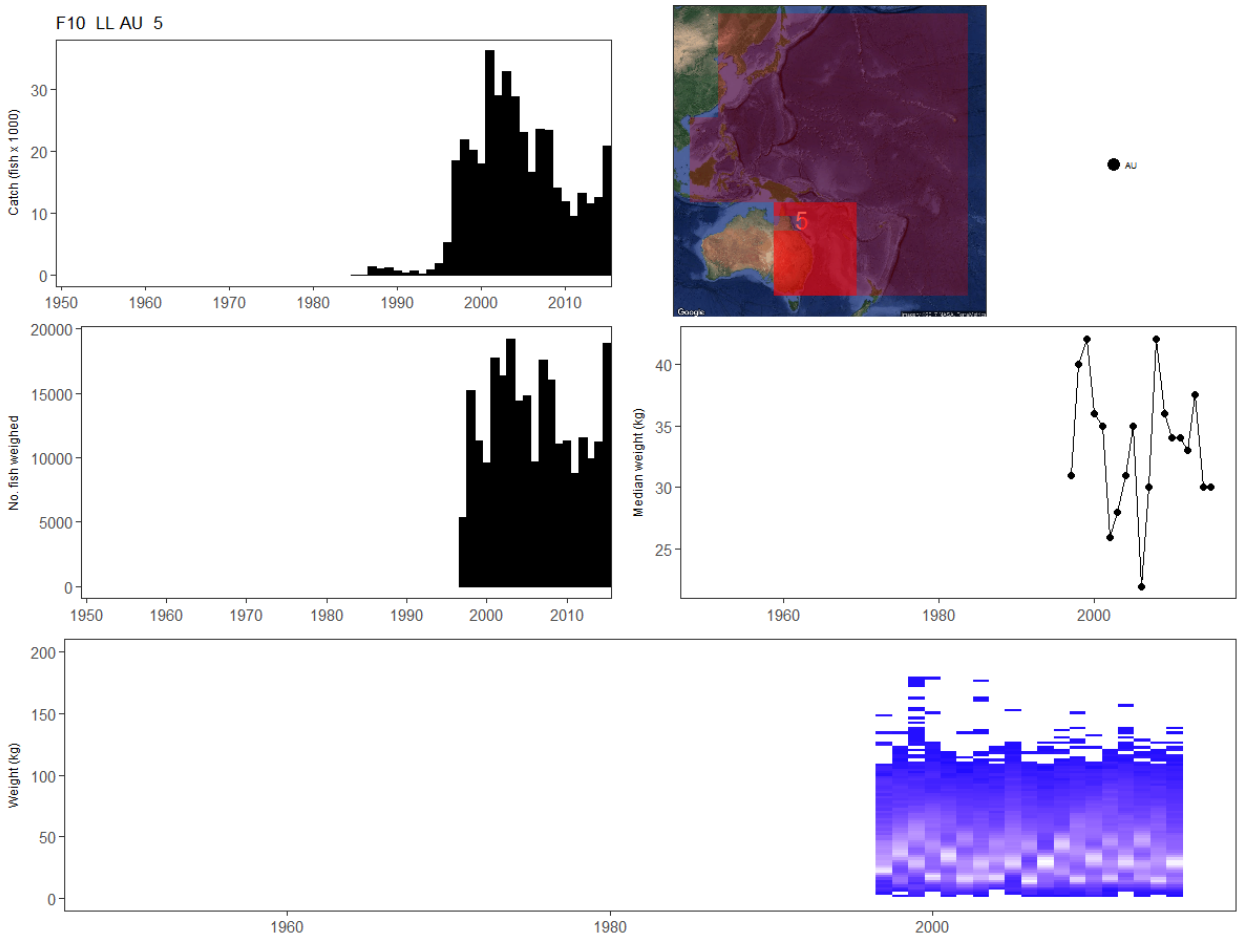

Figure 26: Summary of raw data available for BET fishery 10.

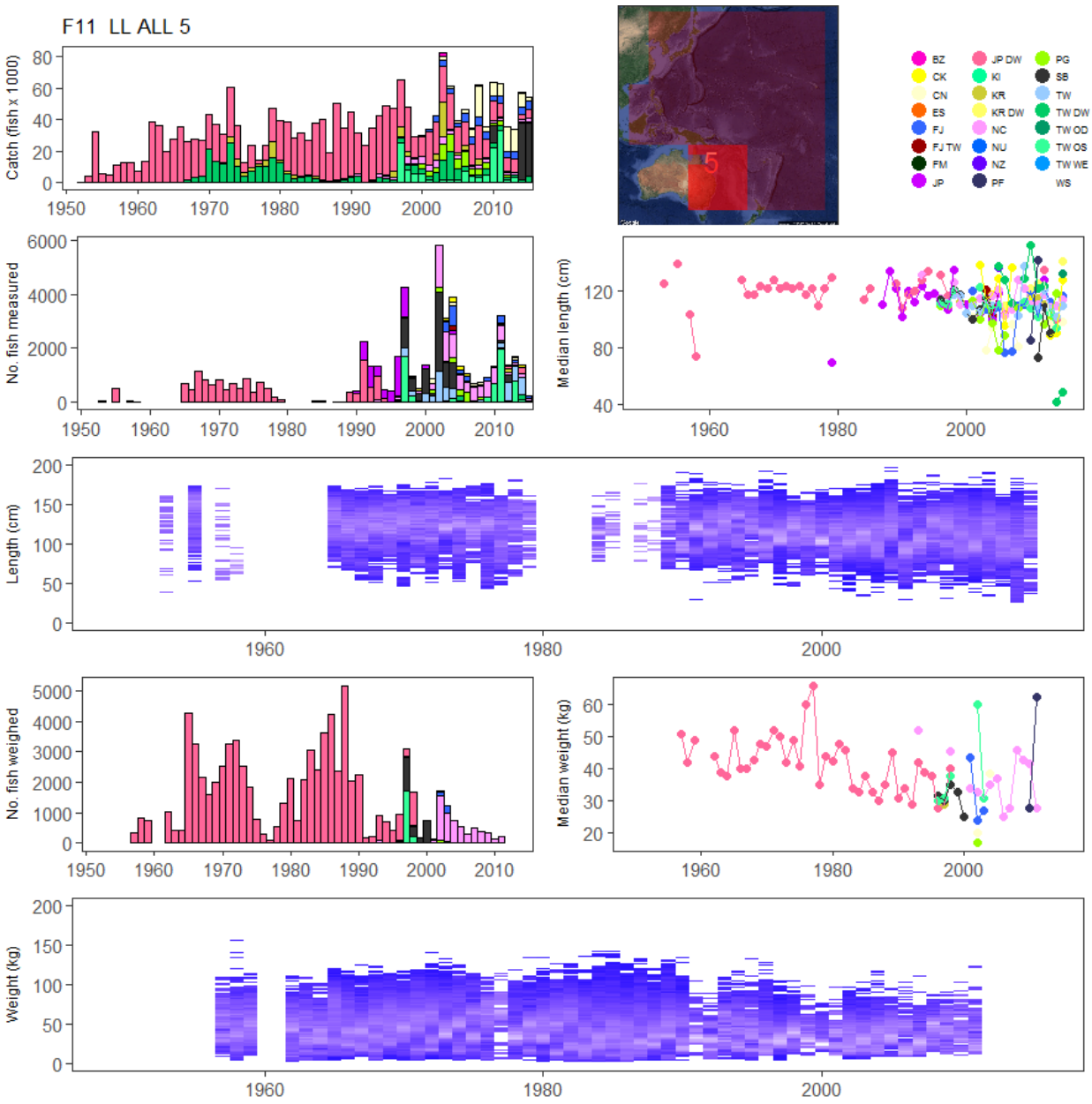

Figure 27: Summary of raw data available for BET fishery 11.

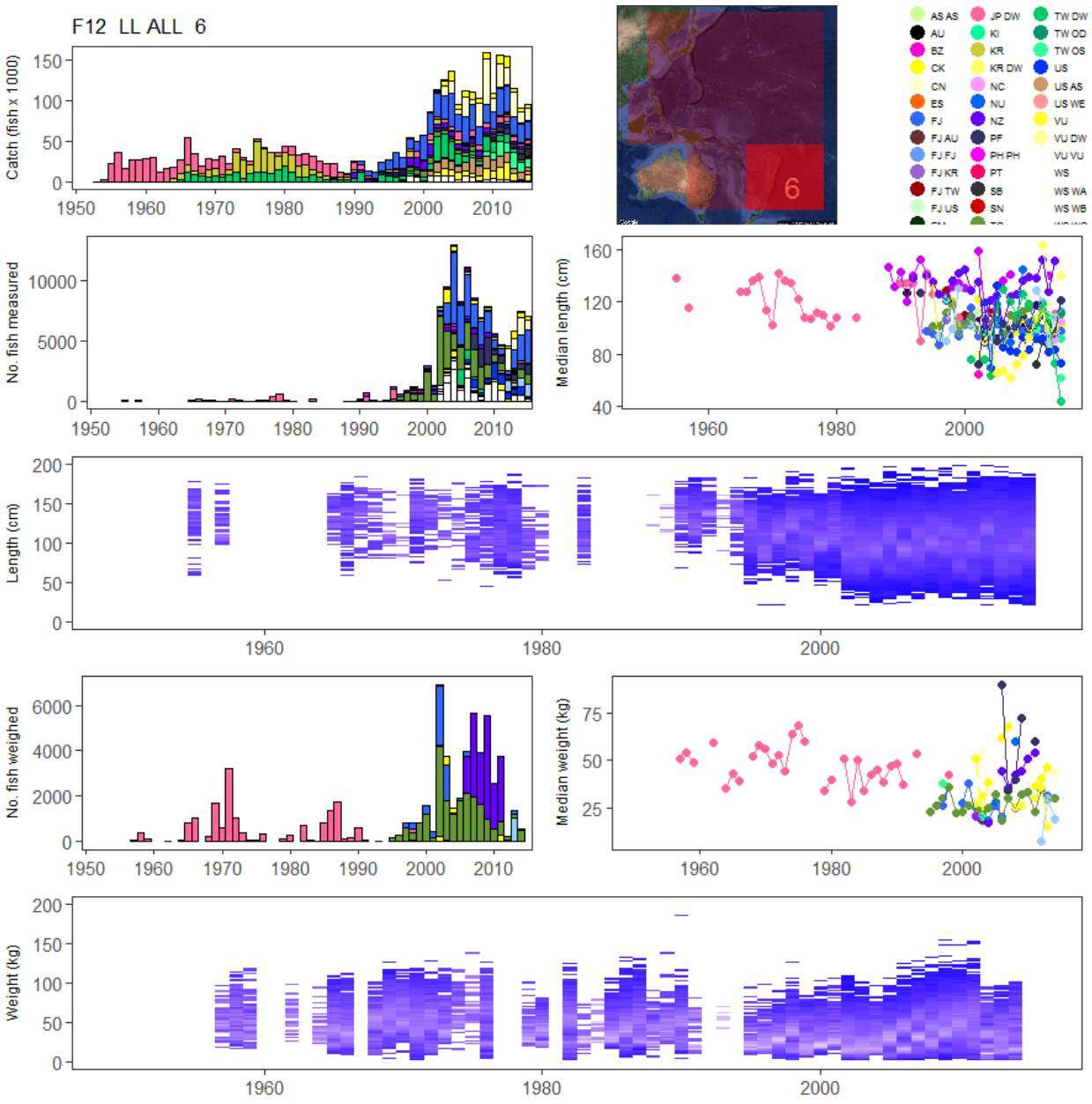

Figure 28: Summary of raw data available for BET fishery 12.

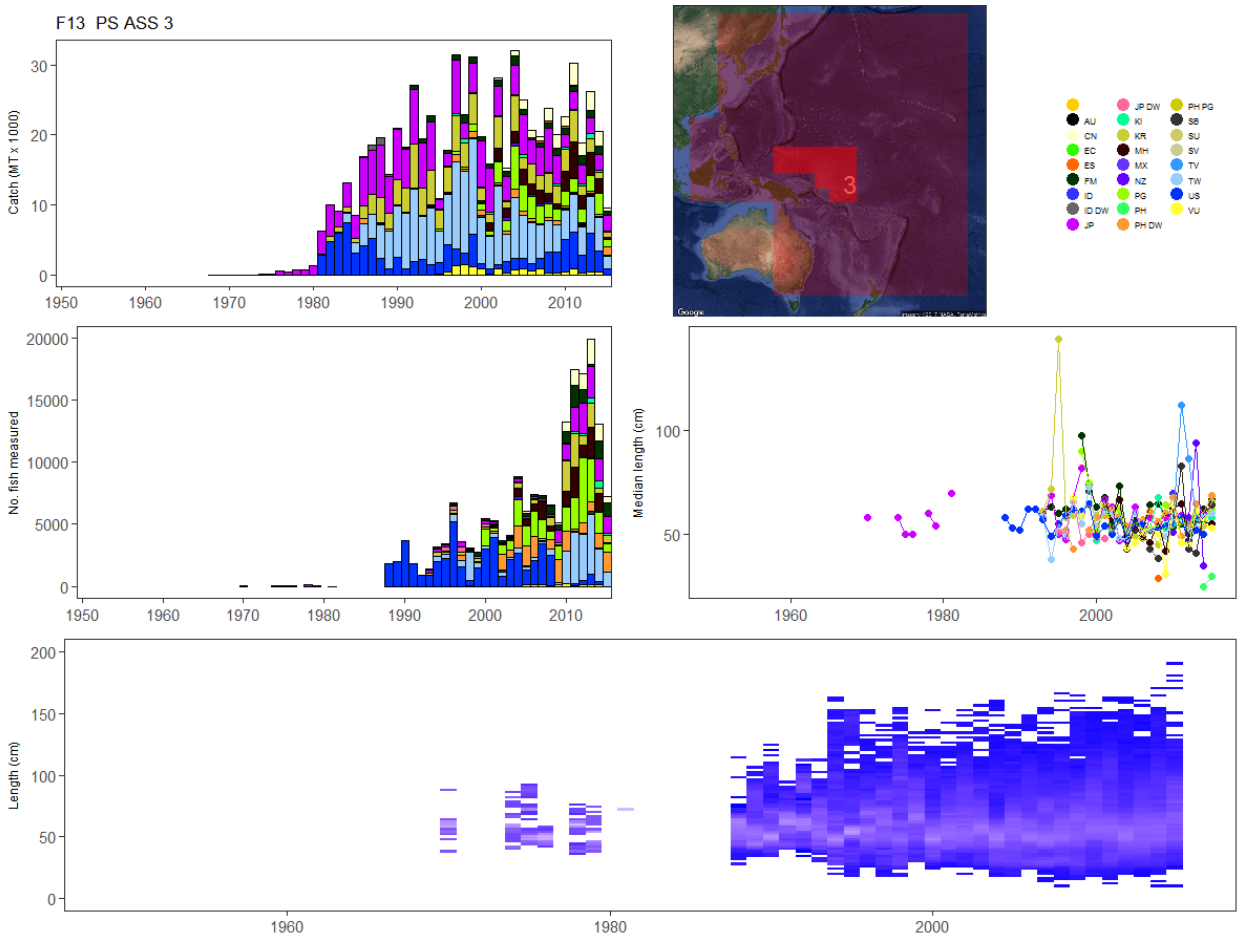

Figure 29: Summary of raw data available for BET fishery 13.

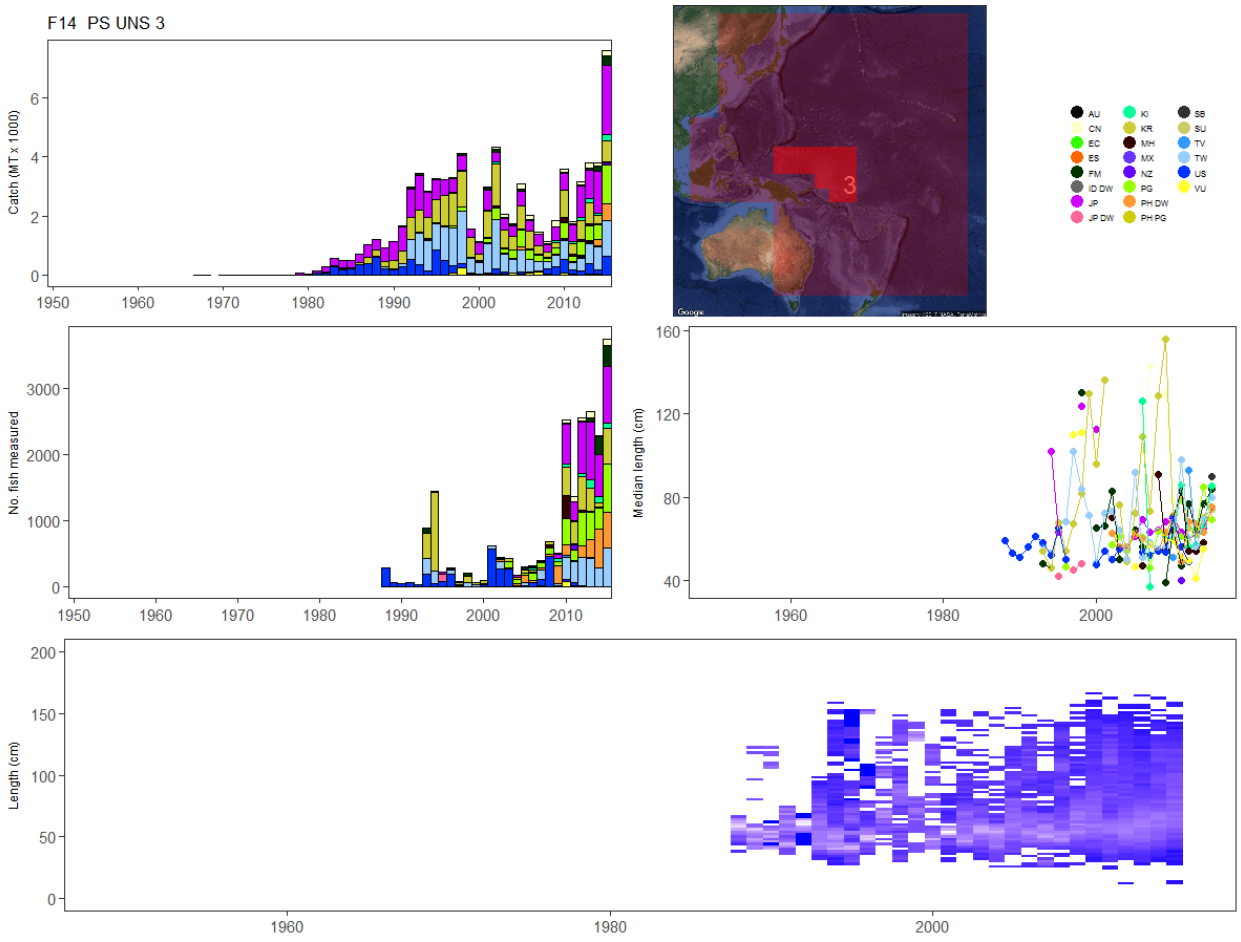

Figure 30: Summary of raw data available for BET fishery 14.

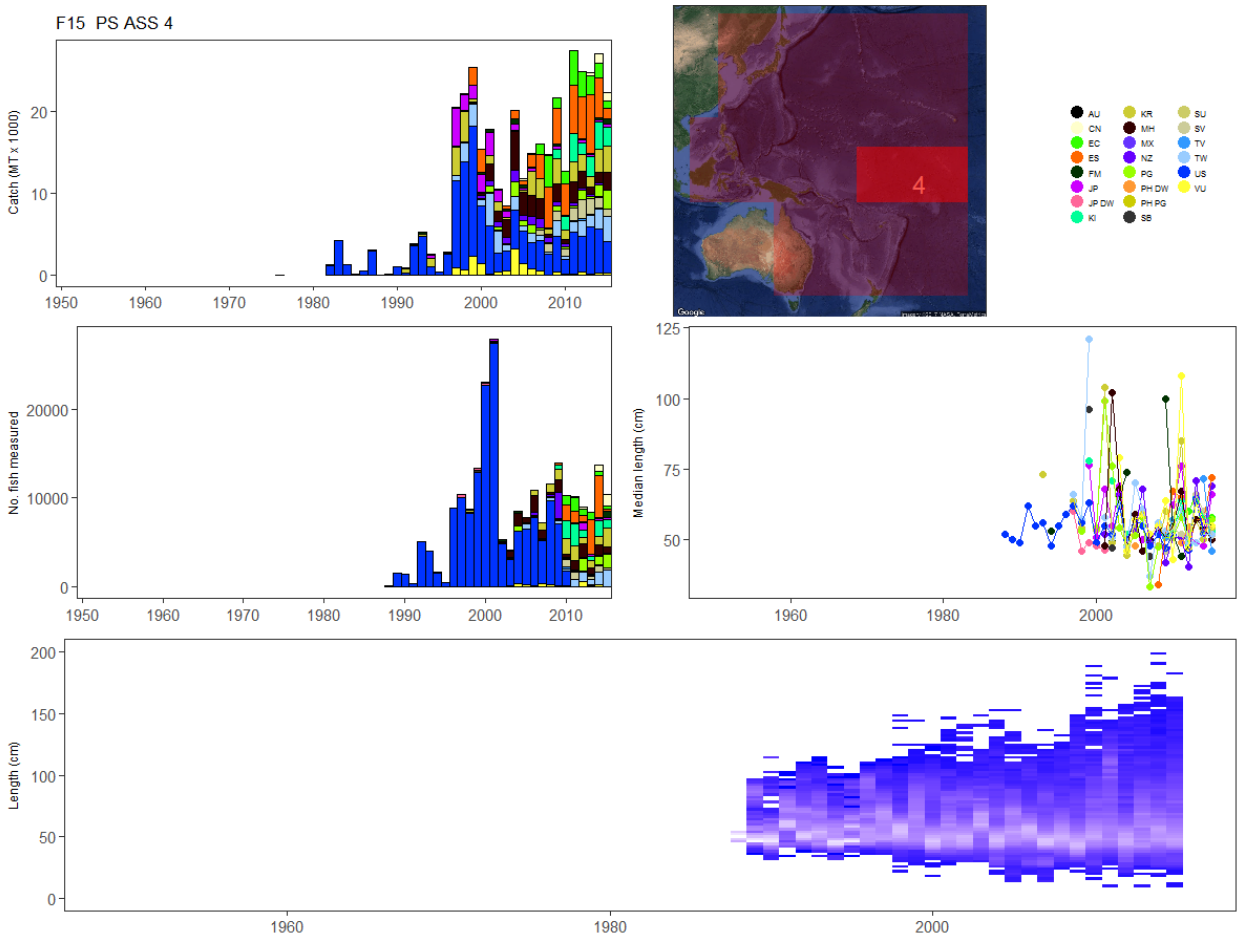

Figure 31: Summary of raw data available for BET fishery 15.

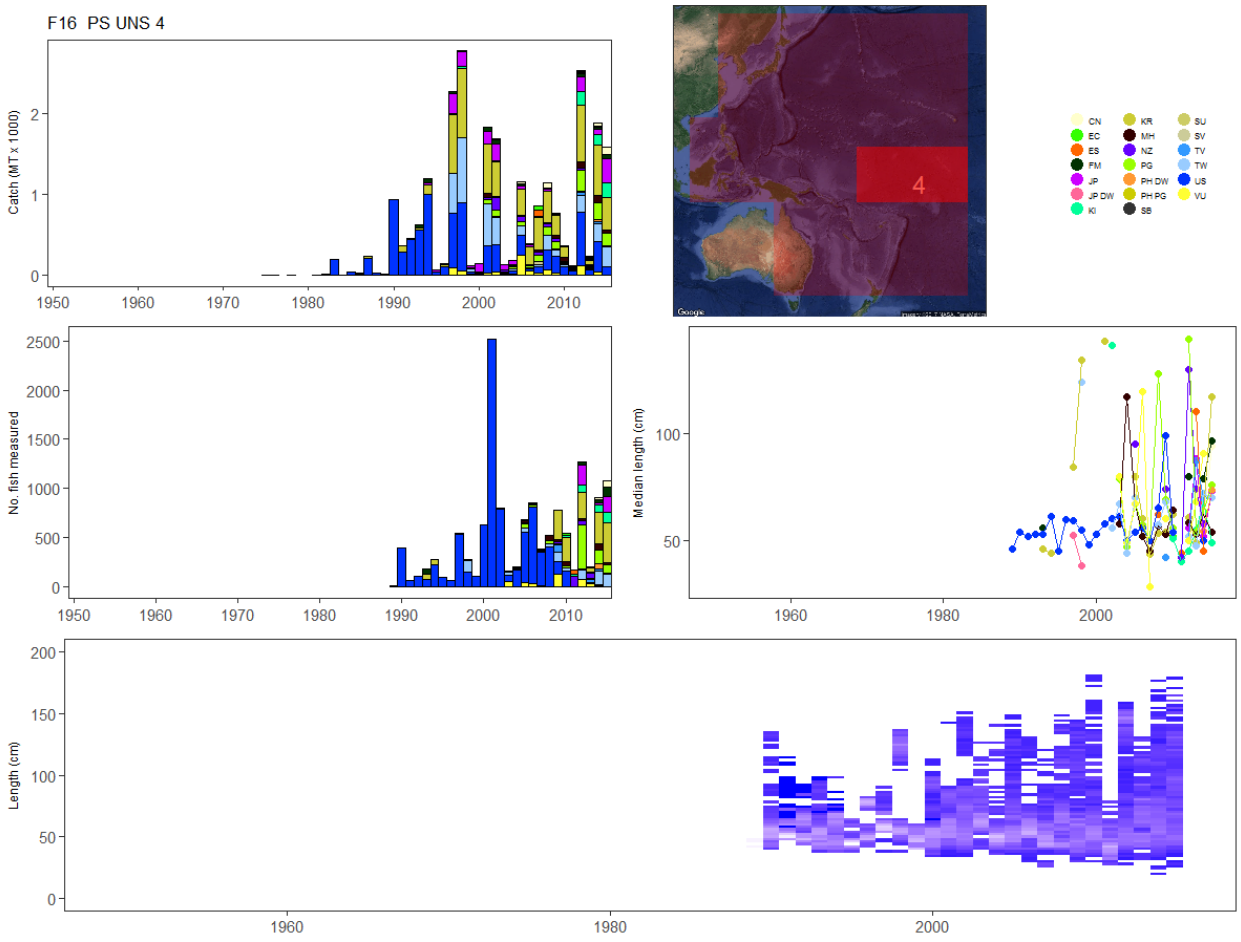

Figure 32: Summary of raw data available for BET fishery 16.

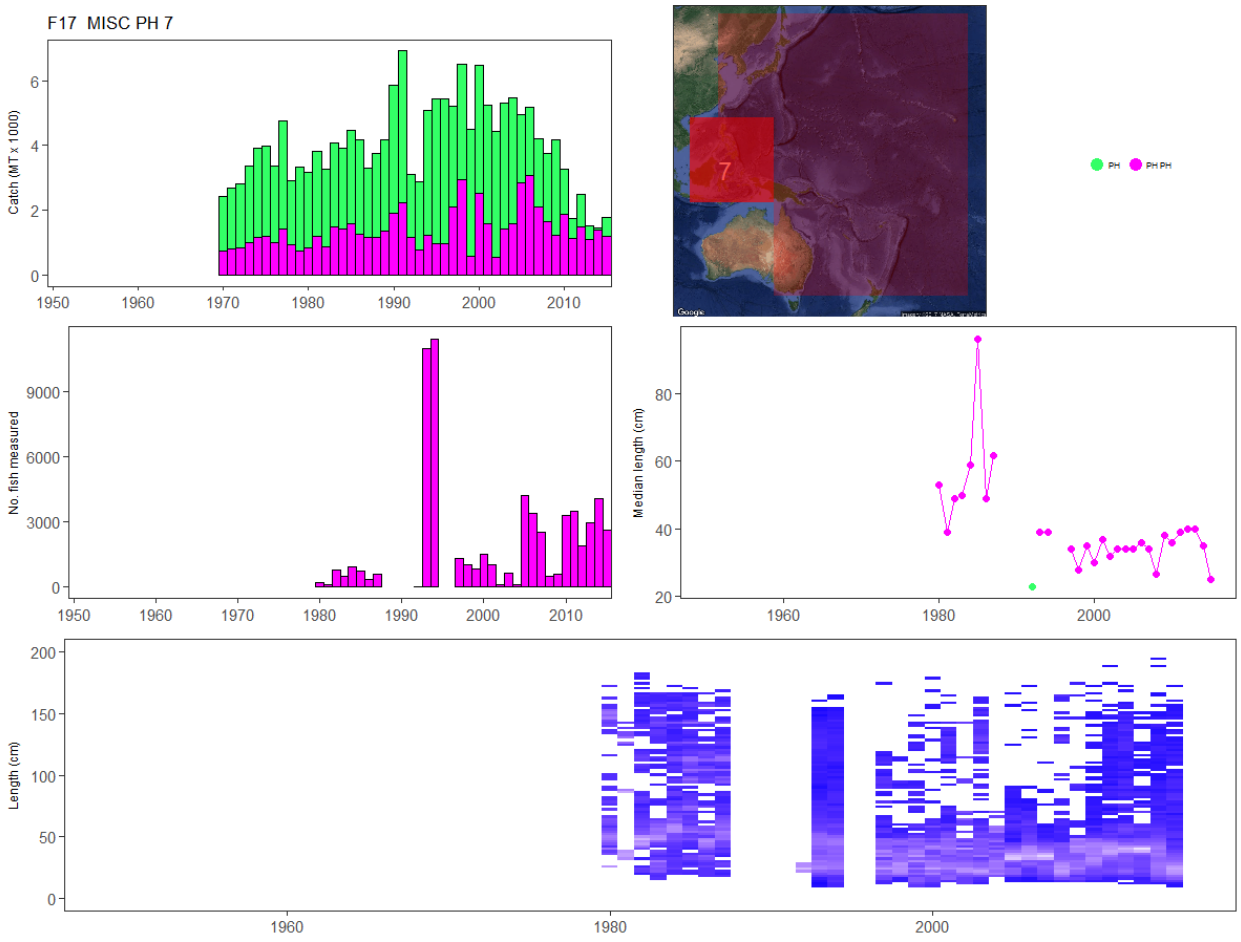

Figure 33: Summary of raw data available for BET fishery 17.

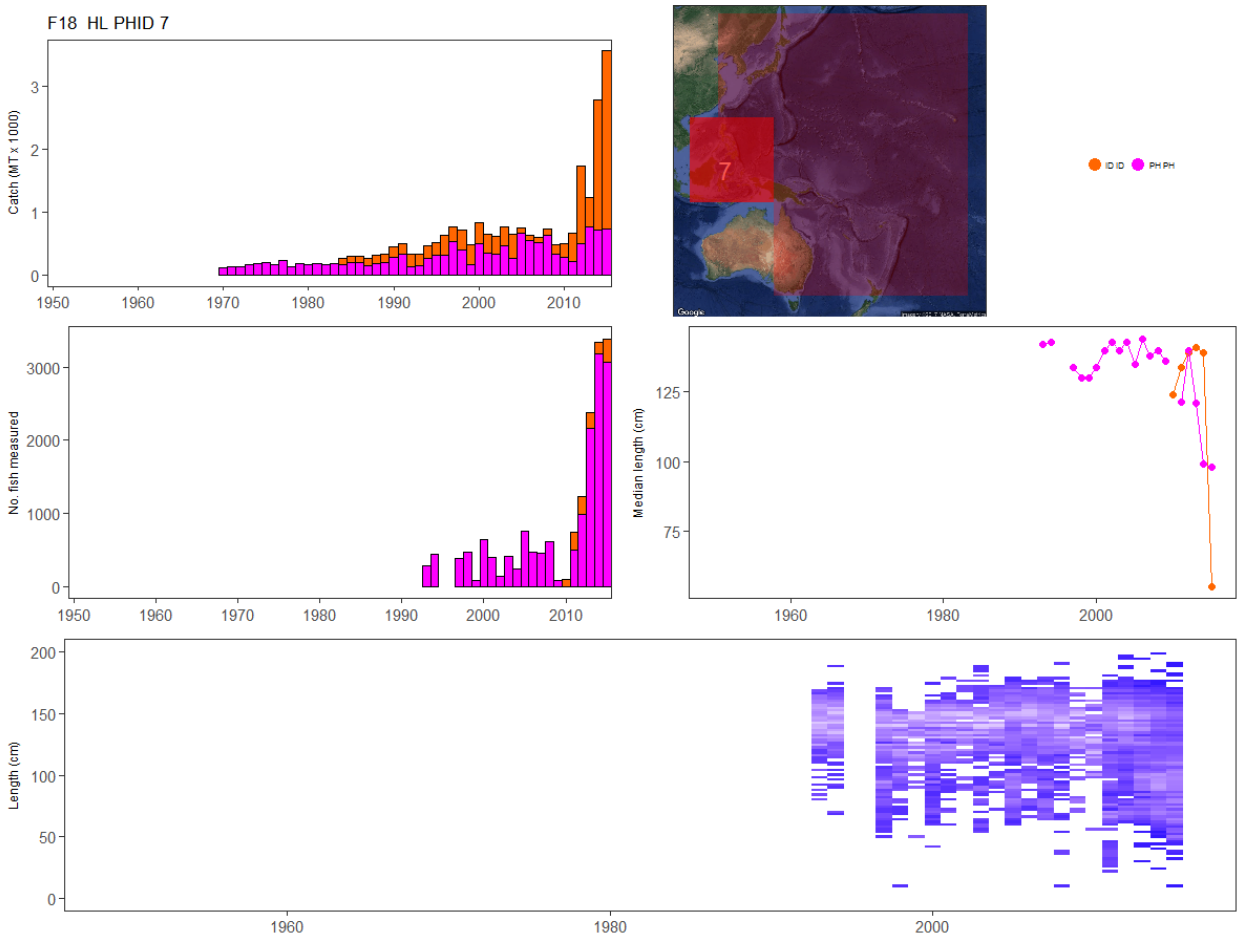

Figure 34: Summary of raw data available for BET fishery 18.

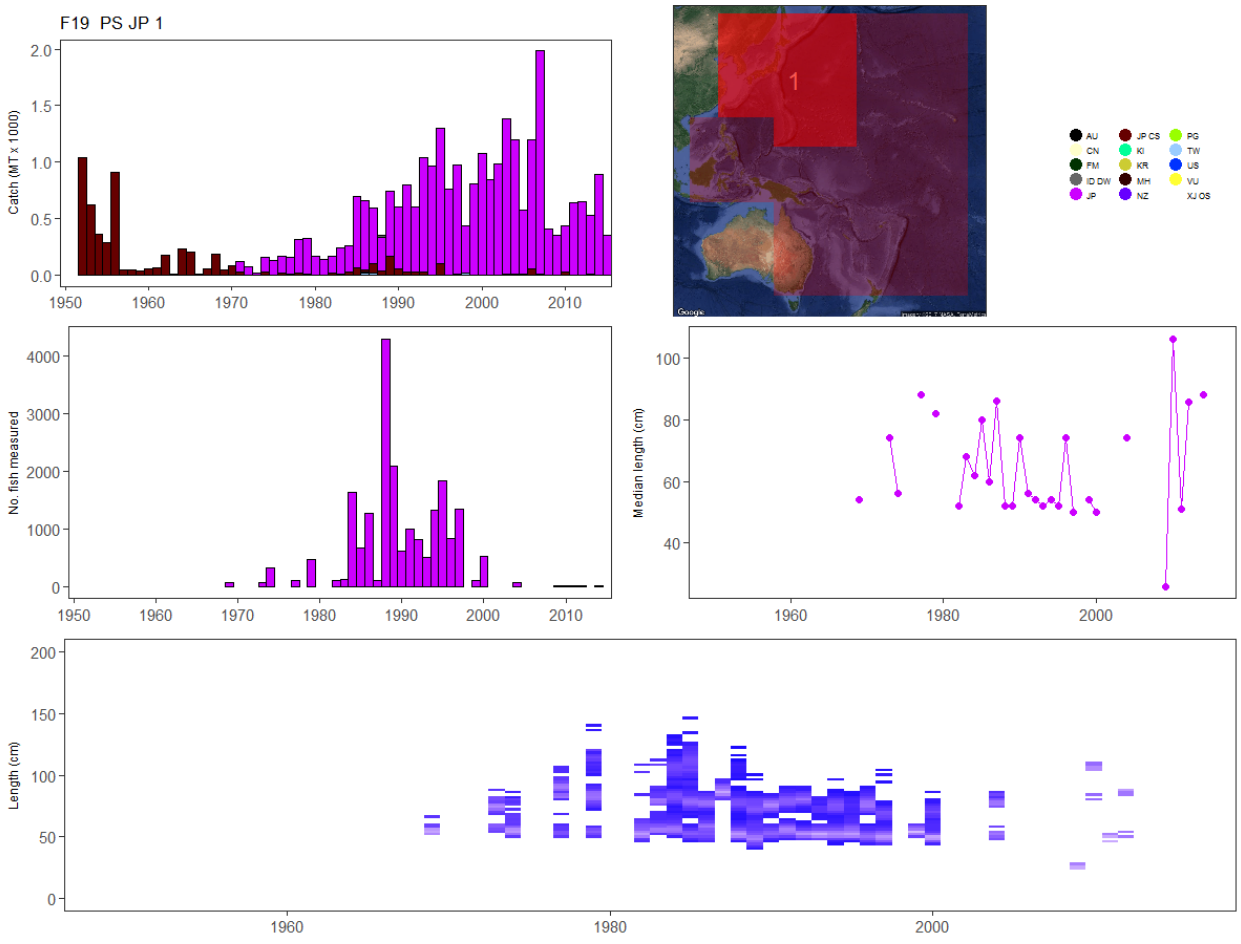

Figure 35: Summary of raw data available for BET fishery 19.

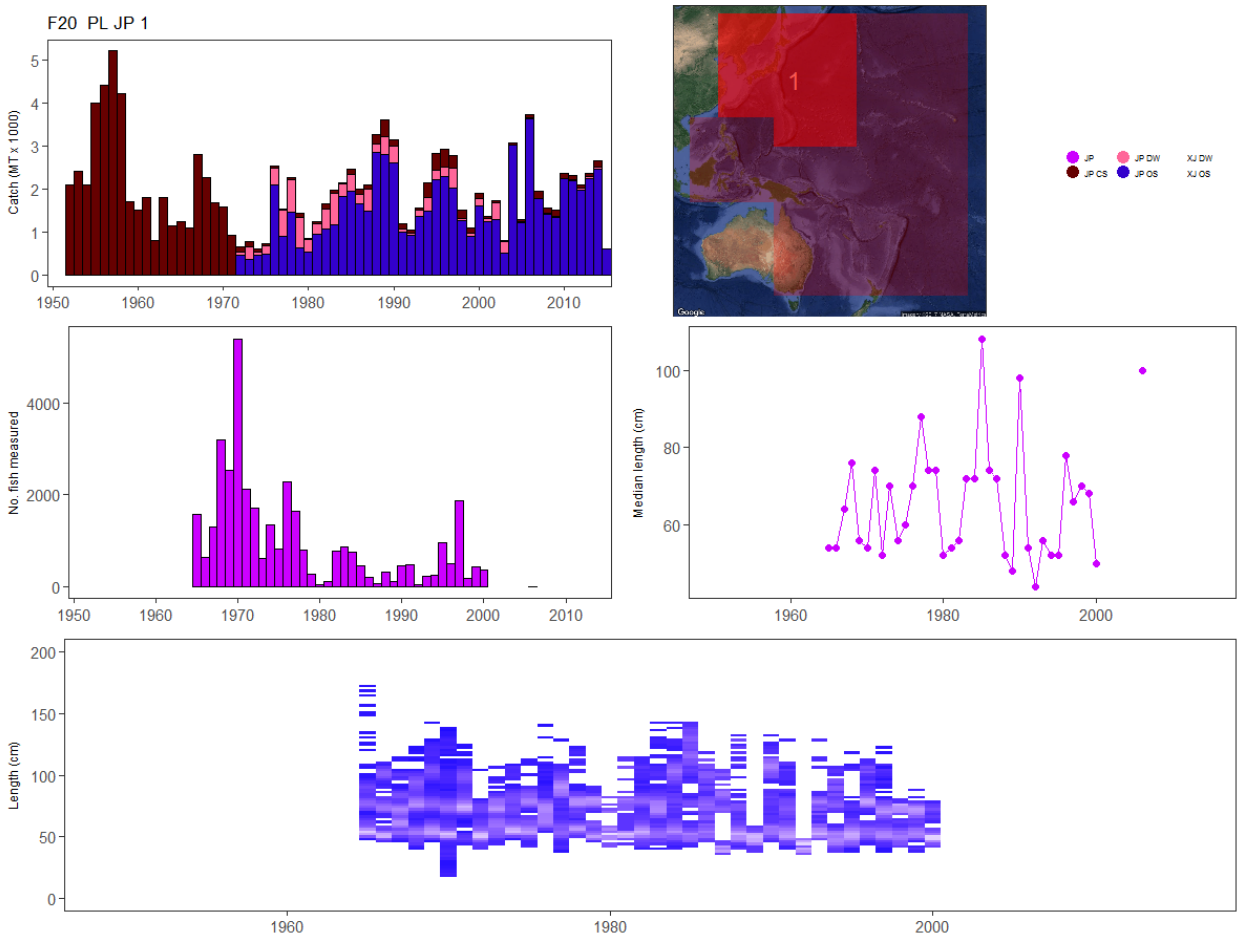

Figure 36: Summary of raw data available for BET fishery 20.

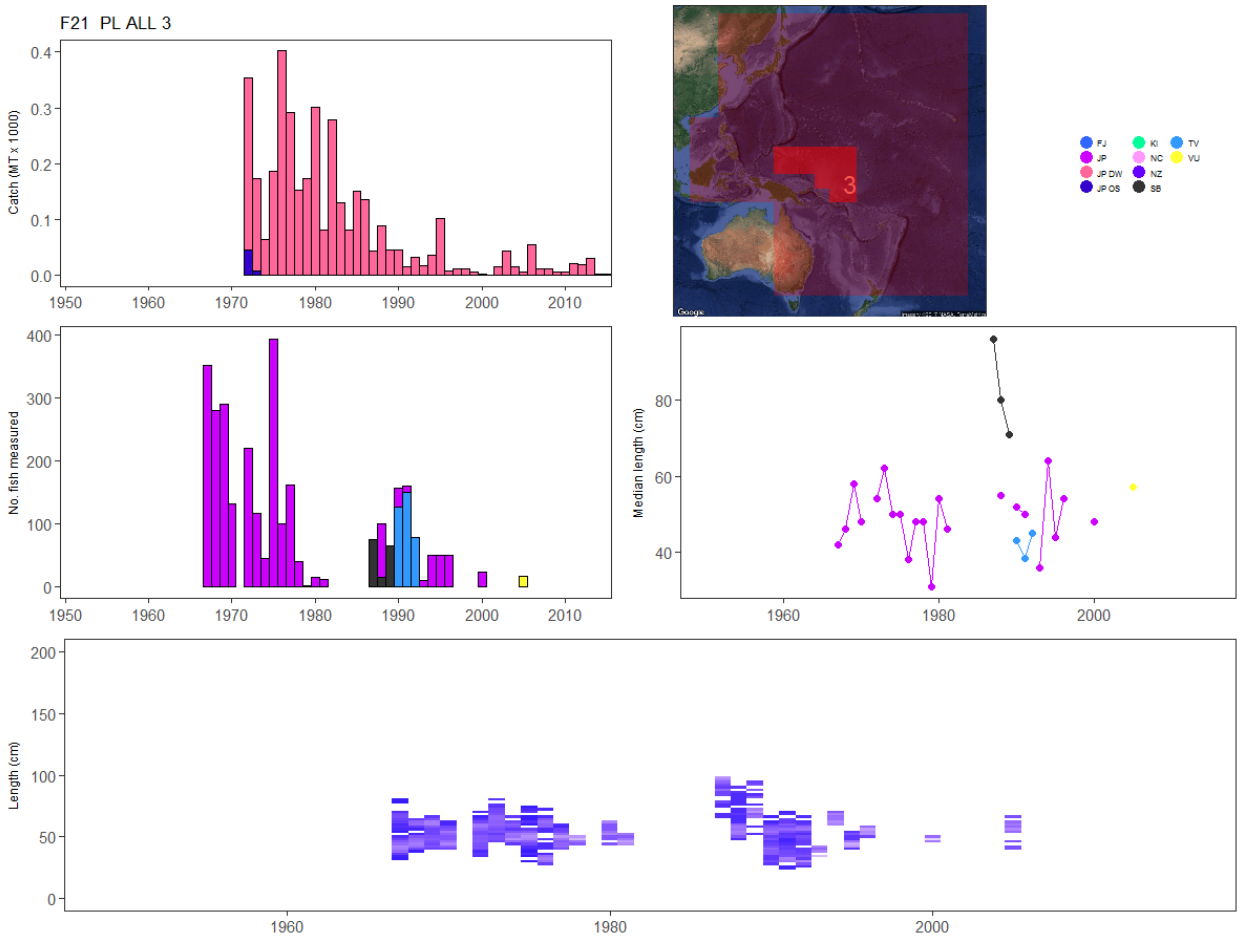

Figure 37: Summary of raw data available for BET fishery 21.

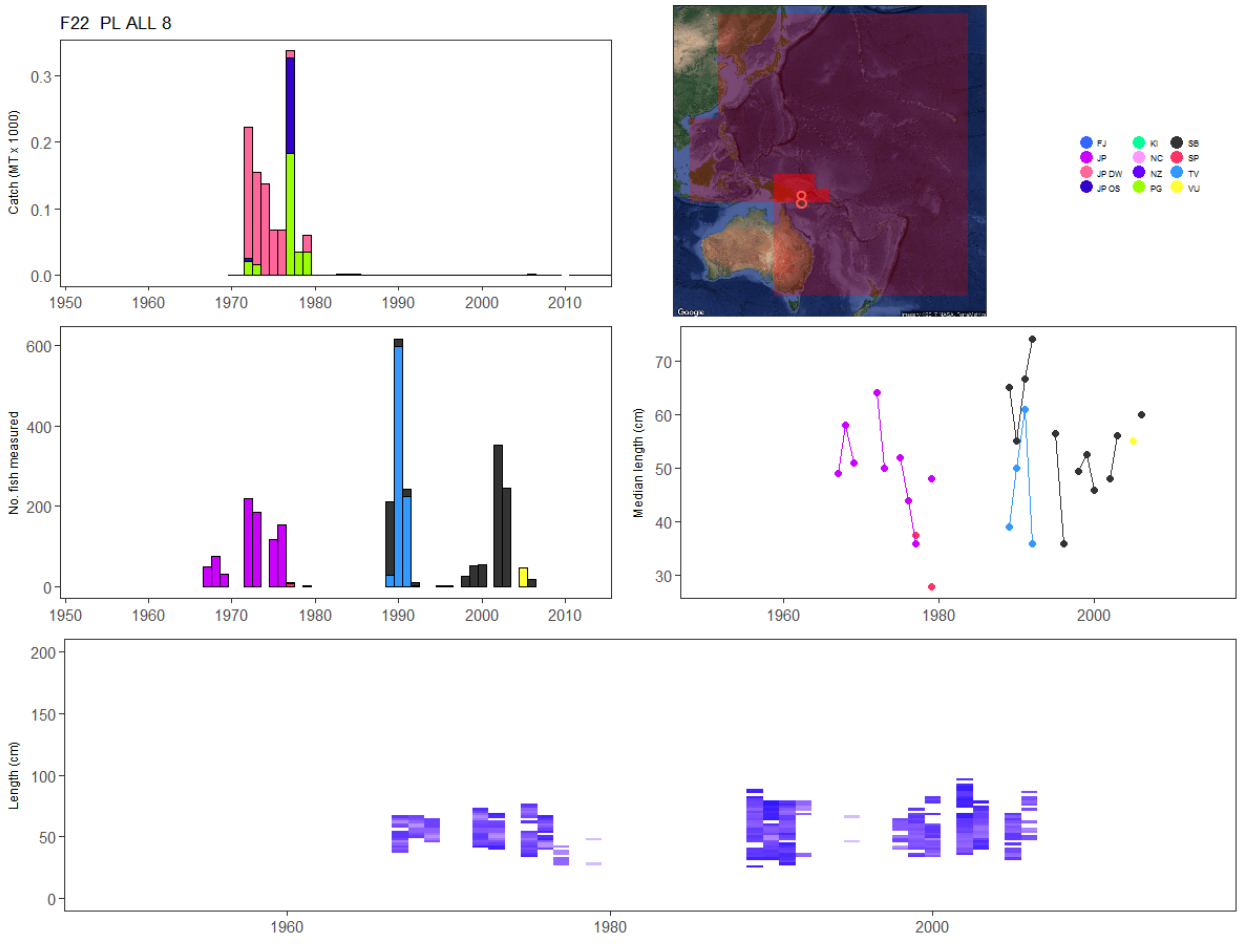

Figure 38: Summary of raw data available for BET fishery 22.

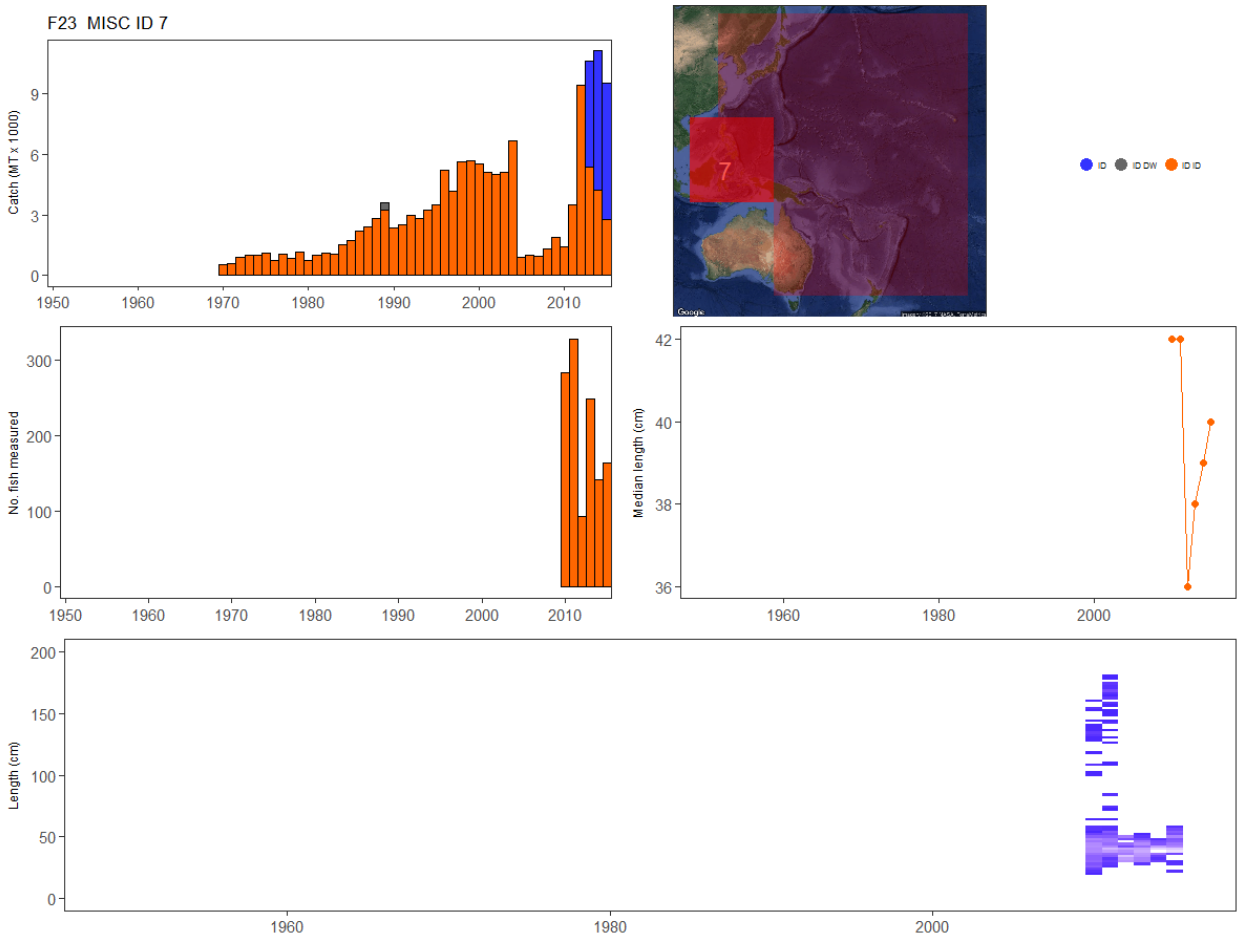

Figure 39: Summary of raw data available for BET fishery 23.

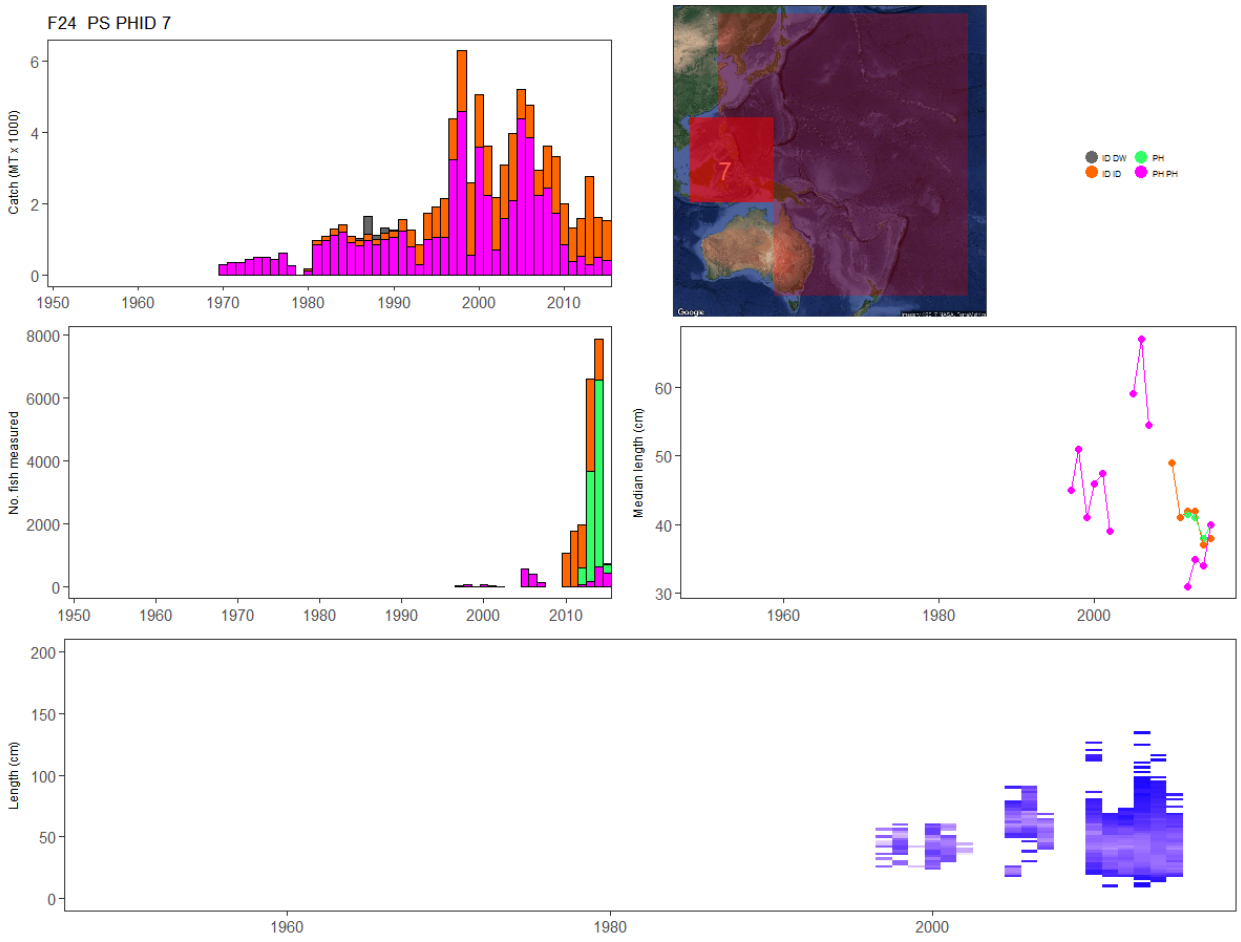

Figure 40: Summary of raw data available for BET fishery 24.

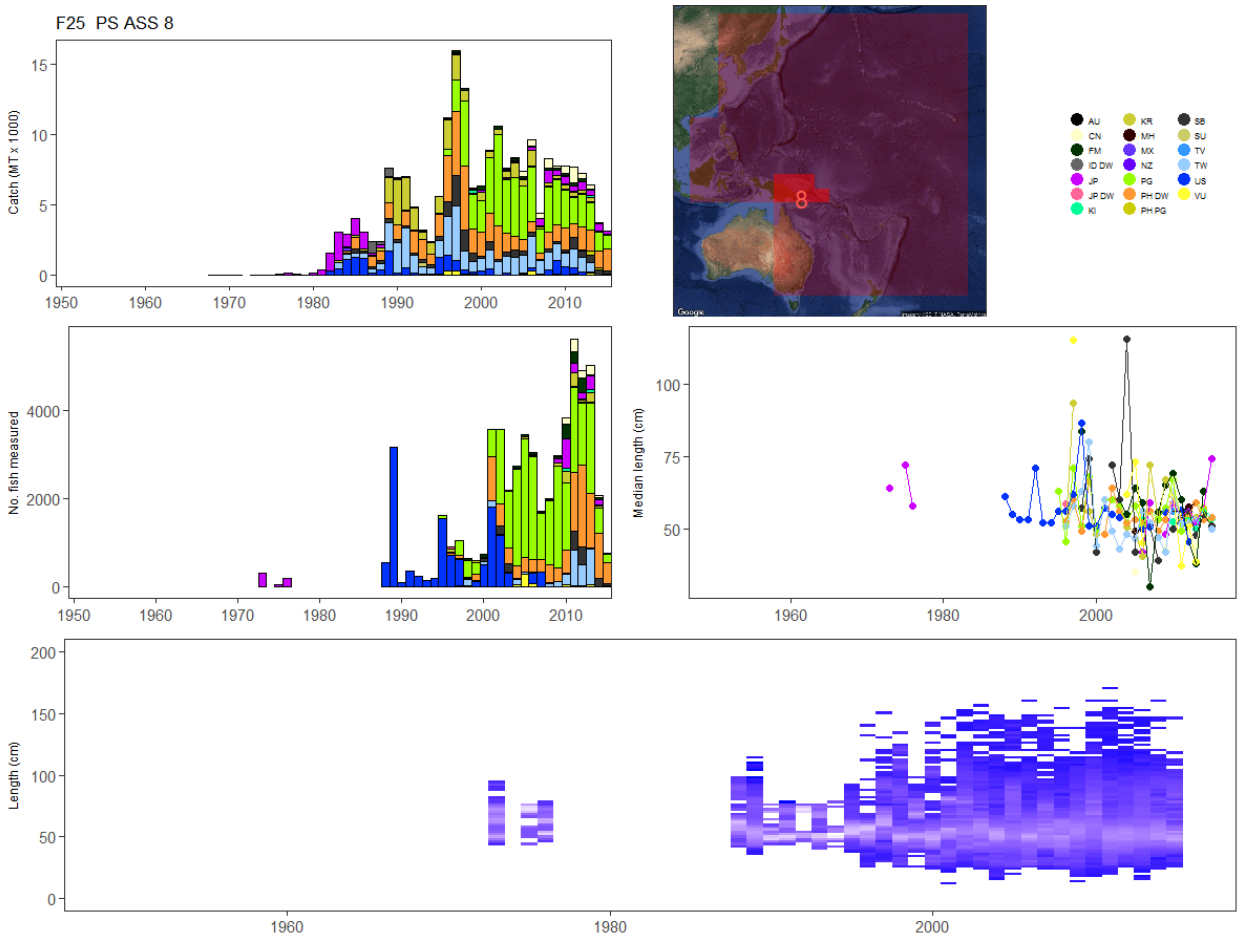

Figure 41: Summary of raw data available for BET fishery 25.

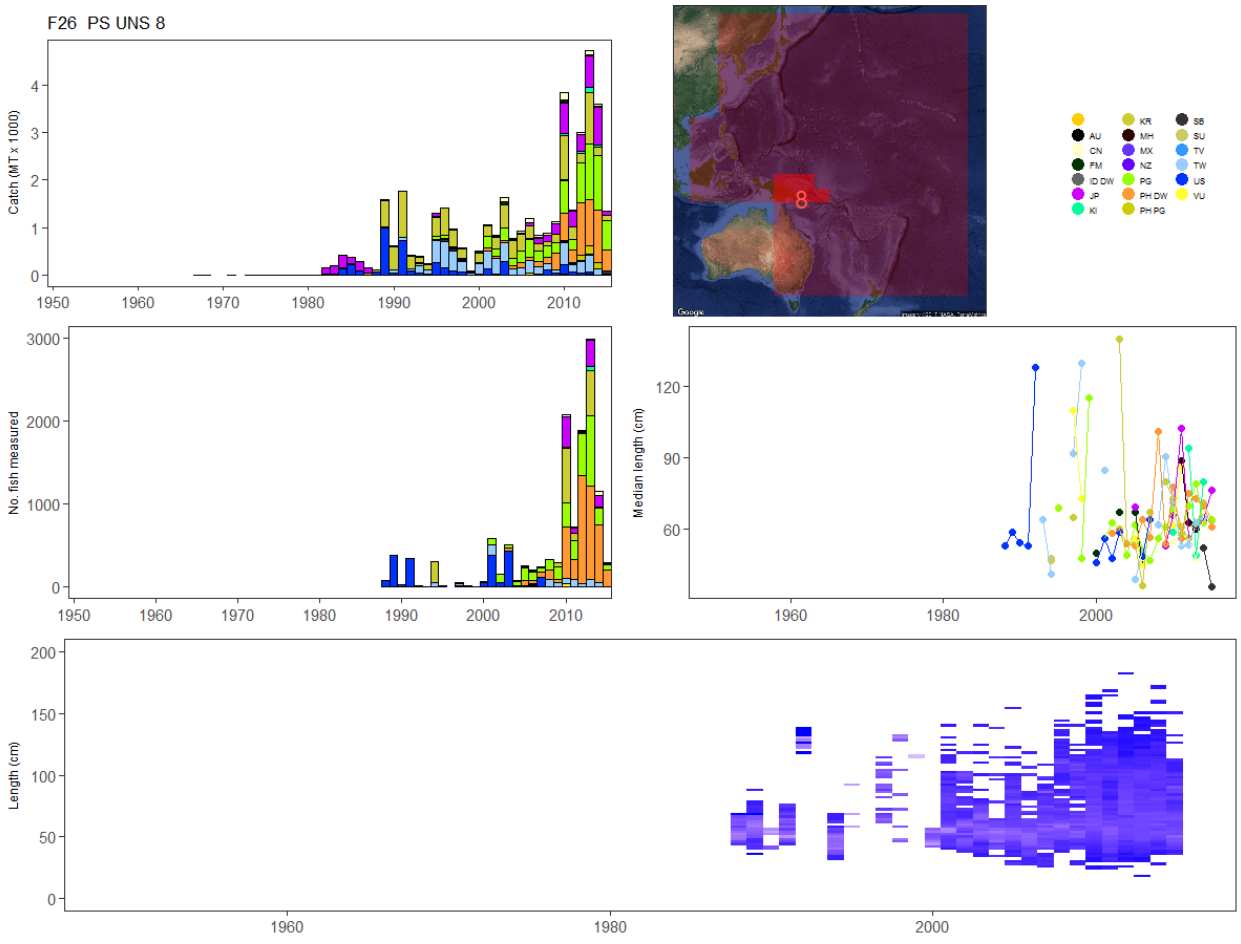

Figure 42: Summary of raw data available for BET fishery 26.

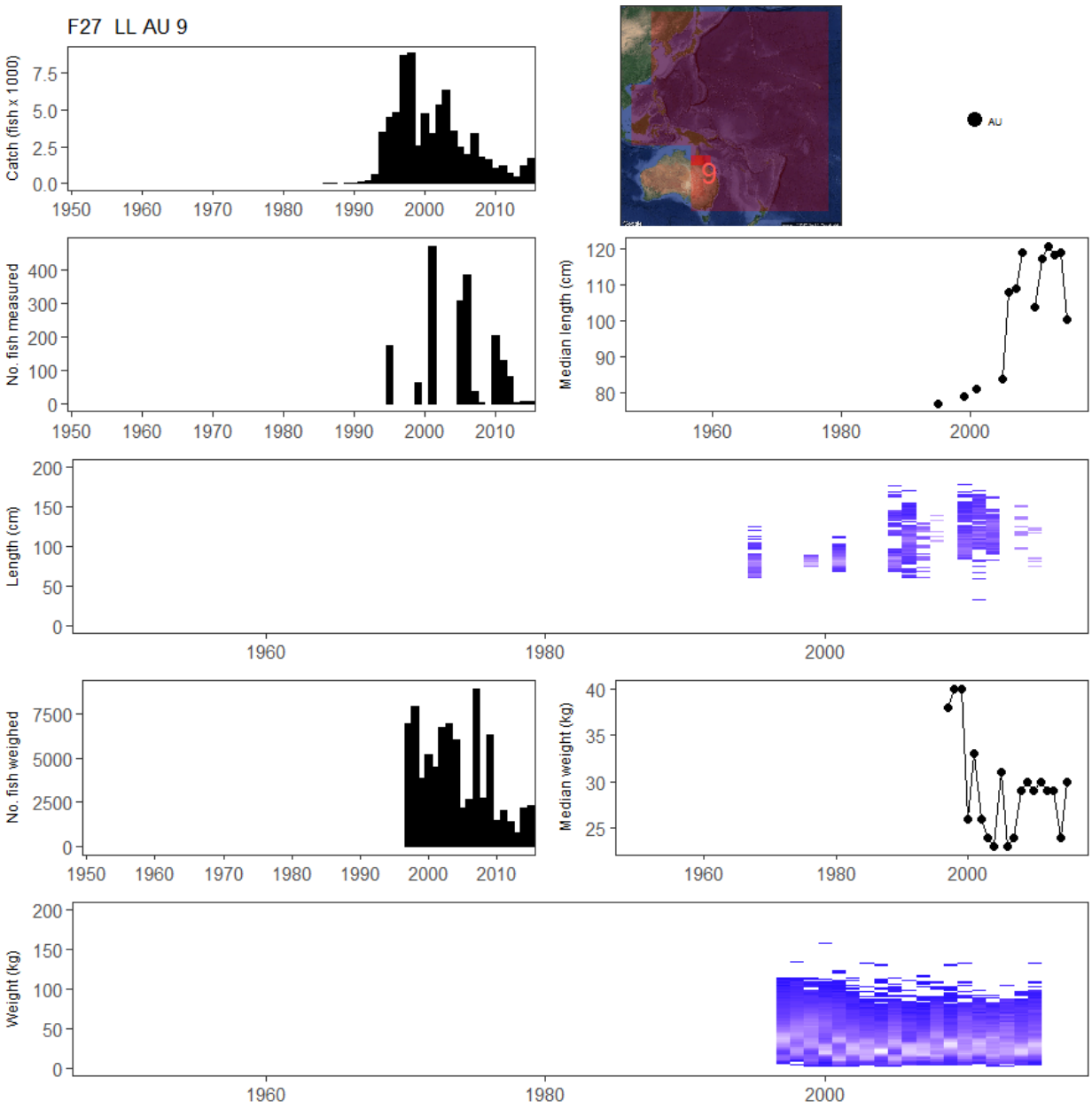

Figure 43: Summary of raw data available for BET fishery 27.

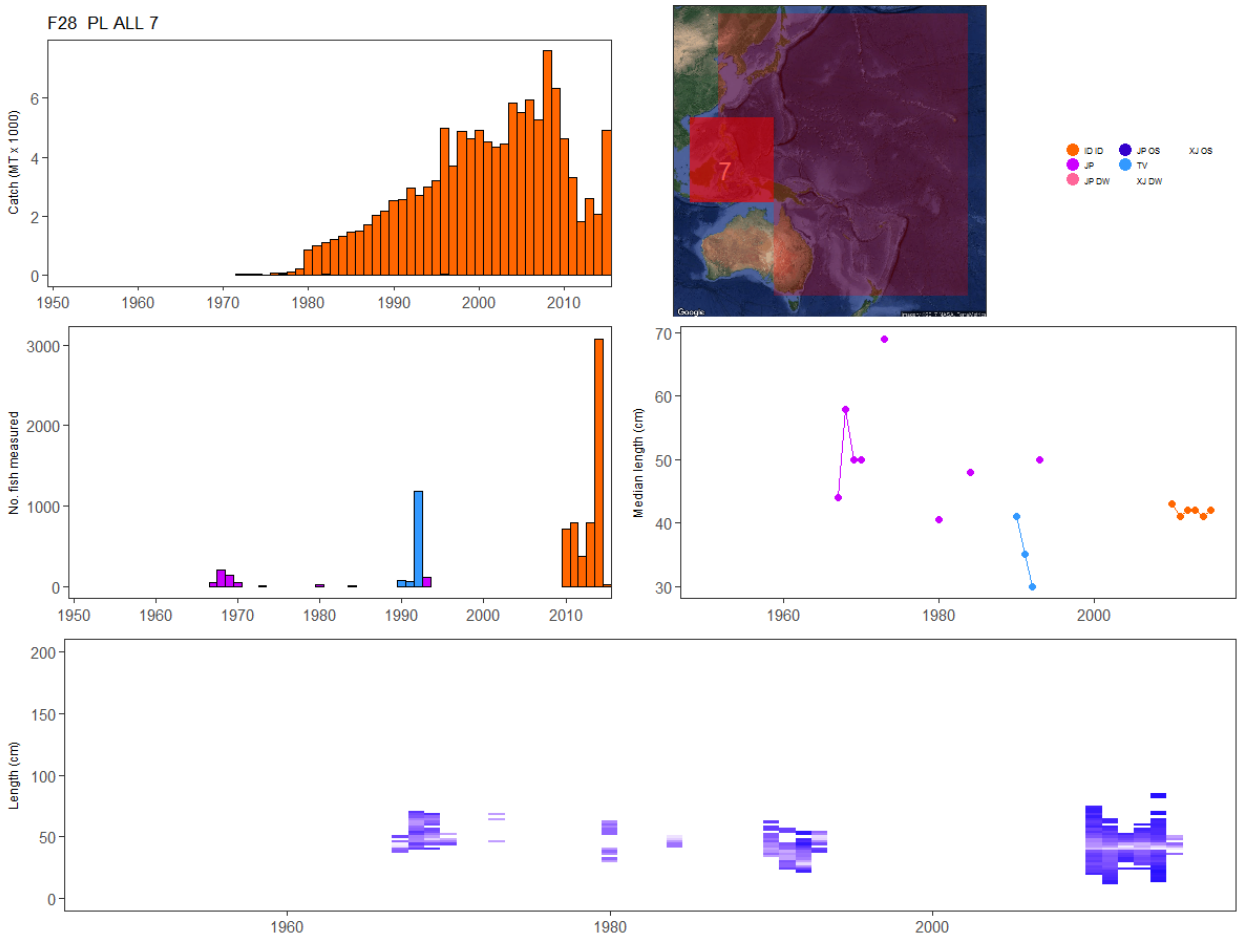

Figure 44: Summary of raw data available for BET fishery 28.

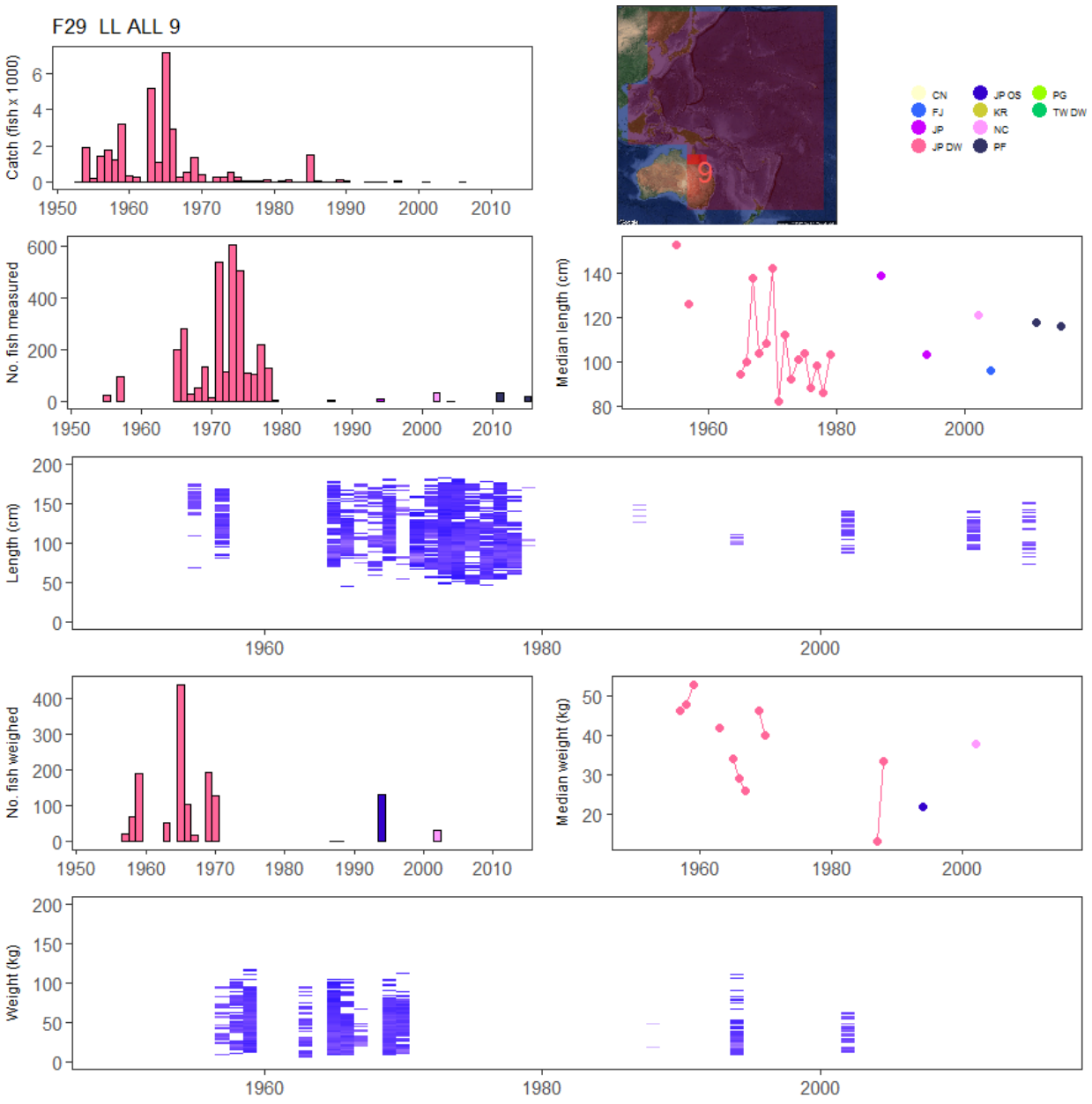

Figure 45: Summary of raw data available for BET fishery 29.

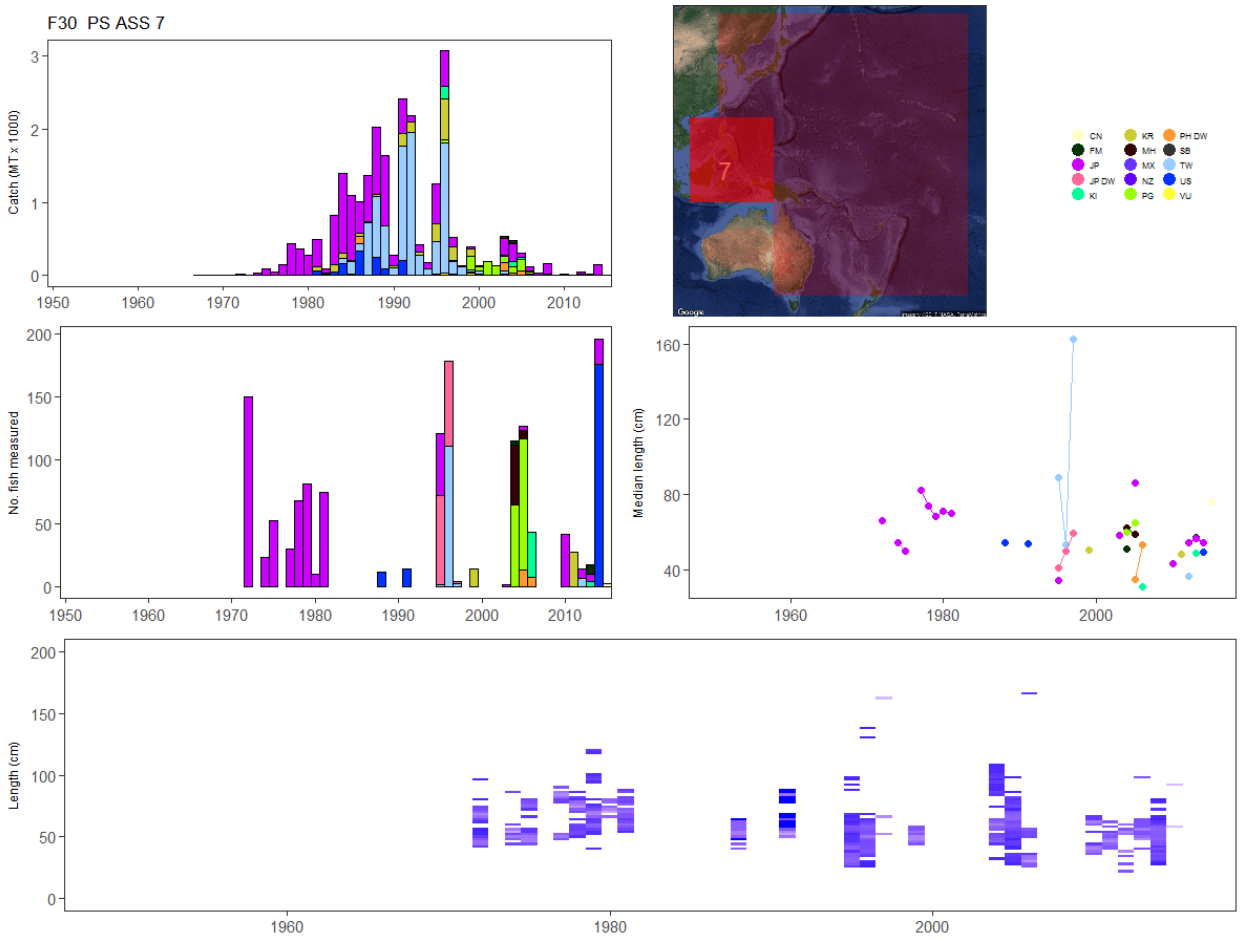

Figure 46: Summary of raw data available for BET fishery 30.

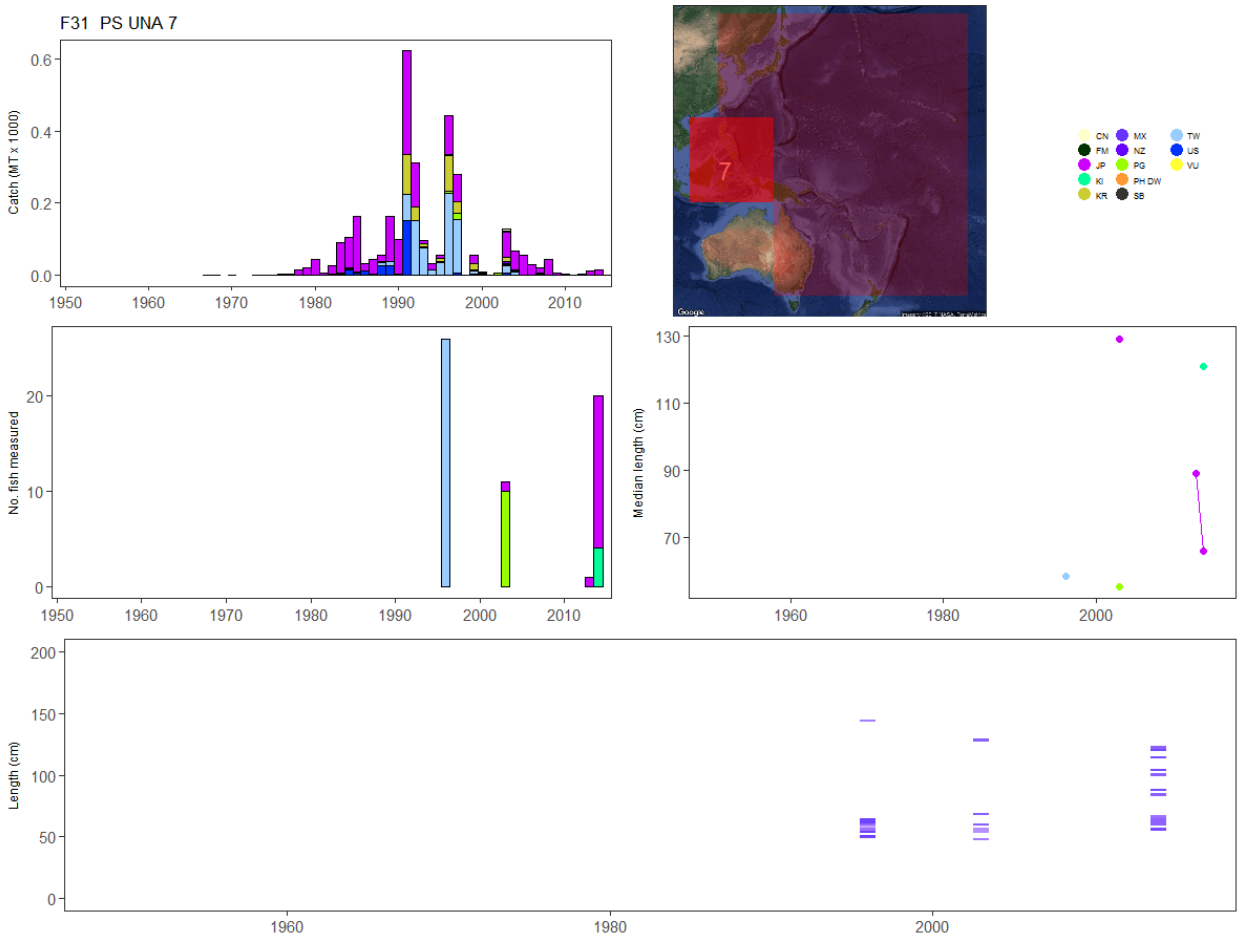

Figure 47: Summary of raw data available for BET fishery 31.

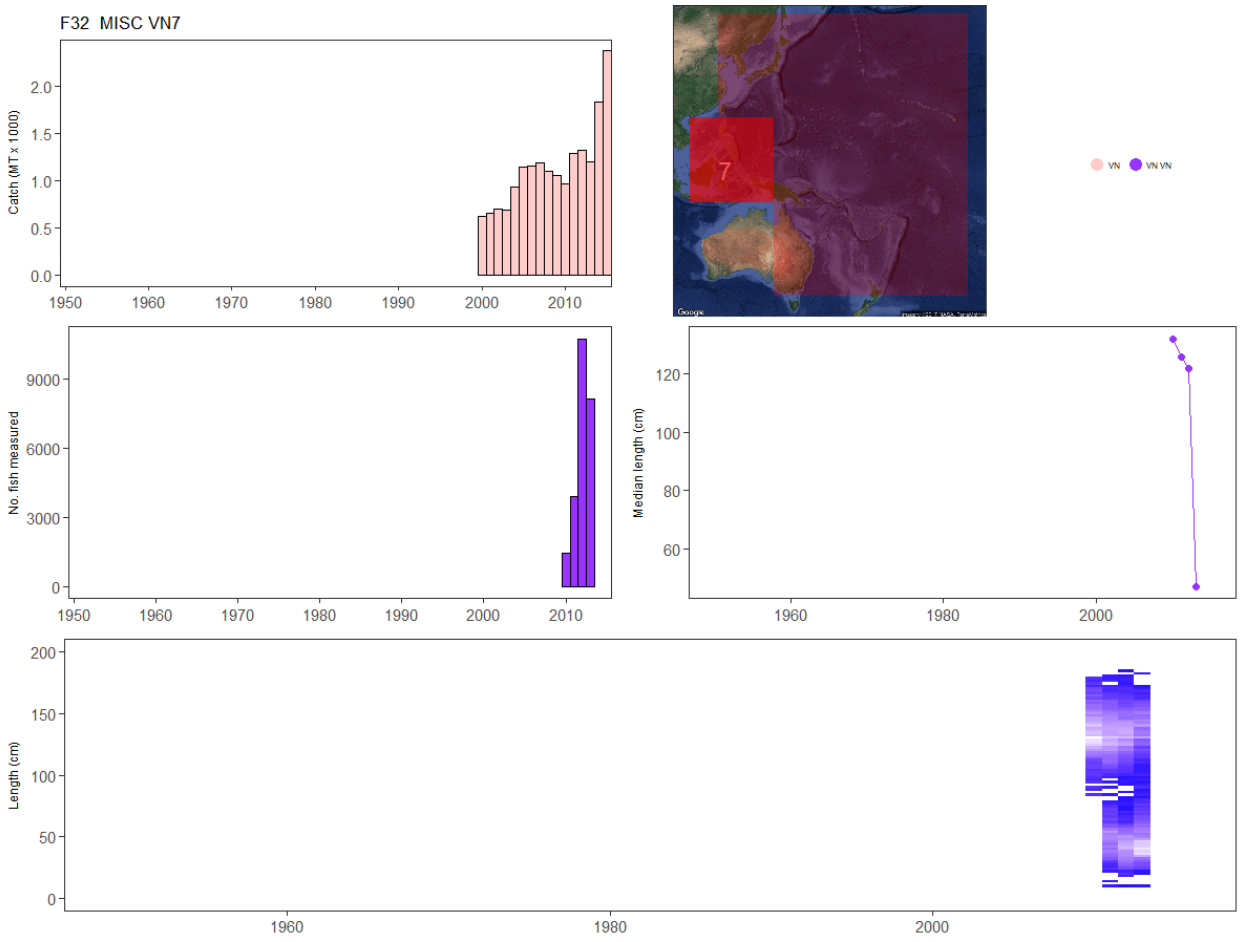

Figure 48: Summary of raw data available for BET fishery 32.

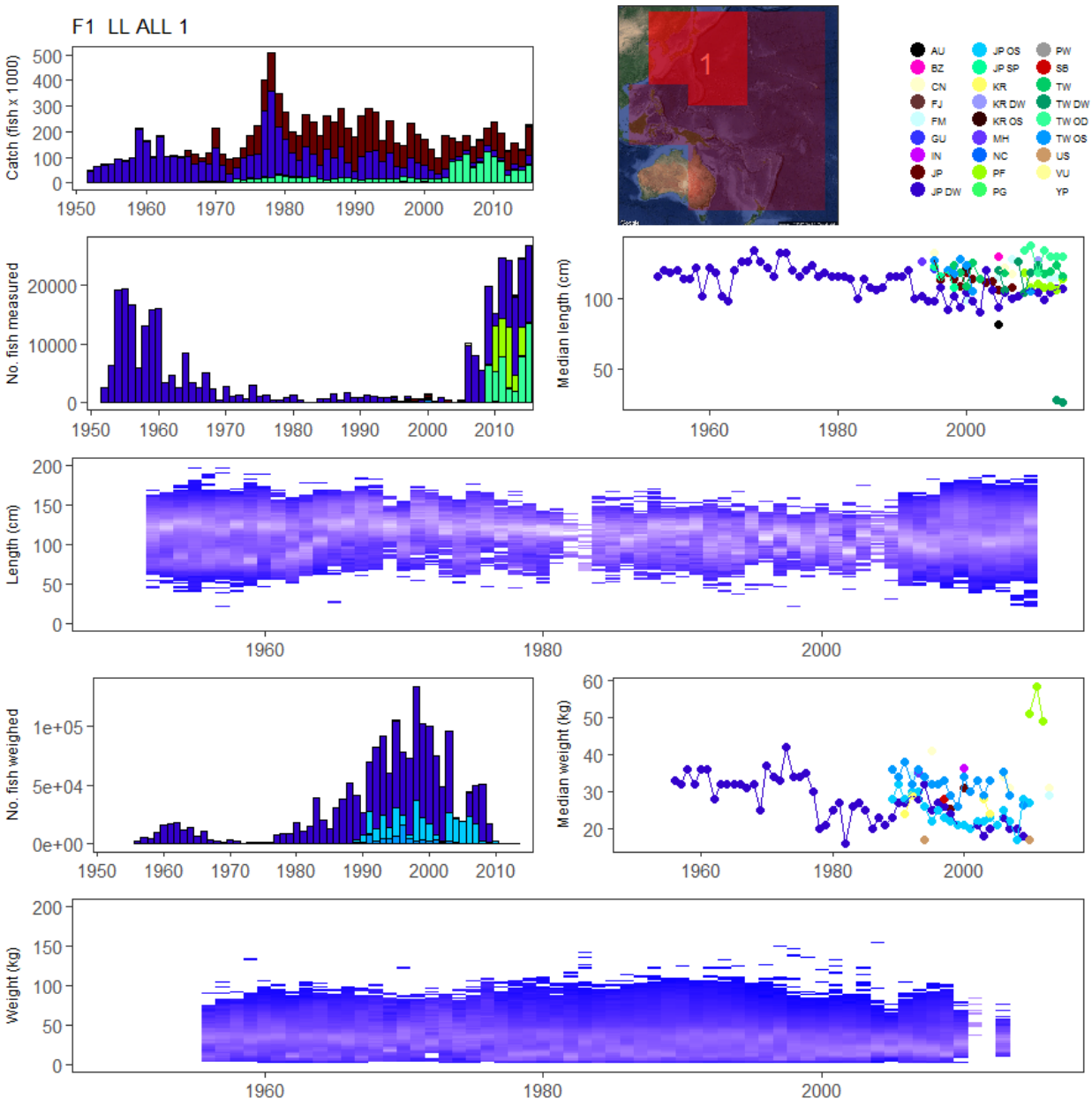

Figure 49: Summary of raw data available for fishery 1 of the 2017 YFT stock assessment in the WCPO. The panels display; annual catch (top left), region of occurrence (top right), the annual number of fish with measured length (top middle left), median length of available length composition data (top middle right), a tile plot of the annual length distribution of fish (middle), the annual number of fish with measured weight (bottom middle left), median weight of available weight composition data (bottom middle right), and a tile plot of the annual weight distribution of fish (bottom).

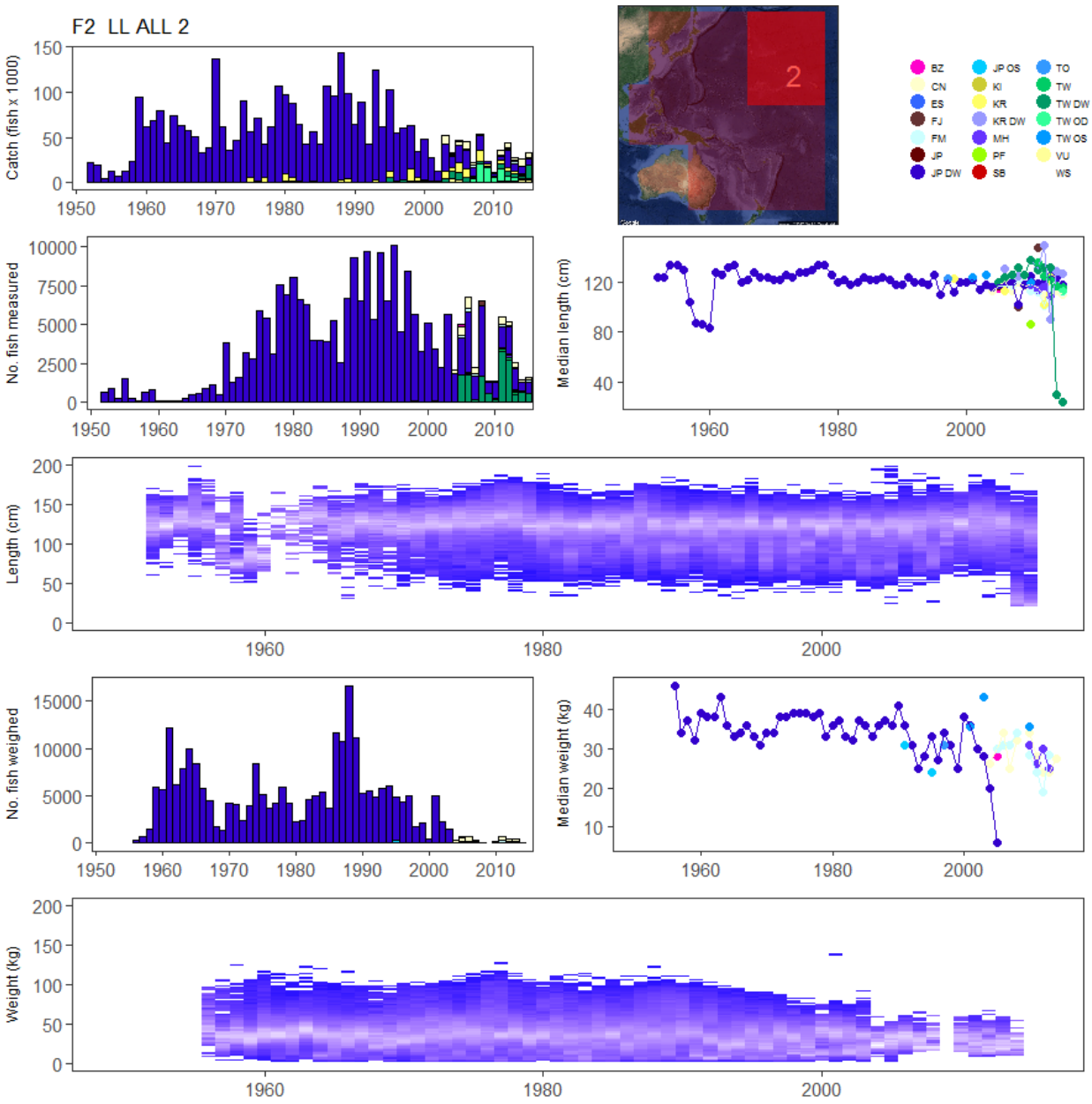

Figure 50: Summary of raw data available for YFT fishery 2.

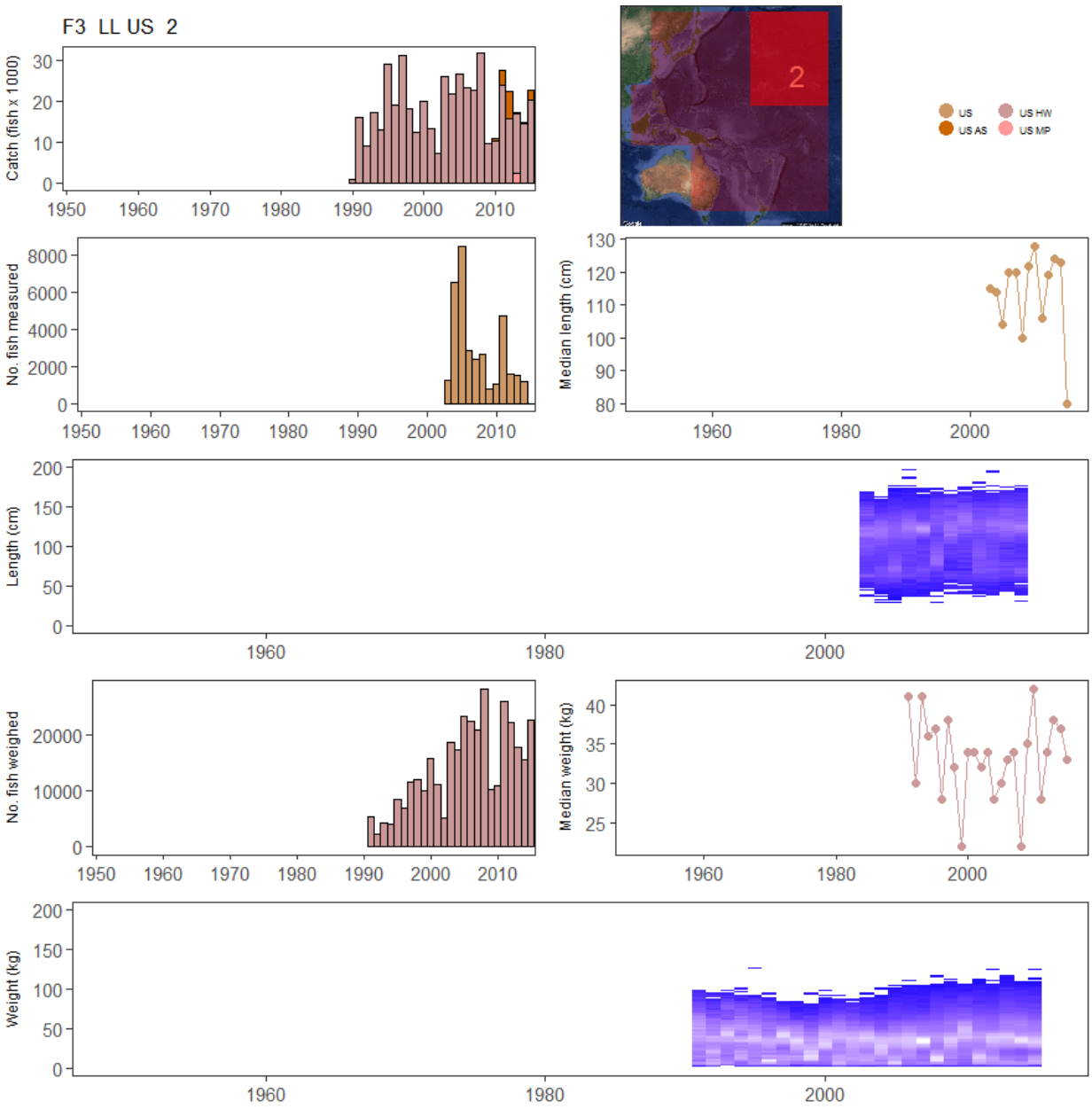

Figure 51: Summary of raw data available for YFT fishery 3.

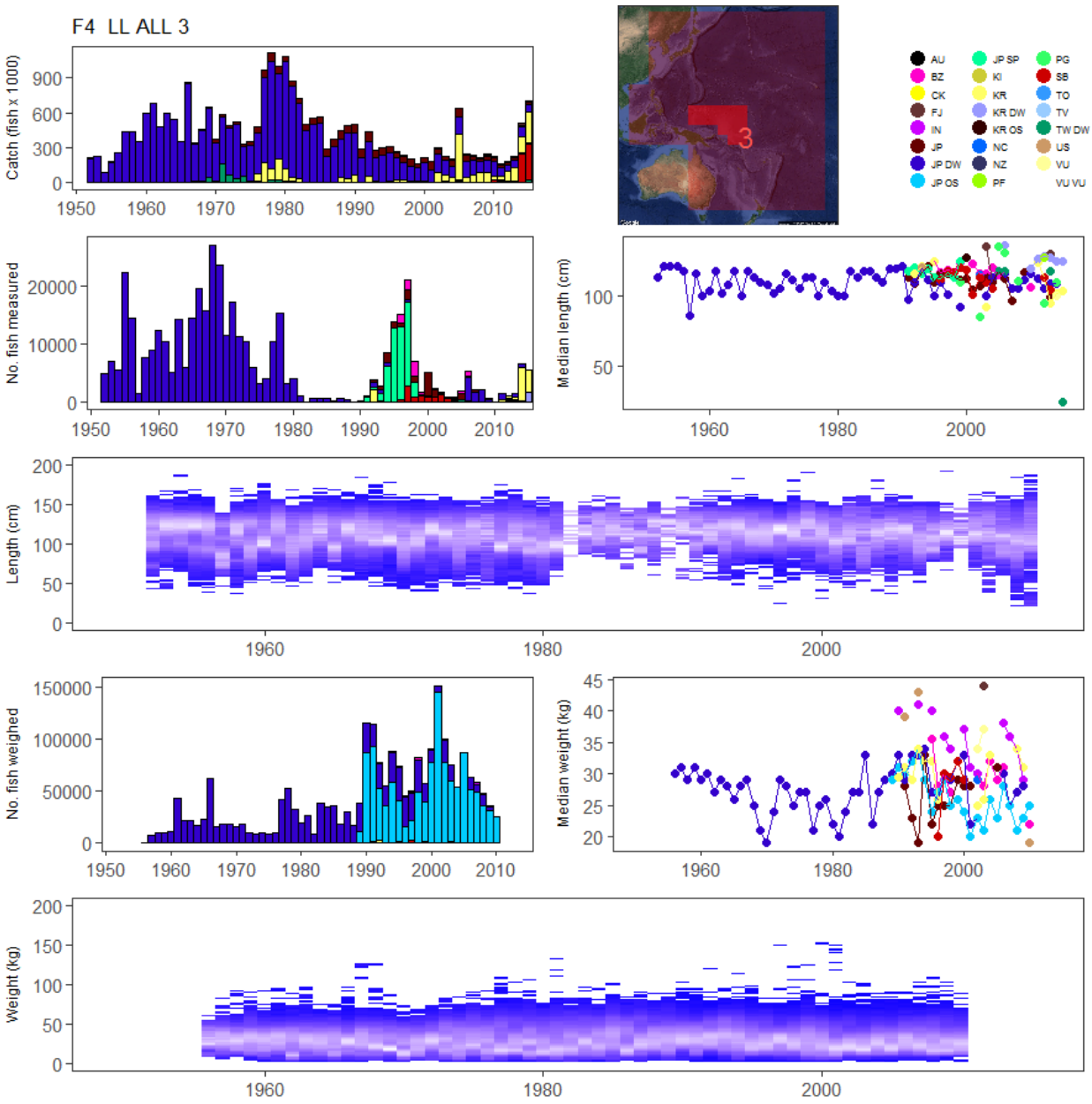

Figure 52: Summary of raw data available for YFT fishery 4.

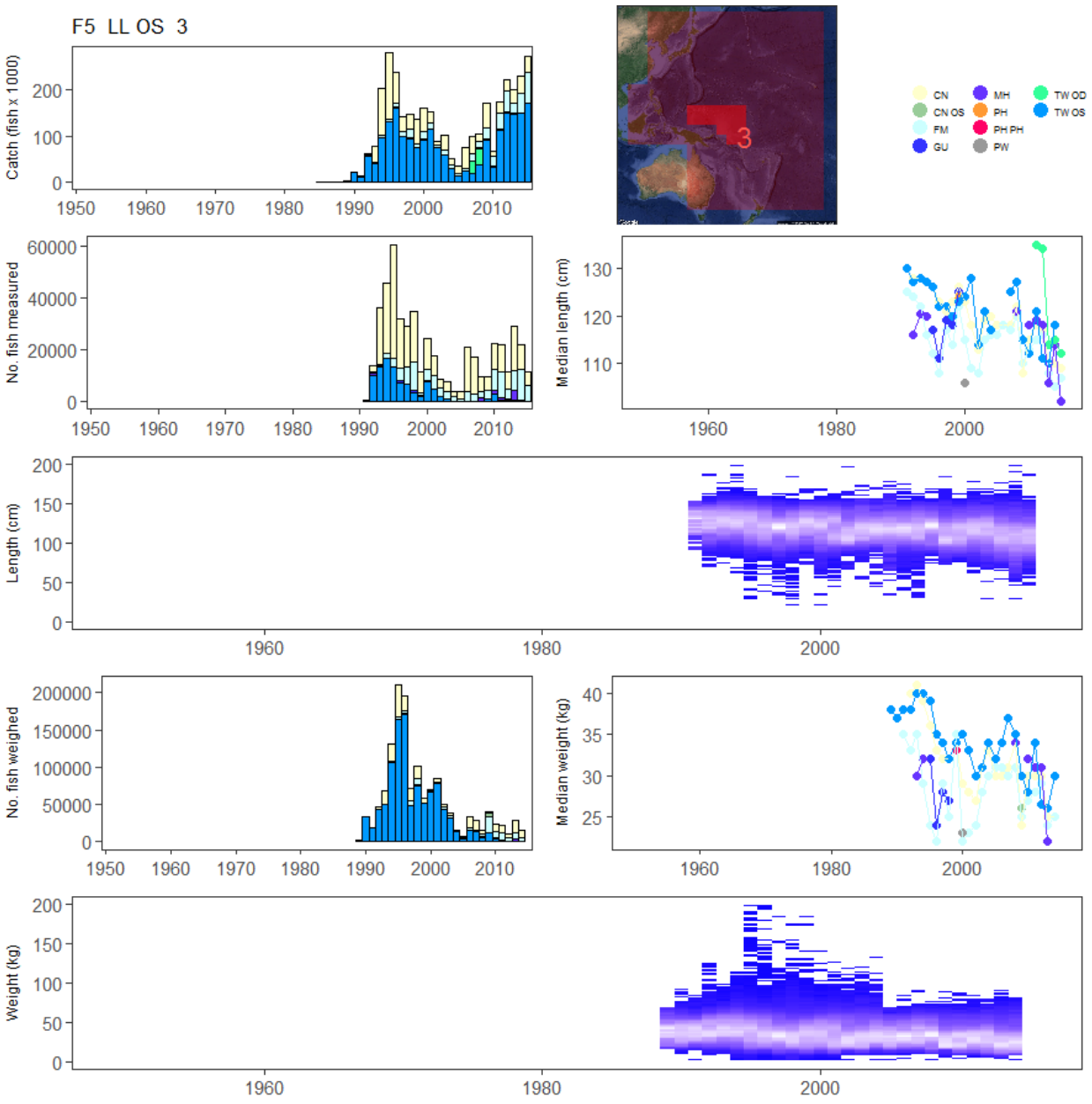

Figure 53: Summary of raw data available for YFT fishery 5.

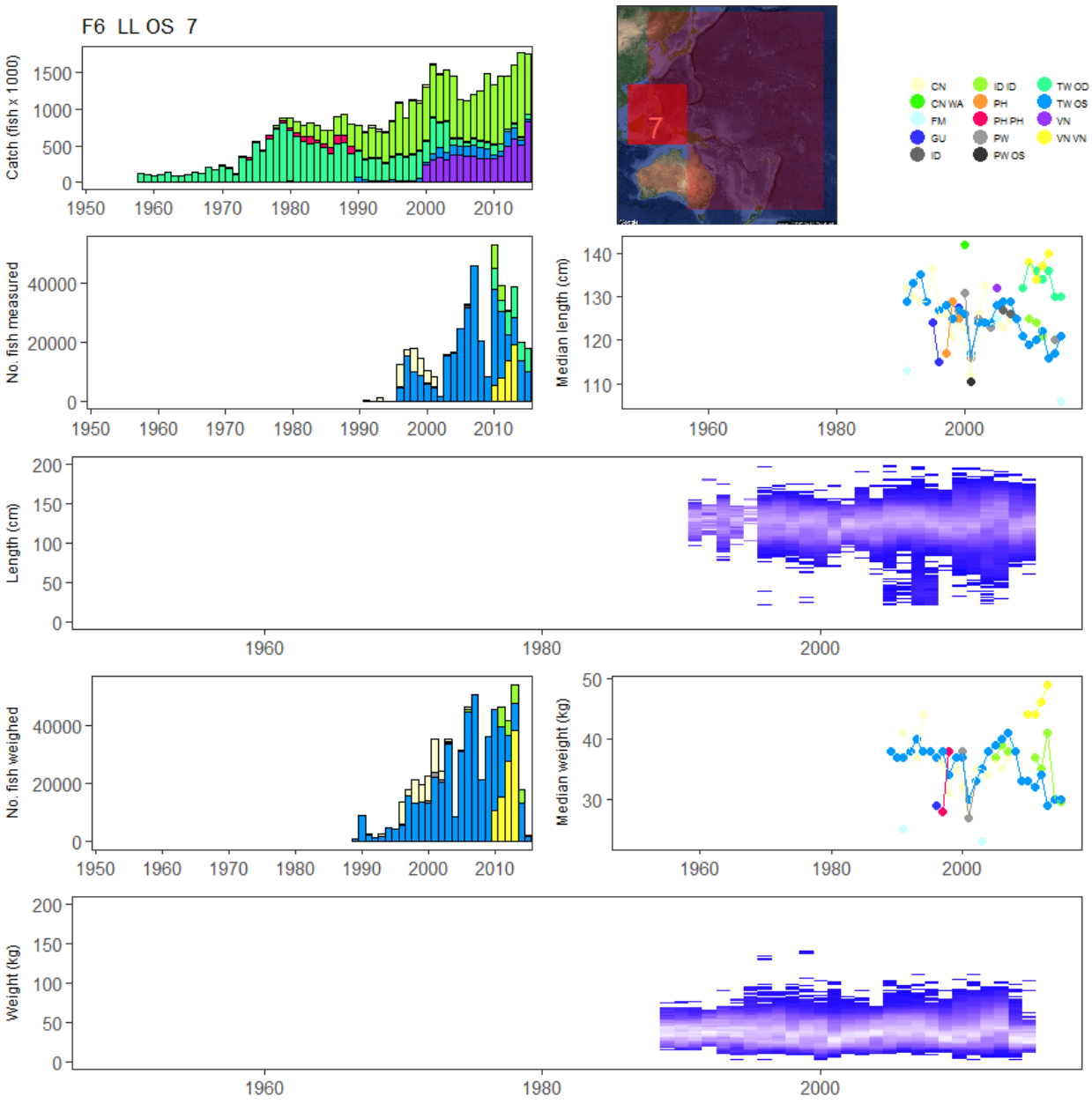

Figure 54: Summary of raw data available for YFT fishery 6.

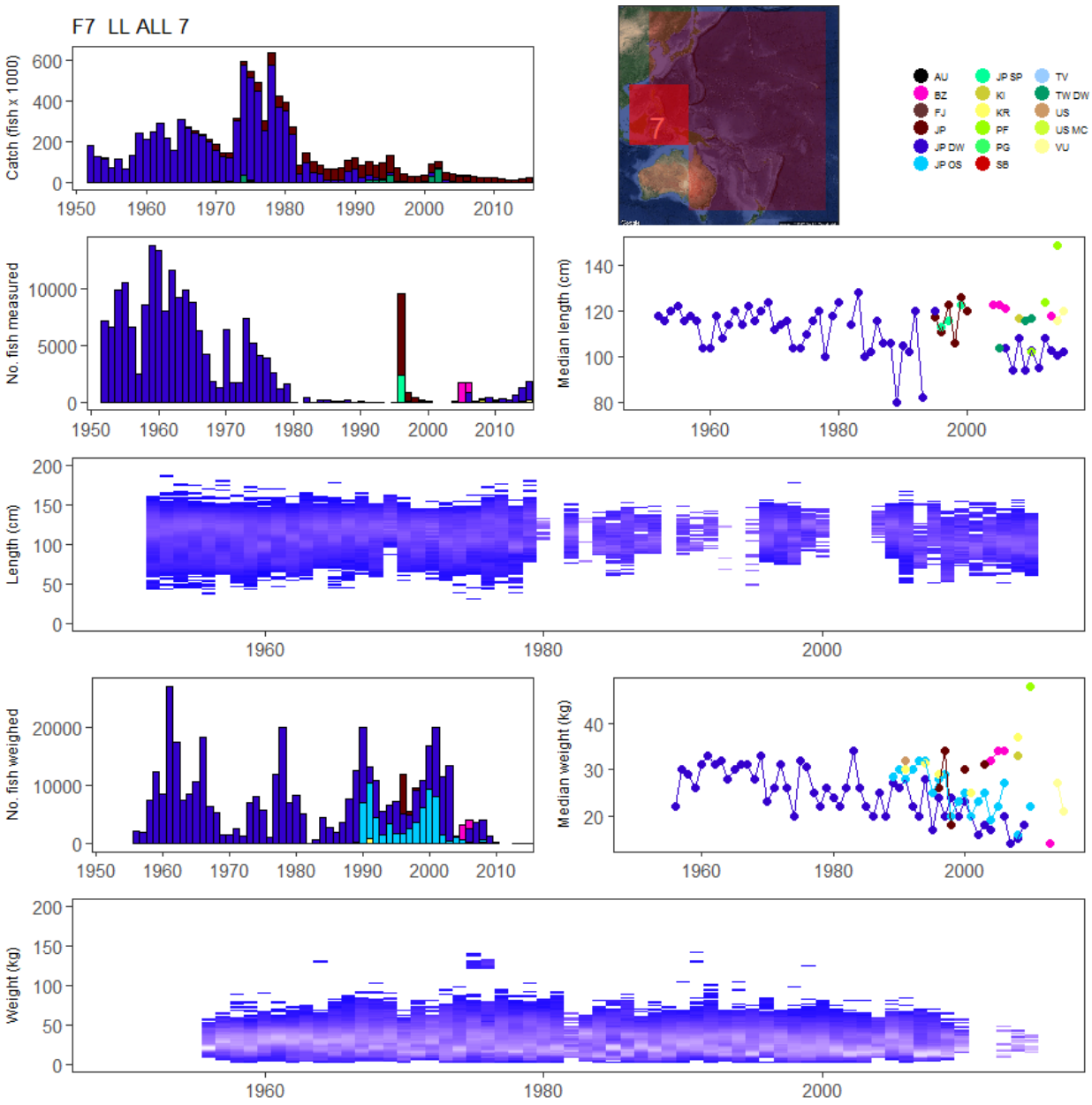

Figure 55: Summary of raw data available for YFT fishery 7.

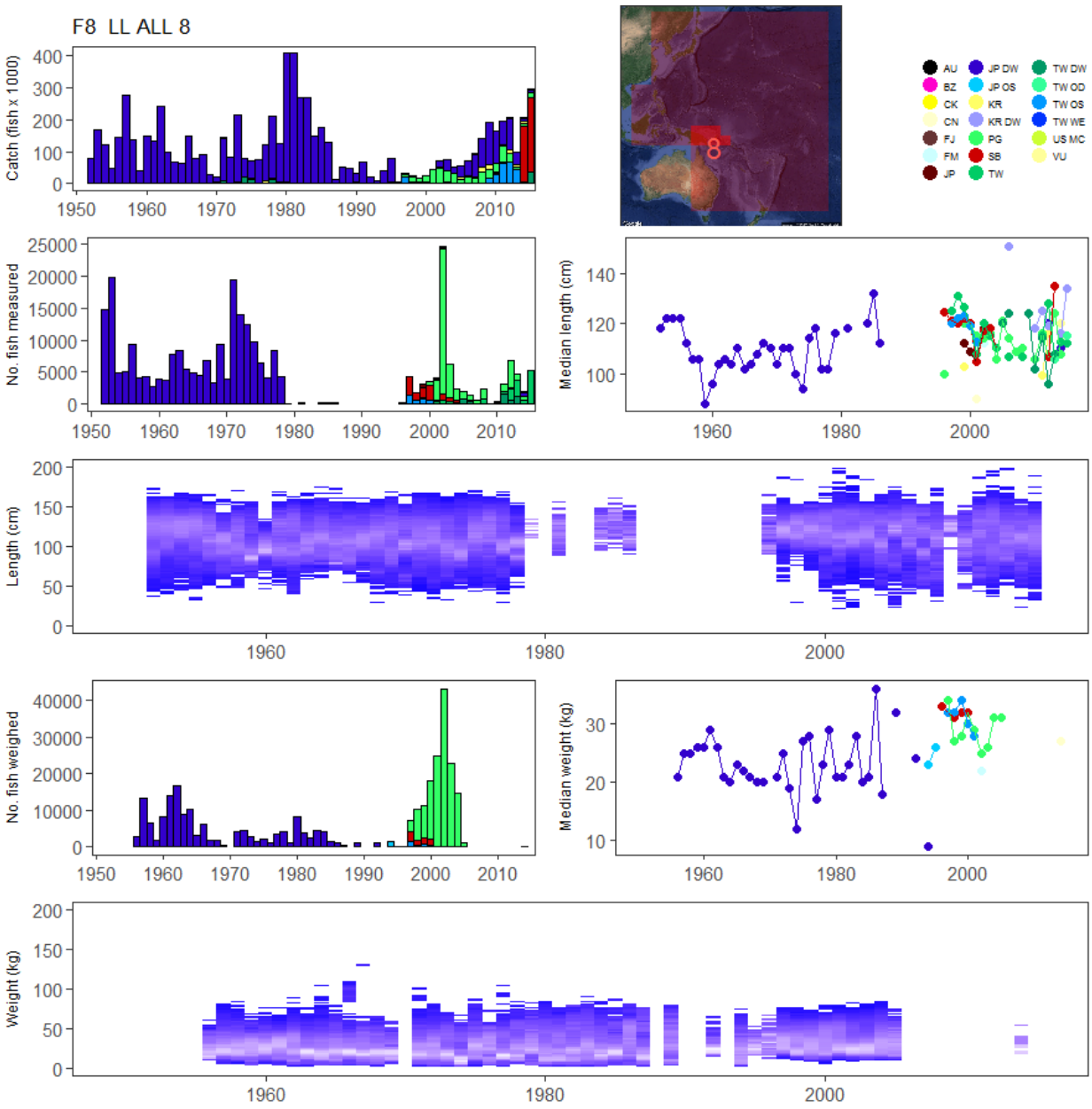

Figure 56: Summary of raw data available for YFT fishery 8.

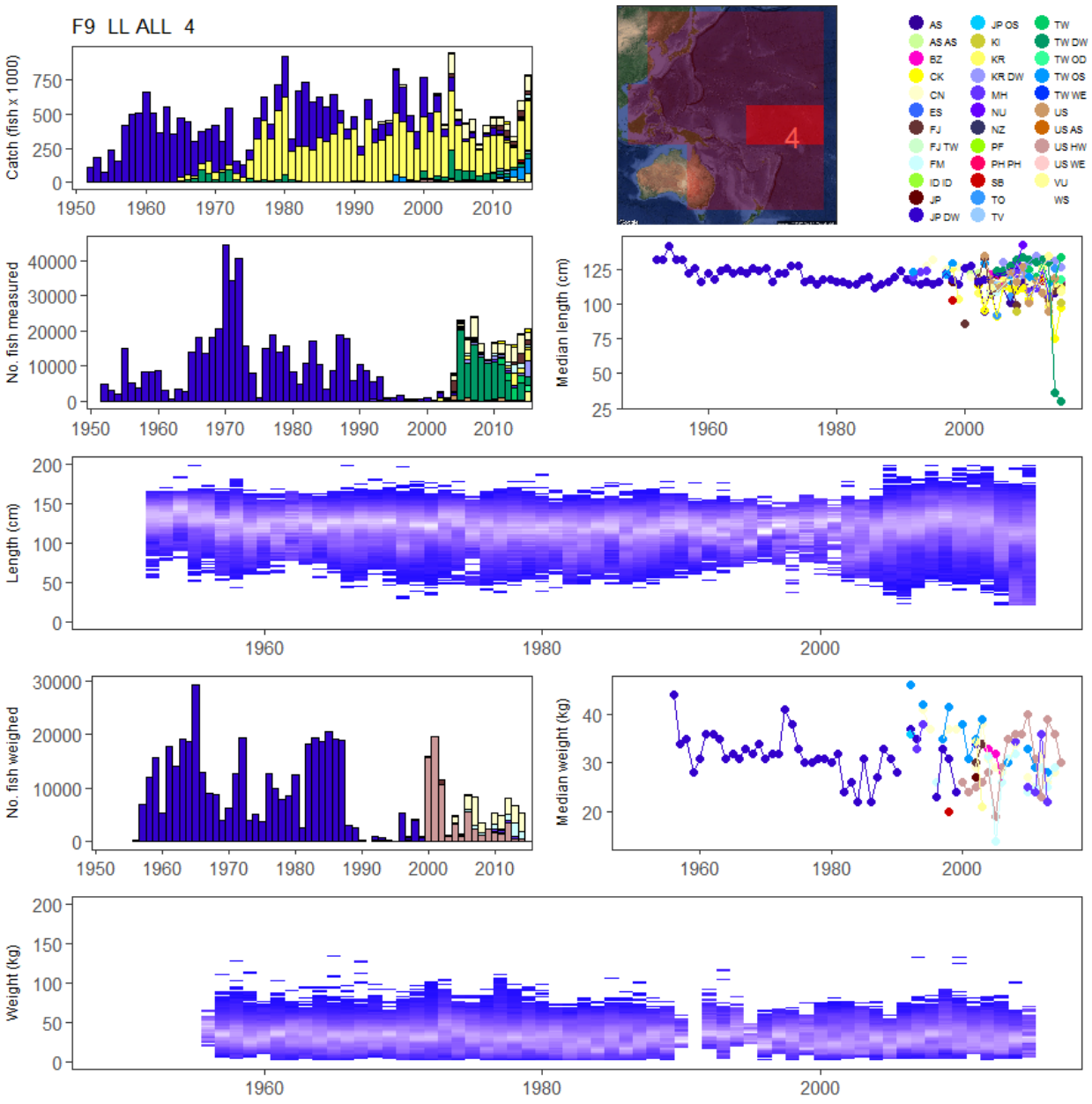

Figure 57: Summary of raw data available for YFT fishery 9.

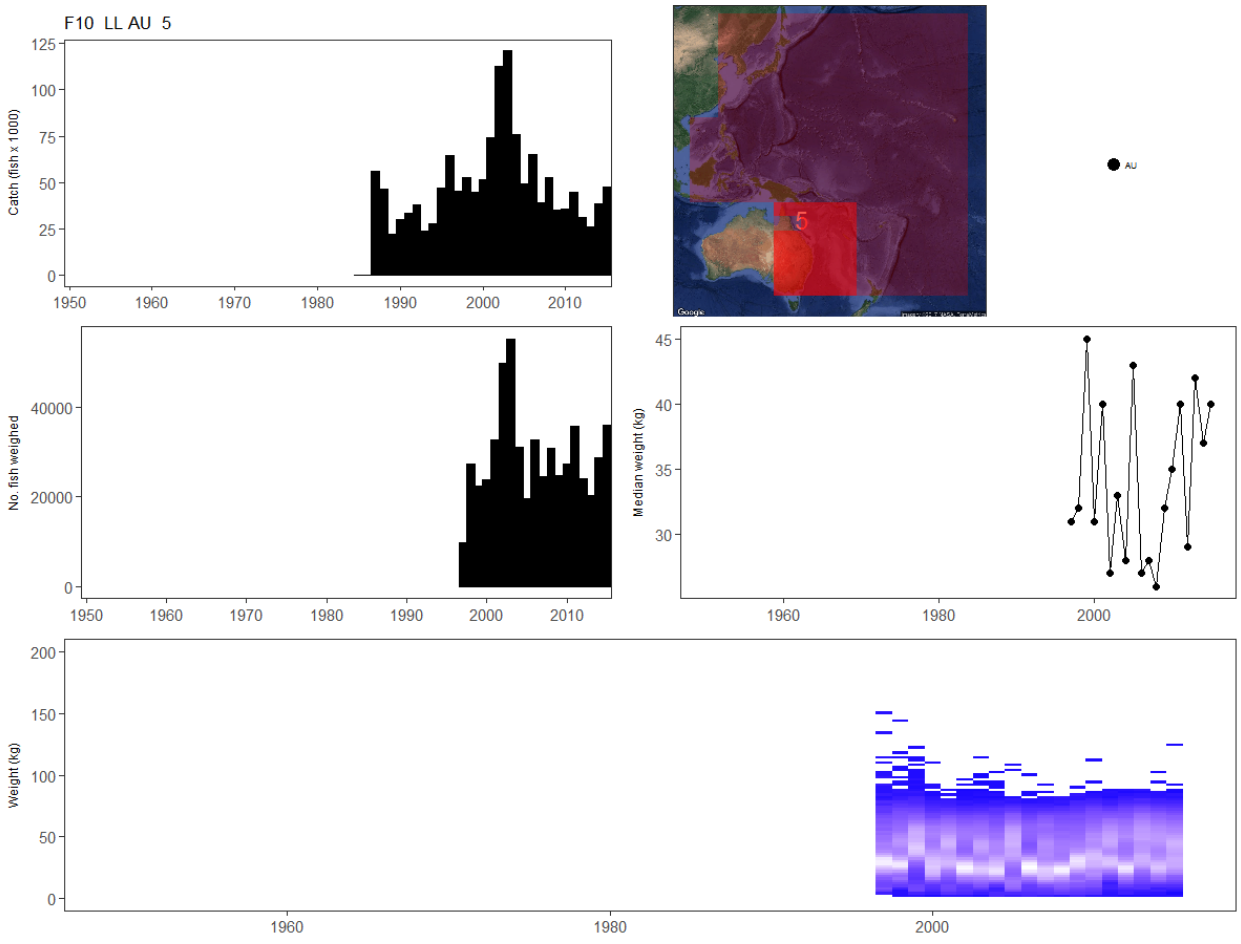

Figure 58: Summary of raw data available for YFT fishery 10.

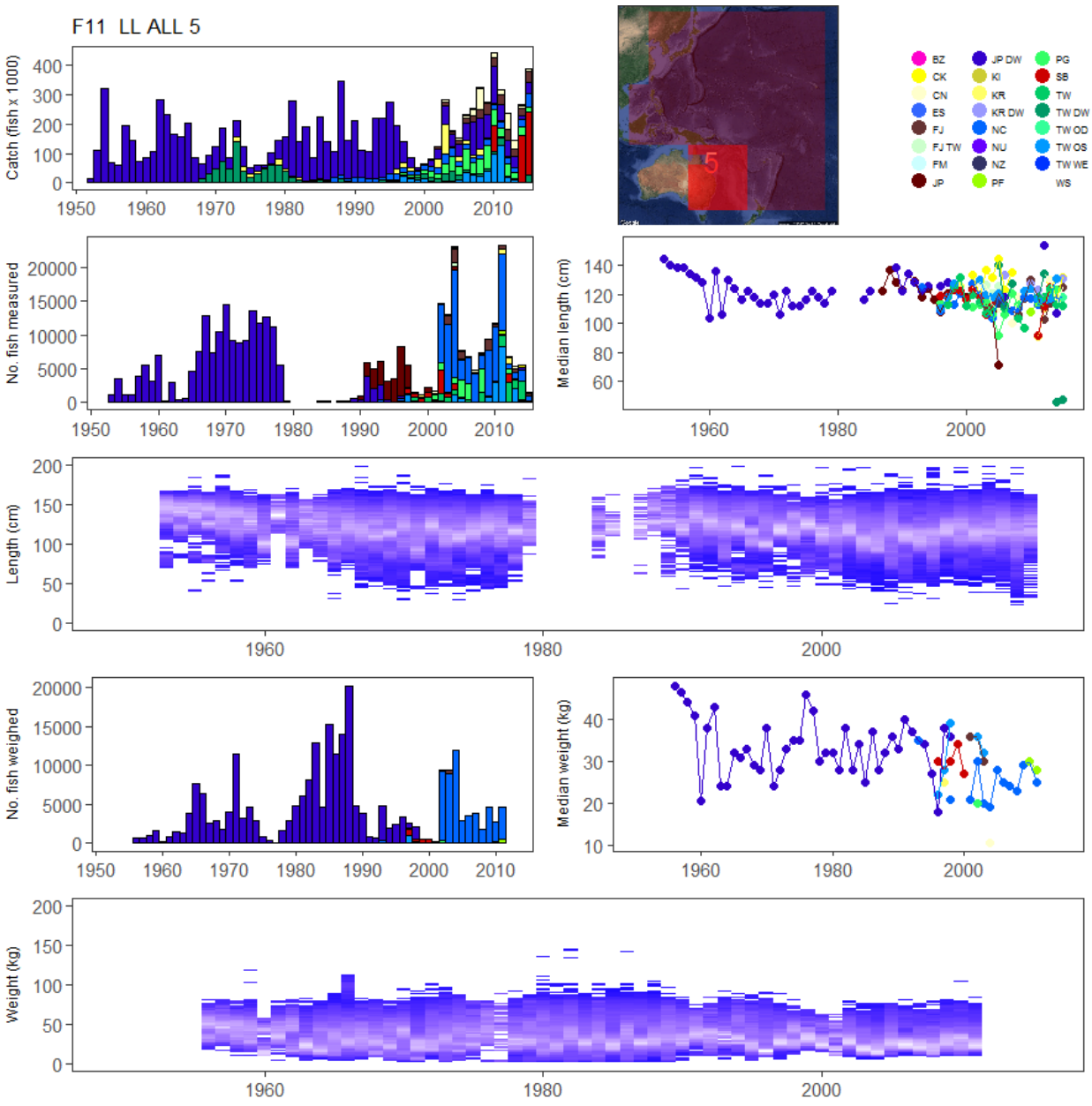

Figure 59: Summary of raw data available for YFT fishery 11.

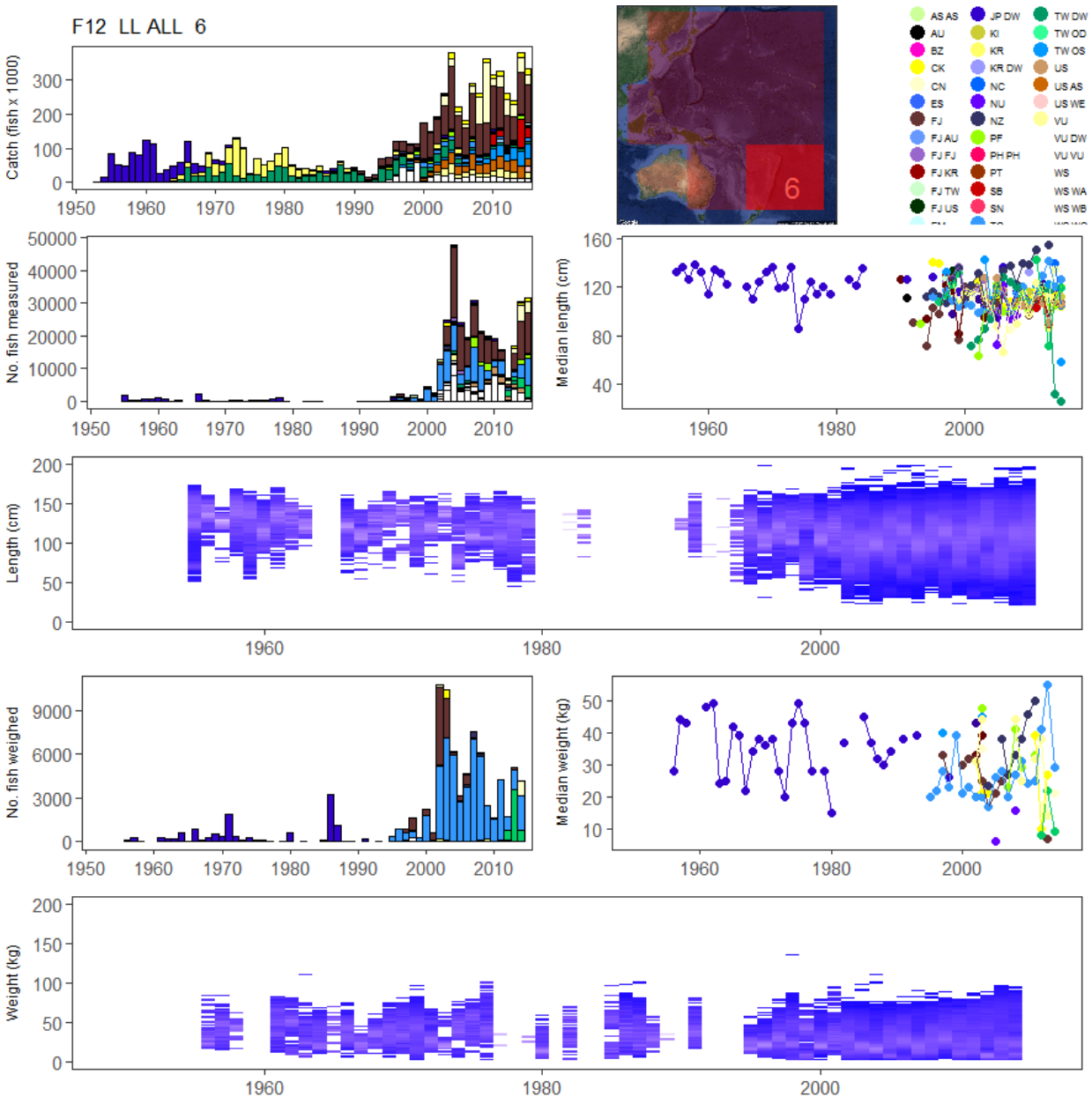

Figure 60: Summary of raw data available for YFT fishery 12.

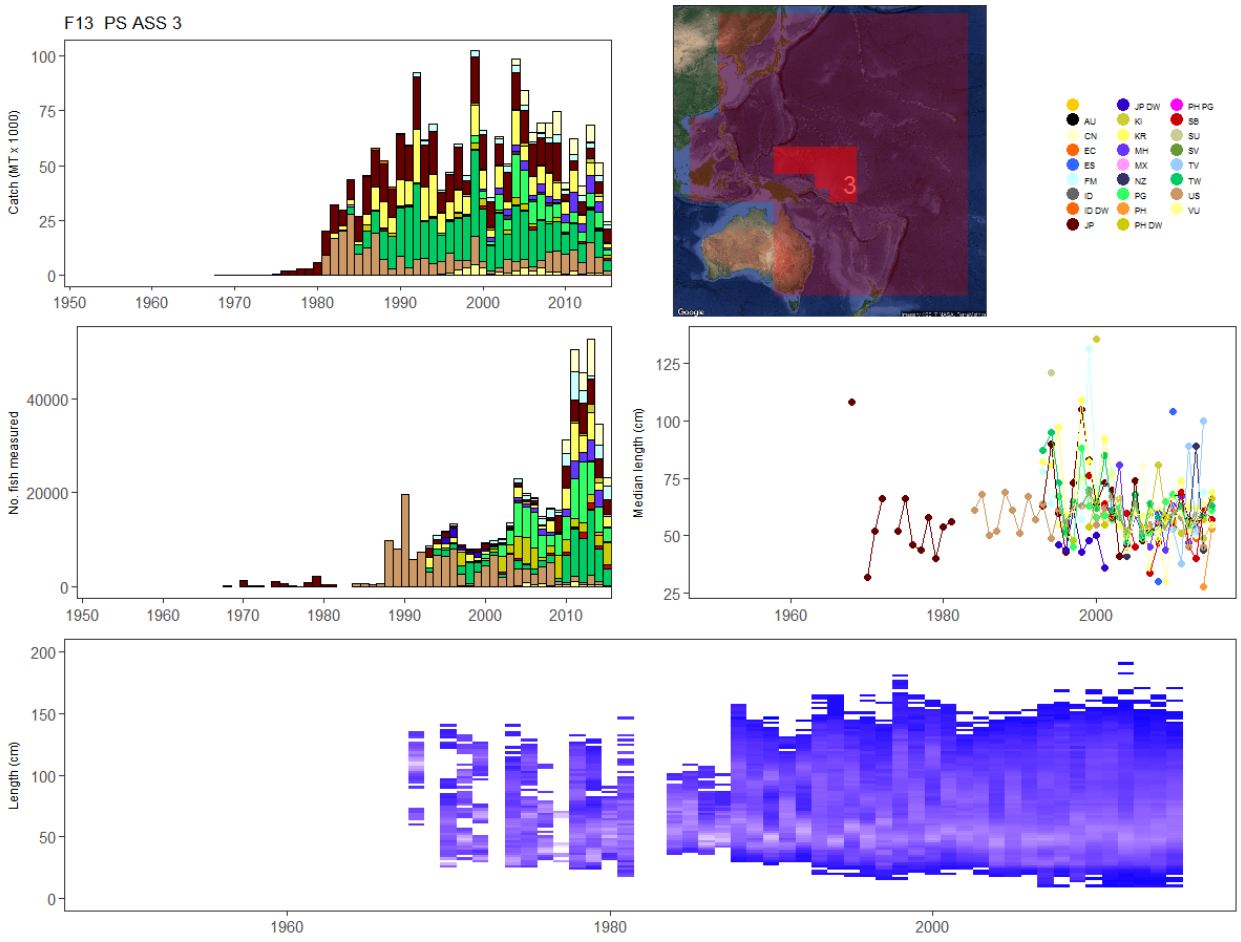

Figure 61: Summary of raw data available for YFT fishery 13.

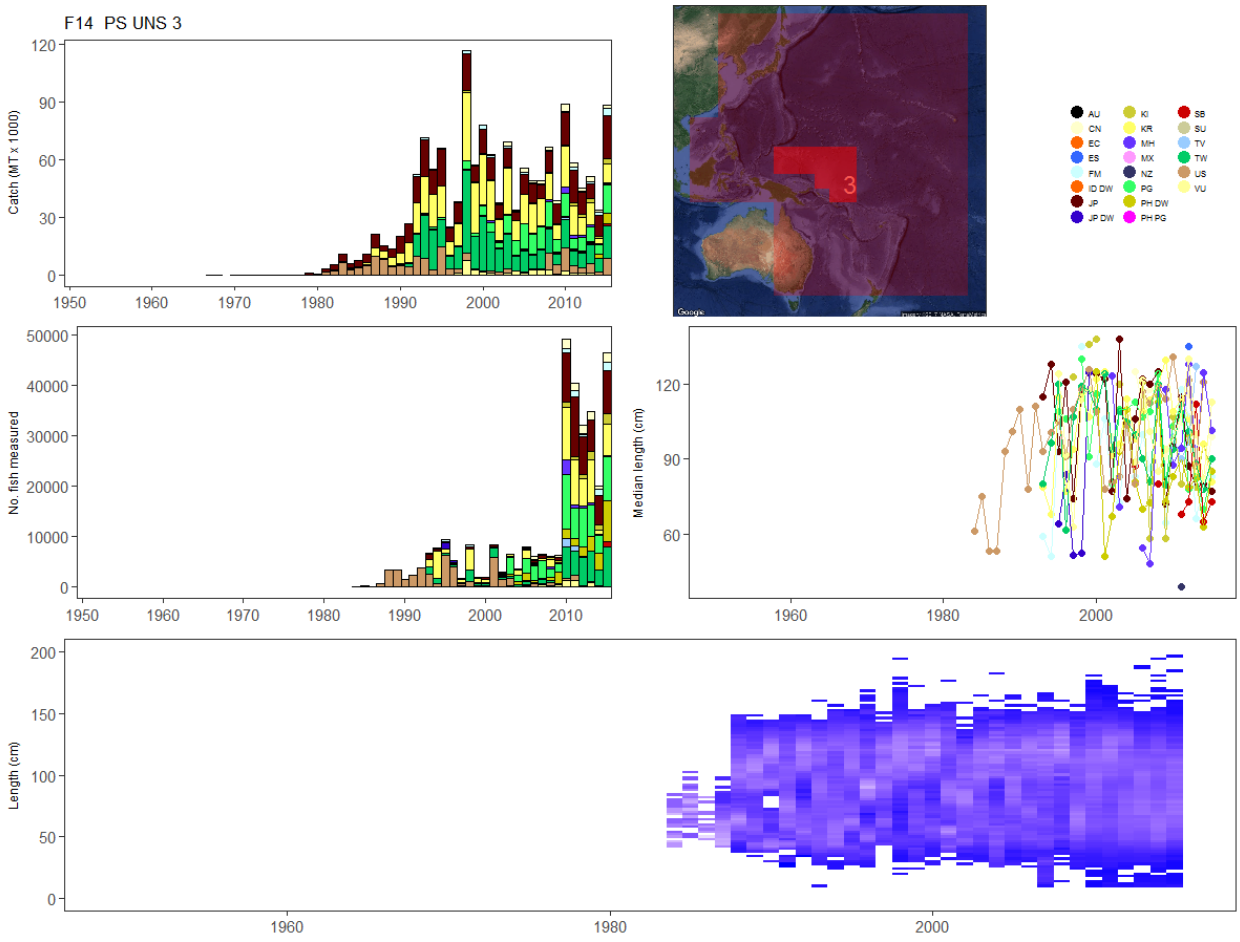

Figure 62: Summary of raw data available for YFT fishery 14.

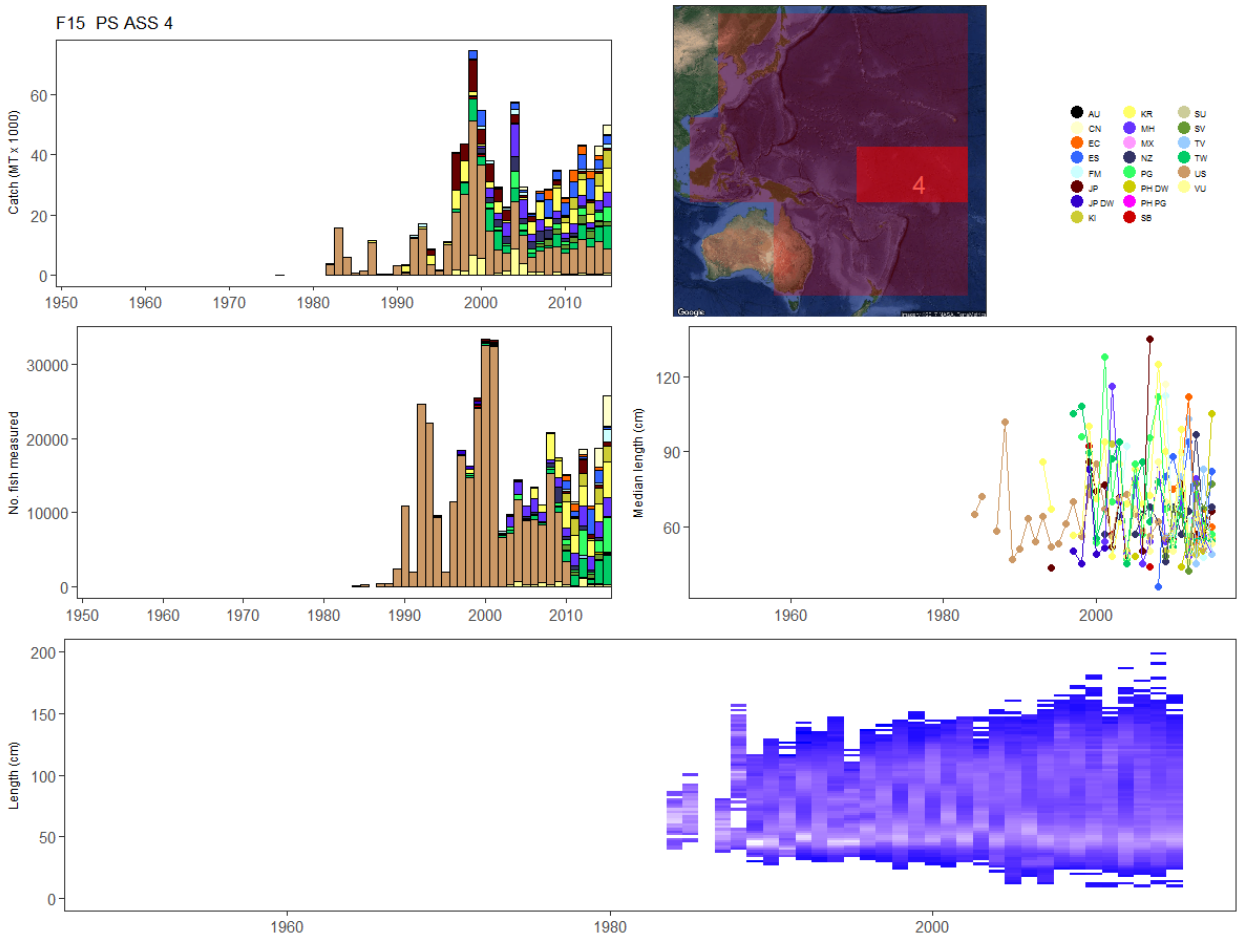

Figure 63: Summary of raw data available for YFT fishery 15.

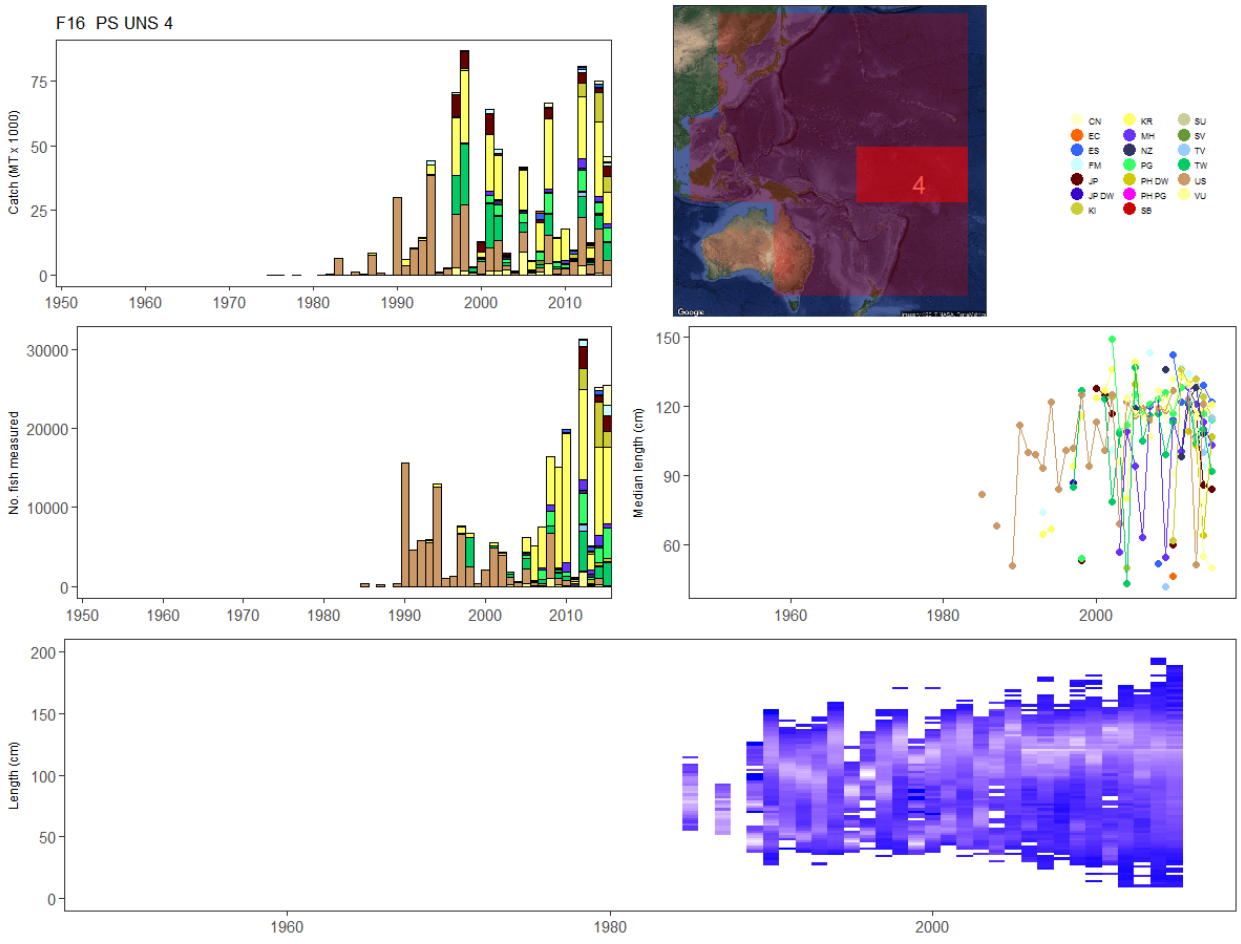

Figure 64: Summary of raw data available for YFT fishery 16.

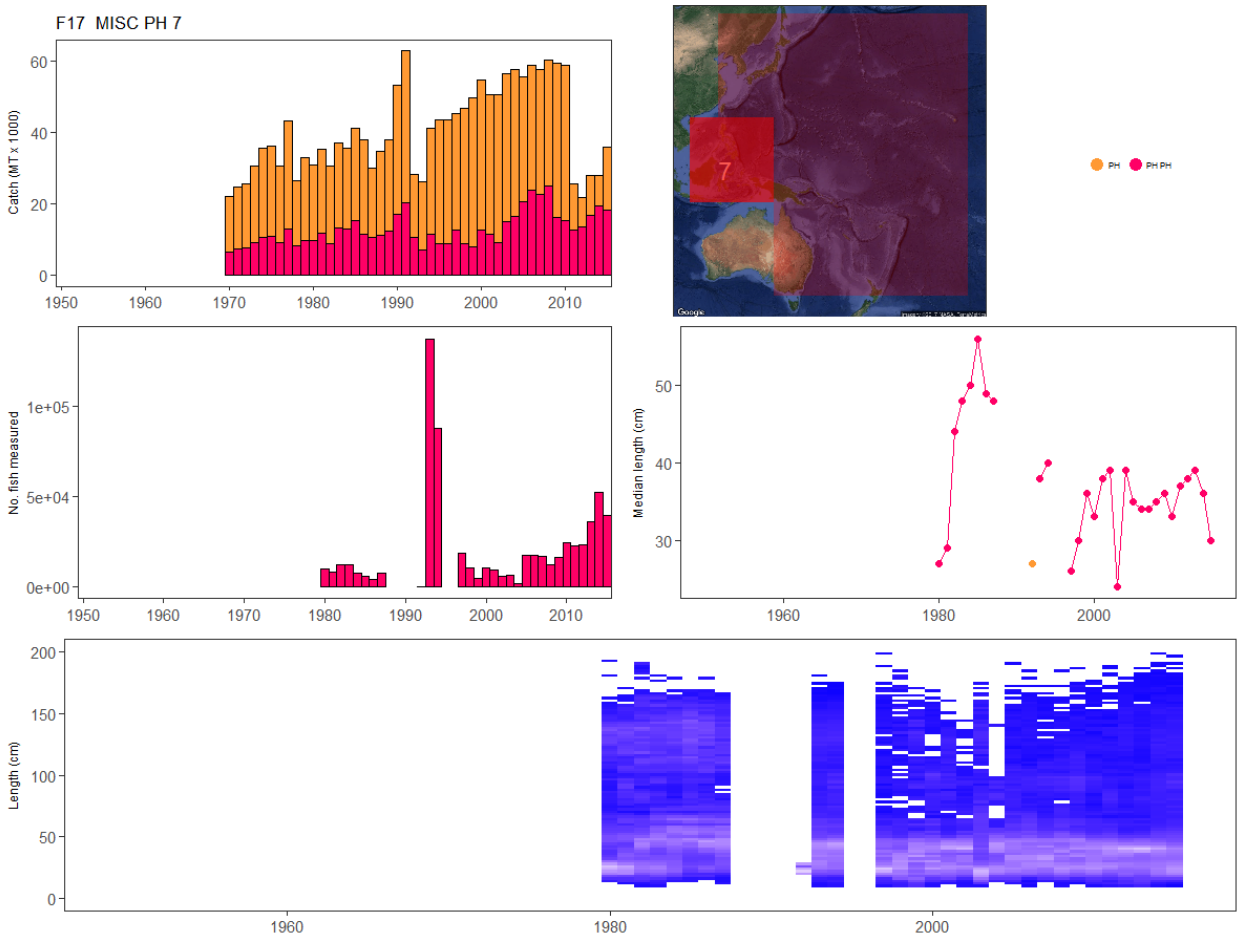

Figure 65: Summary of raw data available for YFT fishery 17.

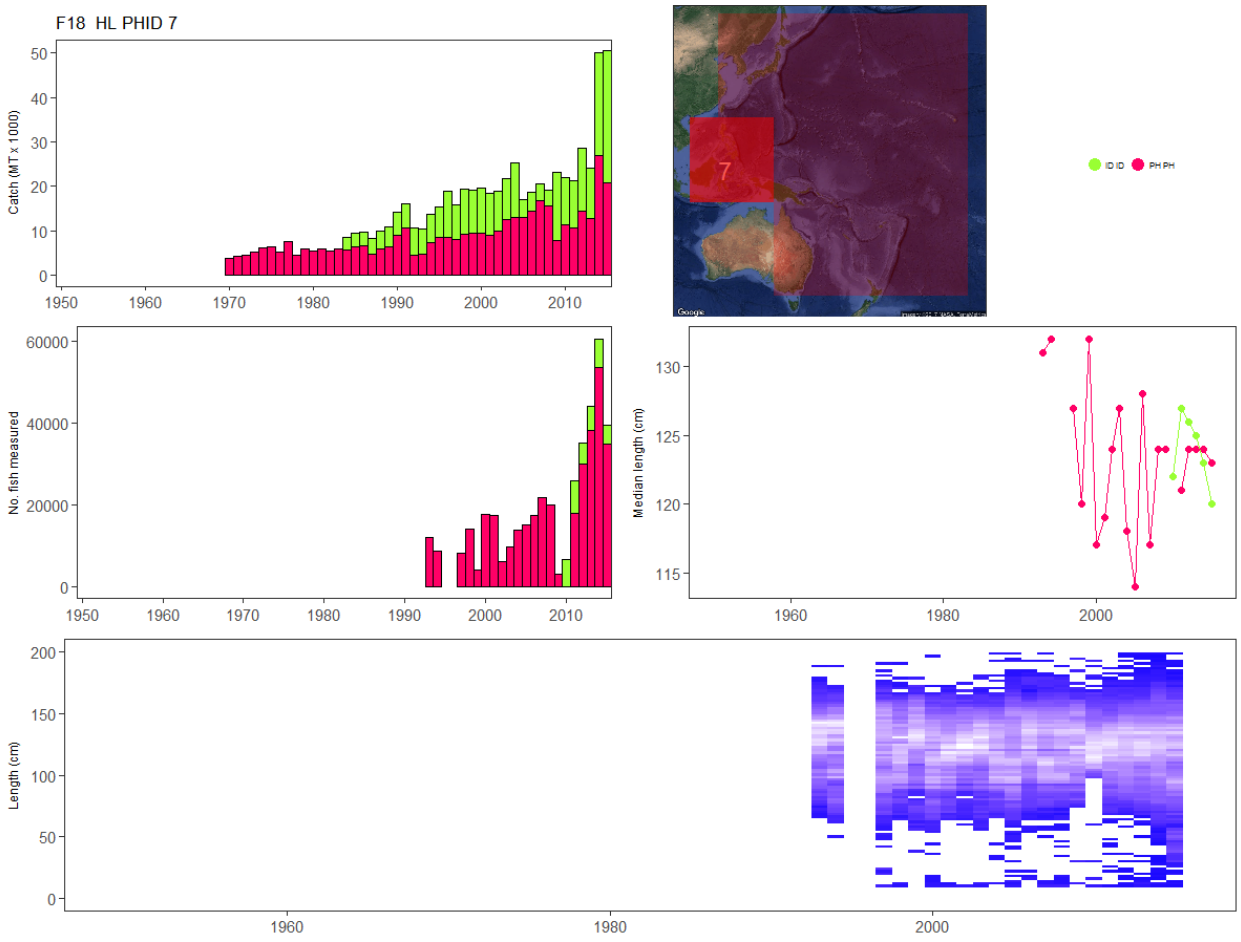

Figure 66: Summary of raw data available for YFT fishery 18.

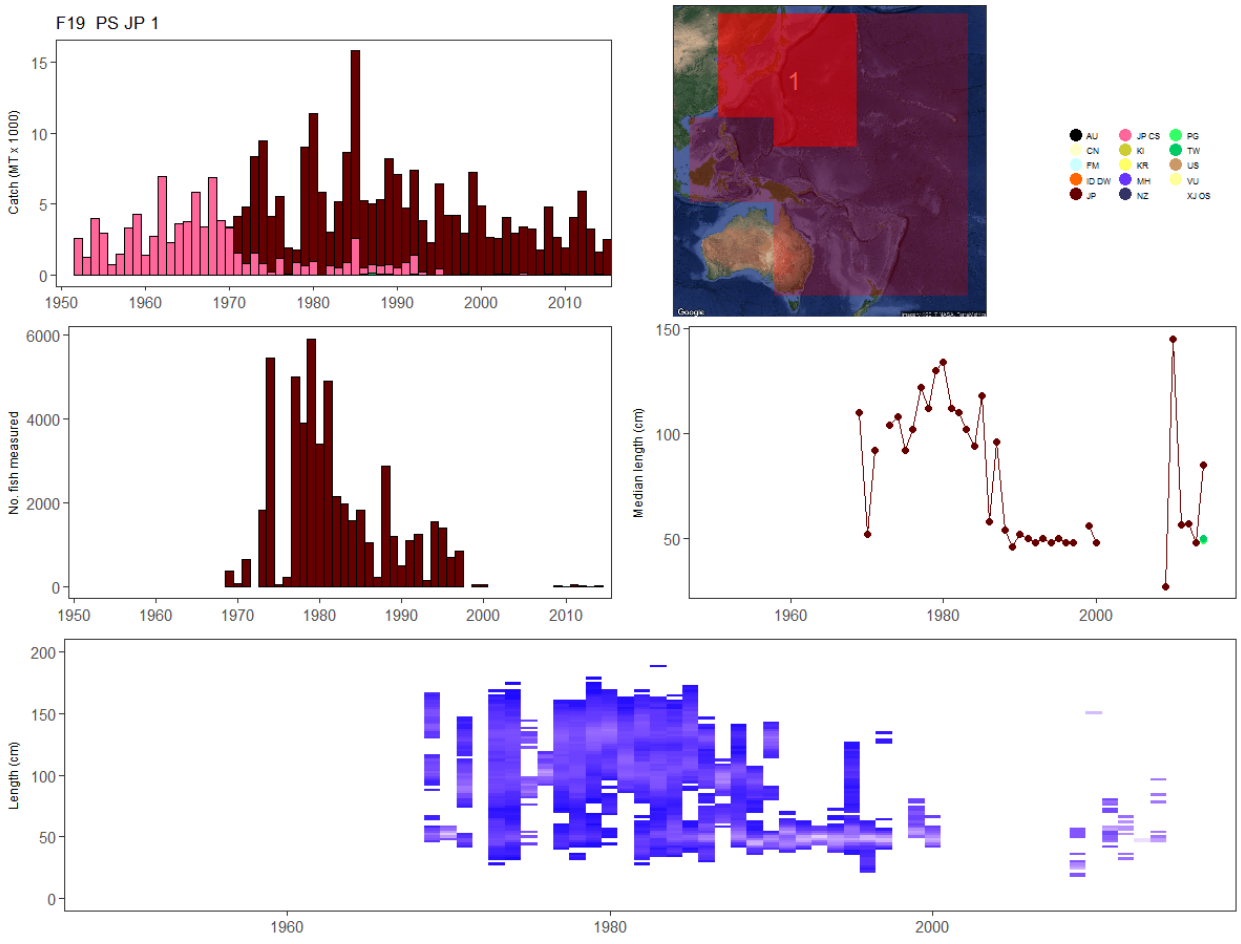

Figure 67: Summary of raw data available for YFT fishery 19.

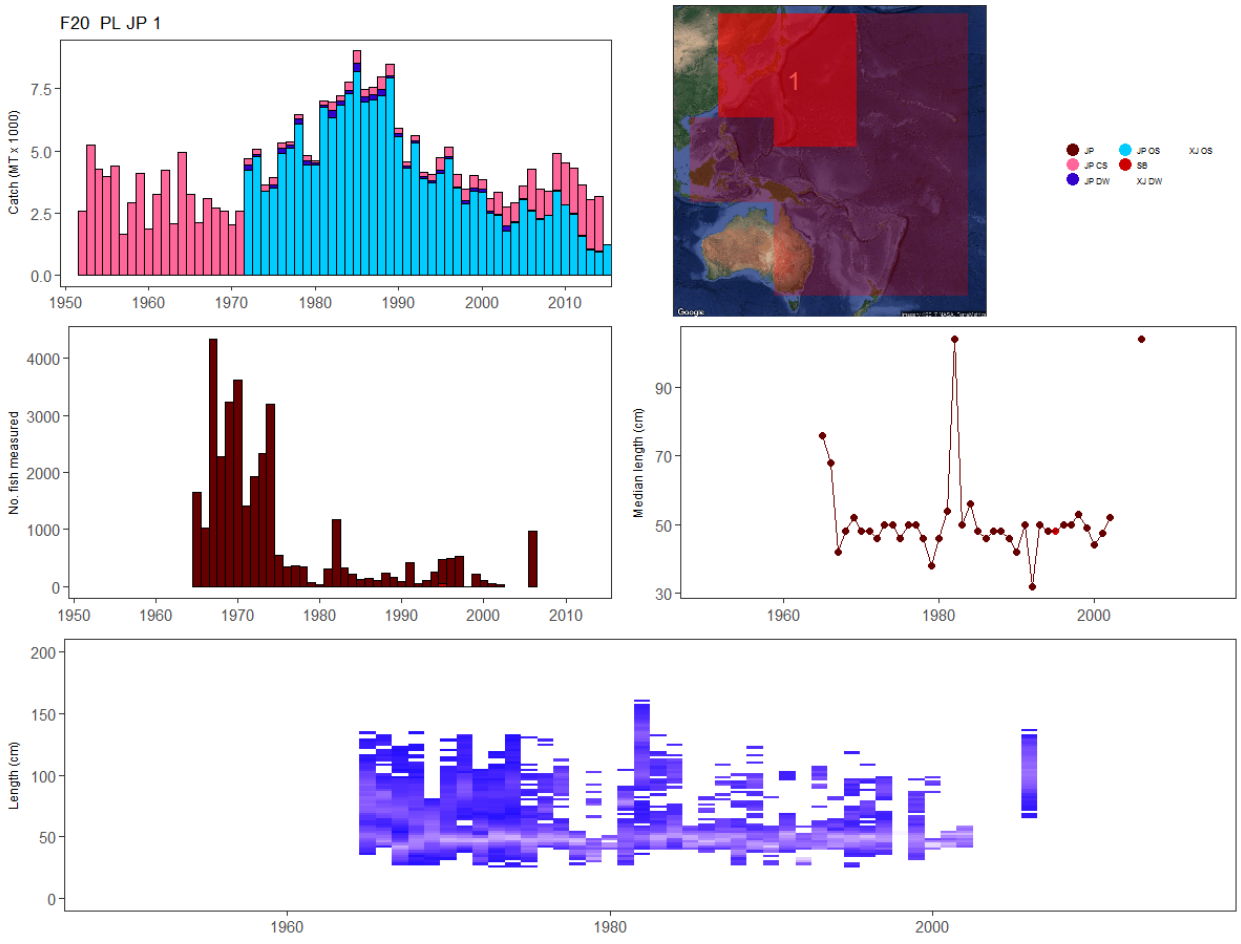

Figure 68: Summary of raw data available for YFT fishery 20.

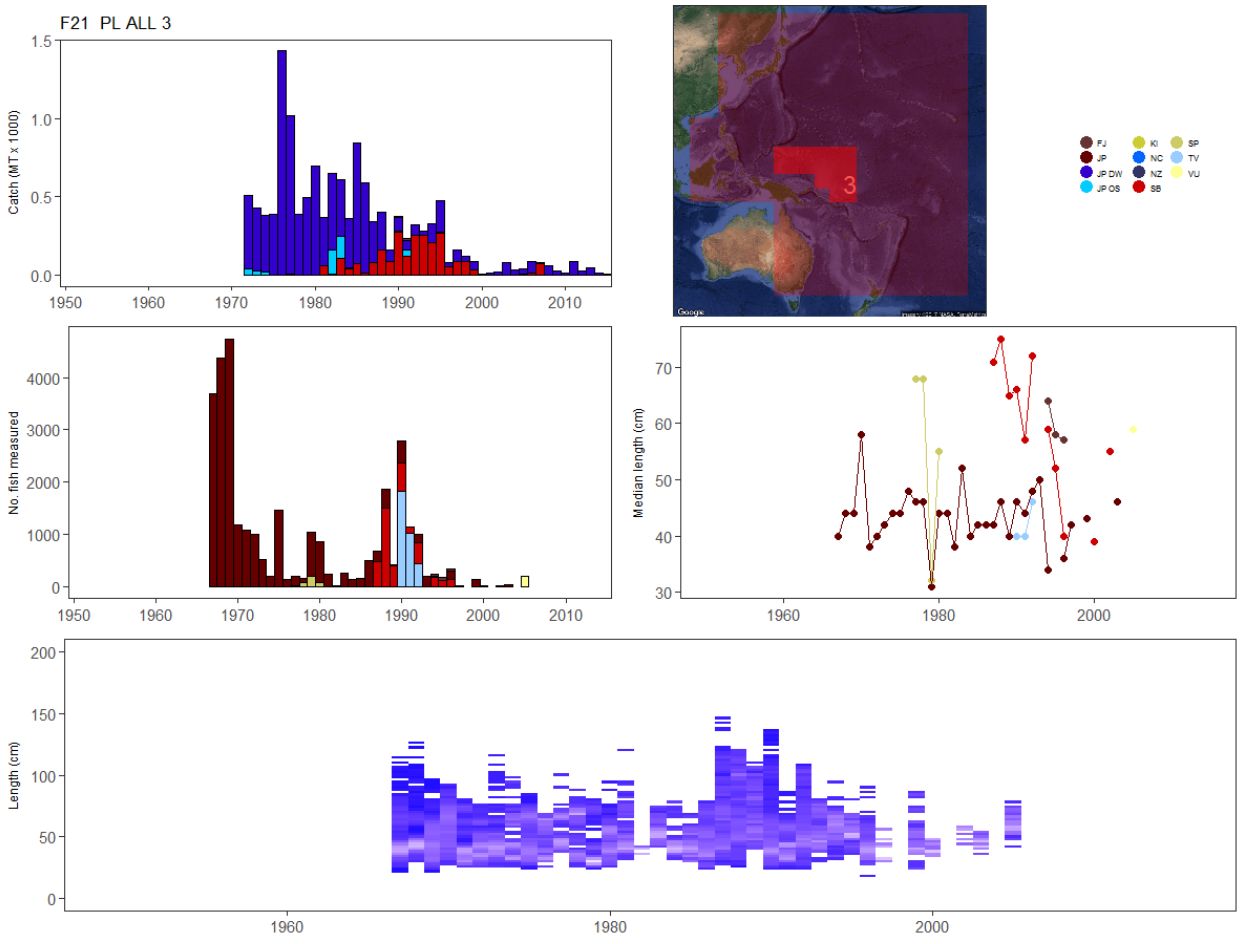

Figure 69: Summary of raw data available for YFT fishery 21.

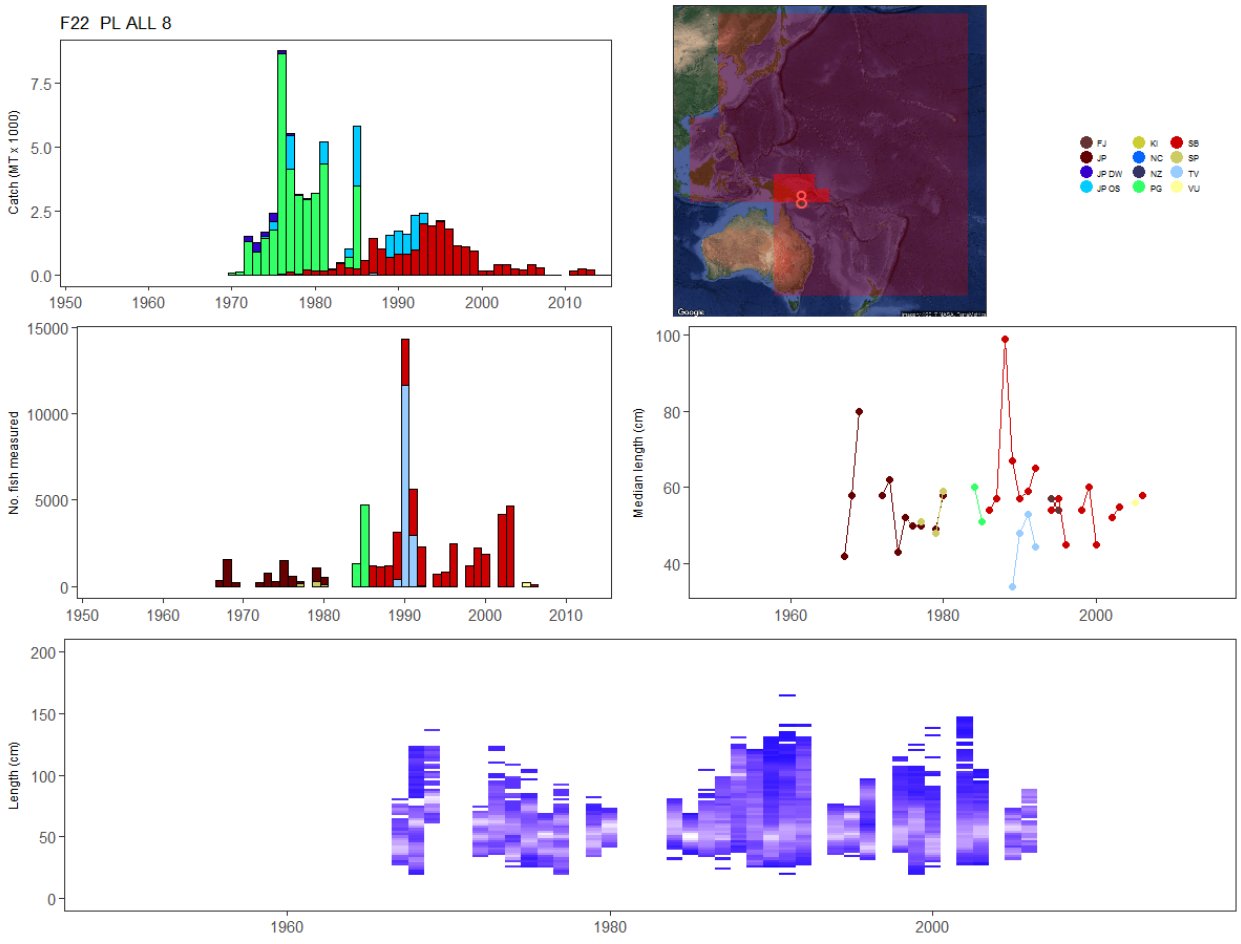

Figure 70: Summary of raw data available for YFT fishery 22.

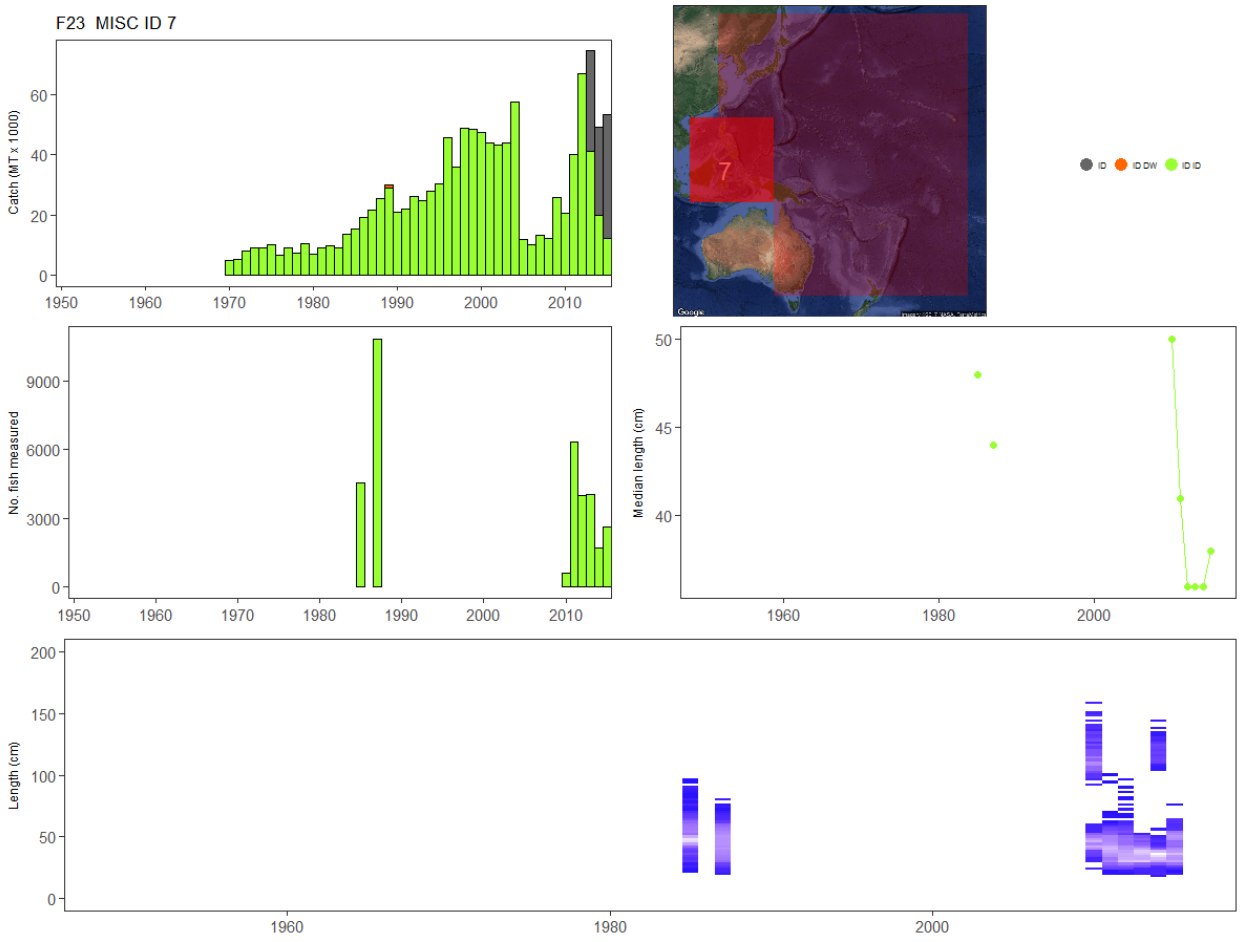

Figure 71: Summary of raw data available for YFT fishery 23.

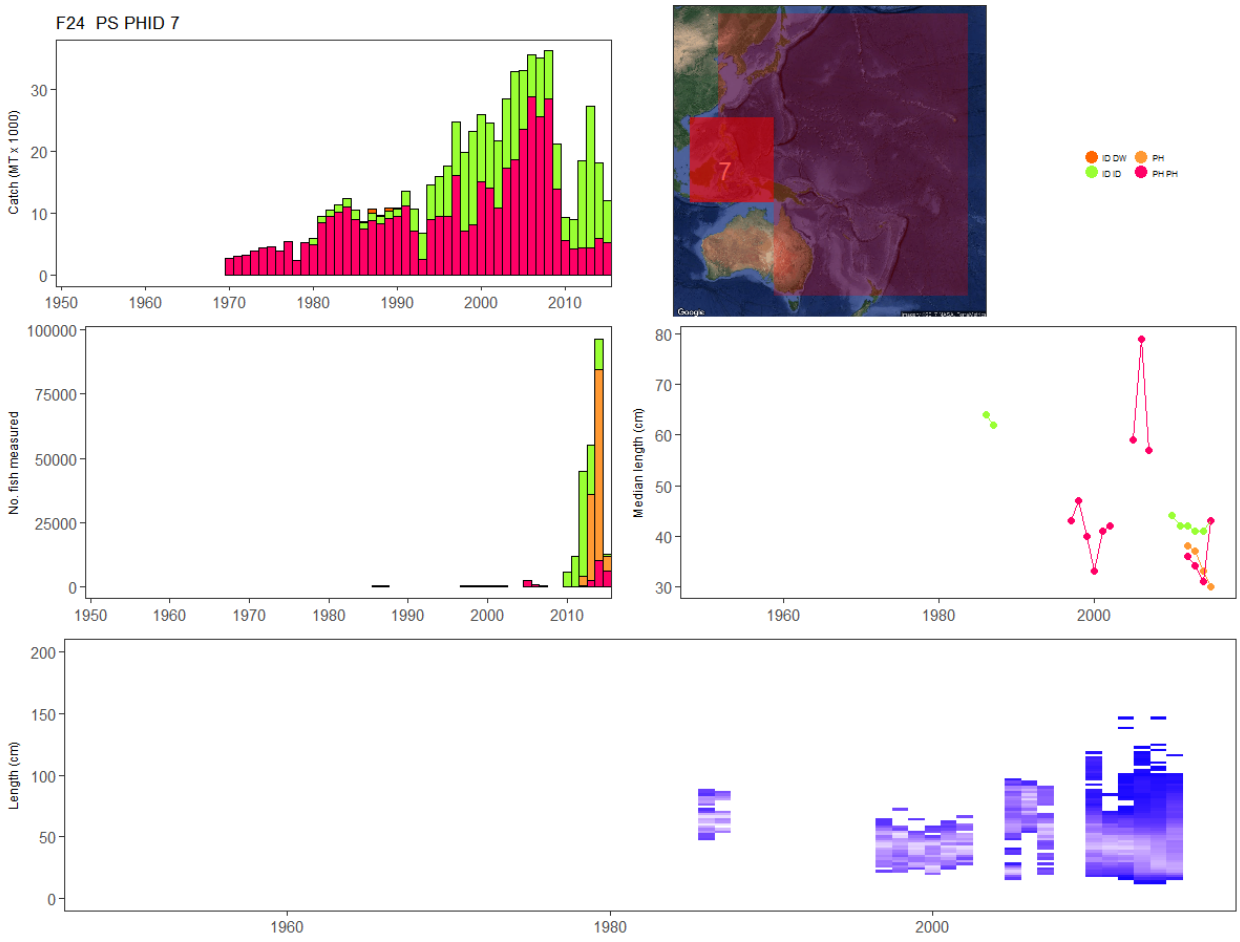

Figure 72: Summary of raw data available for YFT fishery 24.

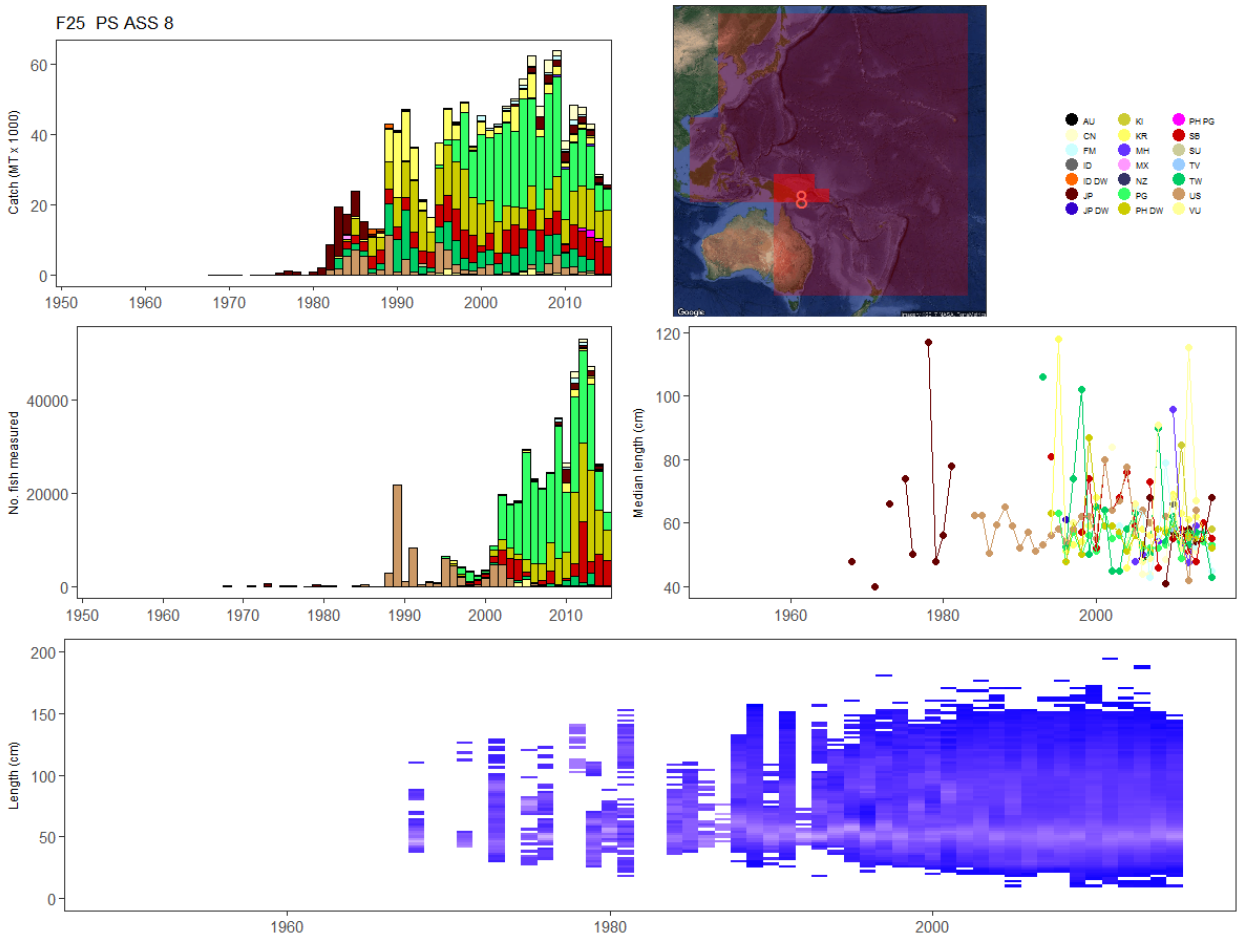

Figure 73: Summary of raw data available for YFT fishery 25.

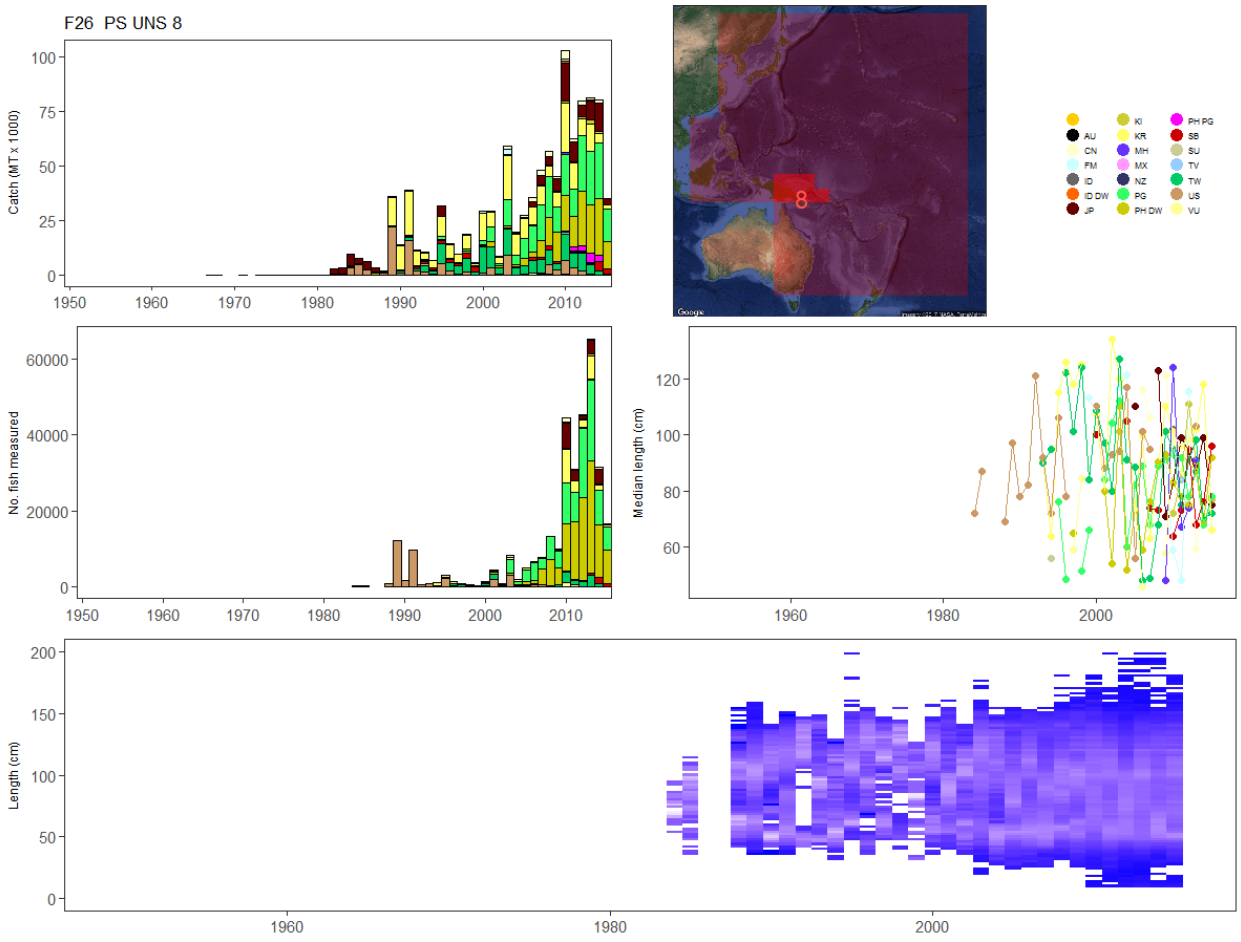

Figure 74: Summary of raw data available for YFT fishery 26.

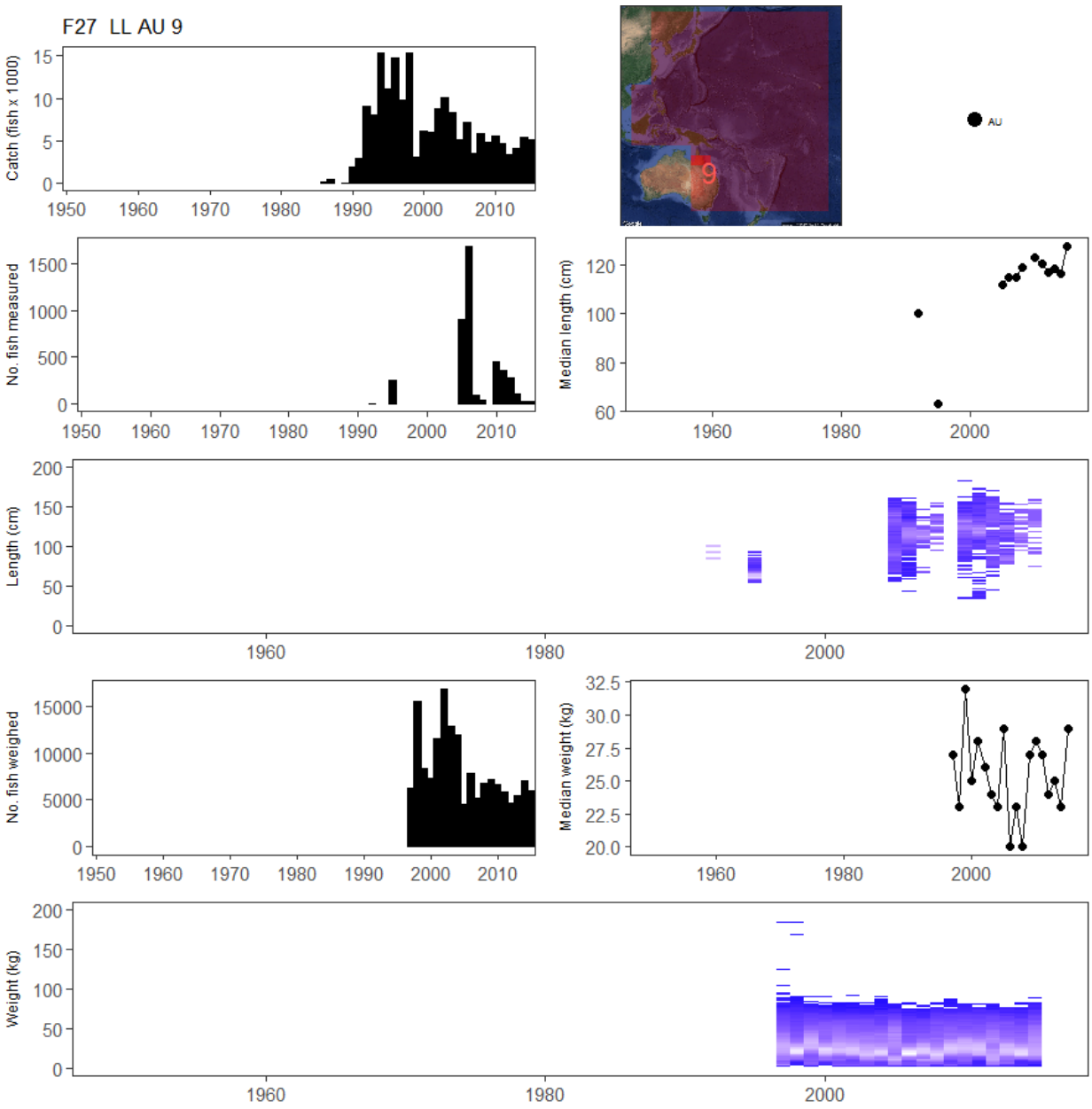

Figure 75: Summary of raw data available for YFT fishery 27.

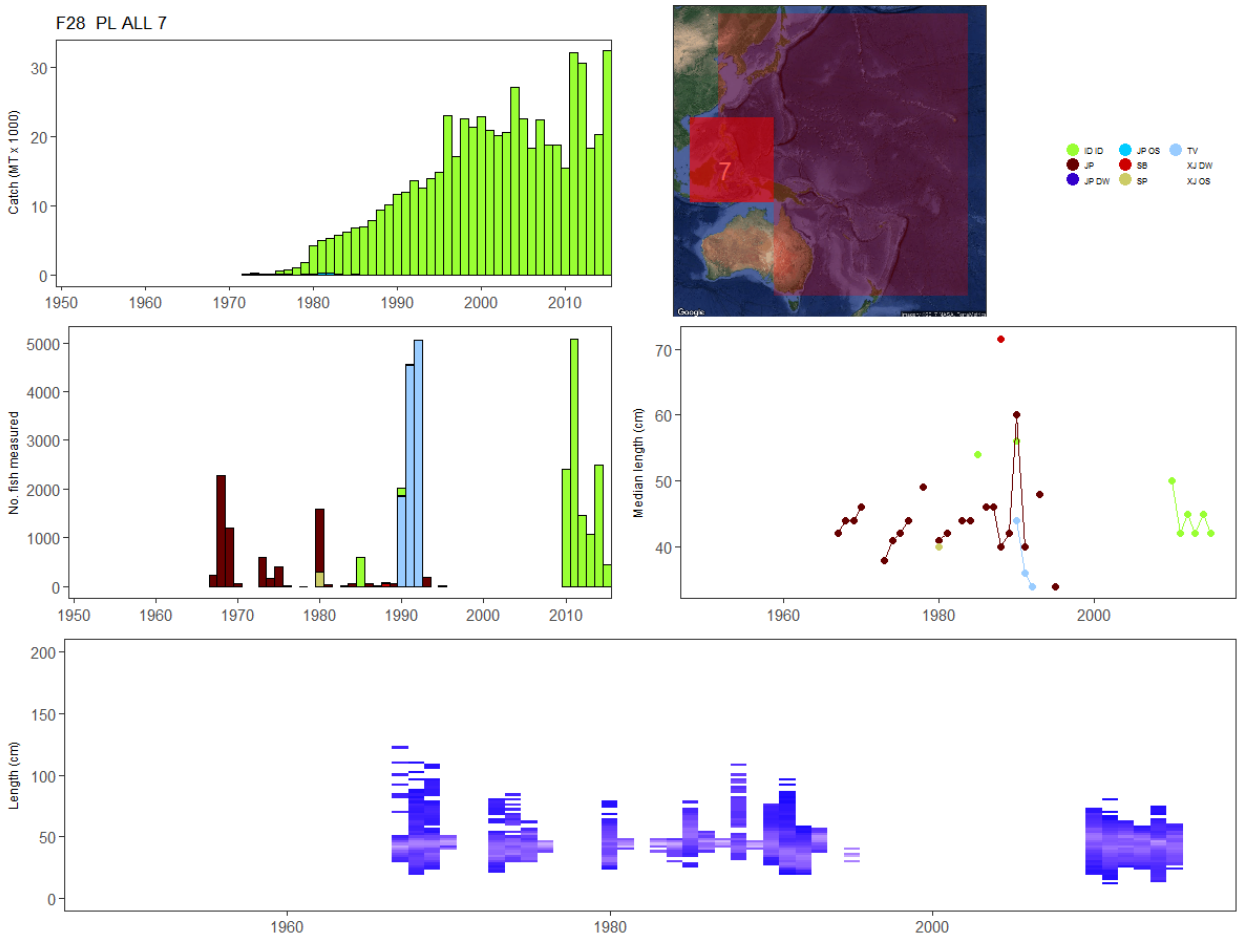

Figure 76: Summary of raw data available for YFT fishery 28.

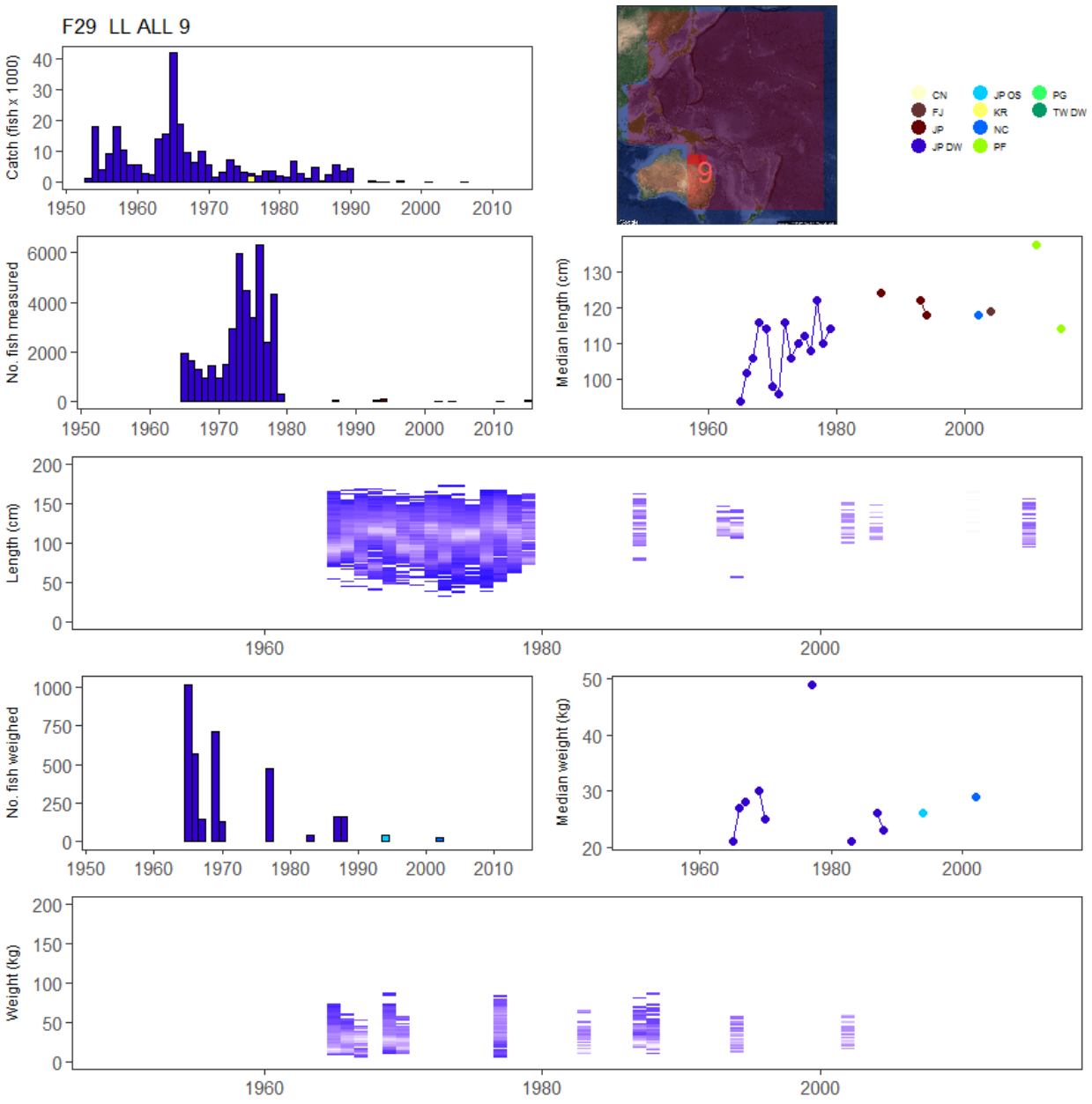

Figure 77: Summary of raw data available for YFT fishery 29.

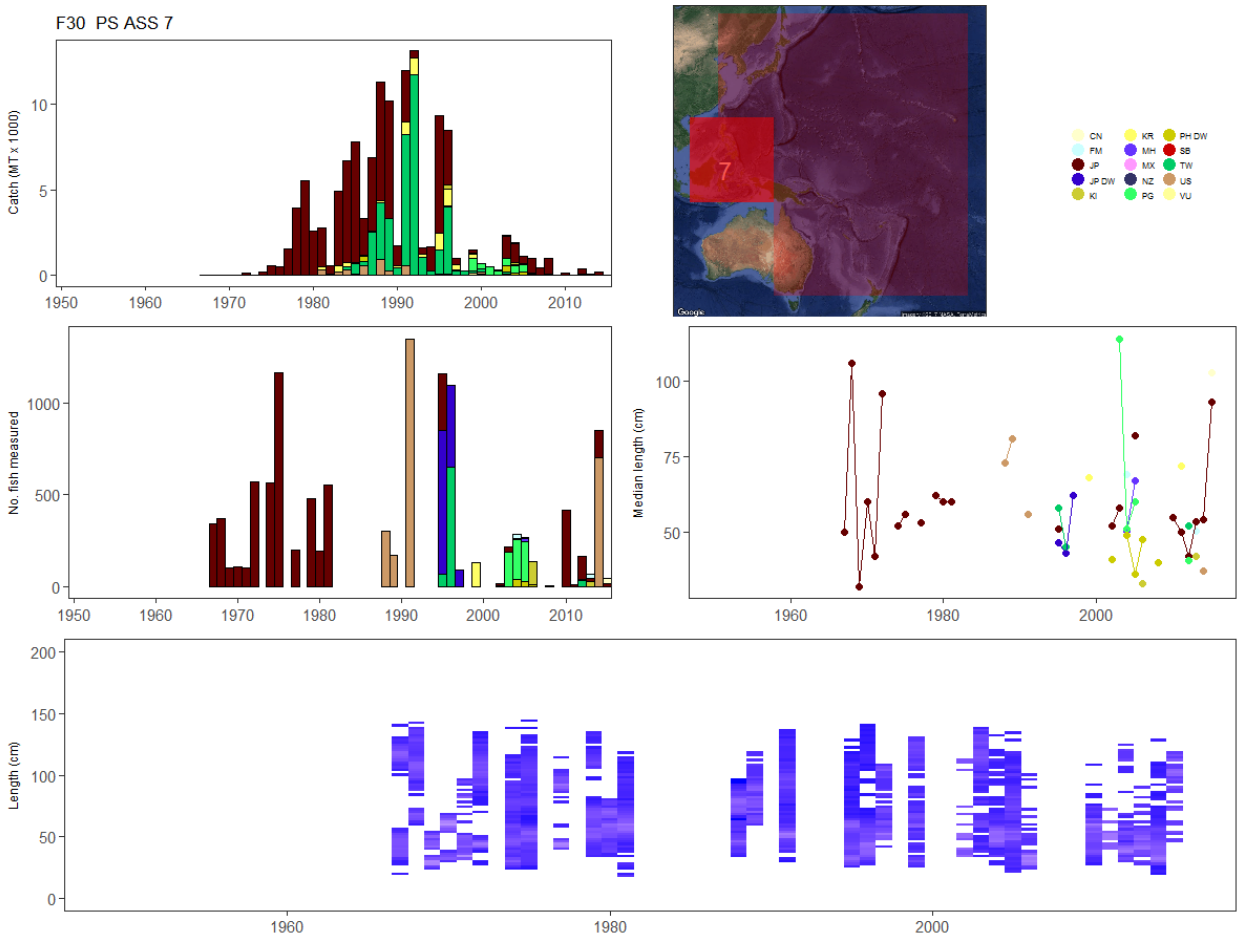

Figure 78: Summary of raw data available for YFT fishery 30.

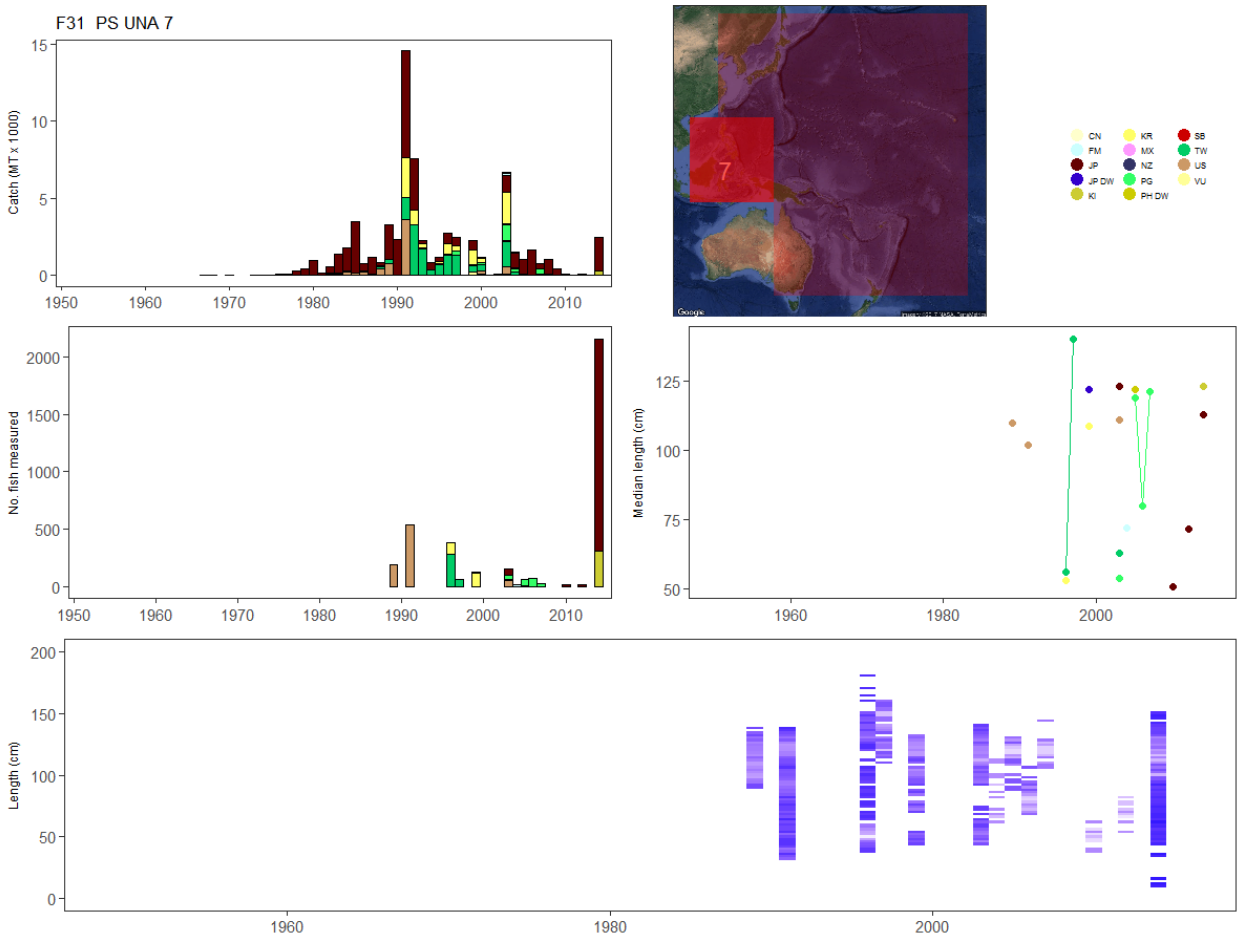

Figure 79: Summary of raw data available for YFT fishery 31.

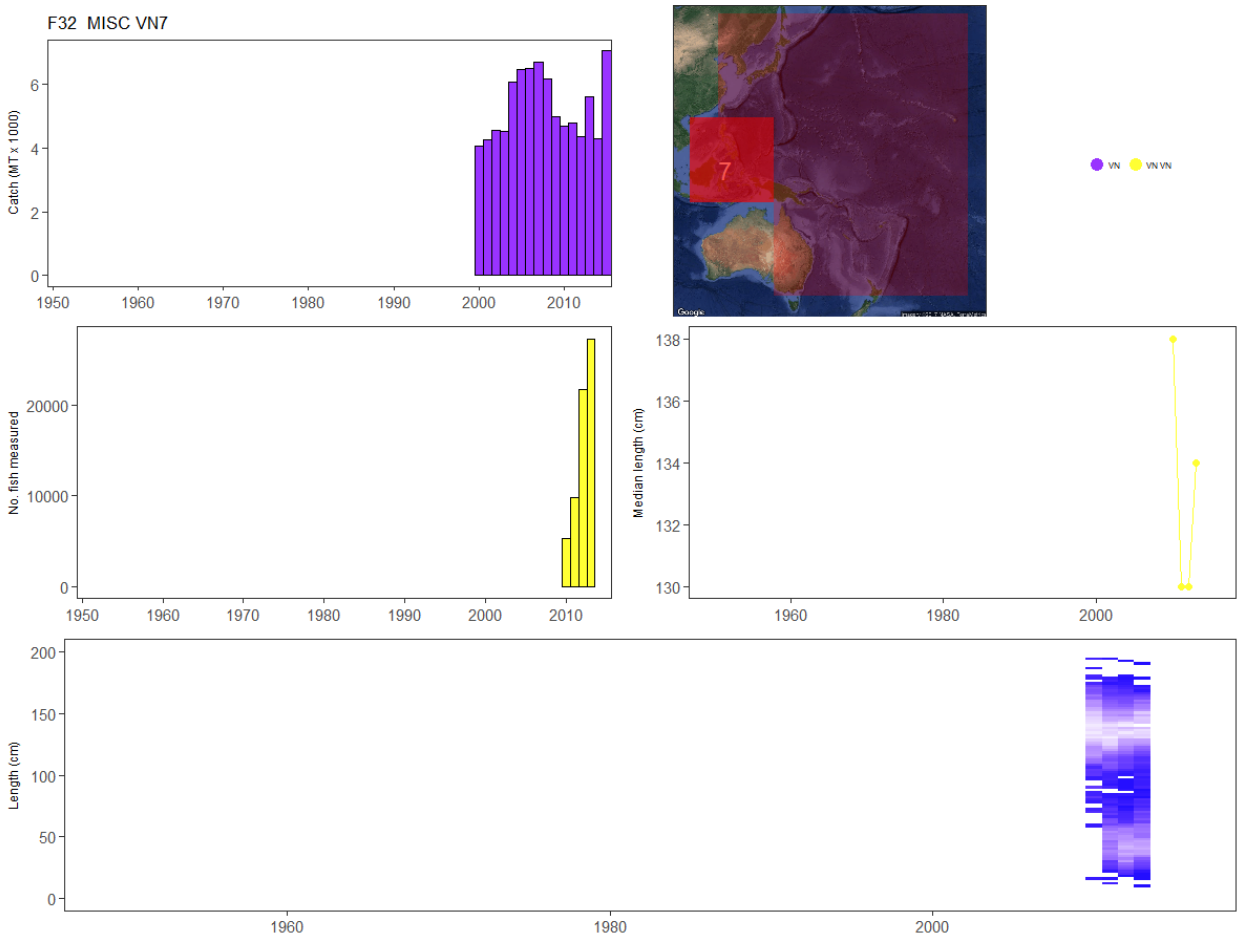

Figure 80: Summary of raw data available for YFT fishery 32.

Diagnostic plots

The following plots show several variations of diagnostics for the standardised CPUE analyses used in the diagnostic case models for the BET (Figures 81–96) and YFT (Figures 97–112) stock assessments. Plots are ordered firstly by species (BET then YFT), then region (1–8) and finally component (binomial and lognormal). The top left panel for the binomial model is the observed value vs the fitted value, while for the lognormal component they are the observed CPUE distribution with the simulated distribution based on the model fit. The top right panels are qqplots of the the model fit, which are quantile residuals for the binomial component and standardised residuals for the lognormal component. The second from top panel on the left is the plot of residuals vs fitted values for both components. All other panels display the estimated distribution of residuals (quantile residuals for binomial and standardised residuals for lognormal) by the potential factor levels - cell, cluster, and year-quarter levels (which were fitted in the model) and vessels (which were excluded).

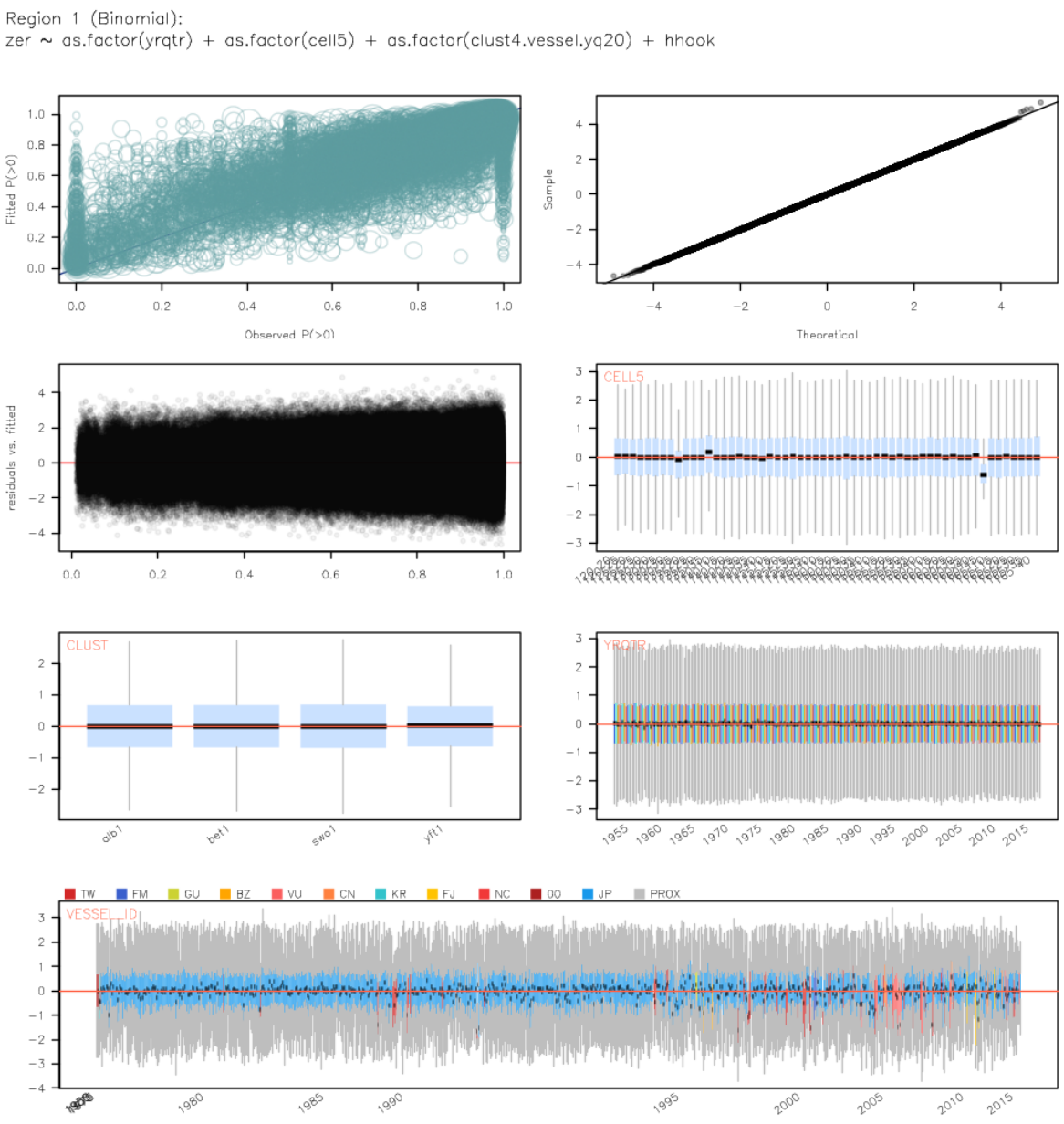

Figure 81: Diagnostics for the binomial GLM fitted to the BET CPUE data for region 1.

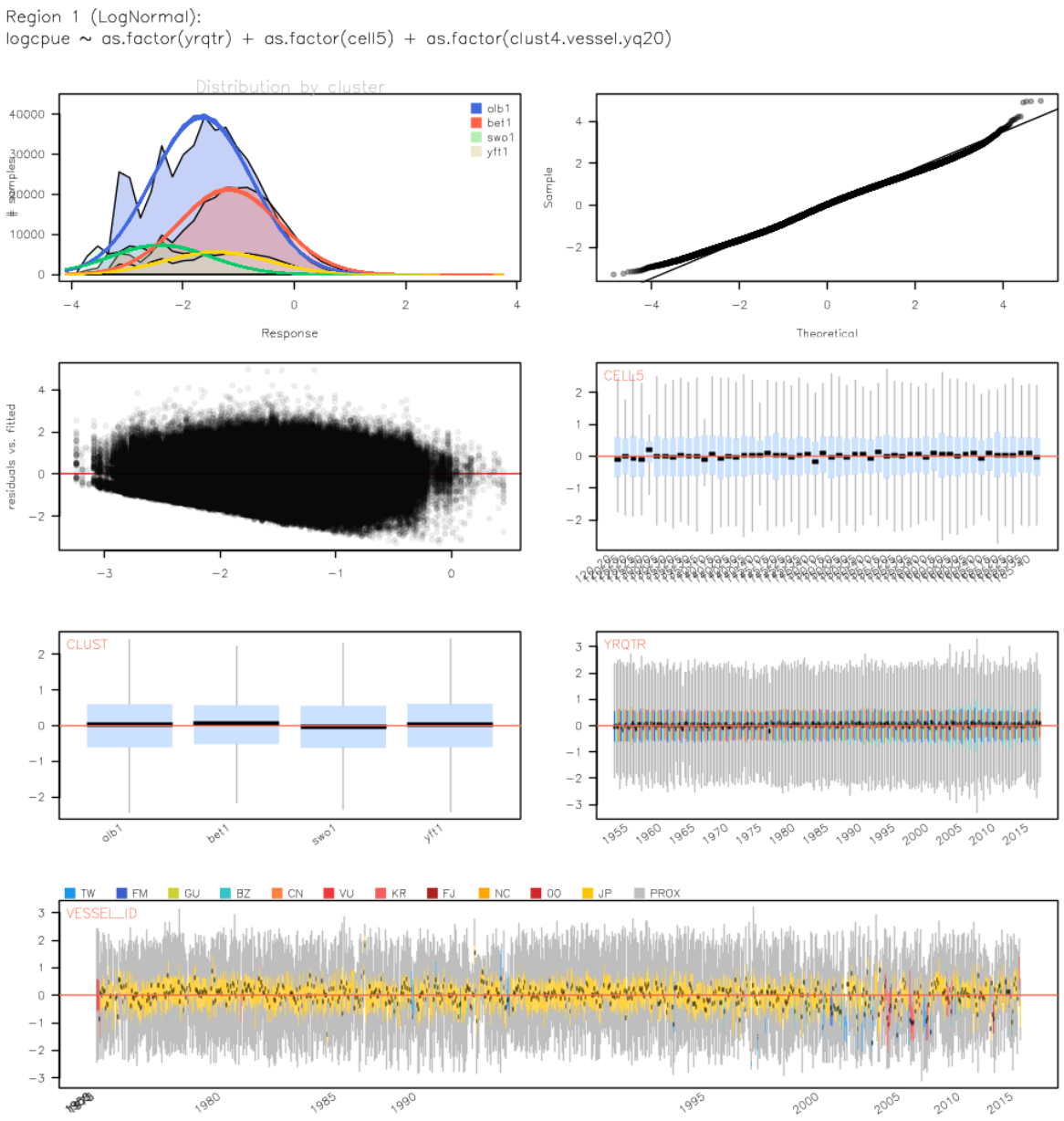

Figure 82: Diagnostics for the log normal GLM fitted to the BET CPUE data for region 1.

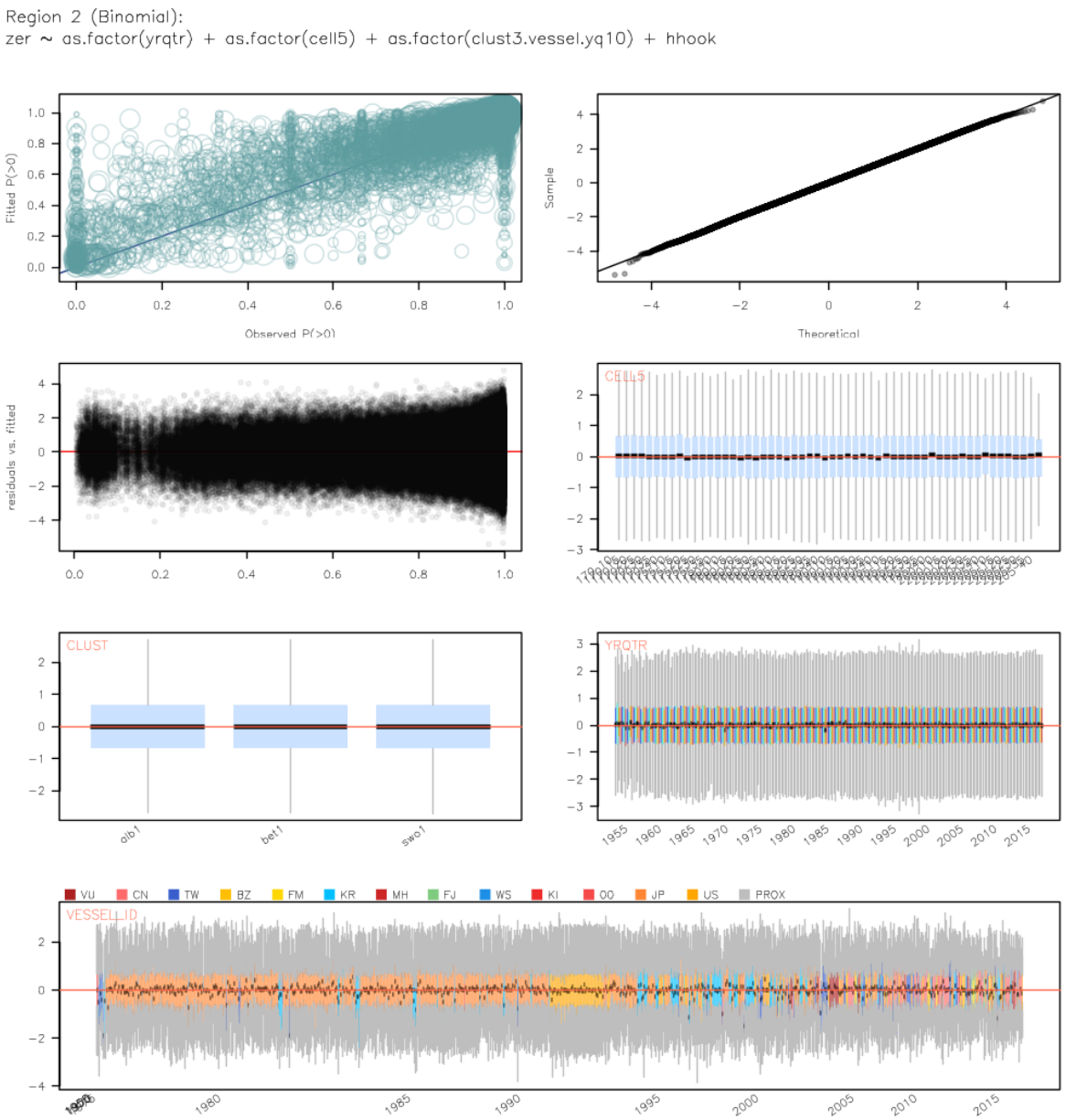

Figure 83: Diagnostics for the binomial GLM fitted to the BET CPUE data for region 2.

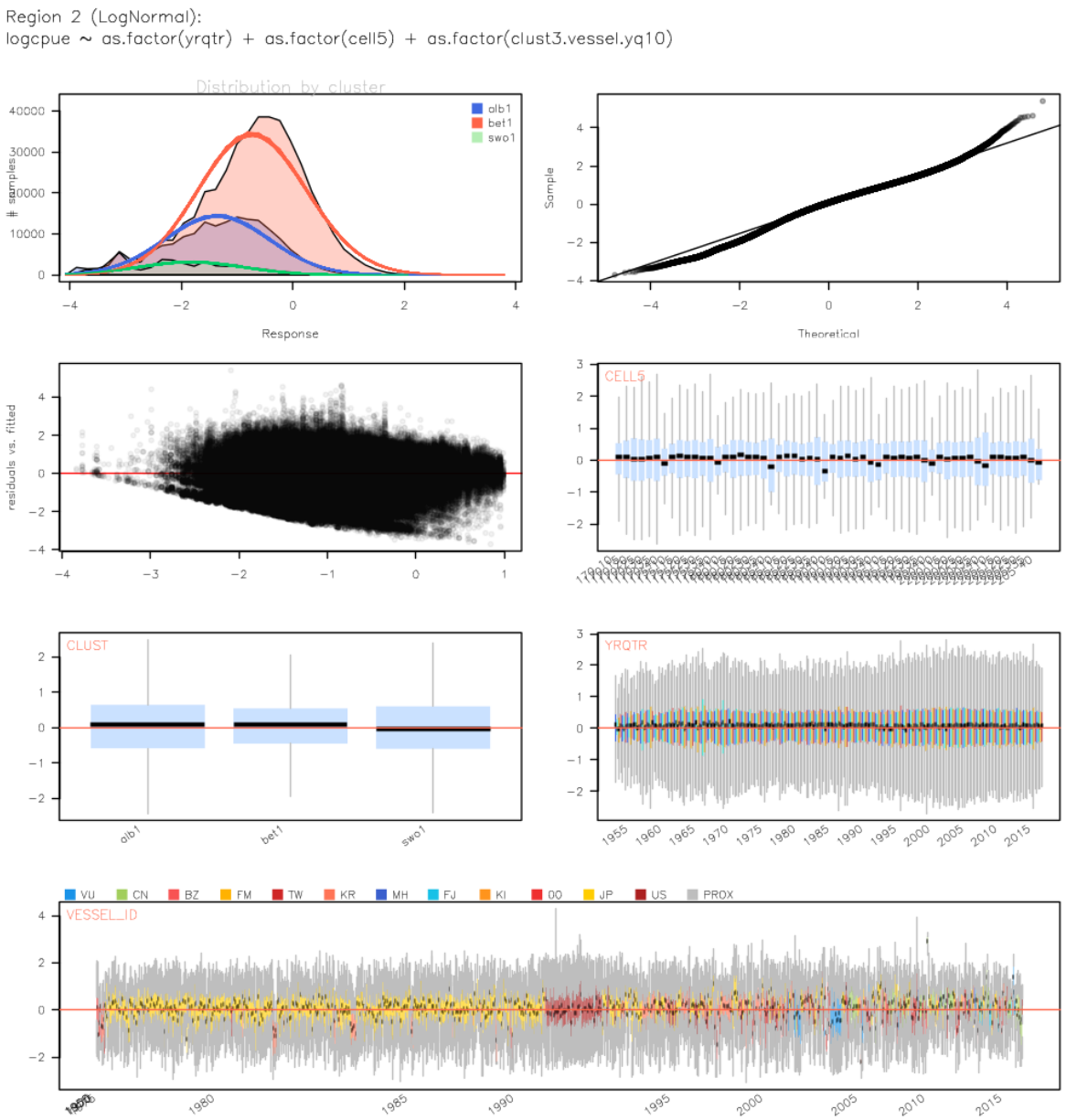

Figure 84: Diagnostics for the log normal GLM fitted to the BET CPUE data for region 2.

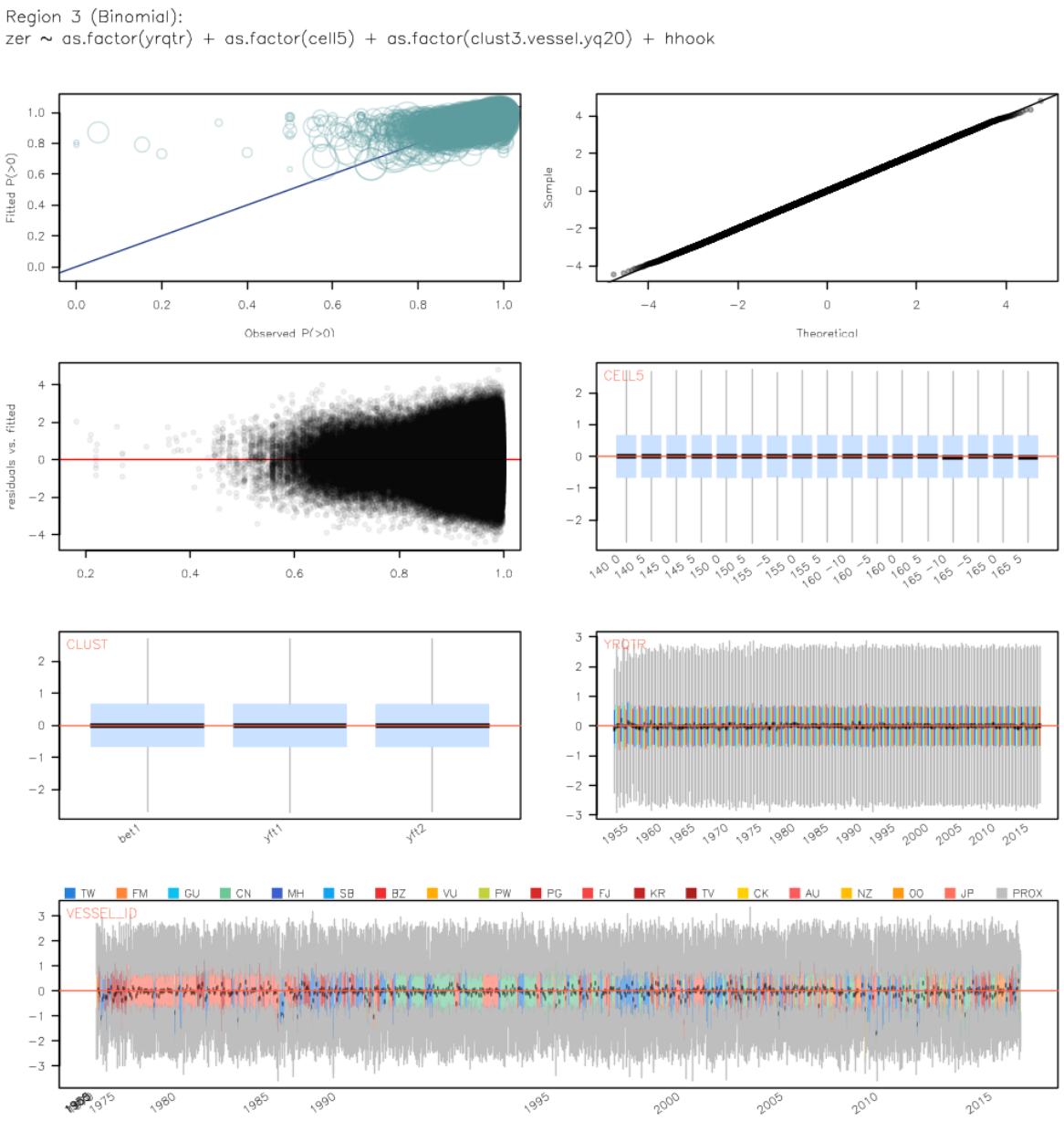

Figure 85: Diagnostics for the binomial GLM fitted to the BET CPUE data for region 3.

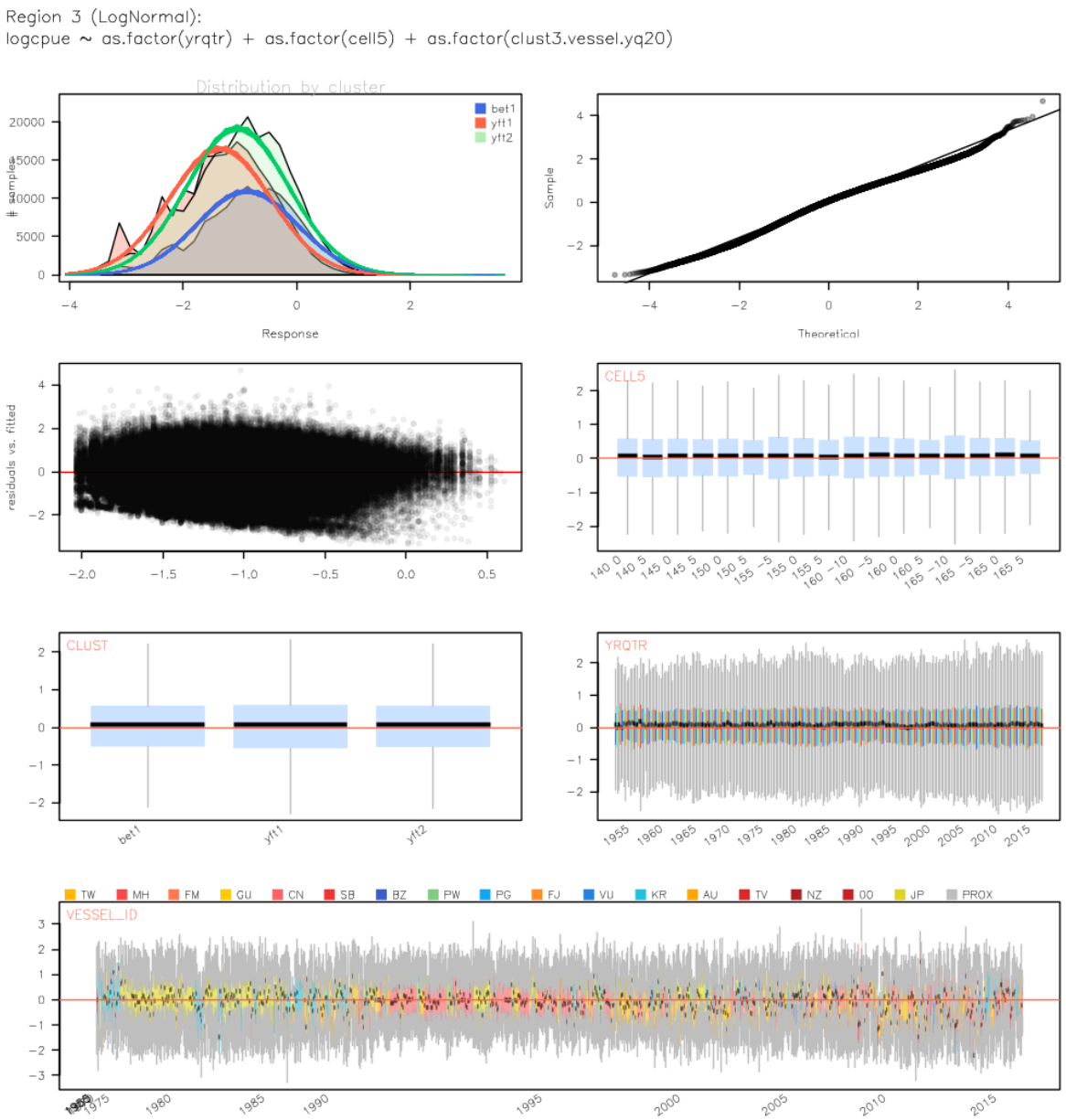

Figure 86: Diagnostics for the log normal GLM fitted to the BET CPUE data for region 3.

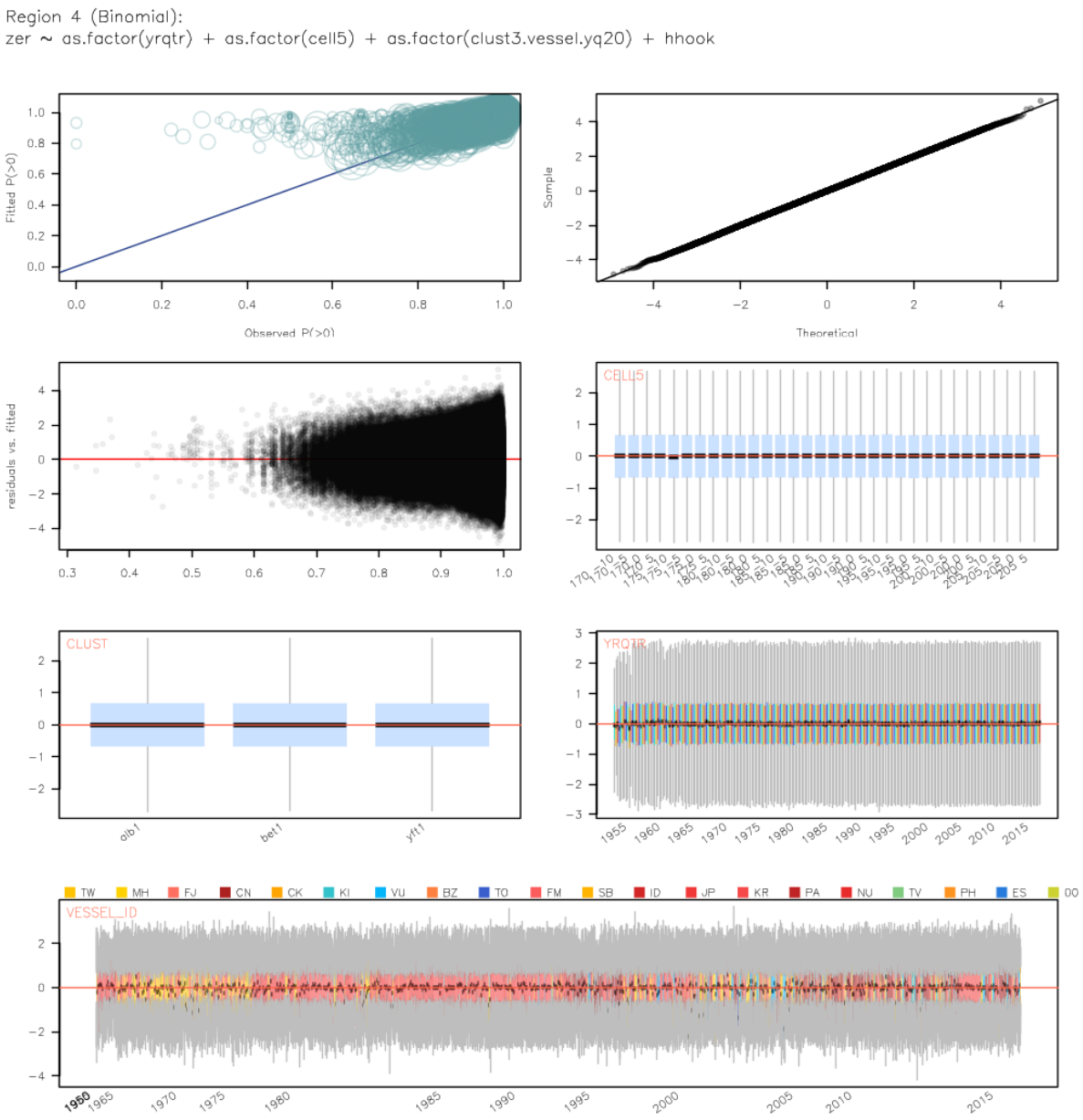

Figure 87: Diagnostics for the binomial GLM fitted to the BET CPUE data for region 4.

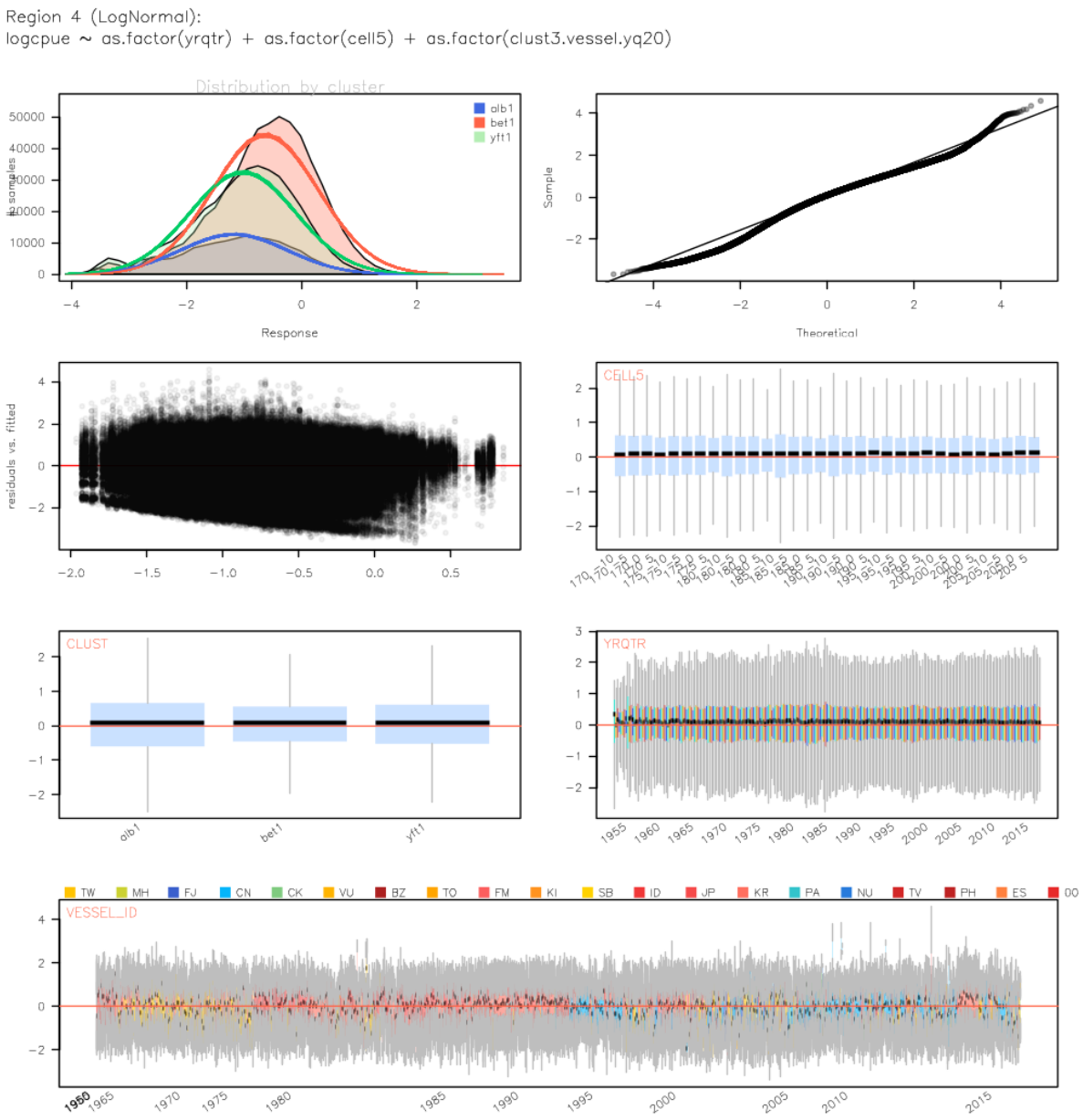

Figure 88: Diagnostics for the log normal GLM fitted to the BET CPUE data for region 4.

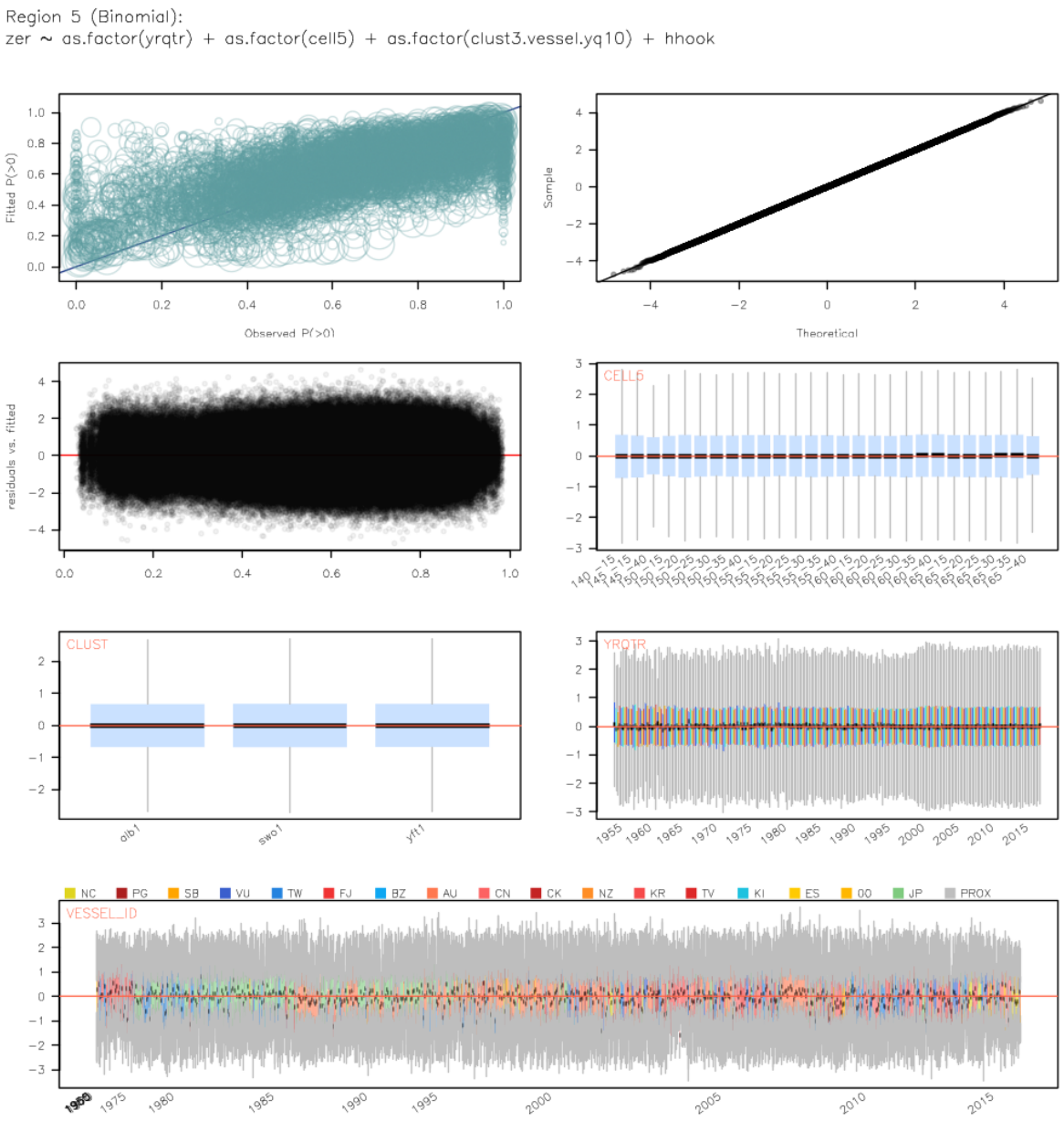

Figure 89: Diagnostics for the binomial GLM fitted to the BET CPUE data for region 5.

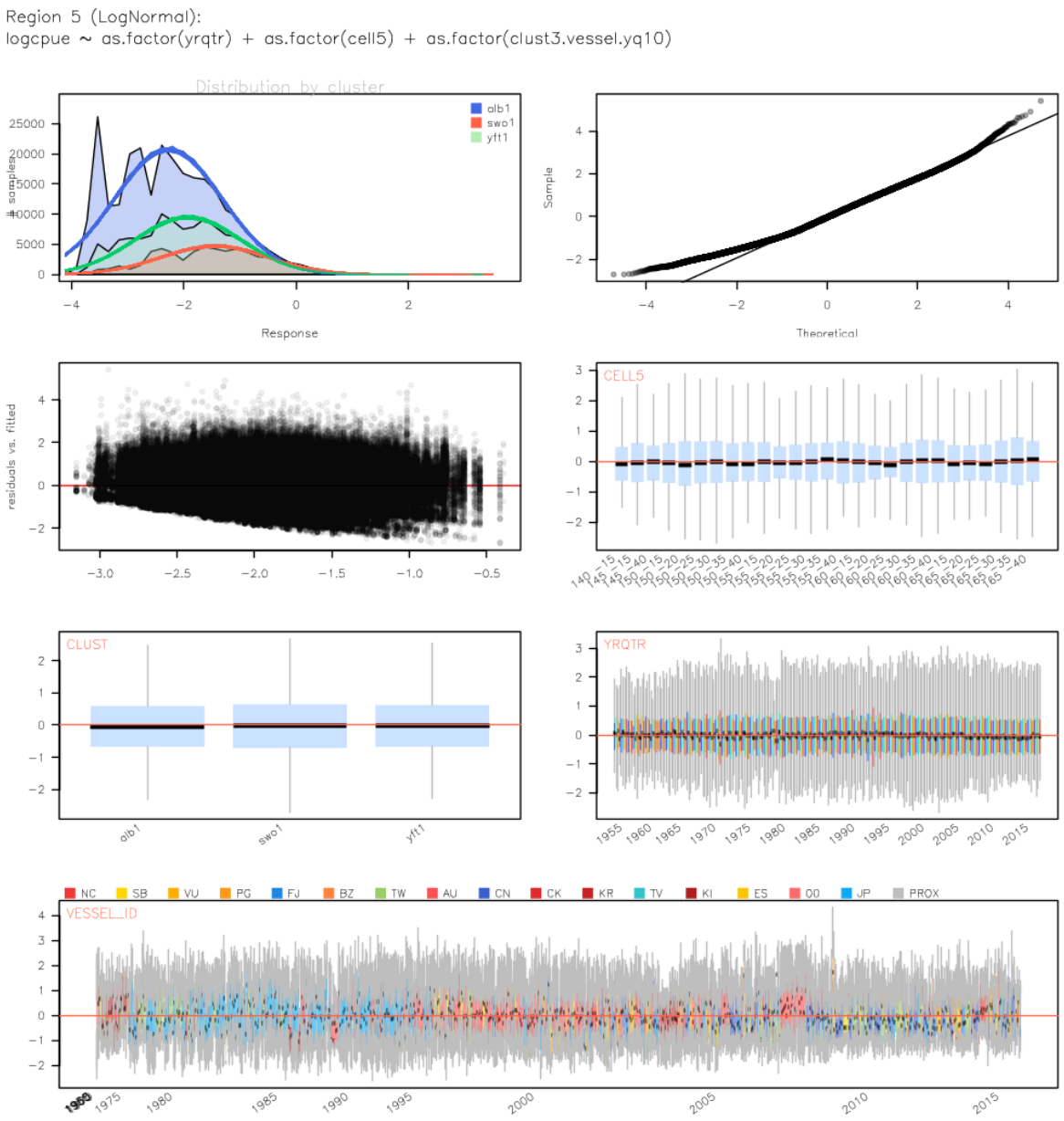

Figure 90: Diagnostics for the log normal GLM fitted to the BET CPUE data for region 5.

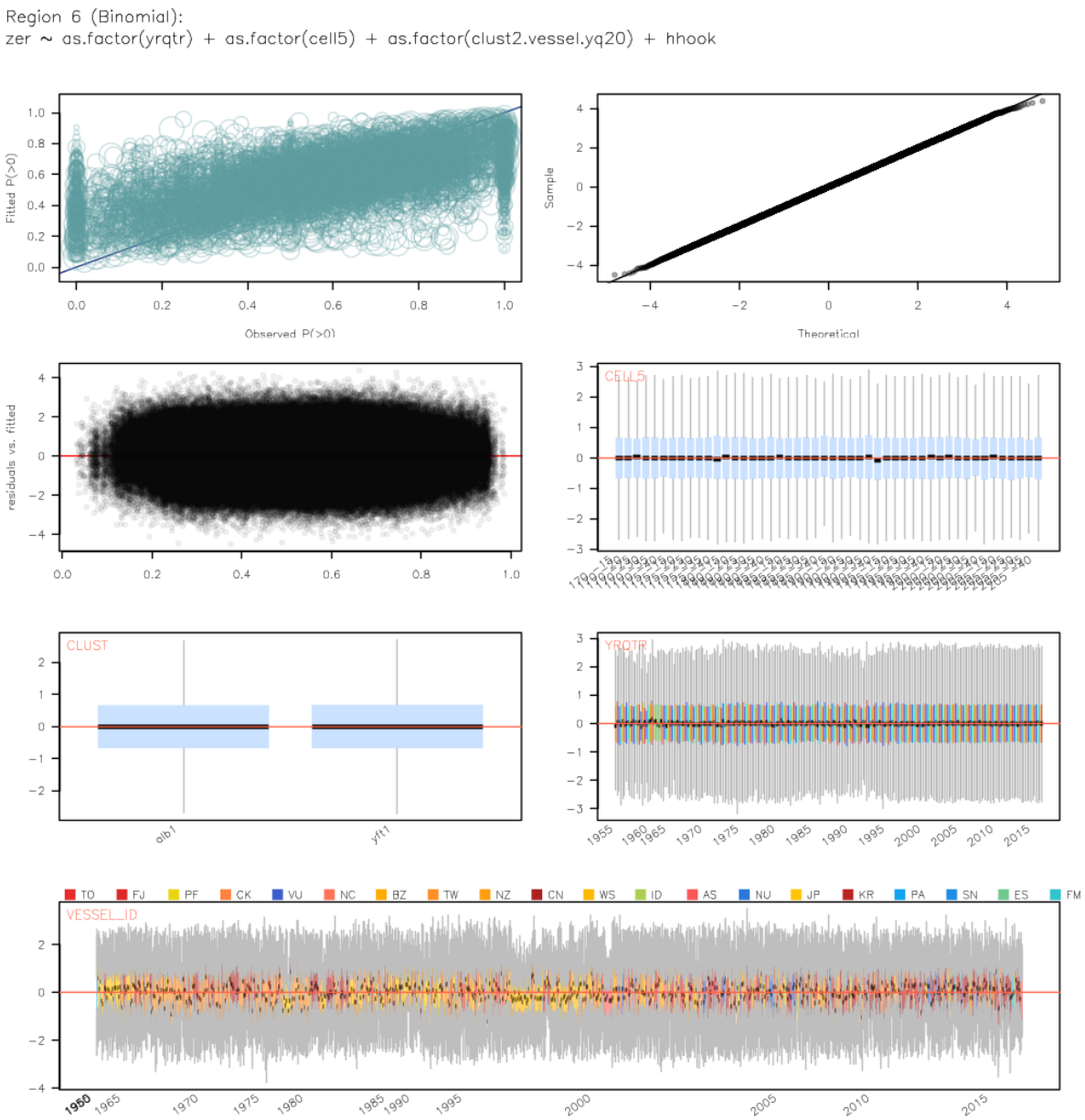

Figure 91: Diagnostics for the binomial GLM fitted to the BET CPUE data for region 6.

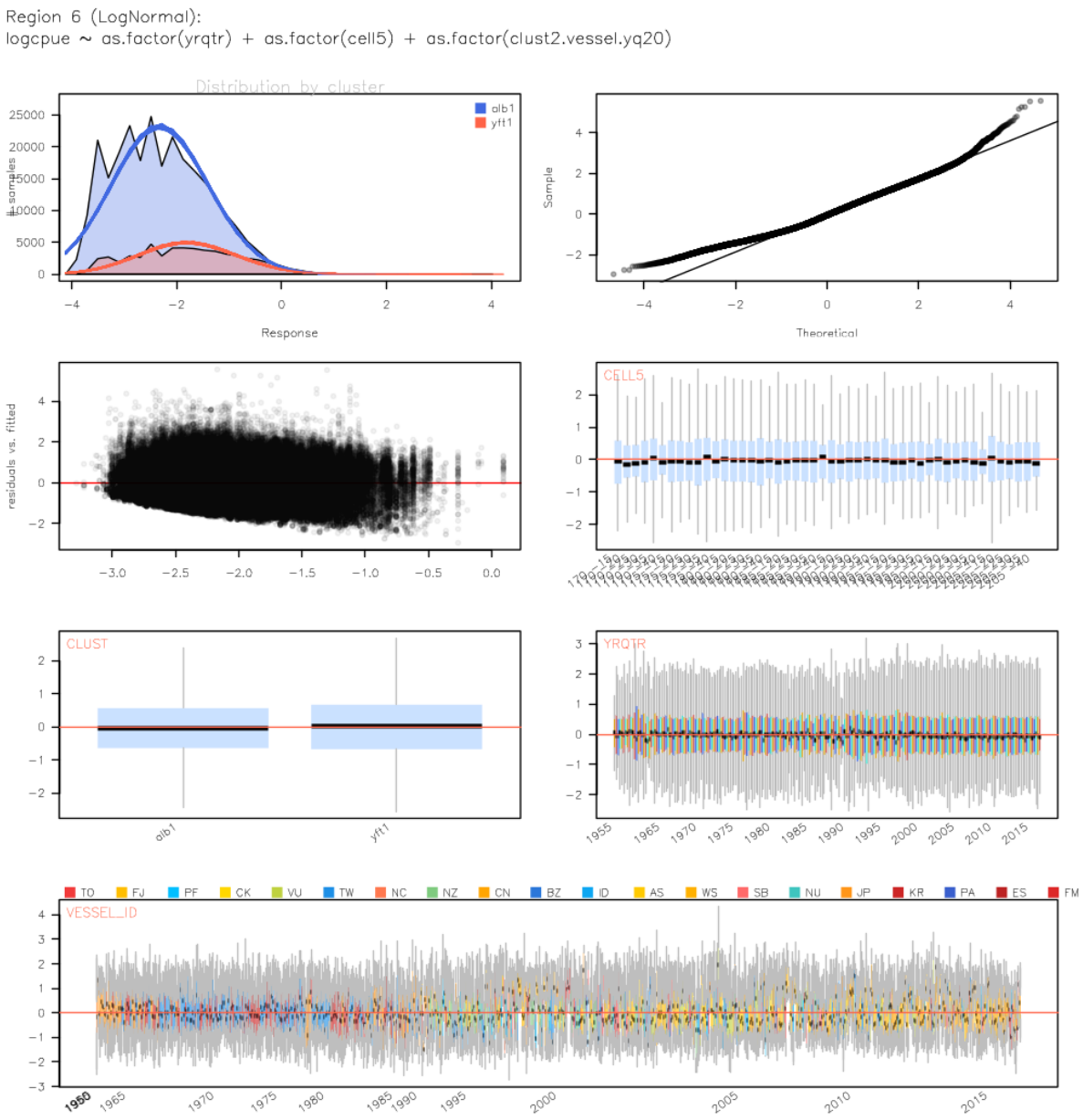

Figure 92: Diagnostics for the log normal GLM fitted to the BET CPUE data for region 6.

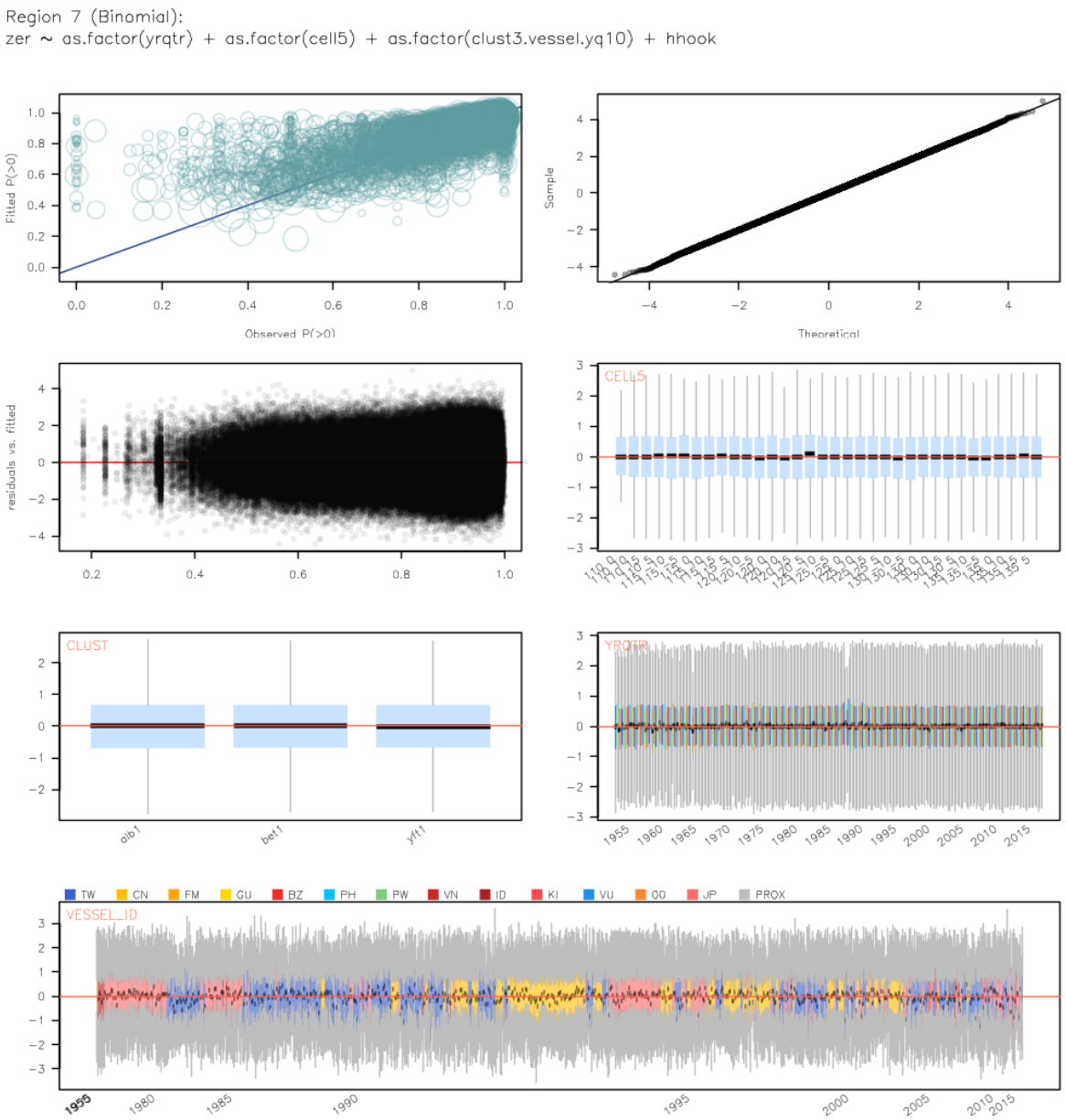

Figure 93: Diagnostics for the binomial GLM fitted to the BET CPUE data for region 7.

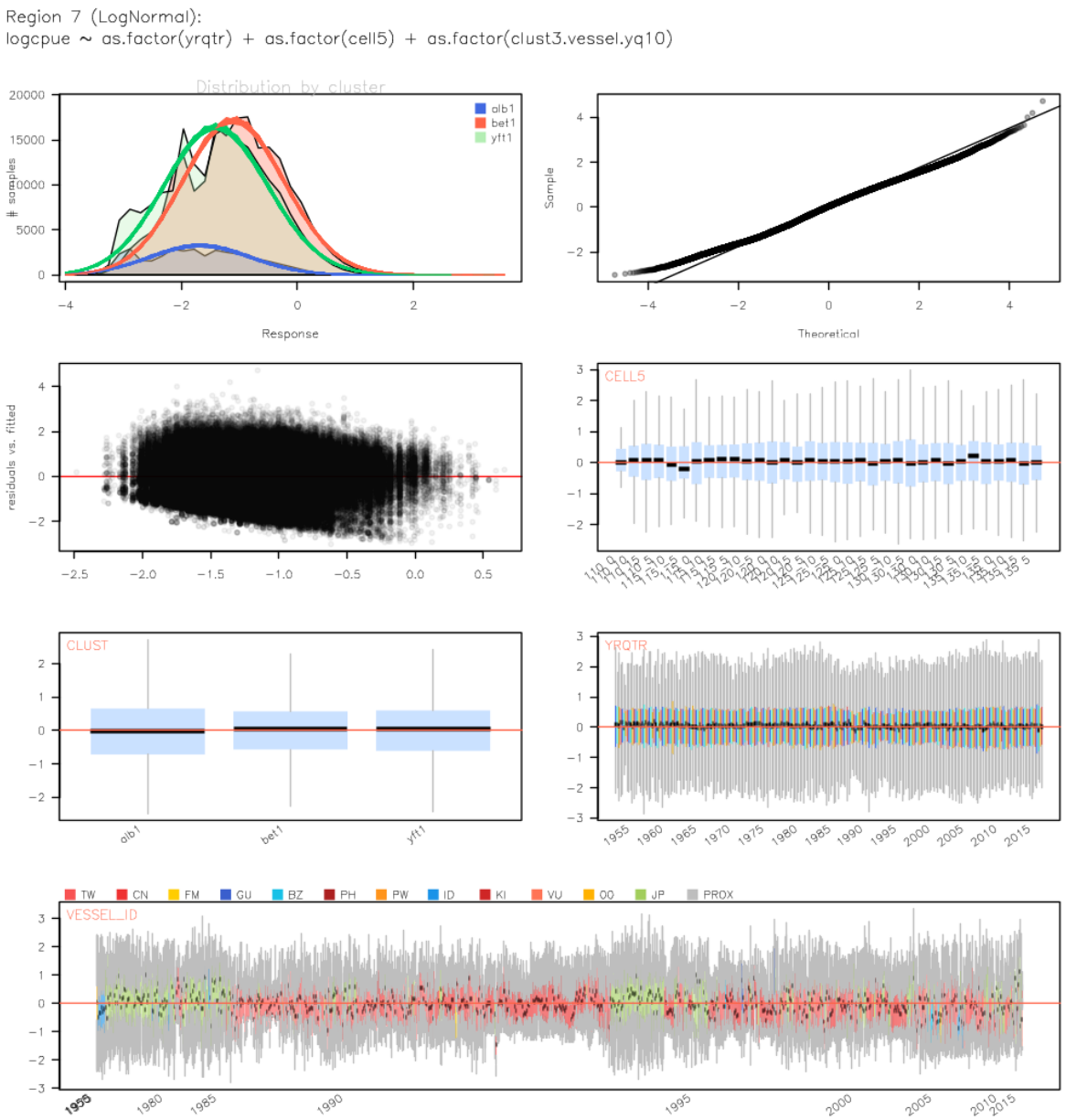

Figure 94: Diagnostics for the log normal GLM fitted to the BET CPUE data for region 7.

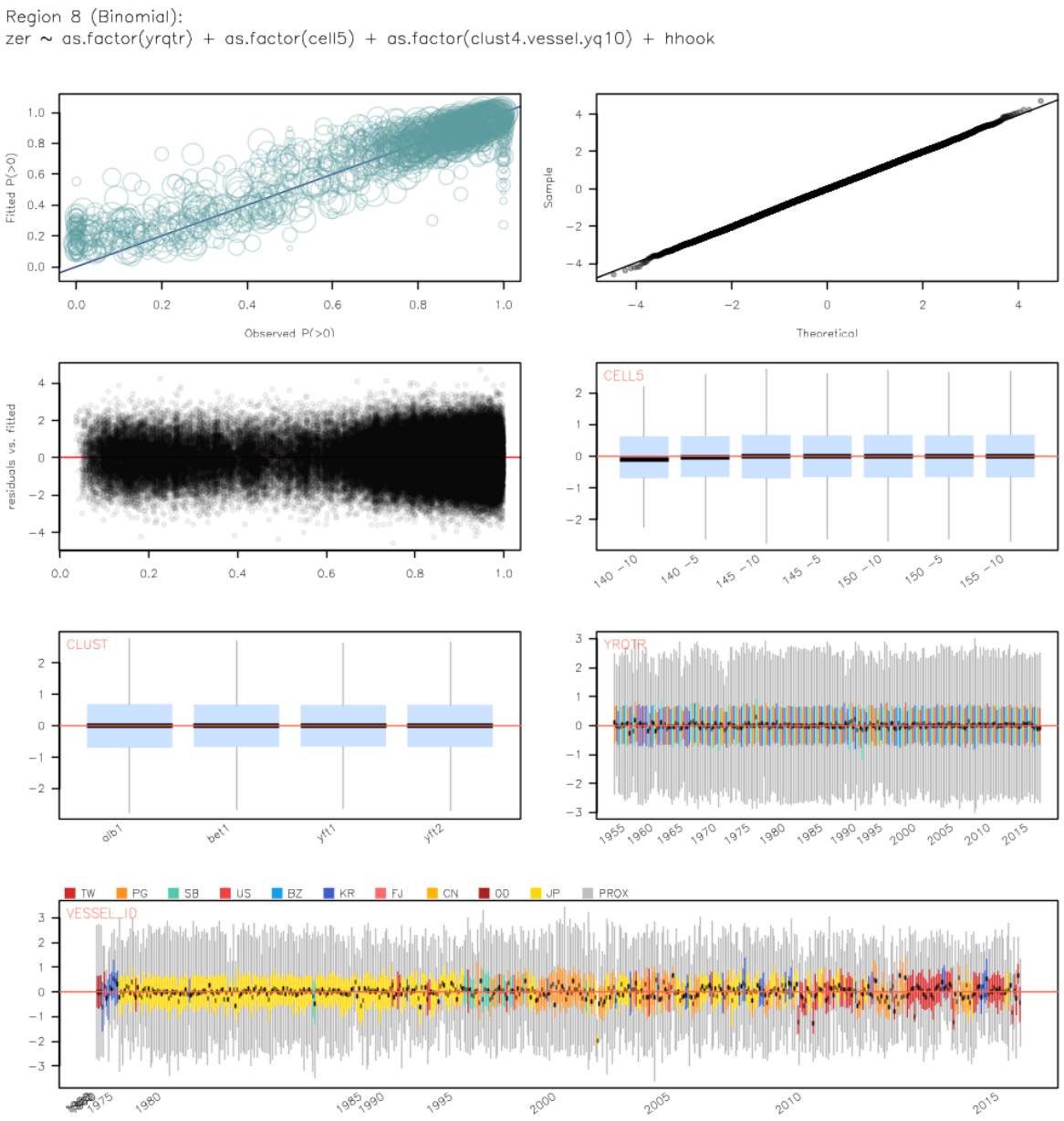

Figure 95: Diagnostics for the binomial GLM fitted to the BET CPUE data for region 8.

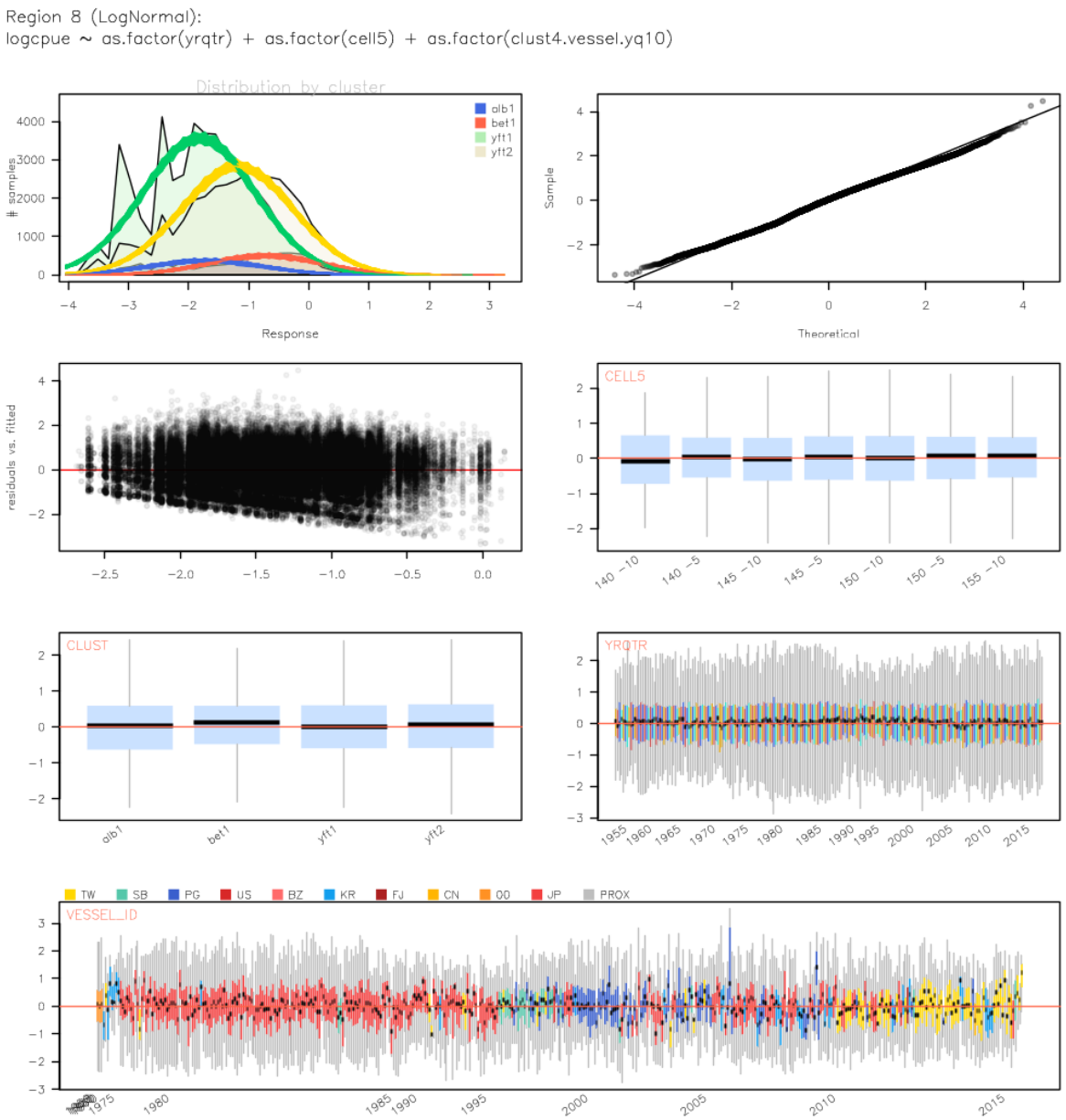

Figure 96: Diagnostics for the log normal GLM fitted to the BET CPUE data for region 8.

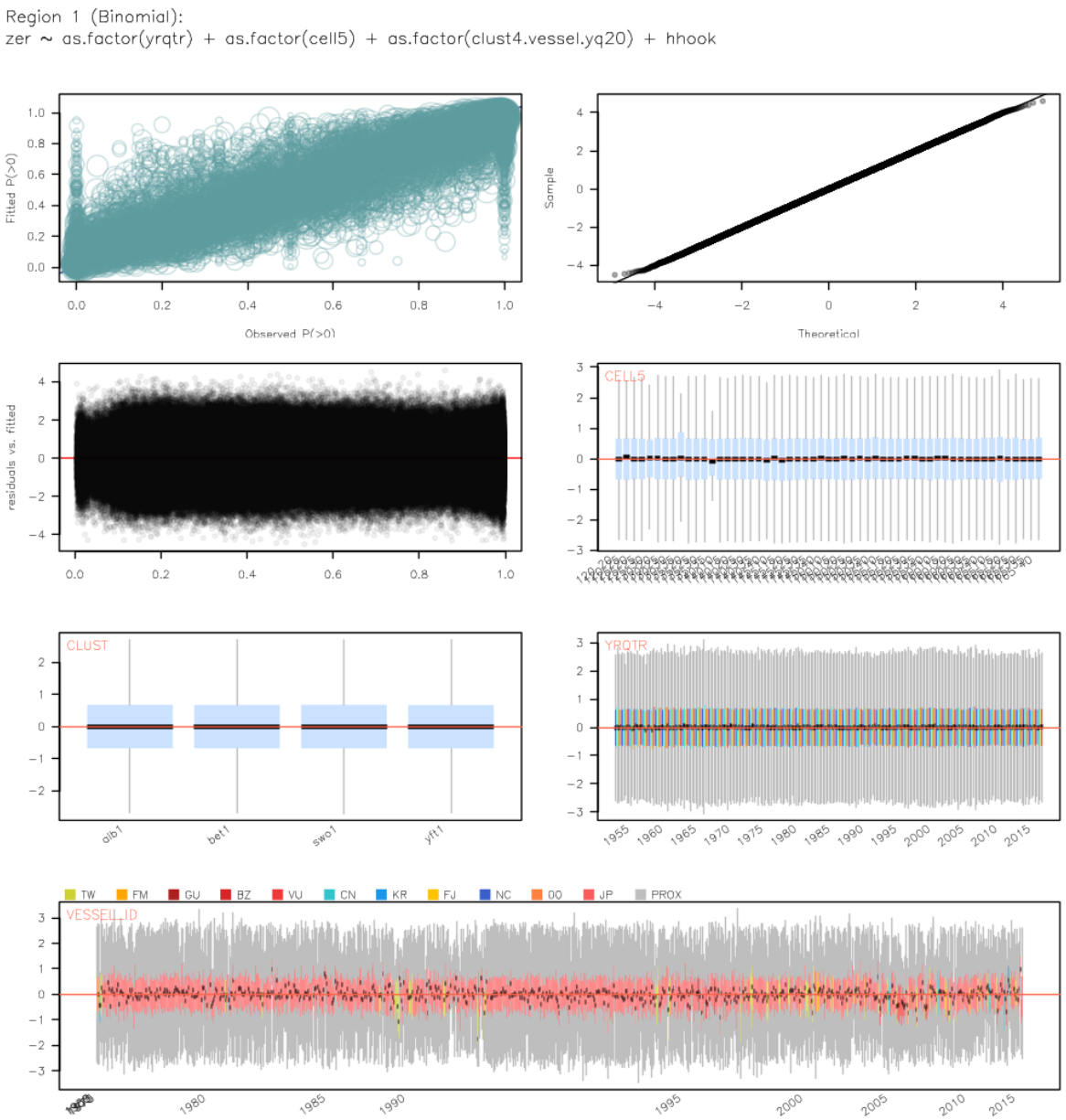

Figure 97: Diagnostics for the binomial GLM fitted to the YFT CPUE data for region 1.

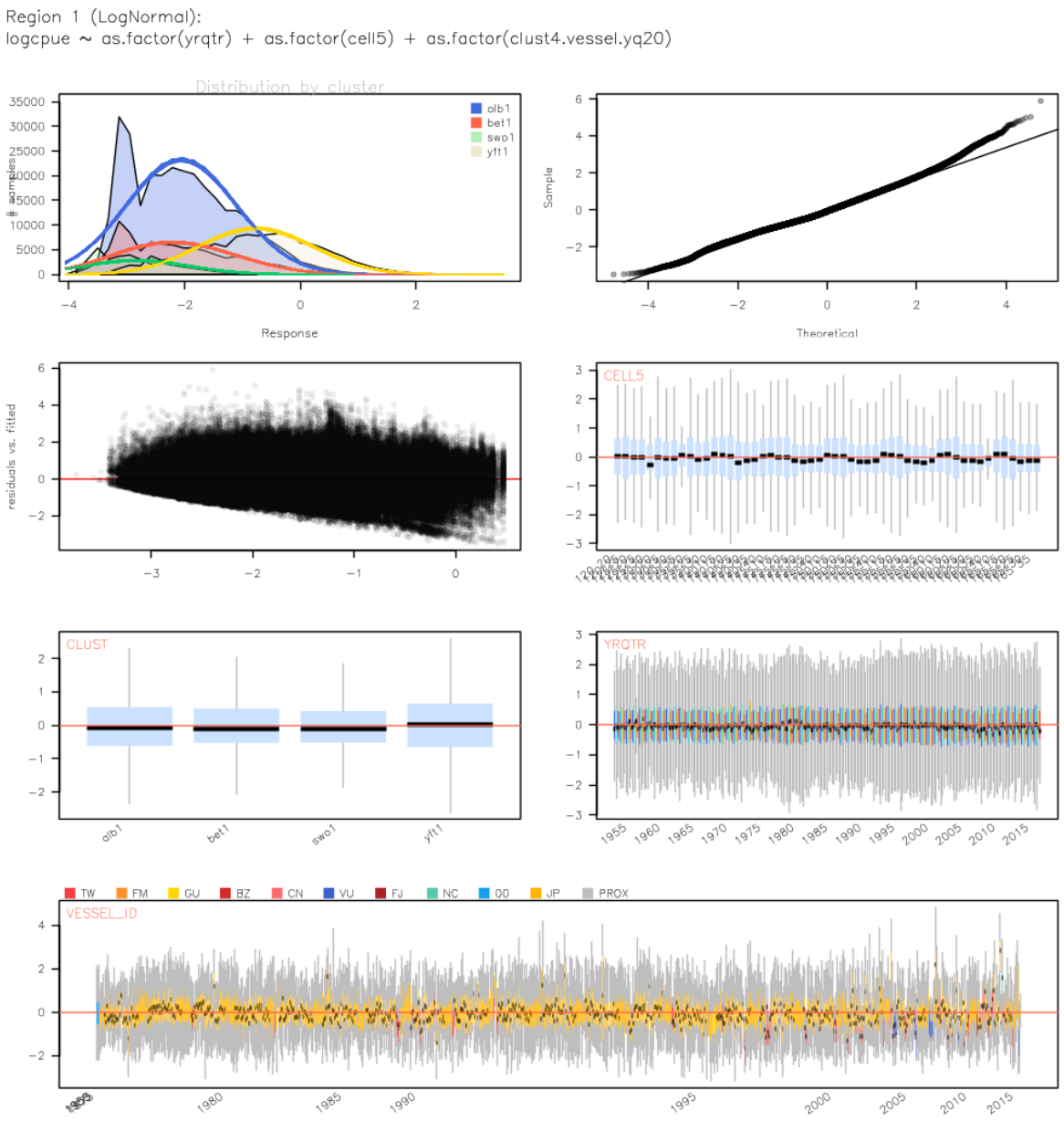

Figure 98: Diagnostics for the log normal GLM fitted to the YFT CPUE data for region 1.

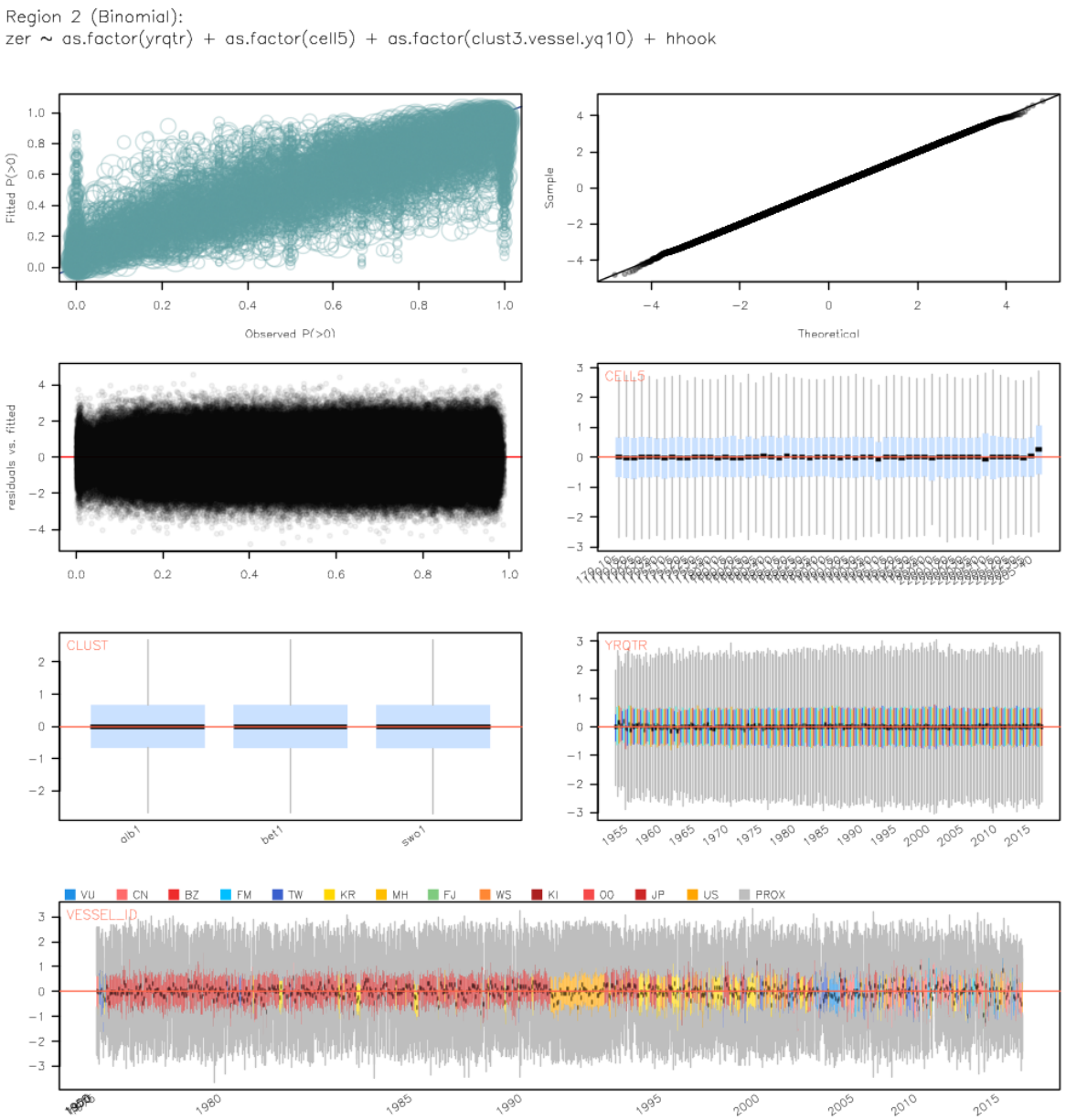

Figure 99: Diagnostics for the binomial GLM fitted to the YFT CPUE data for region 2.

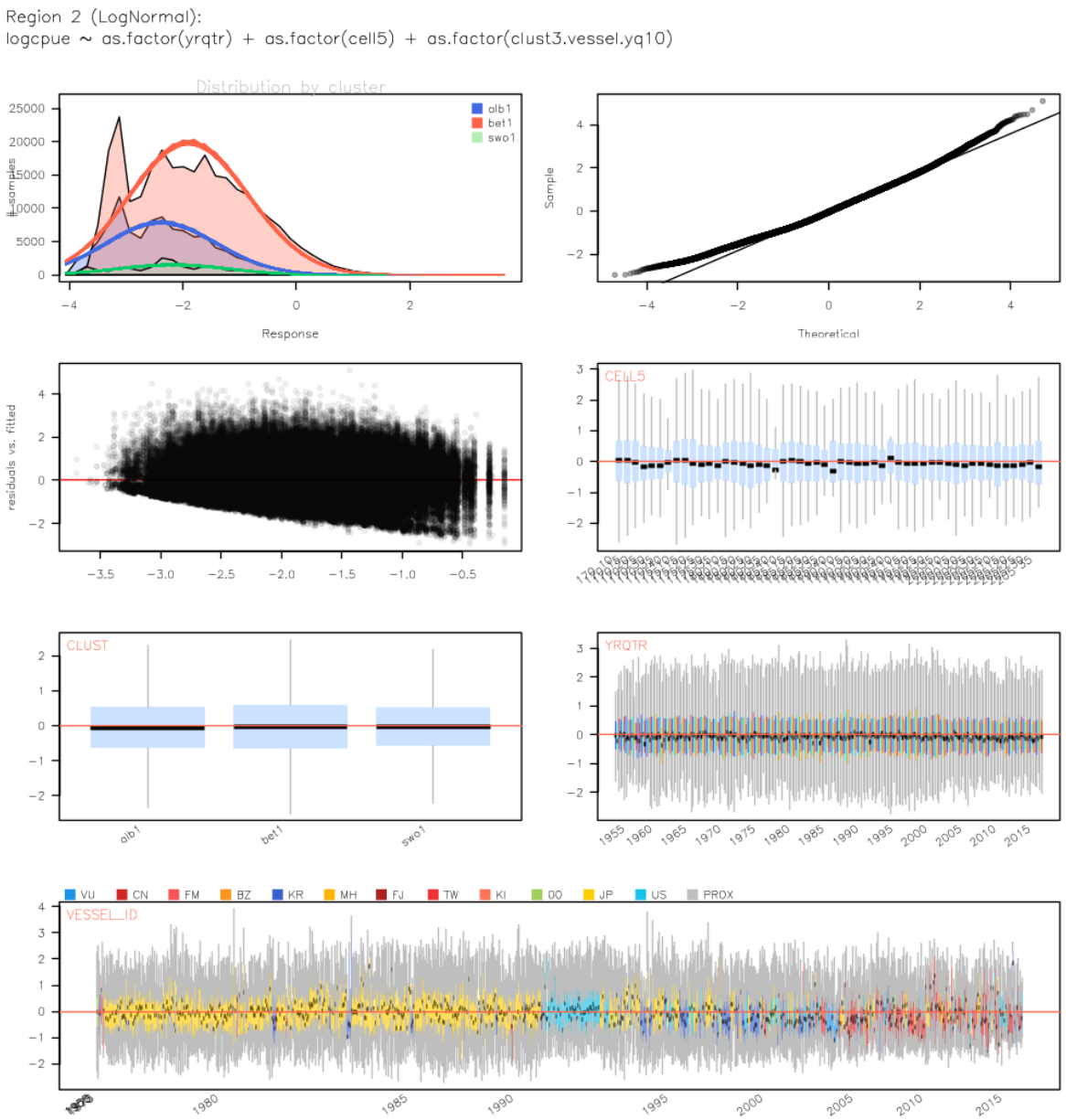

Figure 100: Diagnostics for the log normal GLM fitted to the YFT CPUE data for region 2.

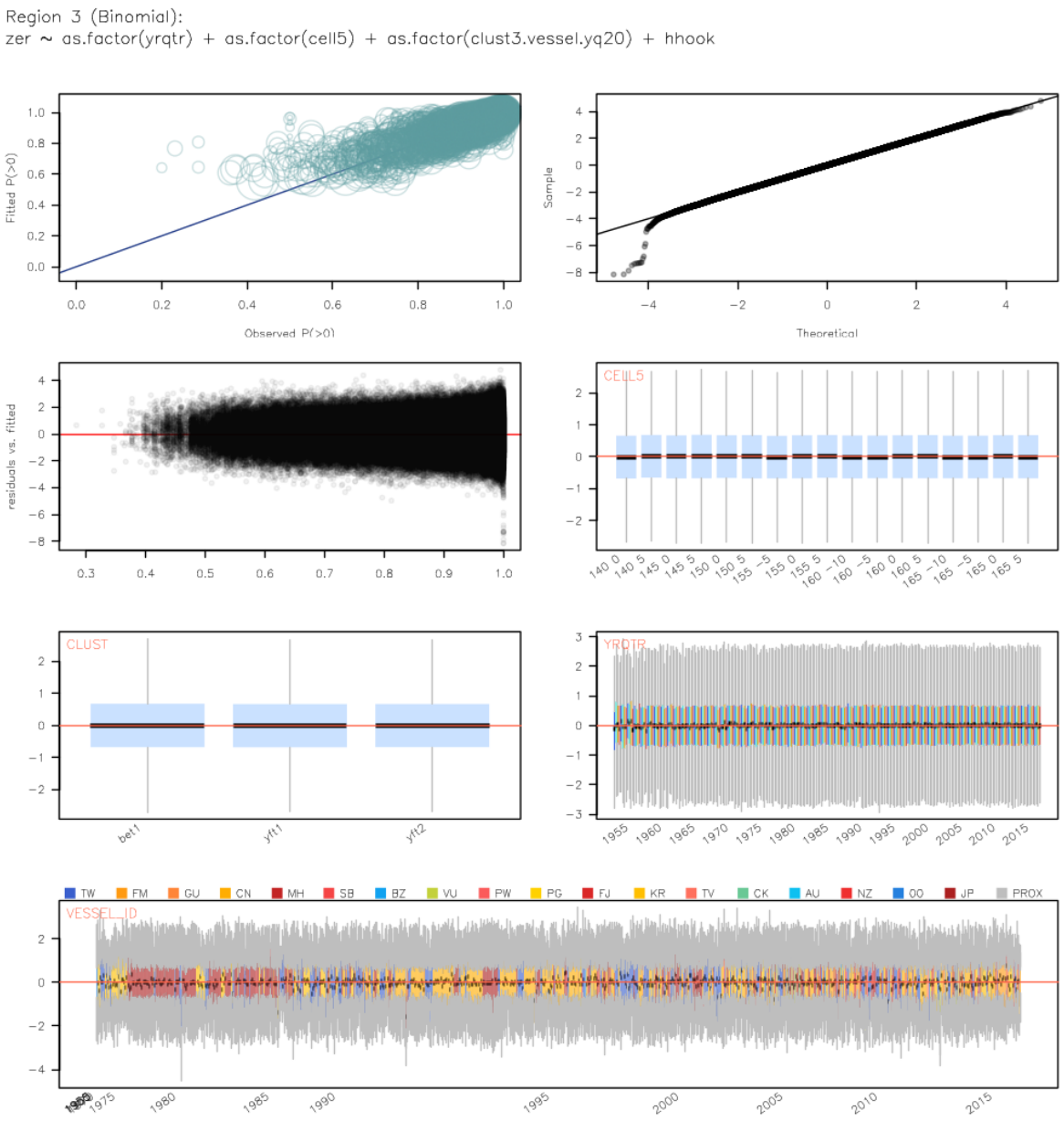

Figure 101: Diagnostics for the binomial GLM fitted to the YFT CPUE data for region 3.

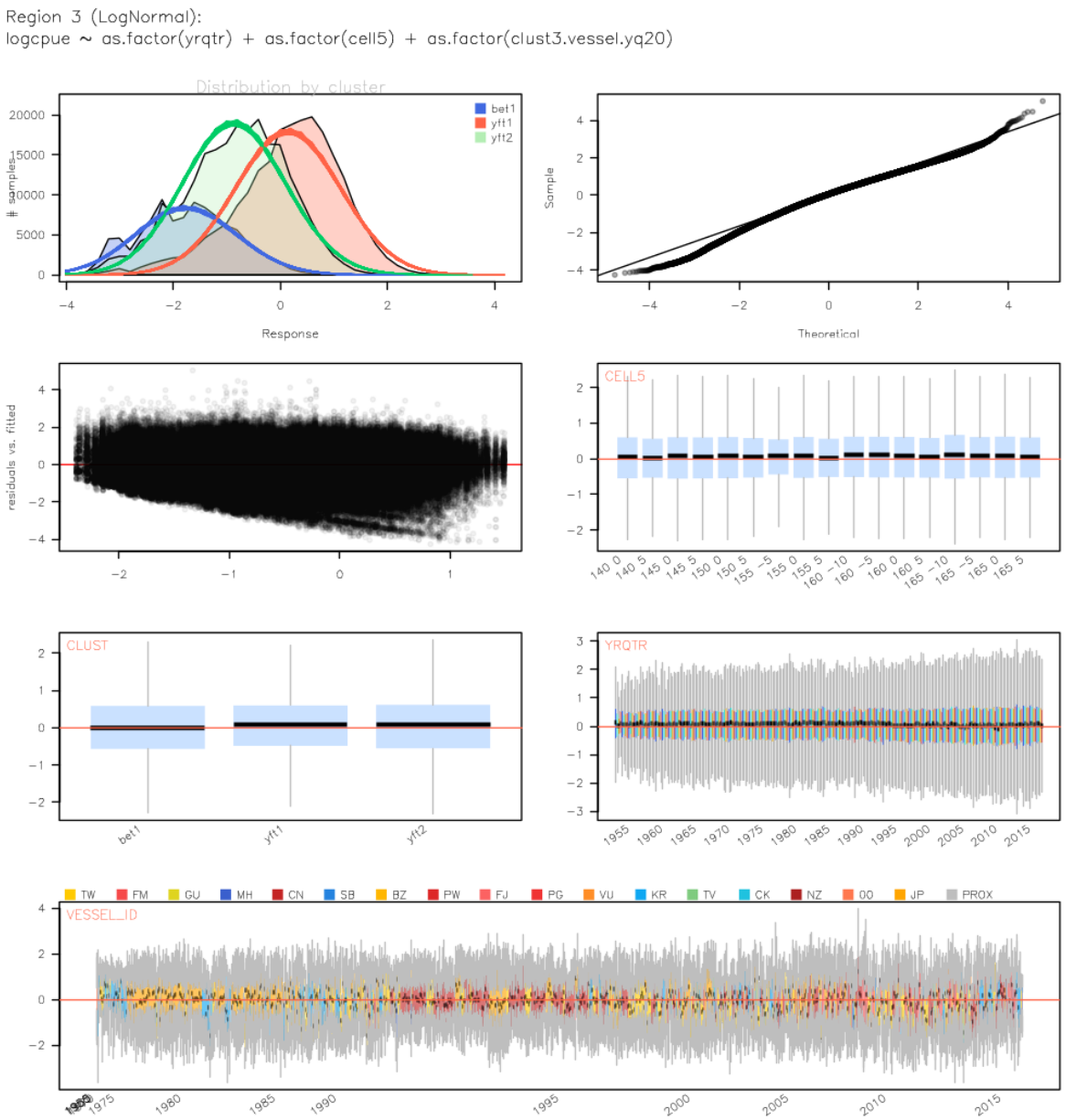

Figure 102: Diagnostics for the log normal GLM fitted to the YFT CPUE data for region 3.

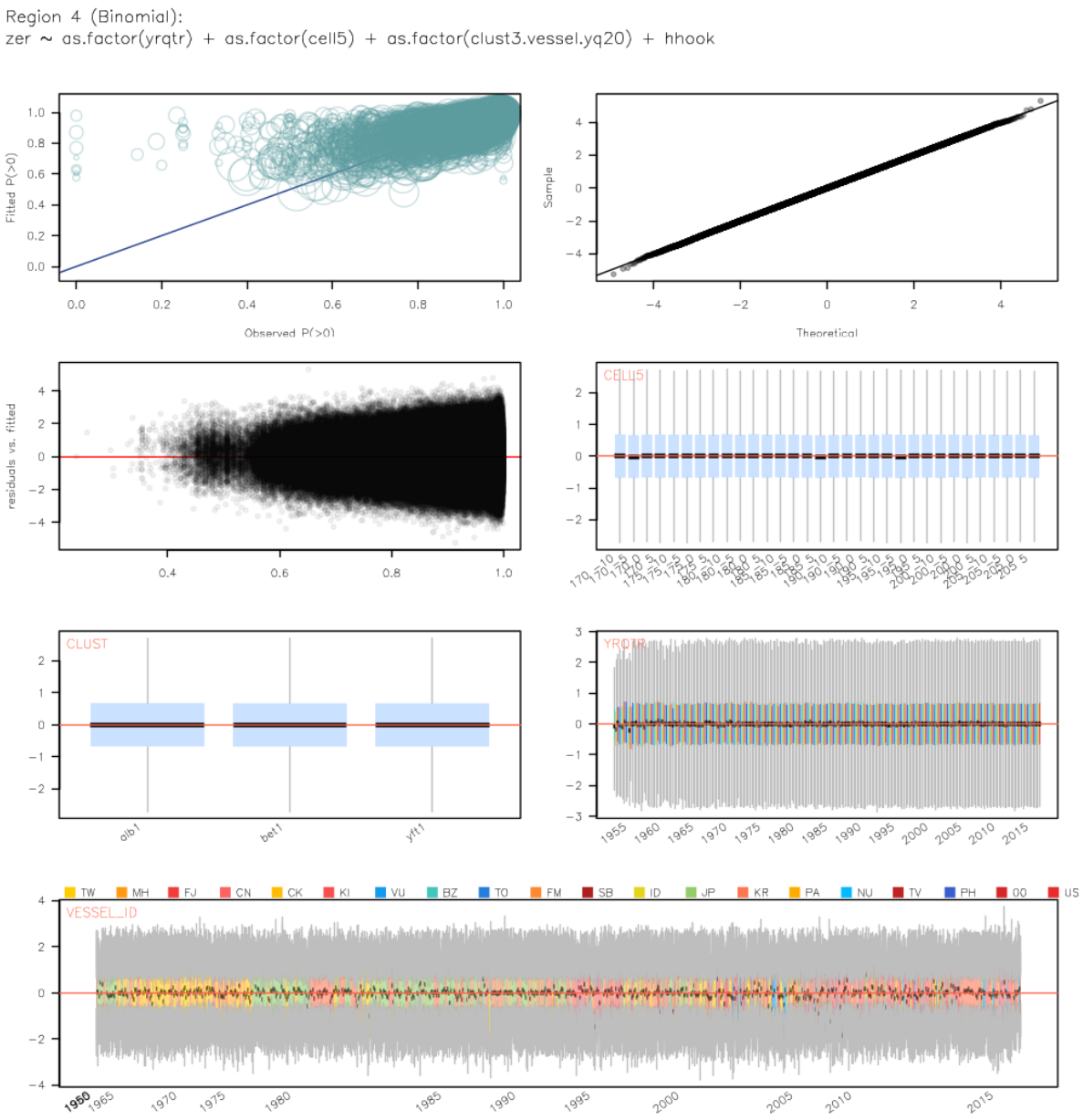

Figure 103: Diagnostics for the binomial GLM fitted to the YFT CPUE data for region 4.

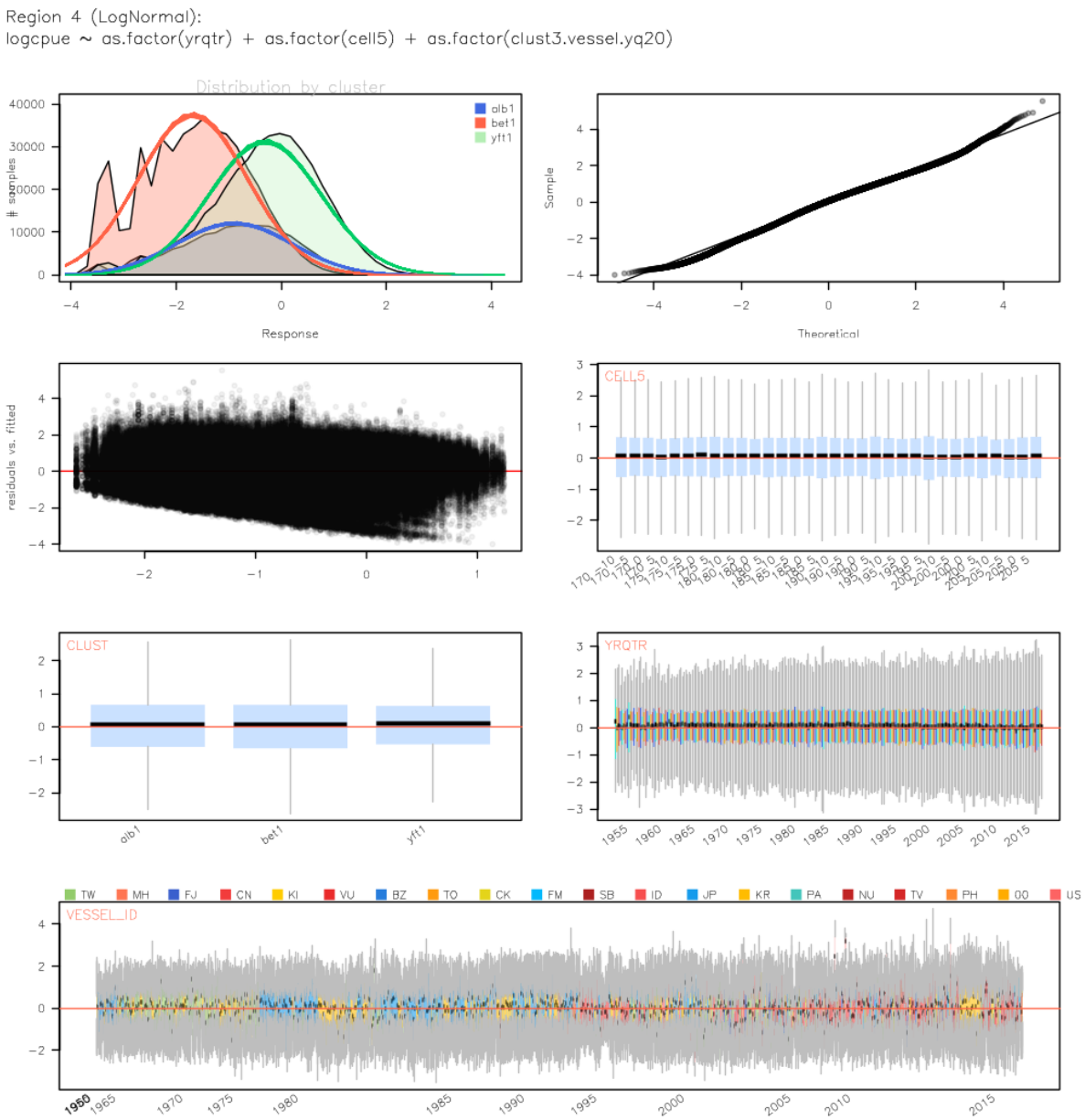

Figure 104: Diagnostics for the log normal GLM fitted to the YFT CPUE data for region 4.

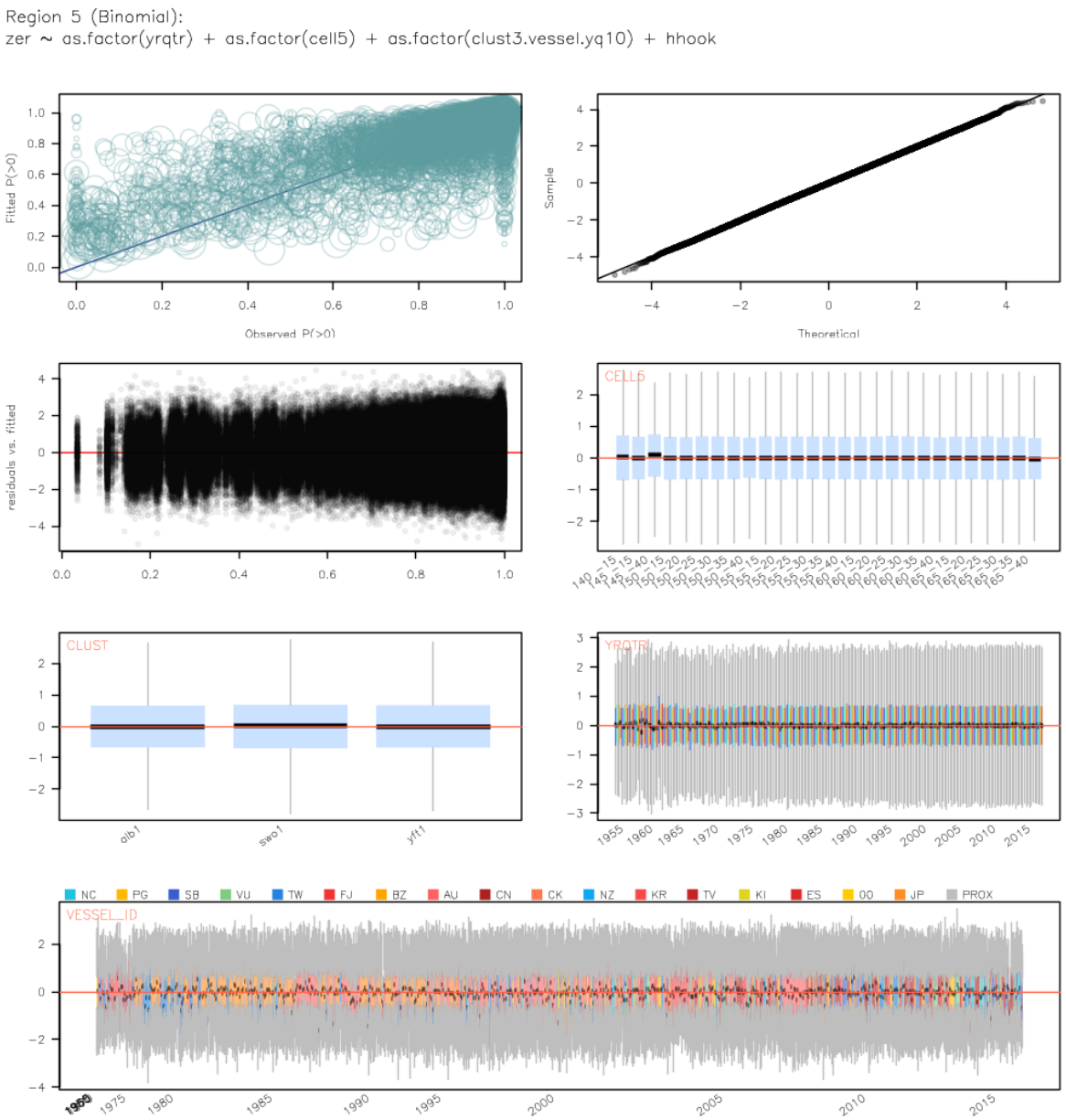

Figure 105: Diagnostics for the binomial GLM fitted to the YFT CPUE data for region 5.

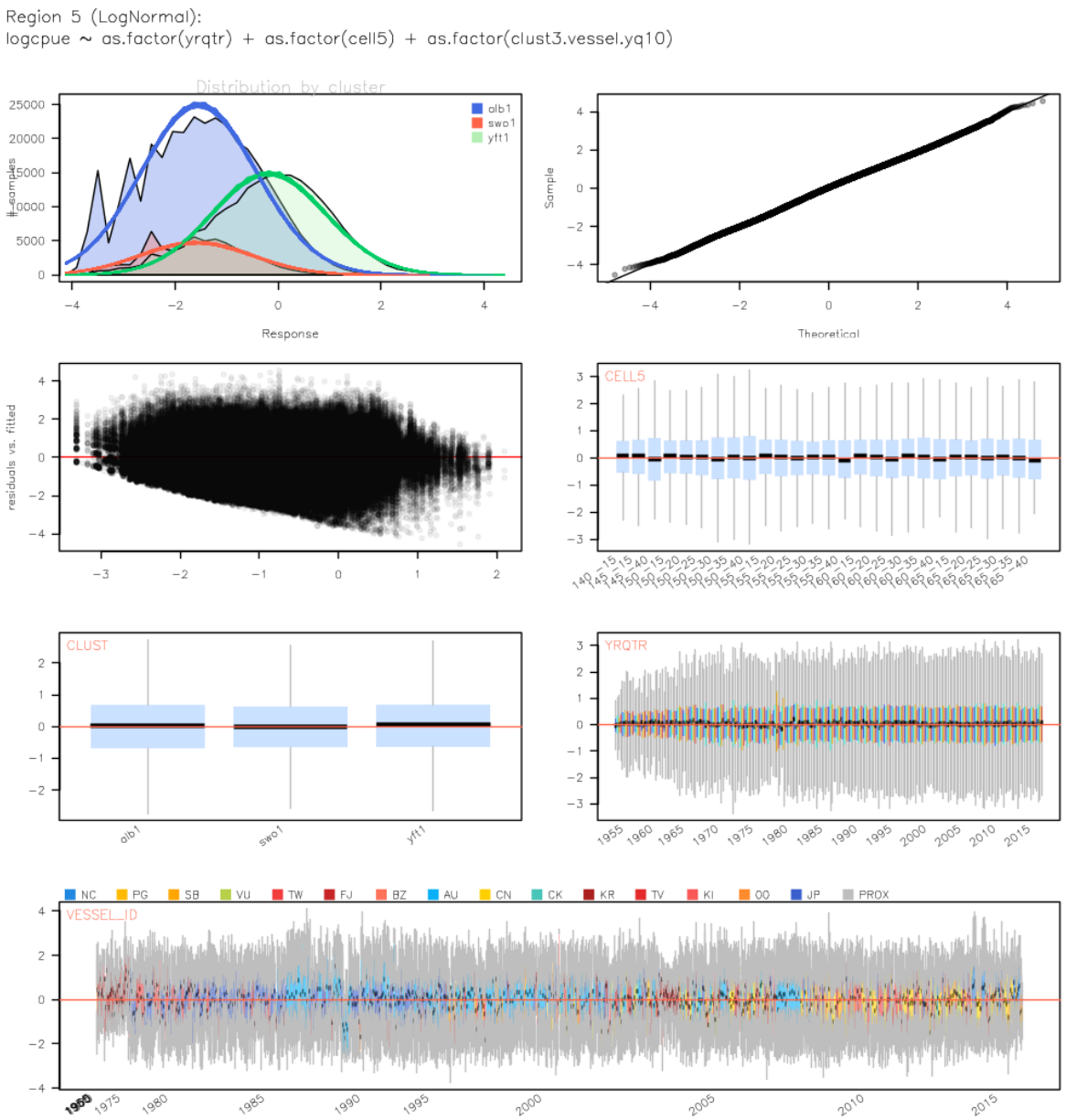

Figure 106: Diagnostics for the log normal GLM fitted to the YFT CPUE data for region 5.

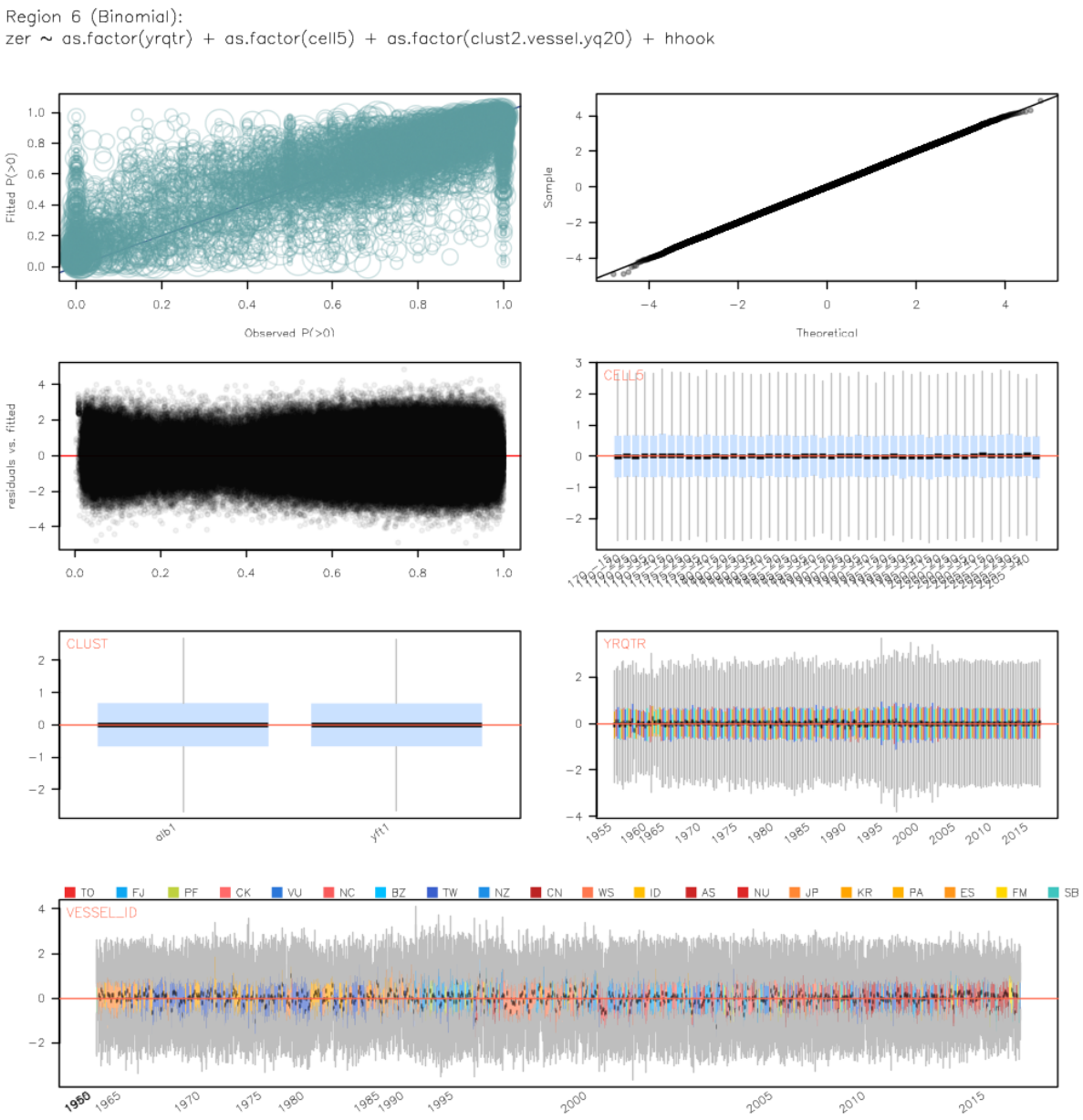

Figure 107: Diagnostics for the binomial GLM fitted to the YFT CPUE data for region 6.

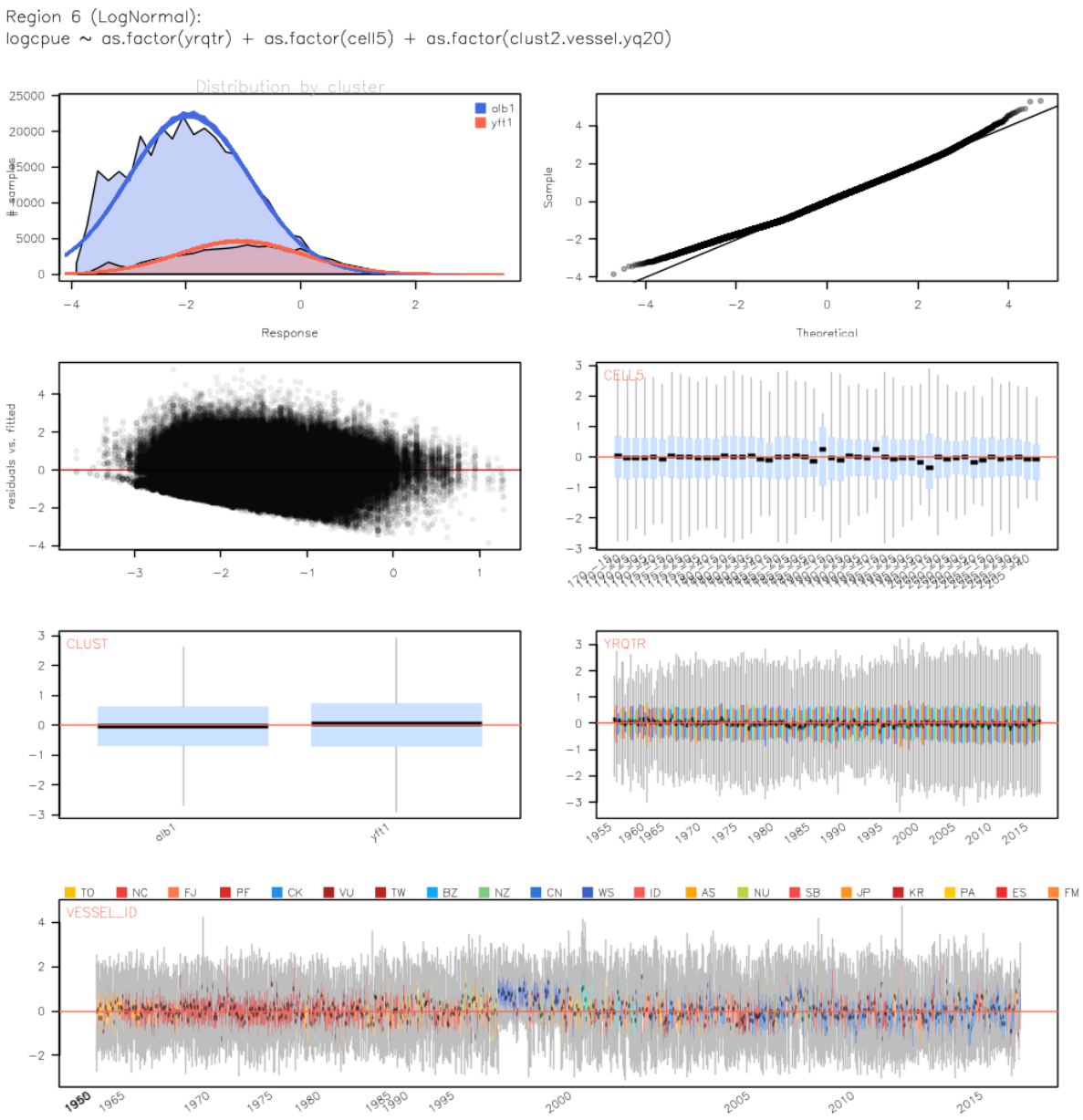

Figure 108: Diagnostics for the log normal GLM fitted to the YFT CPUE data for region 6.

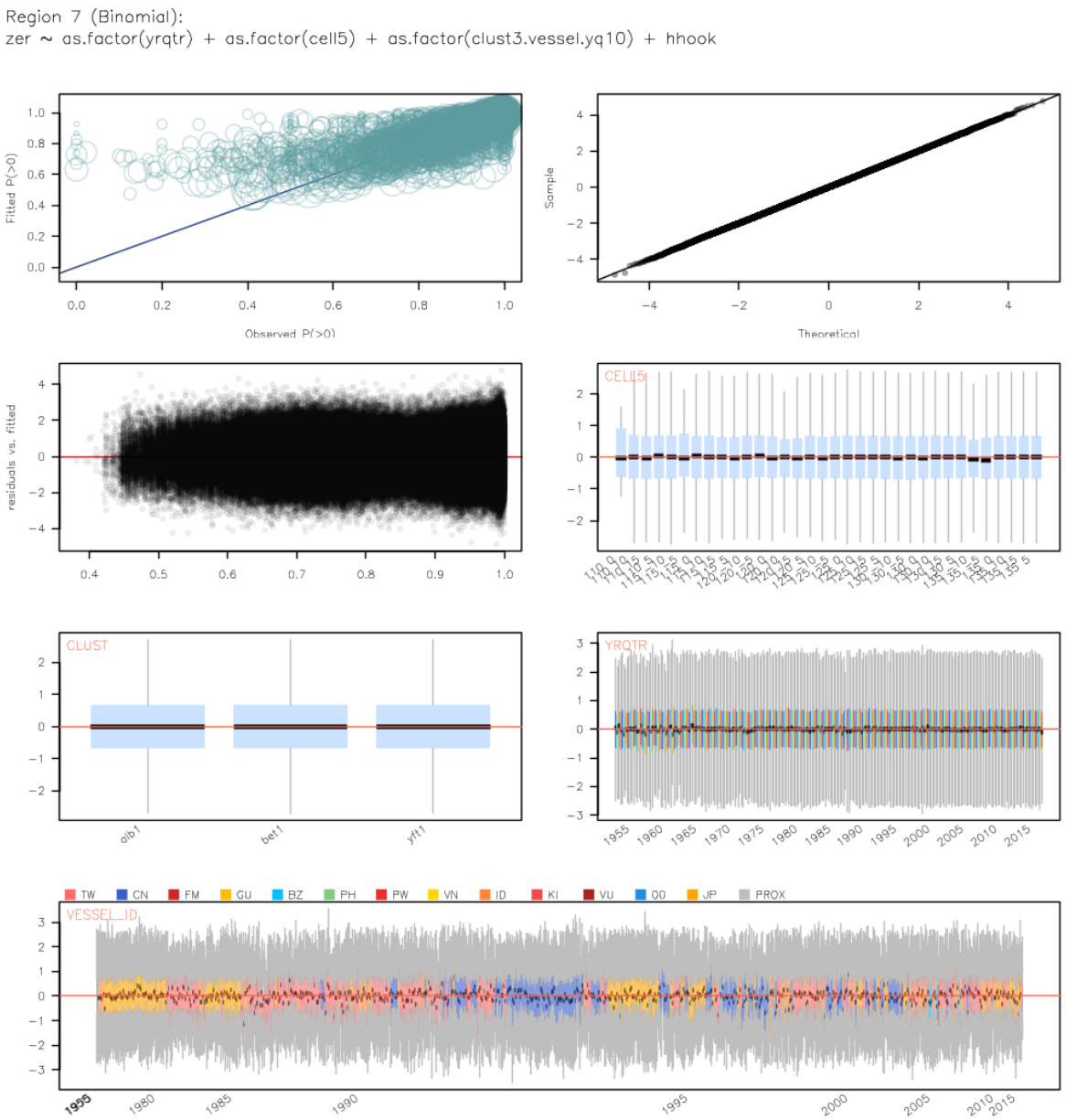

Figure 109: Diagnostics for the binomial GLM fitted to the YFT CPUE data for region 7.

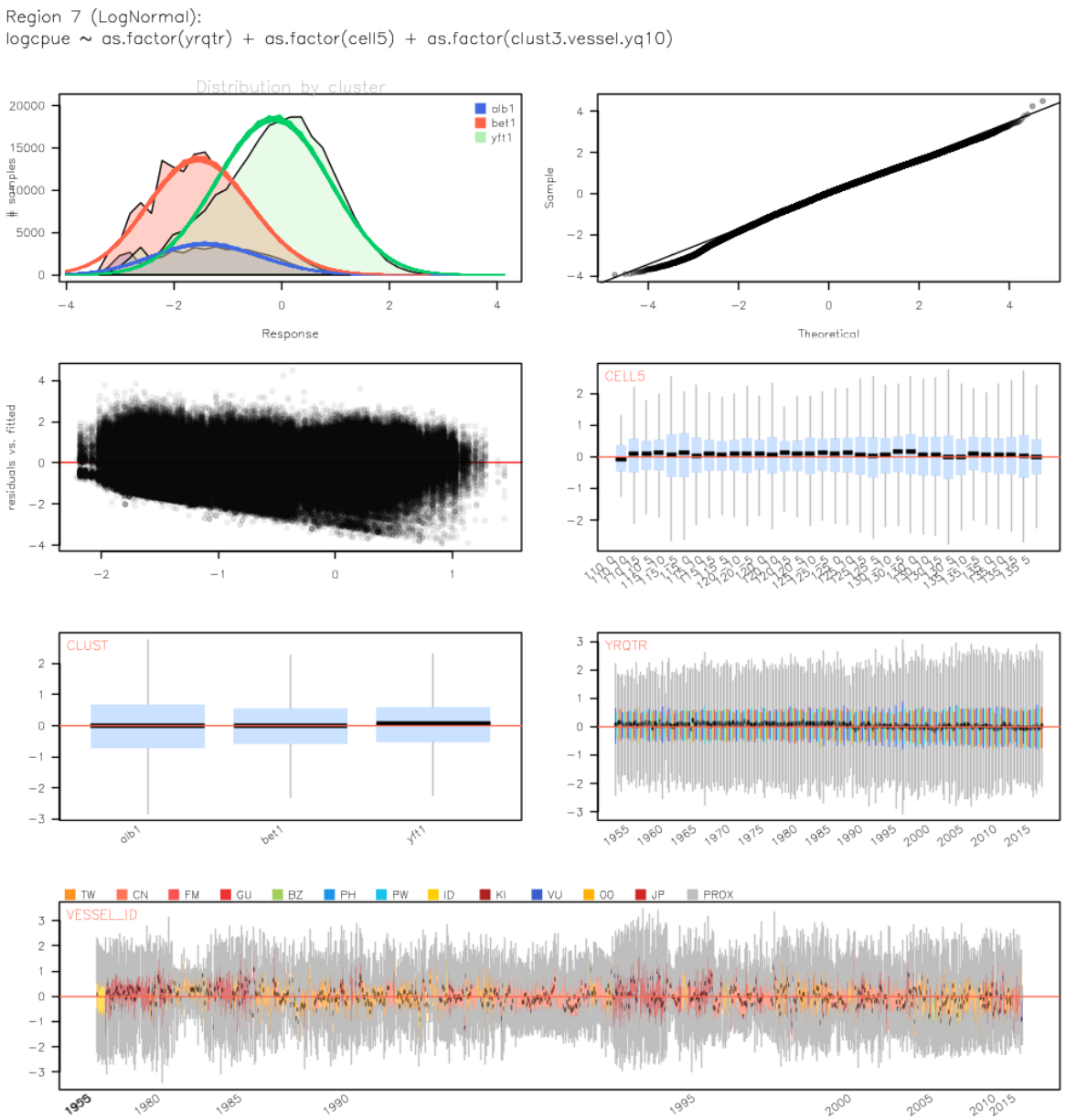

Figure 110: Diagnostics for the log normal GLM fitted to the YFT CPUE data for region 7.

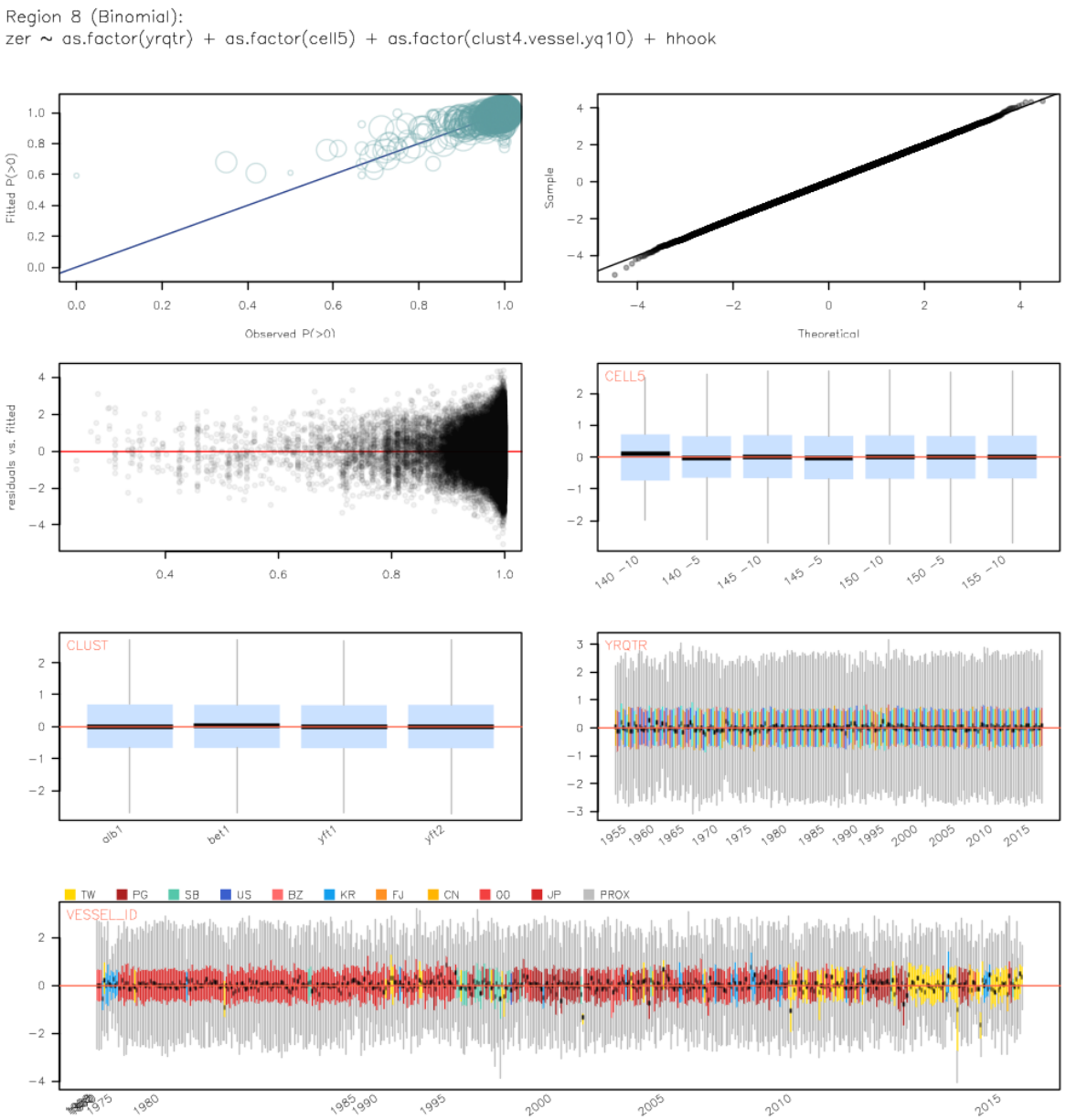

Figure 111: Diagnostics for the binomial GLM fitted to the YFT CPUE data for region 8.

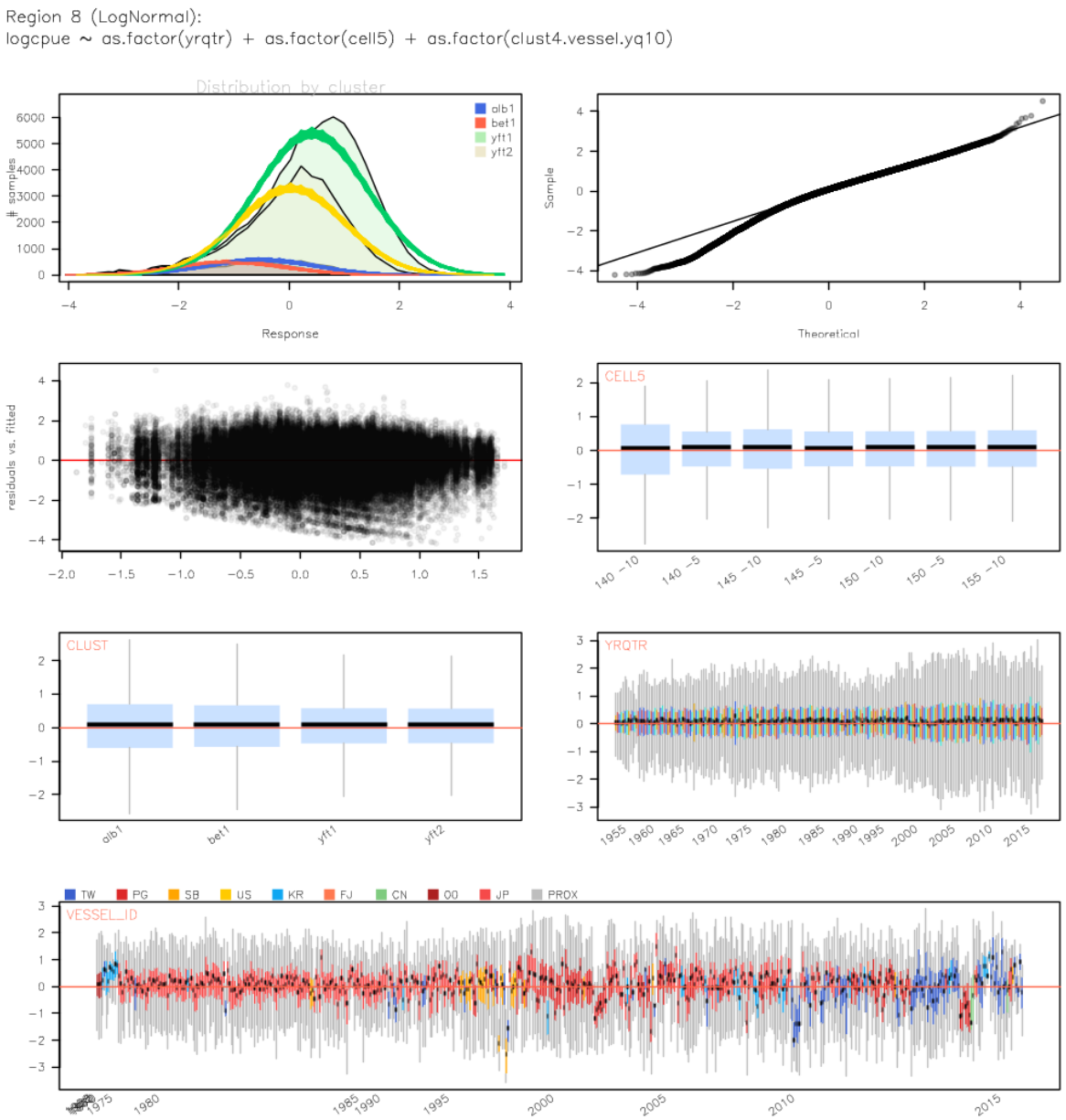

Figure 112: Diagnostics for the log normal GLM fitted to the YFT CPUE data for region 8.